

PDF hosted at the Radboud Repository of the Radboud University Nijmegen

The following full text is a publisher's version.

For additional information about this publication click this link.

<http://hdl.handle.net/2066/124938>

Please be advised that this information was generated on 2018-07-07 and may be subject to change.

The research presented in this doctoral thesis was carried out at the Donders Institute for Brain, Cognition and Behaviour, Radboud University Nijmegen, The Netherlands.

Design by

Niels van der Wegen and Freek van Ede

Printed by

Ipskamp Drukkers BV, Enschede, The Netherlands

ISBN: 978-94-91027-82-6

Preparing for perception

On the attentional modulation, perceptual relevance
and physiology of oscillatory neural activity

Proefschrift

ter verkrijging van de graad van doctor

aan de Radboud Universiteit Nijmegen

op gezag van de rector magnificus prof. mr. S.C.J.J. Kortmann,

volgens besluit van het college van decanen

in het openbaar te verdedigen op dinsdag 18 maart 2014

om 14.30 uur precies

door

Frederik Lammert van Ede

geboren op 18 januari 1985

te Den Helder

Promotor:

Prof. dr. M. Ullsperger

Copromotor:

Dr. E.G.G. Maris

Manuscriptcommissie:

Prof. dr. P. Fries

Prof. dr. P.R. Roelfsema (UvA)

Prof. dr. P. Brown (Universiteit van Oxford, UK)

Table of content

Chapter 1	General introduction and outline of thesis	6
	Part 1: The phenomenon	
Chapter 2	Tactile expectation modulates pre-stimulus beta-band oscillations in human sensorimotor cortex (<i>Neuroimage</i> , 2010)	18
Chapter 3	Orienting attention to an upcoming tactile event involves a spatially and temporally specific modulation of sensorimotor alpha- and beta-band oscillations (<i>J Neurosci</i> , 2011)	40
	Part 2: Perceptual and neural consequences	
Chapter 4	Attentional cues affect accuracy and reaction time via different cognitive and neural processes (<i>J Neurosci</i> , 2012)	62
Chapter 5	Beyond establishing involvement: Quantifying the contribution of anticipatory alpha- and beta-band suppression to perceptual improvement with attention (<i>J Neurophysiol</i> , 2012)	74
Chapter 6	Anticipation increases tactile stimulus processing in the ipsilateral primary somatosensory cortex (<i>Cereb Cortex</i> , 2013)	94
	Part 3: Relation to other physiological phenomena	
Chapter 7	Dissociable spectral signatures of somatosensory attention during anticipation and stimulus processing	114
Chapter 8	Somatosensory demands modulate muscular beta oscillations, independent of motor demands (<i>J Neurosci</i> , 2013)	128
Chapter 9	Phase relation diversity in neural oscillations and the interpretation of observed amplitude modulations	146
Chapter 10	General discussion	162
	References	170
	Nederlandse samenvatting (Dutch summary)	179
	Publications	182
	Curriculum Vitae	183
	Acknowledgements	184
	Donders series	186

General introduction and outline of thesis

1



1.1 Introduction

1.1.1 Perception: selection and preparation

Our senses are continuously confronted with a far greater amount of sensory information than can be perceived. As a consequence, a major challenge that must be resolved by our nervous system is to selectively process those aspects of our environment that are relevant to current goals, while ignoring others. For example, imagine that your goal is to grasp and drink coffee from the mug depicted in Figure 1.1. With this goal in mind, you must selectively process those sensory aspects of your environment that are relevant to this goal (the location of the mug, the size of its handle, how full it is, etc.), while ignoring others (e.g. the image printed on the mug). Conversely, if your goal would be to learn more about the anatomy of the human brain, you must now selectively process the image printed on the mug, while ignoring other aspects of your environment such as the size of the mug's handle. This process of selecting sensory information that is relevant to one's current goals is referred to as *selective attention*.

In many situations, perception does not only require us to select relevant information while it is present, but also to prepare for this information, prior to its occurrence. This is particularly important when sensory information is only briefly presented and/or when this information is immediately relevant. For example, upon initial contact with the mug, it is essential to immediately evaluate the incoming touch sensation with high fidelity because this will determine how the arm's movement must be adjusted to avoid spilling coffee over the table. To this end, primates (and several other species) have developed the remarkable ability to extract regularities from the environment in order to anticipate forthcoming sensory events. Indeed, while reaching out for the mug of coffee, you will be able to anticipate with relatively high precision when and where you will be touching this mug (e.g. in approximately 300 ms, with your right hand). This allows you to prepare for this sensation such that, upon contact, your perception of this relevant part of your environment will immediately be favored over other, non-relevant, parts (e.g. your left hand). It is this type of *preparatory selective attention* (also termed *voluntary orienting of attention*) that is the main focus of my thesis.

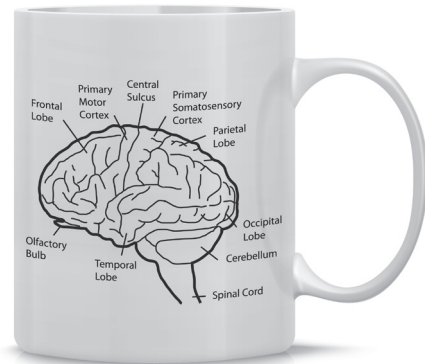


Figure 1.1. Perception requires selection and preparation. Selection example: imagine your goal is to grasp this mug to drink coffee from it. This will require you to first selectively process those sensory aspects of your environment that are relevant to this goal (e.g. the mug's location, the size of its handle, etc.) while ignoring others (e.g. the image printed on the mug). Preparation example: while reaching out for this mug, you can prepare for the upcoming touch sensation in your right hand. Upon initial contact with the mug, this will allow you to process this relevant touch sensation with immediate high fidelity.

In the laboratory, preparatory selective attention is typically studied by presenting symbolic cues (e.g. left- or rightward pointing arrows) that indicate where an upcoming stimulus is most likely to occur (e.g. on the left or right side of the screen). Seminal work by Michael Posner (1980a; 1980b) has demonstrated that such cues result in faster reactions to stimuli presented at cued (i.e. most probable) locations, compared to non-cued locations. Similarly, stimuli are best perceived when they are presented at expected moments in time (reviewed in Nobre, 2001). These studies thus demonstrate that expectations can be utilized by our nervous system to facilitate the processing of anticipated sensory information. A fundamental question is how the nervous system accomplishes this. In other words, what are the neurophysiological mechanisms by which preparatory selective attention improves perception?

1.1.2 Preliminary outline thesis

In this doctoral thesis, I describe a series of eight studies that target different aspects of this central question. These studies focus on the role of oscillatory neural activity (see 1.2) that I have investigated mainly in the human somatosensory modality (i.e. the modality concerned with touch perception; also termed *tactile* perception).

Conceptually, this thesis can be divided into three parts. **Part 1 (chapters 2 and 3)** puts forward the primary phenomenon detailed in this thesis; that orienting attention to an expected touch sensation involves a preparatory suppression of alpha and beta oscillations in the contralateral primary somatosensory cortex (S1; the first stage at which tactile information is processed in the cortex). **Part 2** builds on this central observation by addressing how this relates to the attentional improvement in perception (**chapters 4 and 5**), and via which neural mechanisms during stimulus processing this improvement might be mediated (**chapter 6**). Finally, **part 3** places this central observation into a broader perspective by (1) comparing it to the attentional modulation of neural oscillations during stimulus processing (**chapter 7**), (2) investigating attentional modulations throughout the widely distributed somatomotor network (**chapter 8**), and (3) elaborating on and investigating the mechanisms underlying observed modulations of oscillatory amplitude (**chapter 9**).

In the remainder of this chapter, I first introduce neural oscillations (1.2) and describe the general methodology of my studies (1.3). Where appropriate, I will also point to relevant chapters for more detailed information. Thereafter, I provide an elaborate overview of this thesis (1.4). In this overview, I will also (1) explain the rationale behind each study, and (2) point out how these studies have advanced our understanding of how preparatory attention improves perception by relating these studies to prior literature.

1.2 Neural oscillations

1.2.1 Introduction neural oscillations

Oscillations are a pervasive feature of neural activity. When Hans Berger (the inventor of the Electroencephalogram, or EEG) made his first scalp recordings of human brain activity in the mid 1920's, the first thing he noticed was the presence of highly regular waves of activity, fluctuating rhythmically at approximately 10 Hz (i.e. 100 ms/cycle). He termed these rhythmic fluctuations *alpha oscillations* (Berger, 1929). Nowadays, it is widely accepted that the human brain produces a multitude of neural oscillations with their own characteristic frequencies, brain areas and connectivity profiles. This thesis focuses on the role of alpha, beta and gamma oscillations, primarily in the human somatomotor system. Before introducing these particular oscillations, I first state why this type of neural activity is interesting to study in relation to my central research question.

Oscillations are thought to reflect synchronous fluctuations of the membrane potentials across a population of neurons (Hari and Salmelin, 1997; Fries, 2005; Jensen et al., 2007; Thut et al., 2012). A neuron's membrane potential is directly related to the probability of a neuron's input to elicit an action potential (a neuron's output). On the basis of this notion, oscillations have been proposed to play a key role in the routing of information in the brain (Fries, 2005; Jensen and Mazaheri, 2010; Thut et al., 2012). I return to this in 1.2.2 and 1.2.4. Moreover, because oscillations (in particular in the alpha and beta frequency bands) can be sustained without external input, they are a key candidate to be adjusted during the voluntary orienting of preparatory attention (i.e. prior to sensory input).

There are also practical considerations for studying neural oscillations. First, because these oscillations can be recorded outside of the brain (as in Hans Berger's EEG), they allow the non-invasive study of neural activity in human participants. This contrasts with the recording of action potentials which requires invasive procedures and is therefore mainly restricted to animal research. Second, because these oscillations directly reflect neural activity, they can be used to study neural and cognitive operations with high temporal resolution. This contrasts with the study of blood flow (as recorded using functional Magnetic Resonance Imaging; fMRI), which is delayed relative to the actual neural computations.

1.2.2 Alpha oscillations reflect an inhibited state of sensory cortex

Oscillations in the alpha band (8-12 Hz) are a characteristic aspect of neural activity in the visual, auditory, and somatosensory cortices (reviewed in Hari and Salmelin, 1997). In the latter, these oscillations are also paired by oscillations in the beta band (15-30 Hz), and I will return to this in 1.2.3.

Ample evidence suggests that the amplitude of alpha oscillations is inversely related to information processing in the underlying neural populations. For example, alpha oscillations in the sensory cortices are strongest during rest and are suppressed during the processing of sensory input (Hari and Salmelin, 1997; see also **chapters 2, 3, 6, and 7**). Moreover, spontaneous fluctuations in these oscillations are associated with fluctuations

in cortical excitability, where lower amplitudes are associated with higher excitability (Romei et al., 2008; Dugue et al., 2011; Sauseng et al., 2009; Haegens et al., 2011b). At a functional level, such spontaneous fluctuations have also been related to perceptual detection performance. Again, lower amplitudes (in task-relevant sensory cortices) are associated with better detection performance (van Dijk et al., 2008; Jones et al., 2010; see also **chapter 5**). Based on these observations, alpha oscillations have been suggested to reflect an inhibited (or de-activated) state of the brain (Jensen and Mazaheri, 2010).

One particular scheme that has been proposed is that alpha oscillations are generated by ‘pulses of inhibition’ that come at a rate of around 10 Hz (Jensen and Mazaheri, 2010; Mathewson et al., 2011). When these pulses become stronger, there is more inhibition and there are shorter ‘windows of opportunity’ (i.e. periods in which the membrane potential can be easily depolarized to produce an action potential). Conversely, when these pulses become weaker there is less inhibition and there are longer windows of opportunity. This may increase the overall amount of action potentials (Haegens et al., 2011b) and thereby the impact on downstream populations. Hence, the selective suppression of these oscillations in neural populations representing the attended stimulus provides a possible neurophysiological mechanism of attentional selection. Crucially, this also provides a mechanism of preparatory selective attention because this particular brain state may be instantiated already prior to the sensory information (see **chapters 3-7**). Upon sensory input, information processing in these populations will have an immediate advantage over populations in which alpha oscillations were either not suppressed or even amplified.

1.2.3 Beta oscillations reflect an inhibited state of the somatomotor network

Ongoing activity in the primary somatosensory (S1) and motor (M1) cortices (also termed *sensorimotor* or *somatomotor* cortices) are characterized by oscillations in both the alpha and the beta frequency bands. One particular hypothesis about oscillations in these distinct bands holds that alpha oscillations are predominantly involved in somatosensation, while beta oscillations are predominantly involved in action. This notion is primarily based on the observation that the localization of beta oscillations peaks more anterior than that of alpha oscillations (Salmelin and Hari, 1994). However, in contrast to such a strict separation, passive somatosensory input alters both alpha and beta oscillations, even when no movement is required (Cheyne et al., 2003, see also **chapters 2, 3, and 6**). As I will show in **chapters 2-8**, this also holds for preparatory somatosensory attention, also when movement is strictly controlled for.

Like alpha oscillations, beta oscillations in these cortices have also been associated with an inhibited state. For example, the amplitude of these oscillations is strongly increased by the GABA-agonist benzodiazepine (an inhibitory drug; Jensen et al., 2005). At a functional level, inducing beta oscillations by means of transcranial alternating current stimulation slows down movements (Pogosyan et al., 2009) and spontaneous fluctuations in beta amplitude predict somatosensory detection performance, with lower amplitudes

predicting better performance (Palva et al., 2005; Jones et al., 2010; see also **chapter 5**). Therefore, also the selective suppression of these oscillations provides a mechanism via which (preparatory) attention may improve touch perception (see **chapters 2-8**).

The somatomotor alpha and beta oscillations do differ in one critical aspect. Only the beta oscillations occur coherently throughout a widely distributed somatomotor network. This network comprises not only the primary somatomotor cortices (Brovelli et al., 2004; Witham and Baker, 2007), but also the premotor cortex (Ohara et al., 2001), basal ganglia (reviewed in Jenkinson and Brown, 2011), thalamus (Marsden et al., 2000; Paradiso et al., 2004), cerebellum (Aumann and Fetz, 2004; Soteropoulos and Baker, 2006), and even the spinal cord (as evidenced from oscillations in muscular activity; Kilner et al., 2004, Baker, 2007). This aspect is central to the results presented in **chapter 8**.

It is important to distinguish between beta oscillations in- and outside the somatomotor network. In particular, several studies have suggested that coherent beta oscillations across the frontal and parietal cortices are *positively* related to information processing (Liang et al., 2002; Bushman and Miller, 2007; Salazar et al., 2012). Throughout this thesis, when I refer to beta oscillations, I refer to the beta oscillations in the somatomotor network.

1.2.4 Gamma oscillations reflect information processing

In contrast to alpha and beta oscillations, gamma oscillations (ranging between 40 and 100 Hz, depending on the species, sensory modality, and stimulus parameters) have been associated *positively* with cortical information processing. For example, sensory stimuli induce, rather than attenuate, gamma oscillations in sensory cortices (e.g. Hoogenboom et al., 2006; see also **chapter 7**).

It has been proposed that gamma oscillations lead to more synchronized cortical output, thereby rendering cortical communication to downstream areas more effective (e.g. Engel et al., 2001; Fries et al., 2001; 2005; Jensen et al., 2007). Compared to alpha oscillations, gamma oscillations reflect rhythmic fluctuations at a much faster rate. Because of this, the periods of high neural excitability occur relatively frequent and, crucially, are strongly concentrated in time. When these oscillations occur synchronously across a population of neurons, this may ensure that these neurons will fire action potentials (given sufficient input) at roughly the same time. In turn, this will increase the efficacy of this population of neurons in driving a downstream population due to more efficient temporal summation in the downstream neurons (Engel et al., 2001; Fries et al., 2001; 2005; Jensen et al., 2007).

Analogous to the selective decrease of alpha and beta oscillations in neural populations representing the attended stimulus, the selective increase in gamma oscillations in these populations may serve to bias processing towards attended sensory information (Fries et al., 2001; Siegel et al., 2008; Gregoriou et al., 2009). However, as opposed to alpha and beta oscillations, gamma oscillations are most prevalent during, and not prior to, sensory input. This difference is central to the results presented in **chapter 7**.

1.3 Experimental approach and recordings

1.3.1 Experimental approach

I have investigated the neurophysiological mechanisms of preparatory attention in the somatosensory modality. Similar to the example provided in 1.1.1, I have investigated this during preparation for upcoming touch sensations at the left or right fingertips.

Expectations about the location and/or timing of upcoming tactile stimuli were manipulated by either a regular stimulation pattern (**chapter 2**) or by symbolic auditory or visual cues (**chapters 3-8**), as in the Posner cueing paradigm described in 1.1.1. I have used two types of tasks requiring either stimulus identification (“stimulus pattern A or B?”) or detection (“stimulus present or absent?”).

To investigate the neurophysiological mechanisms of preparatory attention, I have contrasted conditions in which participants expected stimuli on the fingertips of either their left or their right hand. In cortex, sensory information from the left/right hand is first received in the hemisphere contralateral to that hand, namely in the right/left primary somatosensory cortex (S1). Therefore, at the level of S1, preparatory modulations of neural activity in the left S1 (during right hand anticipation) can be distinguished from such preparatory modulations in the right S1 (during left hand anticipation), by virtue of their localization. Because the left and right S1 lie relatively far apart, this can even be distinguished for neural activity recorded outside of the brain, as with MEG.

Tactile stimuli were always presented to participants while their hands remained in position. This was done for strictly methodological purposes: only in this way could modulations of neural activity due to covert somatosensory attention be isolated from modulations due to overt motor behavior. To further rule out potential motor confounds, stimulus-response mappings were always independent of the attended side and muscular activity was always recorded as a control signal. Nevertheless, I will state up front that, in everyday situations, touch sensations on the fingertips are most often anticipated while reaching out for objects (such as a mug of coffee). Hence, it will be important for future investigations to establish whether this thesis’ key observations also hold in these situations.

1.3.2 Magnetoencephalography

I have recorded oscillatory neural activity using Magnetoencephalography (MEG). MEG is based on the following principle. Weak electrical currents in the brain produce small magnetic fields. Highly sensitive measuring devices called SQUIDS (superconducting quantum interference devices) are able to record these magnetic fields. For this, the SQUIDS are bathed in liquid helium cooling them to approximately minus 269 degrees Celsius. Only at this temperature can very weak magnetic fields, as those originating from the brain, be detected. In order for these fields to sum to a measurable field outside of the skull, they must also occur synchronously across a large group of aligned neurons. Because apical dendrites of pyramidal neurons have this feature of spatial alignment, it is thought that they are the main contributor to the MEG signal. Likewise, it is thought that MEG is mainly sensitive to

post-synaptic currents because only their fields sum to a measurable signal outside the brain (action potentials are too short-lived and produce fields that cancel each other).

The main benefit over the more common EEG is that the magnetic fields produced by the currents in the brain, unlike the currents themselves, pass the skull without distortion. Thus, while the electrical activity (as recorded with EEG) of a source is strongly smeared out across the skull (due to the skull's poor electric conductance), its magnetic counterpart (as recorded with MEG) is not. For this reason, MEG is said to have a higher spatial resolution.

For all chapters in this thesis, I have recorded neural activity using a CTF MEG system containing 275 axial gradiometers. These gradiometers are built into a helmet and, once the participant is raised in this helmet, they provide whole-brain coverage. A gradiometer contains two magnetometers (i.e. SQUIDS) that are aligned in series (one above the other, in case of an axial gradiometer). This constellation allows the recording of local differences in magnetic field (i.e. magnetic flux). Because a nearby source (i.e. the brain) produces a difference between the two magnetometers that is larger than the difference produced by a more distant source (e.g. a car driving by on a nearby road), this type of gradiometer is ideally suited to measure the weak but localized magnetic fields originating from the brain. To further mitigate external influences, the MEG was housed in a magnetically shielded room.

1.4 Overview, rationale, and relation to prior literature

Because the studies in this thesis build on prior literature, I will here outline my thesis in relation to this literature. I also highlight the main rationale for each study. I do this on the basis of six points.

1.4.1 Generalization

Prior to the studies presented here, it had been established that covert orienting of visual spatial attention involves a spatially specific preparatory modulation of alpha oscillations in visual cortex (e.g. Worden et al., 2000; Thut et al., 2006). In **chapters 2 and 3**, I investigated whether a similar type of modulation occurs in the somatosensory modality. To my knowledge, **chapter 2** is the first study that shows that orienting attention to an upcoming tactile stimulus also involves a spatially specific preparatory modulation of ongoing oscillations in the somatosensory modality. This suggests that this type of modulation is a generalizable phenomenon across the different sensory modalities. Moreover, this chapter reveals that this can already occur at the level of the *primary* sensory cortex. To arrive at this inference, I made use of the fact that, in contrast to the visual system, in the somatosensory system, the primary- and secondary sensory areas are well distinguishable in the MEG signal.

In **chapter 2**, I report the anticipatory modulation with regard to beta oscillations. In later chapters (**chapters 3-7**), I have employed more robust attention paradigms and I will show that this modulation occurs in the alpha band as well.



As pointed out in 1.1.1, preparatory attention can not only be oriented in space, but also in time. If the anticipatory modulation of ongoing oscillations reflects a general mechanism of preparatory orienting of attention, then this modulation should also be specific in time. **Chapter 3** reports precisely this. In addition, this chapter reveals that this modulation occurs in both the alpha and the beta band and that this modulation is constituted by a contralateral decrease rather than an ipsilateral increase.

1.4.2 Perceptual relevance

Together with previous literature, **chapters 2 and 3** demonstrate that preparatory orienting of attention involves an anticipatory modulation of ongoing alpha and beta oscillations in sensory cortex. This is a general phenomenon that occurs in multiple sensory modalities and is specific in both space and time. However, a critical aspect of this phenomenon has remained largely unaddressed: how relevant is this phenomenon for perception? This is a critical question because attention is only interesting by virtue of its ability to improve perception. Therefore, the extent to which any neural correlate of attention provides a satisfactory account of attention is directly related to the extent to which this correlate can explain the associated improvement in perception. In **chapters 4 and 5**, I address this with regard to the observed anticipatory suppression of alpha and beta oscillations.

In **chapter 4**, I show that the time course of this preparatory neural modulation may account for the time course of the attentional improvement in perceptual accuracy, but not reaction time. This shows that additional processes must be considered to account for the effect of attentional cues on reaction time. In **chapter 5**, I go one step further and quantify *how much* of the improvement in perception can be explained by the preparatory modulation of alpha and beta oscillations. To date, cognitive and systems neuroscience have been largely dominated by studies that demonstrate the *involvement* of neural phenomena in cognitive functions and behavior (on the basis statistical significance). An important second step is to quantify the effect size, once such involvement has been established. To illustrate the importance of quantifying effect sizes, consider the following fMRI study by Gonzalez-Castillo et al. (2012). In this study, participants performed a simple visuo-motor task. Now, rather than collecting a single dataset per participant, the authors collected 100 datasets per participant. Strikingly, after 100 datasets, 90 % of the voxels in the brain were significantly activated (i.e. involved) in this simple task. This demonstrates that whether or not a given region (or phenomenon) is involved in a given cognitive function (or behavioral outcome), may depend more on the amount of collected observations than on the degree of its involvement. In **chapter 5**, I therefore aimed at quantifying the effect size of the central phenomenon in this thesis. This revealed that the anticipatory suppression of alpha and beta oscillations can account for up to 30 % of the attentional improvement in perception.

1.4.3 Neural consequences

Chapters 2-5 have revealed that the anticipatory modulation of alpha and beta oscillations

in the contralateral primary somatosensory cortex provides a mechanism that accounts for part of the perceptual improvement in perception. Crucially, this improvement can only occur through altered processing of the anticipated sensory information. A relevant question thus becomes how preparatory attention alters the neural processing of the anticipated sensory information. A classical observation is that preparatory attention amplifies the amplitude of evoked potentials to sensory stimuli (e.g. Mangun and Hillyard, 1991; Miniussi et al., 1999). These evoked potentials reflect early processing stages in sensory cortices contralateral to sensory input. In demanding perceptual tasks, it is likely that neural processes beyond these early stages (such as the readout of sensory information from short-term memory) play a key role in perception as well. However, because the precise timing of these processes may vary from trial to trial, these processes may not show up in evoked (i.e. time-domain averaged) activity. In contrast, such processes might show up in modulations of induced neural activity (i.e. non-phase-locked oscillations; Tallon-Baudry and Bertrand, 1999). In **chapter 6**, I focused on such modulations and report that preparatory attention increases the stimulus-induced response (suppression of beta oscillations) originating from the ipsilateral primary somatosensory cortex. This occurs in the period in which the tactile memory trace is analyzed (300-600 ms post-target) and is correlated with the attentional improvement in tactile perception. If this response reflects stimulus processing, then this implies that preparatory attention may not only boost the processing of sensory information in the contralateral sensory cortex (as previously observed), but also increase the degree to which stimulus processing is distributed across the hemispheres.

1.4.4 Context dependence

In addition to the attentional suppression of alpha and beta oscillations, the attentional amplification of gamma oscillations has also been established as a key signature of attention. However, careful inspection of the literature reveals an important distinction. The attentional suppression of alpha oscillations in the visual modality (Worden et al., 2000; Thut et al., 2006) and alpha and beta oscillations in the somatosensory modality (Jones et al., 2010; see also **chapters 2-6**) is typically reported in studies that investigate attention during anticipation, that is, in the interval between a symbolic cue and an anticipated target. In contrast, the attentional amplification of gamma oscillations is almost exclusively reported in studies in which attention is directed to a sustained stimulus (i.e. during stimulus processing; Fries et al., 2008; Siegel et al., 2008; Gregoriou et al., 2009). Thus, while both signatures have been well-established, an important issue has remained obscure: namely, whether these different signatures co-occur or, alternatively, are unique to the specific sensory context in which attention is investigated (i.e. before or during the stimulus). In **chapter 7**, I directly compare the spectral signatures of somatosensory attention during anticipation and stimulus processing. I will show that the attentional modulation of alpha and beta oscillations is largely restricted to the preparatory interval and is replaced by the attentional modulation of gamma oscillations during stimulus processing.



1.4.5 Network perspective

As stated previously, beta oscillations do not only occur in the primary somatomotor cortices, but instead occur coherently throughout a widely distributed somatomotor network. In accordance with the anatomy of this network, these oscillations have traditionally been studied almost exclusively with regard to motor function. However, **chapters 2-7** have shown that beta oscillations are also modulated by strictly somatosensory demands and moreover predict somatosensory perception (**chapters 5 and 6**). In **chapter 8**, I address whether these beta oscillations that are relevant for tactile perception are actually part of the coherent somatomotor network that has traditionally been studied only in the context of motor tasks. Based on the inter-areal coupling of these oscillations (e.g. Baker et al., 1997; Brovelli et al., 2004), I hypothesized that, if this is the case, then beta modulations associated with somatosensory demands (in anticipation and during the processing of tactile information) should also be observed in motor parts of this network. In accordance with this hypothesis, **chapter 8** shows that the somatosensory driven modulation of beta oscillations does not only occur in cortex (**chapters 2-7**), but is even visible in the patterns of muscular activity. Critically, this occurs independent of motor demands.

1.4.6 Interpretation

In **chapters 2-8**, the main neural signatures of interest all involve modulations in the observed amplitude of neural oscillations. In fact, over the last two decades, this type of modulation has emerged as one of the core indices of neural computations and cognition (reviewed in Hari and Salmelin, 1997; Kahana et al., 2001; Jensen et al., 2007). To contribute to a mechanistic understanding of cognition (i.e. preparatory attention), it is thus essential to understand how such observed amplitude modulations come about.

In **chapter 9**, I elaborate on three alternative scenarios that may produce amplitude modulations, as observed in a recording site at some distance from the sources (see Fig. 9.1 in **chapter 9**). In this chapter, I also take a first step towards disentangling these alternatives by evaluating diversity in the between-channel phase relations for conditions that differ markedly in amplitude. I will show that, at least for neural populations that can be distinguished by MEG, amplitude modulations are not paired by changes in the diversity of the phase relations *between* these populations. Rather, such modulations co-exist in multiple underlying neural structures, while these maintain their average phase relations. This narrows down the possible interpretations and functional consequences of observed amplitude modulations. Nevertheless, such modulations may still have a number of different causes, as described in **chapter 9**. Thus, while tentative, this chapter provides a first step towards understanding the physiological principles that govern the phenomenon that will be central to this thesis: the preparatory *amplitude suppression* of alpha and beta oscillations recorded above the contralateral primary somatosensory cortex.

The following eight chapters (**chapters 2-9**) present each of these studies in detail. I provide a general discussion in **chapter 10**.

Tactile expectation modulates pre-stimulus beta-band oscillations in human sensorimotor cortex

Adapted from van Ede F, Jensen O, Maris E (2010) *Tactile expectation modulates pre-stimulus β -band oscillations in human sensorimotor cortex*. Neuroimage 51:867-876.



2

Abstract

Neural oscillations are postulated to play a fundamental role in top-down processes of expectation. We used magnetoencephalography (MEG) to investigate whether expectation of a tactile event involves a pre-stimulus modulation of neural oscillations in human somatosensory cortex. In a bimodal attention paradigm, participants were presented with a predictable spatio-temporal pattern of lateralized tactile stimulations and simultaneously occurring non-lateralized auditory stimuli. Before the onset of a series of such combined audio-tactile stimuli, a cue was presented that indicated the sensory stream that had to be attended. By investigating lateralized patterns of oscillatory activity, we were able to study both attentive (when the tactile stream was attended) and non-attentive (when the auditory stream was attended) tactile expectation. For both attention conditions, we observed a lateralized modulation of the amplitude of beta band oscillations prior to a predictable – and accordingly lateralized – tactile stimulus. As such, we show that the anticipatory modulation of ongoing oscillatory activity is not restricted to attended sensory events. Attention did enlarge the size of this modulation. We argue that this modulation constitutes a suppression of beta oscillations that originate at least partly from the primary somatosensory cortex (S1) contralateral to the expected stimulation. We discuss our results in the light of the hypothesis that ongoing beta oscillations over sensorimotor cortex reflect a brain state in which neural processing efficacy is low. Pre-stimulus suppression of these oscillations then prepares the system for future processing. This shows that perception is an active process that starts even prior to sensation.

2.1 Introduction

Perception is not mere registration of sensory input. Rather, it is an active process in which top-down mechanisms play important roles. Expectation constitutes one such top-down mechanism. Specifically, expectations about upcoming sensory events can be utilized to prepare sensory cortices by instantiating a neural context that allows for enhanced processing of the forthcoming event (Engel et al., 2001). Neural oscillations might define such a context, as they have been hypothesized to be involved in gating neural activity (Pfurtscheller and Lopes da Silva, 1999; Engel et al., 2001; Fries et al., 2001; 2005; Salinas and Sejnowski, 2001). In particular, because neural oscillations reflect rhythmic shifts of excitability they influence spike timing and synchronicity (Lampl and Yarom, 1993; Volgushev et al., 1998). Accordingly, pre-stimulus modulations of oscillatory activity may affect cortical information transfer of initial afferent input and is therefore considered a mechanism by which expectation can guide perception. Here we investigated whether expectation of a tactile event involves a pre-stimulus modulation of neural oscillations in human somatosensory cortex.

Because neural oscillations can be sustained in the absence of identifiable sensory input or motor output, they are likely to be involved in the neurophysiological mechanisms behind top-down influences such as expectation. These sustained neural oscillations can be identified because they are region and frequency specific (Hari and Salmelin, 1997). For instance, over posterior sites of the brain, alpha oscillations (8-12 Hz) are observed. This rhythm is affected by information processing, because its amplitude is modulated by visual input, as was already shown by Hans Berger (1929). Importantly, the alpha rhythm is also affected by top-down influences, as is demonstrated by the fact that its amplitude is modulated in anticipation of a visual stimulus (Foxe et al., 1998; Worden et al., 2000; Sauseng et al., 2005; Kelly et al., 2006; Thut et al., 2006; Rihs et al., 2007; Wyart and Tallon-Baudry, 2008). Similarly, over sensorimotor cortex, alpha (8-12 Hz) and beta (15-35 Hz) rhythms are observed, whose amplitudes are reduced over the contralateral hemisphere not only during, but also prior to voluntary movement (Jasper and Penfield, 1949; Nagamine et al., 1996; Pfurtscheller and Lopes da Silva, 1999; Taniguchi et al., 2000; Zhang et al., 2008a). It has further been shown that the sensorimotor alpha rhythm is reduced in anticipation of nociceptive stimuli (Babiloni et al., 2003). The present paper provides evidence for another type of pre-stimulus modulation of an ongoing oscillation. Specifically, we show that the amplitude of beta oscillations over sensorimotor cortex is modulated by expectation of a tactile stimulus.

Because sensory afferents enter the cortex in the primary sensory cortices, this is the first neocortical terminal in which information can be gated. In studies measuring the BOLD-signal, expectation-related increases in regional blood flow have been observed in V1 (Kastner et al., 1999; Ress et al., 2000; McMains et al., 2007), S1 (Carlsson et al., 2000), early auditory cortices (Voisin et al., 2006) and even the LGN (O'Connor et al., 2002). Precise localizations on the basis of extra-cranial recordings of human electromagnetic

brain activity are generally more problematic. Consequently, studies that implicate primary sensory cortices in anticipatory modulations of neural oscillations are rare. The human somatosensory system provides a unique system for investigating the role of primary sensory cortices in relation to expectation-induced modulation of neural activity. This is because, in the somatosensory system, only the primary sensory cortex (S1) receives (thalamic) input unilaterally (Burton, 1976; Hari et al., 1993). We made use of this fact by having participants expect either a left or right hand stimulation. Importantly, left and right hand stimulations are processed by the same S2 cortices, but different S1 cortices. By contrasting expected events with a different lateralization we could thus deduce the neural origin without the need for assumption-dependent source localization methods. As such, the present paper provides evidence for the involvement of S1 in oscillatory dynamics during expectation.

Empirically, effects of expectation have often been conflated with those of attention (Summerfield and Egnér, 2009). For example, in the Posner cueing paradigm (a paradigm used in many of the abovementioned studies) expectation constitutes the primary source for the endogenously directed focus of attention. Anticipatory processes of expectation are, however, not necessarily confined to attended events. In the present study, we therefore examined whether the expectation-induced modulation of pre-stimulus oscillatory activity was restricted to task-relevant stimuli. For this, expectation was manipulated by a predictable spatio-temporal pattern of tactile stimulations. Because stimulus patterns are predictable regardless of their task-relevance, they allow for a dissociation between effects of attentive and non-attentive expectation. Interestingly, we provide evidence that the pre-stimulus modulation of beta oscillations is not restricted to task-relevant and therefore attended events.

2.2 Materials and Methods

Participants

A total of 22 healthy subjects voluntarily participated in the experiment (12 male, mean age: 24y, range: 20-33y). Four participants were excluded from the analysis due to excessive artifacts. Two participants returned for a follow-up session, about two months after their first session. All participants provided written consent and were paid in accordance with guidelines of the local ethics committee (CMO Committee on Research Involving Humans subjects, region Arnhem-Nijmegen, the Netherlands). The experiment was in compliance with national legislation as well as the code of ethical principles (declaration of Helsinki).

Apparatus

Both tactile and auditory stimuli were presented. For tactile stimulation, piezoelectric Braille cells (Metec, Stuttgart, Germany) were used. A single Braille cell consists of eight pins, aligned in two series of four, that can be raised and lowered. Five such cells, together with a response button, were built in to a graspable device (see Fig. 2.1A), one for each hand.

Tactile stimuli were produced by transiently raising the pins of all Braille cells overlying the five fingertips of a single hand. The pins were lowered into the cells again 20 ms after being raised, rendering the subjective experience of a tactile stimulus as a tap on the fingers. Auditory stimuli consisted of brief (80 ms) noise bursts that were presented binaurally via MEG compatible air-tubes. The complete experiment was programmed and run using the software package Presentation (<http://nbs.neurobs.com>).

MEG recording

The MEG system (CTF MEG TM Systems Inc., Port Coquitlam, Canada) contained 275 axial gradiometers and was housed in a magnetically shielded room. Additionally, a bipolar surface-ECG was recorded using two Ag/AgCl electrodes. All data were low-pass filtered by an analogue filter (300 Hz cutoff), digitized at 1200 Hz, and stored for offline analysis.

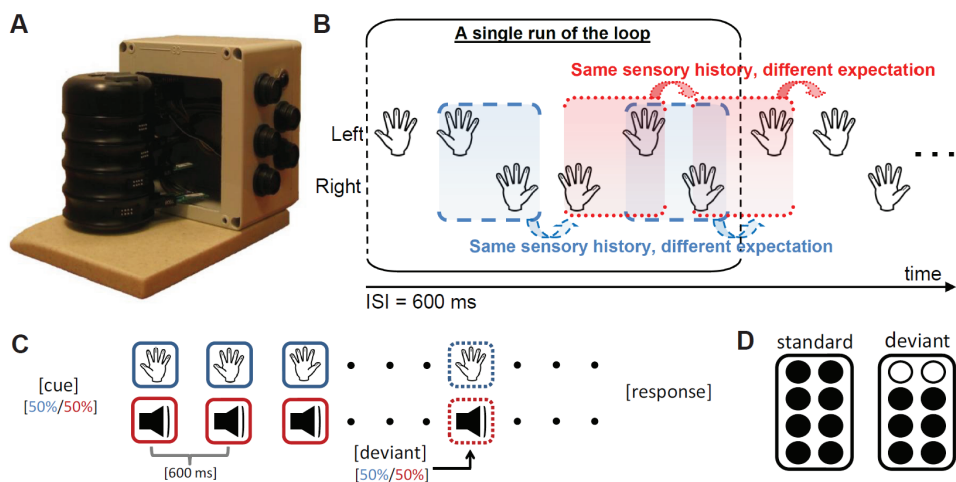


Figure 2.1. Stimulation apparatus, the spatio-temporal pattern used to manipulate tactile expectation, the trial structure and the tactile deviants. (A) Stimulation apparatus. Built-in are five Braille cells (four on the side, one on the top) and a response button (also on the top). Individual Braille cell positions are adjustable. When grasped, all five fingertips overlie a Braille cell. (B) Spatio-temporal pattern of tactile stimulation. First the left hand is stimulated twice, then the right hand is stimulated twice, then the left hand is stimulated once and finally the right hand is stimulated once. This series of six stimulations is then looped. Note the presence of identical tactile stimulation segments (i.e. histories) with different forthcoming predictable tactile events. That is: after the sensory history Left-Right (LR, blue boxes) once the right hand and once the left hand is stimulated. Likewise for the sensory history Right-Left (RL, red boxes). It is here, prior to these predictable events, where windows of analysis are situated. (C) Schematic representation of a single trial. At the beginning of each trial a cue is presented that indicates the sensory stream in which a deviant stimulus has to be detected. Cues to the auditory and tactile stream have an equal probability of occurrence. A deviant stimulus can occur in either modality (hence can be either a target or a distracter), comes between the fifth and forty-fifth stimulus position and replaces a standard. After a deviant, the trial is continued for up to four to seven stimulations, allowing the subject to respond. Note that each depicted tactile event denotes the stimulations of a single hand. Six such events make up the pattern depicted in B. (D) Schematic representation of a standard and a deviant tactile stimulus. While a standard tactile stimulation consist of a transient raise of all eight pins of each of the five Braille cells stimulating a single hand, a deviant is characterized by only six pins being transiently raised for each of those cells. In the auditory stream, a deviant was of lower dB than a standard.

No EOG data were recorded because subjects were instructed to close their eyes during the experiment.

Experimental design & paradigm

The factors expectation and attention were experimentally manipulated in a crossed two-factorial design. Expectation was manipulated by presenting a recurrent, and thus predictable, spatio-temporal pattern of tactile stimulations (see Fig. 2.1B). In this pattern, participants could at any time predict whether the right or the left hand would be stimulated and when this would happen. The prediction of the forthcoming stimulus within such a pattern is based on its tactile history. To control for the sensory effects of the tactile history, a pattern was used that contains left and right hand stimulations that are each preceded by identical segments of tactile stimulations. This is shown in Figure 2.1B by the blue (red) boxes, which contain the same segment of tactile stimulations, but once followed by a stimulation of the left and once by a stimulation of the right hand. The presence of identical tactile stimulation histories (boxes of the same color), with different forthcoming and predictable events thus allows for an investigation of expectation while controlling for tactile history.

On top of the stream of tactile stimulations, we presented a binaural auditory stream consisting of brief noise-bursts (see Fig. 2.1C). Sensory events occurred simultaneously in the tactile and the auditory modality. Attention was manipulated by instructing participants to attend to either modality. Specifically, before the onset of a series of simultaneously occurring tactile and auditory stimuli, a cue was presented signaling the sensory modality in which deviant stimuli had to be detected and responded to by means of a button-press. It must be noted that the auditory stream was only included for the purpose of experimental control. Our data analyses (see further) focused on lateralized expectation-related activity, and since only tactile stimulations occurred lateralized, only tactile expectation was investigated. Thus, tactile expectation was investigated once when the tactile stream was attended and once when it was not.

Attention was manipulated by instructing subjects to detect deviant stimulations in one of the two sensory modalities. In both modalities, deviant stimulations were defined by their strength. An auditory deviant was characterized by a lower amplitude (individually adjusted; on average 4.1 dB, SD = 1.1). A tactile deviant was characterized by the fact that six instead of eight pins were raised in each of the Braille cells stimulating a single hand (see Fig. 2.1D), subjectively appearing as a tap on the fingers of lower intensity.

Figure 2.1C schematically depicts the structure of a trial. A single trial consisted of a cue followed by a sequence of up to 50 combined audio-tactile stimulations with an interval of 600 ms between the onsets of the combined audio-tactile stimulation. The cue was a one second repetitive stimulus presented in either the tactile or the auditory modality. With regard to the tactile stream, the pattern of tactile stimulations would start randomly at one of the six stimulations of which the pattern consists. Each trial contained a single deviant that could either be a target (presented in the cued modality) or a distracter (presented in the non-



cued modality). The uncued stream always had to be ignored. As a consequence, the cued stream was maximally attended. As a drawback, we were not able to quantify the strength of attention orienting on the basis of detection performance (as no behavioral responses were given to unattended stimuli). The deviant stimulus was randomly presented between the fifth and forty-fifth stimulus-position and replaced the standard. The trial ended either after the participant had pressed the response button, or within four to seven stimulations after a deviant (giving enough time to respond in case a target was detected). Thereafter, a new cue was presented starting the next trial. Each cue was chosen randomly resulting in both attention conditions being randomly intermixed. After nine trials, there was a rest period that the participant could terminate by pressing the response button. In total, the experiment consisted of seven such blocks containing nine trials and lasted about 1 hour.

Experimental procedure

Before data acquisition, participants were familiarized with the pattern of tactile stimulations as well as the deviant stimuli. Thereafter, ECG electrodes were placed and the participant was positioned into the MEG that was put into supine position. After instruction of the task, lights were turned off and the recording and experimental session started. Afterwards, participants were debriefed on the aims of the experiment.

Data analysis

Data were analyzed using Matlab (Mathworks, <http://www.mathworks.com>). We made extensive use of FieldTrip (Oostenveld et al., 2011), an open source Matlab toolbox developed at the Donders Institute for Brain, Cognition and Behaviour (Nijmegen, The Netherlands).

Both pre- and post-stimulus activity was analyzed. Data of pre- and post-stimulus segments were cut out and processed separately to avoid bleeding in of post-stimulus activity into pre-stimulus segments (e.g. as a result of digital filtering). For the analysis of the post-stimulus activity, we used all left and all right hand stimulations, irrespective of the experimental condition. Around 1000 trials were obtained for each hand. For the analysis of pre-stimulus activity, only a sub-set of pre-stimulus segments were of interest, namely those with a different expectation while controlling for tactile history. This resulted in four distinct pre-stimulus segments ([1] LR->R, [2] LR->L, [3] RL->R and [4] RL->L, see Fig. 2.1B) per attention condition. The segments following the deviants were not analyzed. Around 80 trials were obtained for each of the four segments.

To clean up the data, we first removed ECG-components. An automatic routine that was implemented in FieldTrip detected QRS peaks in the ECG channel. Segments from 200 ms before until 400 ms after the QRS peak were selected and an independent component analysis was performed on the MEG data in this window. Components whose virtual time-courses were highly coherent with the ECG were then removed from the data. Next, segments were visually inspected and those contaminated by artifacts were removed. We also removed channels that were excessively noisy. Line noise was removed by calculating

the Discrete Fourier Transform (DFT) of the epochs at 50, 100 and 150 Hz and then subtracting the sine waves that were constructed from the DFT-estimated amplitudes and phases. Finally, we removed the DC-component of the signals (which includes the offset of the SQUIDS) by subtracting the mean of each segment.

We calculated power spectra for all MEG channels. This produces two-dimensional arrays with a spatial (the MEG channels) and a spectral (the frequencies) dimension. However, these spatio-spectral arrays were reduced to a single value that was subsequently contrasted between the two experimental conditions: left and right hand expectation. Specifically, participant-specific post-stimulus induced modulations of oscillatory activity were used to zoom in on pre-stimulus oscillatory activity. The rationale behind this approach is double: (1) we want to increase sensitivity by reducing the influence of inter-individual variability in the spatial and spectral domain, and (2) we want to reduce the number of statistical comparisons in subsequent analysis over subjects. The steps involved in this reduction are the following:

1. Determination of every individual's temporo-spectral locus of the oscillatory activity that is modulated by tactile stimulation
2. Determination of every individual's spatial locus of the modulated oscillatory activity, which involves a selection of channels above left and right S1
3. Estimation of pre-stimulus power in the selected frequency band and visualization of effects of expectation
4. Calculation of a pre-stimulus lateralization index of the power in the specified frequency band by contrasting channels above left and right S1

In the following, we elaborate on each of the above steps. We describe these steps for oscillatory activity in the beta band. However, the exact same analysis was done for alpha and gamma band activity. Several steps in this analysis are graphically depicted in Supplementary Figure 2.1.

Step 1. For both left and right hand stimulation segments, trials were baseline corrected (with a baseline-window of 50 milliseconds pre-stimulus) and averaged. Topographies of these averages showed a clear dipolar pattern over the contralateral hemisphere between 40 and 60 ms post-stimulus, which will be denoted as the M50 (see Supplementary Fig. 2.1A). To extract the one-dimensional topography of this dipolar pattern, we applied singular value decomposition (SVD) to the spatiotemporal array of evoked responses between 40 and 60 ms. The first singular vector was then taken as the topography of the M50 source. We subsequently projected the single-trial data on this singular vector and in this way obtained an S1 virtual channel. We did this separately for left and right hand stimulations, and thus obtained two S1 virtual channels, one for the right and one for the left hemisphere, respectively. Oscillatory power of both virtual S1 channels was then estimated with a short-



time Fourier analysis (5-100 Hz), involving 200 ms sliding time-windows, 5 ms steps, and a Hanning taper. This resulted in a time-frequency representation (TFR) of the data. Per virtual channel we then contrasted the oscillatory power for contralateral and ipsilateral stimulations and normalized this difference (contra minus ipsi) by dividing it by the summed power over both conditions (contra plus ipsi). This was done per time-frequency sample. Subsequently, we averaged the normalized TFRs of both virtual channels. For every participant, a time-frequency window was selected that captured the contralateral suppression of the power in the beta band. This was done on the basis of visual inspection of the TFR (see Supplementary Fig. 2.1B). On average, beta ranged from 16 to 33 Hz and was suppressed between 100 and 350 ms post-stimulus.

Step 2. Power in the participant-specific beta-range was estimated for all MEG channels over the participant-specific time-window. We estimated the power using the multitaper method (Percival and Walden, 1993). Herein, squared Fourier coefficients of differently tapered data (all Slepian tapers) are averaged to estimate the power in a frequency interval. On average, 5 tapers were used. Besides these power estimates for the original axial gradiometer data, we also calculated power estimates for synthetic planar gradiometer data. The synthetic gradiometer data for a given channel consists of two components, of which one measures the spatial derivative along the anterior-posterior axis of the MEG helmet, and the other along the left-right axis. These synthetic planar gradiometer data for a given channel were calculated as linear combinations of the axial gradiometer data for this channel plus all neighboring channels. Every synthetic planar gradiometer pair defines a plane, and we linearly combined (rotated) the two components of the synthetic planar gradiometer using coefficients that maximized the power of this linear combination. In this way, the two-component synthetic planar gradiometer data were mapped onto a single-component measure of oscillatory power. For every channel, we then calculated an independent samples t-statistic in which we contrasted the trials with a right and a left hand stimulation (right minus left). Channels to be used for pre-stimulus analysis were selected on the basis of these results. The selection was based on the following criteria: (1) channels must have a t-value higher (lower) than 1.96 (-1.96) and (2) they must be within 8 cm from the right (left) virtual S1 channel (see Supplementary Fig. 2.1F for an example of selected channels). The position of this virtual channel was calculated as a linear combination of all channel coordinates, with the elements of the defining singular vector (see Step 1) being the coefficients of this linear combination.

Step 3. After identifying the participant's spatial and spectral locus of the post-stimulus beta modulation, pre-stimulus oscillatory activity in the selected participant-specific frequency interval was analyzed. The pre-stimulus window was chosen to be the interval [-350, 0] ms, with 0 ms being stimulus onset. Two separate analyses were then performed, one focusing on the visualization of the pre-stimulus expectation and the post-stimulus stimulation effect (Step 3), and one focusing on the quantification of the pre-stimulus expectation effect as

a single number (Step 4). For visualization, we calculated channel-specific quantifications of the expectation and the stimulation effect in the following way. For each channel, mean power during left hand expectation/stimulation was subtracted from mean power during right hand expectation/stimulation. This was then divided by the summed mean power in the two experimental conditions, resulting in a normalized topography of the beta modulation. Normalized topographies were then averaged across subjects, yielding a grand average topography. These calculations were performed on the power estimates obtained from the synthetic planar gradiometer data. For the participant showing the strongest effect, we additionally performed the same calculations on the power estimates obtained from the axial gradiometer data. For the same participant, we also performed a time-resolved frequency analysis on the virtual S1 channels for the pre-stimulus segment. For this, we used the short-time Fourier analysis described in Step 1.

Step 4. In this step, we combine the pre-stimulus oscillatory activity that is observed over the selected channels (see Step 2) and quantify the extent to which it is modulated by expectation. For every trial, we estimated the power in the selected frequency interval and averaged it over the selected channels above left and right S1. The average power over right S1 was then subtracted from the average power over left S1, and we normalized this difference by the trial-specific summed power over both channel subsets:

$$\text{Lateralization index} = \frac{\text{mean power}(\text{left channels}) - \text{mean power}(\text{right channels})}{\text{mean power}(\text{left channels}) + \text{mean power}(\text{right channels})}$$

This is a lateralization index, similar to Thut et al. (2006) that is positive when the channels above left S1 have a higher power, and that is negative when the channels above right S1 have a higher power. Because selection of the frequency range and the channels was done on the basis of post-stimulus activity, our lateralization index is an unbiased measure. And because this selection is participant-specific, it is likely to be sensitive to a pre-stimulus modulation of neural activity in the same areas that produce this post-stimulus activity. This lateralization index was averaged separately over the left and the right hand expectation trials. If expectation of a lateralized tactile stimulus results in a lateralization of pre-stimulus oscillatory activity, then expectation of left and right hand tactile stimuli should produce different values of our index.

Statistical evaluation

In all statistical evaluations, lateralized events were contrasted. That is, for the pre-stimulus period, left and right hand expectation were compared, and for the post-stimulus period, left and right hand stimulation were compared. Since binaural auditory events were identical during left and right hand stimulation, our statistical comparisons will not be affected by auditory-related activity.

For the selection of the participant-specific channel subsets (Step 2), independent samples t-tests were performed *within* participants (treating the trials as statistical

replications). All statistical evaluations of the expectation effect were performed *across* participants (treating the participants as statistical replications). The dependent variable for this statistical evaluation was the trial-averaged lateralization index, calculated separately for the left and the right hand expectations. The expectation effect was statistically tested by means of a paired-samples t-test. This statistical test was performed for both attention conditions (tactile and auditory) separately. Additionally, a repeated-measures ANOVA was performed on the factors expectation (left and right) and attention (tactile and auditory).

Follow-up session

Two participants, whose MEG data showed the strongest expectation effect, returned for a follow-up session in which also EMG activity was recorded. In all trials, these participants were cued to attend to the tactile modality. Two new blocks were added in which participants were asked to contract their left and right hand either strongly or weakly. We indicated which hand the participants had to contract by means of a transient tactile stimulation of their thumb. Bipolar surface-EMG was measured from both arms using two Ag/AgCl electrodes. The electrodes were placed over the flexors of the forearm, with one electrode placed near the wrist and the other near the elbow in order to map digit a-specific contractions. For analysis, EMG traces were high-pass filtered (40 Hz cutoff) and rectified. For every EMG channel, we calculated the difference between two experimental conditions, each corresponding to one of the two hands. In the contraction blocks, every experimental condition corresponds to one contracted hand, and in the tactile stimulation block, it corresponds to one hand that was expected to be stimulated. We normalized every difference by dividing it by the summed power over the conditions. Finally, we averaged the normalized difference time-courses of both EMG-channels in the following way: we averaged the difference [left-right] contraction/stimulation for the left hand EMG with the difference [right-left] contraction/stimulation for the right hand EMG. Thus, we averaged the differences [ipsi-contra] of the two EMG channels.

2.3 Results

Behavioral performance

Average detection rates, expressed as the percentage of targets detected, were 69.7 (SD = 27.7) for tactile targets and 75.1 (SD = 24.3) for auditory targets. Few participants detected all targets in either sensory stream. All participants reported the task to be difficult and attention-demanding, consistent with the detection rate.

Pre-stimulus beta activity reflects tactile expectation (a representative participant)

Figure 2.2 shows our main result for this single participant: an expectation-induced pre-stimulus modulation of oscillatory activity in the beta band. In Figure 2.2A, a representation of the time-resolved power difference between contralateral and ipsilateral virtual

S1 channels is shown. Following a tactile stimulus (right TFR), there is a contralateral suppression of beta power, as indicated by the white box. This is in accordance with previous studies that applied tactile stimulation to the human hand region (Bauer et al., 2006; Cheyne et al., 2003; Gaetz and Cheyne, 2006). Interestingly, in anticipation of a lateralized tactile stimulus (left TFR), a similar modulation of beta power is observed. Starting from around 300 ms prior to the expected stimulation, lower power in the beta band is observed over contralateral relative to ipsilateral sensorimotor cortex. This effect increases over time and is therefore consistent with a role in sensory preparation.

We selected the spectral-temporal window in which beta power was suppressed after a tactile stimulus (as indicated by the white box in Fig. 2.2A) and estimated power within this window for all channels. We then contrasted conditions of right and left hand stimulation (right minus left). Figure 2.2C shows the topography of this contrast. Evidently, over

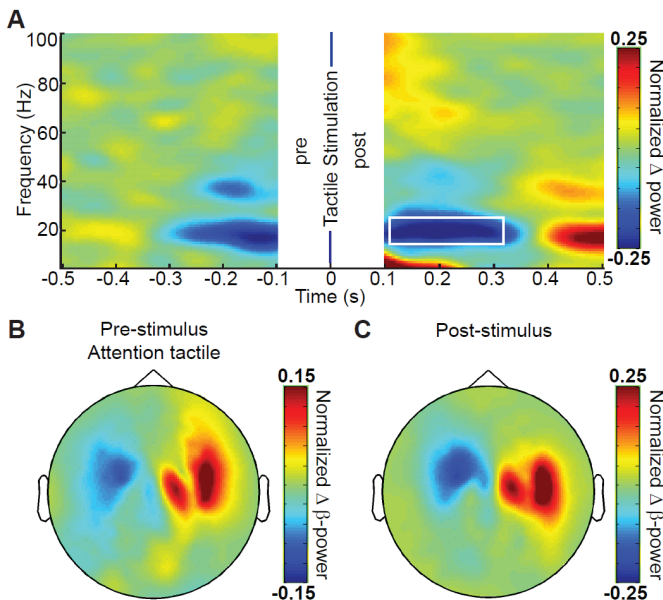


Figure 2.2. Expectation and stimulation induced modulations of beta (representative participant). (A) Pre- and post-stimulus representations of the time-resolved power difference between contralateral and ipsilateral virtual S1 channels (contralateral minus ipsilateral). The gap in the middle is due to the sliding-window being 200 ms for both pre- and post-stimulus data segments that were cut-out separately. The white box in the post-stimulus TFR represents the selected beta band for this participant. (B) Topography of the beta modulation during attentive-expectation of a lateralized tactile stimulus. Beta power was estimated over a window 350 ms to stimulus onset. Color coded is the normalized difference in beta power between conditions of right and left hand expectation (i.e. [right minus left] / [right plus left]). The modulation topography was calculated on the axial gradiometer data. (C) Topography of the beta modulation following a lateralized tactile stimulus. Same conventions as for B, except beta was estimated for the post-stimulus window indicated in the white box in A.

left sensorimotor cortex beta power is lower after stimulation of the right hand (negative values), whereas over right sensorimotor cortex beta power is lower after stimulation of left hand (positive values). Figure 2.2B shows a similar contrast topography that was now calculated for the selected beta-range over a window of 350 ms to stimulus onset, thus during tactile expectation. Importantly, the topography of the pre-stimulus modulation of beta power strongly resembles the post-stimulus modulation. Thus, whereas Figure 2.2A shows spectral correspondence between the stimulation- and expectation-induced modulation of beta,

Figure 2.2B and 2.2C show that the pre-stimulus effect resembles the post-stimulus effect also in terms of spatial topography. Strikingly, both modulation topographies show dipolar patterns¹ that are similar between pre- and post-stimulus modulations of beta. This is suggestive of a common neural generator of the beta oscillation that is suppressed not only by stimulation but also by expectation. These topographies furthermore resembled the dipolar topographies of the M50 components of the ERF (see Supplementary Fig. 2.1A). Note that pre- and post-stimulus data segments were cut-out and processed separately, excluding the possibility of post-stimulus effects bleeding into pre-stimulus windows.

Grand average beta modulation during tactile expectation

In Figure 2.3, we show the grand average topographies of the stimulation- and the expectation-induced beta modulation. Beta power was calculated on the synthetic planar gradient data (see Materials and Methods), which is robust against inter-individual differences in source orientation because its greatest activity lies directly above the source (Hämäläinen et al., 1993). Figure 2.3A shows the stimulus-induced modulation of beta power. This serves as a reference for evaluating the topographies of the two expectation-induced modulations of pre-stimulus beta power. Figure 2.3B shows the topography of the expectation-induced modulation of pre-stimulus beta power that is observed during states of attentive expectation (i.e. when the tactile stream is behaviorally relevant). It is very clear that this topography is highly similar to the

topography of the stimulus-induced modulation of beta power. Figure 2.3C shows the topography of the expectation-induced modulation of pre-stimulus beta power that is observed during states of non-attentive expectation (i.e. when the non-lateralized auditory stream is behaviorally relevant). Over left sensorimotor

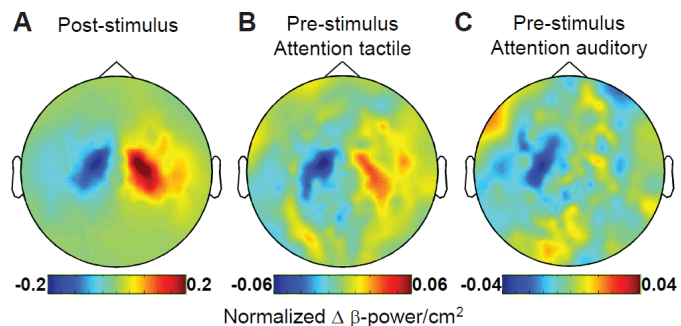


Figure 2.3. Grand average beta modulation topographies of post- and both pre-stimulus attention conditions. (A) Topography of the post-stimulus induced beta modulation. Color coded is the normalized difference in beta power between left and right hand stimulation (i.e. [right minus left] / [right plus left]). Depicted are grand average values of this contrast. Note that these differences were calculated on the synthetic planar gradient data. (B) Topography of the modulation of pre-stimulus beta power during states of attentive expectation (i.e. when the tactile stream is behaviorally relevant). Same conventions as for A (i.e. right minus left). (C) Topography of the modulation of pre-stimulus beta power during states of non-attentive expectation (i.e. when the non-lateralized auditory stream is behaviorally relevant). Same conventions as for A.

1. The two areas within both the positive and the negative clusters of the topographies suggest the presence of two dipolar sources. These sources both produce a magnetic out- and influx, oscillating at beta frequency. Importantly, in a power representation, out- and influx have the same sign. The topography would be comparable to that of the M50 if one would square the M50 signal and subtract conditions of right and left hand stimulation (see e.g., Bauer et al., 2006 [Fig. 6]).

cortex, we again observe an expectation-induced modulation of pre-stimulus beta power, i.e. beta-power over left sensorimotor cortex differentiates between conditions of left and right hand expectation. This modulation is, however, not clear over the right sensorimotor cortex, at least not in the grand average topography.

Because participants take different positions in the MEG-helmet and have a different head-shape and cortical folding, topographies calculated over subjects (as in Fig. 2.3) are not optimally sensitive. We therefore devised a measure that is robust against inter-individual variability in both the spectral and the spatial domain, the *participant-specific lateralization index* (see Materials and Methods, and Supplementary Fig. 2.1G). Figure 2.4 shows the mean lateralization indices for the four conditions of our experimental design. The negative values in all conditions indicate a general hemispheric asymmetry in beta power (which is on average higher over the right than over the left channels) and is not of further interest. We are mainly interested in differences between the conditions with respect to the

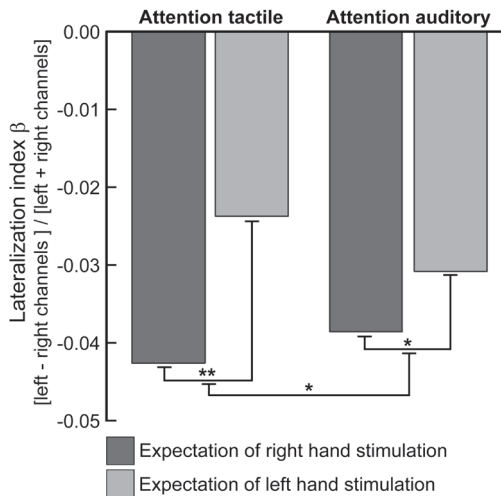


Figure 2.4. Grand average lateralization index values during left and right hand expectation for both attention conditions. For all four experimental conditions we calculated a lateralization index over the pre-stimulus interval of 350 ms to stimulus onset. This was done with respect to power in the post-stimulus selected beta band, using post-stimulus selected (synthetic planar gradient) channels above left and right sensorimotor cortex. Depicted are grand average values of this index. For both attention conditions a significant difference in the values of the lateralization index is observed between conditions of left and right hand expectation. Furthermore, this difference is significantly greater during the tactile attention condition, thus during states of attentive-expectation. The direction of the differences shows that for both attention conditions beta power is lower over contralateral compared to ipsilateral channels, relative to the upcoming tactile event. * = $p < 0.05$; ** = $p < 0.001$ (two-tailed).

lateralization index. For both attention conditions, the lateralization index is significantly more negative during expectation of right as compared to left hand stimulation ($t_{(17)} = -4.43$, $p < 0.001$, for the tactile attention condition; $t_{(17)} = -2.54$, $p < 0.05$, for the auditory attention condition). This implies that beta power is significantly lower over channels contralateral as compared to channels ipsilateral to the forthcoming tactile stimulus. Thus, tactile expectation modulates the (lateralization of) beta power while attending as well as while not attending the tactile input stream. Analysis of variance further showed a significant main effect of expectation ($F_{(1,17)} = 20.15$, $p < 0.001$) and a significant interaction between expectation and attention ($F_{(1,17)} = 6.19$, $p < 0.05$). The latter shows that there is a stronger expectation-induced modulation of beta power for attended as compared to unattended upcoming tactile events.

Similar analyses for alpha and gamma power yielded no significant



results. It must be noted that, for the alpha and gamma bands, we could not select participant-specific frequency bands on the basis of the stimulus-induced effect. This is because post-stimulus modulations in alpha and gamma band oscillations were less strong and not detectable in all subjects. Therefore, we did our analyses with predefined frequency-bands: 8-12 Hz for mu and 60-90 Hz for gamma.

Refutation of a motor confound

A major concern relates to the involvement of primary motor cortex (M1) in our task. This is because M1 and S1 both process information in a lateralized fashion and lie next to each other on the cortical surface. As a result, M1 and S1 have a large common projection to the SQUIDs.

A motor confound would be picked up by our analysis if (and only if) motor activity follows the pattern of tactile stimulations. This is the case when participants actively contract along with the forthcoming stimulation. To rule out this interpretation of our results, EMG was recorded in a follow-up session with the two participants that showed the strongest neural expectation effect. In separate blocks, these participants were instructed to either strongly or weakly contract one of their hands. Figure 2.5A and 2.5B show that during strong (A) and weak (B) contractions, a reliable increase in the EMG difference signal (ipsi-contra) could be detected. In Figure 2.5C, we show the EMG difference signals for the pre-stimulus period in which the participants expected a tactile stimulus. As is clear from Figure 2.5C, there is no expectation-induced modulation of the EMG difference signal. Thus, expectation of a lateralized tactile stimulus is not accompanied by a contraction of the hand on which the tactile stimulation is expected to occur. During these follow up sessions also MEG data were collected and the expectation-induced modulation

of beta was again observed.

Another potential confound is pre-stimulus response preparation. However, this potential confound is refuted because of the following simple fact: participants had a preferred response hand with which they responded, irrespective of location of the target.

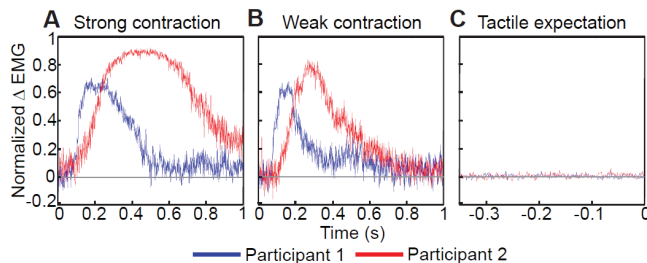


Figure 2.5. EMG activity during contraction and expectation. (A) EMG difference signal (i.e. ipsi minus contra) during explicitly instructed strong contraction of the whole hand. Shown are data from two participants that were recorded in a follow-up session. As expected, contraction of the hand results in a significant increase in muscular activity over the contracted hand. (B) EMG difference signal during explicitly instructed weak contraction of the whole hand. Contraction can still reliably be detected. (C) EMG difference signal during tactile expectation, shown for the time-window in which the cortical effect is observed. Evidently, expectation of a lateralized tactile stimulus is not accompanied by a contraction of the hand on which the tactile stimulation is expected to occur.

2.4 Discussion

We set out to investigate whether expectation of an upcoming tactile event involves a pre-stimulus modulation of oscillatory neural activity in human somatosensory cortex, and in particular S1. Additionally, we set out to test whether such a modulation would be restricted to attended events. During expectation of a lateralized tactile event, we observed an accordingly lateralized modulation of oscillatory neural activity in the beta band. This modulation resembled the modulation observed post-stimulus, both in terms of spectral content as in spatial topography. The effect was specific to the beta band and could not be explained by motor planning or behavior. Although we observed a stronger modulation during states of attentive expectation, we observed a qualitatively similar effect during states of non-attentive expectation. Thus, the anticipatory modulation of oscillatory activity was not restricted to attended events. These observations are well in line with previous studies – primarily in the visual and motor domain – that implicate a modulation of ongoing oscillatory activity in anticipation of neural processing. Our observations complement this literature by showing such a modulation (1) in the tactile domain, and (2) during states of both attentive and non-attentive expectation. In the following we speculate about the neural origin of the observed lateralized modulation, discuss our result against the background of the hypothesis that ongoing oscillations reflect a brain state in which neural processing efficacy is low and elaborate on attention in relation to expectation.

The neural origin of the expectation-induced modulation of beta oscillations

The most straightforward interpretation of the observed lateralized modulation of beta band oscillatory activity is a modulation within contralateral S1. In fact, this is the first neocortical area where the forthcoming information will be processed. However, there is increasing evidence that areas not receiving the expected thalamocortical input also show anticipatory modulation of oscillatory activity. For example, during anticipation of a visual stimulus, alpha activity does not only decrease over areas receiving input from the attended visual field (Sauseng et al., 2005; Thut et al., 2006; Wyart and Tallon-Baudry, 2008), but also increases over areas receiving input from the unattended visual field (Worden et al., 2000; Kelly et al., 2006; Rihs et al., 2007). In the absence of a neutral baseline, we contrasted conditions of left and right hand expectation directly. Accordingly, we were not able to dissociate an ipsilateral increase from a contralateral decrease. We nevertheless believe that our observed modulation at least partially involves a contralateral suppression. First, we observed a qualitatively similar modulation in both attention conditions. If beta were involved in active inhibition of non-relevant stimuli (i.e. disengagement of the cortical areas that process these non-relevant stimuli), as was suggested for alpha on the basis of aforementioned findings, then this is not expected. Rather, with attention directed to the auditory modality, one would expect to find either no lateralization (in case of general disengagement of both S1 cortices) or even a reversed lateralization (in case of a selective disengagement of that S1 that will receive the distracting input). Second, it has been hypothesized that the observed increases



in alpha power in aforementioned studies relate to distracter suppression (Worden et al., 2000; Kelly et al., 2006). In the present study, no distracters were presented on the non-expected hand. Third, we observed a highly similar spatial topography and spectral signature in the pre- and the post-stimulus modulation of beta. This is suggestive of a common neural generator of the beta oscillation that is affected both by stimulation and expectation. Despite above arguments, new experiments are required to address this issue properly.

We also argue that the observed pre-stimulus modulation of beta originates at least partly from the post-central gyrus and therefore indexes anticipation of somatosensory processing. The main argument for this claim is that this pre-stimulus modulation could not be related to motor planning or behavior. We further argue that this pre-stimulus modulation originates from *primary* somatosensory cortex. This follows from the fact that a lateralized pre-stimulus modulation most likely originates from the primary sensorimotor cortex, as only here information is processed in a lateralized fashion. That is, left and right hand stimuli are processed by different S1 cortices but the same S2 cortices. Therefore, the observed difference between left and right hand expectation most likely originates from primary rather than secondary somatosensory cortex. Thus, we have evidence for the involvement of S1 in expectation-induced modulations of oscillatory brain activity. This implies that S1 is subject to top-down influences and that expectations are effective from the initial cortical processing stages on. This complements the existing literature on sensory expectation by showing that a primary sensory cortex is involved in anticipatory modulations of oscillatory activity.

Regarding the rolandic rhythms, traditionally mu is considered to be primarily a post-central rhythm whereas beta is considered to be primarily a pre-central rhythm (Salmelin and Hari, 1994). Accordingly, beta is attributed to the motor and mu to the somatosensory system. This notion is in conflict with our interpretation that the observed beta modulation indexes somatosensory anticipation. However, recent evidence suggests that this traditional view is probably an oversimplification. First, tactile stimulation induces changes in beta power (present study; Cheyne et al., 2003; Bauer et al., 2006; Gaetz and Cheyne, 2006). Second, intracranial electrophysiological measurements, directly on the post-central gyrus, have shown beta oscillations that originated from S1 (Crone et al., 1998; Brovelli et al., 2004). Witham and Baker (2007) even recorded stronger beta oscillations in S1 than in M1. Finally, pre- and post-stimulus beta oscillations are related to conscious detectability of tactile stimuli (Linkenkaer-Hansen et al., 2004; Palva et al., 2005). All three sets of observations, together with our observation, show that beta oscillations play a role in somatosensation.

Ongoing oscillations reflect a non-efficacious mode of processing and are susceptible to top-down influences of expectation

Oscillations impact upon neural excitability and therefore produce a neural context that affects the processing of sensory input and motor output. There is ample evidence that oscillations that can be sustained in the absence of sensory input and motor output are

inversely related to processing efficacy. For instance, pre-stimulus alpha power has been shown to be negatively correlated with visual discrimination performance (van Dijk et al., 2008), detection performance (Ergenoglu et al., 2004; Hanslmayr et al., 2007), speed of visuomotor processing (Thut et al., 2006; Zhang et al., 2008b) and cortical excitability (Romei et al., 2008). Also sensorimotor alpha and beta oscillations have been associated with reduced cortical excitability (Chen et al., 1998; Tamura et al., 2005; Sauseng et al., 2009), at least in the motor domain. Applying transcranial alternating-current stimulation (tACS) at 20 Hz to the contralateral motor cortex, Pogosyan and colleagues (2009) were even able to slow down movement. Pre-stimulus sensorimotor mu and beta oscillations have furthermore been related to conscious detectability of tactile stimuli (Linkenkaer-Hansen et al., 2004). Taken together, there is ample evidence that ongoing oscillations produce a brain state in which neural (e.g. sensory) processing efficacy is low. It follows that the neural processing efficacy can be enhanced by altering these oscillations prior to an expected sensory event. In particular, suppressing these oscillations (beta) in regions where the upcoming event will be processed (contralateral S1), may affect cortical transfer of initial afferent input. (Note that an increase of beta in ipsilateral S1 might also be beneficial, as a disengagement of ipsilateral S1 may suppress competing input.) We provide evidence for such a mechanism by showing an amplitude modulation of beta in anticipation of a tactile stimulus. This observation is in line with similar observations in the visual modality, involving an amplitude modulation of the posterior alpha oscillations in anticipation of a visual stimulus (Foxe et al., 1998; Worden et al., 2000; Sauseng et al., 2005; Kelly et al., 2006; Thut et al., 2006; Rihs et al., 2007; Wyart and Tallon-Baudry, 2008). The observation of a similar phenomenon in a different sensory modality speaks to a general neural mechanism of anticipation.

Surprisingly, it has been reported that pre-stimulus beta oscillations in prefrontal cortex are positively correlated with states of anticipation, with higher beta power and coherence being associated with faster reaction times and higher amplitudes of visual-evoked potentials in a visuomotor task (Liang et al., 2002; Zhang et al., 2008b). Likewise, pre-stimulus beta oscillations from parietal cortex have shown to be positively correlated with tactile detection performance (Linkenkaer-Hansen et al., 2004). Thus, brain oscillations in the same frequency band may have a different function dependent on their origin (i.e. prefrontal/parietal versus sensorimotor beta).

Tactile stimuli not only generate a post-stimulus beta suppression; they also generate a beta rebound. In our experiment, this rebound emerges within the time window between two successive tactile stimuli (see Fig. 2.2A). This is consistent with the timing of the beta rebound, as has been reported in several studies (Cheyne et al., 2003; Bauer et al., 2006; Gaetz and Cheyne, 2006). This means that our analysis windows (from 250 ms after the previous stimulus until the next stimulus) also contain the beta rebound in response to the previous stimulus. This implies that the lateralized beta modulation may also be caused by an expectation-induced reduction of the amplitude of the beta rebound. (This would then



only apply to those time segments where the upcoming event is on the same hand as the previous stimulation.) Although this clearly is an expectation-induced modulation of beta, it may suggest a different mechanism. From the perspective of metabolic efficiency, in anticipation of an upcoming stimulus that will produce a post-stimulus beta-suppression, it is not desirable to have a rebound. Thus, an account in terms of metabolic rather than sensory efficacy is conceivable. However, two observations go against this interpretation. First, we did not observe a relationship across participants between characteristics of their beta-rebound (i.e. strength, starting-point) and the size of their expectation effect. Second, attention led to a stronger modulation of beta. The latter is clearly predicted from our first account, but not from the metabolic one.

Expectations are effective outside the realm of attention

Remarkably, we observed that the involvement of neural oscillations in sensory expectation is not restricted to attended sensory events. Thus, even when participants were attending the non-lateralized auditory stream, a lateralized modulation of beta oscillations was observed. This implies that participants not only make predictions about unattended events, but also that these predictions are effective in modulating ongoing oscillatory activity in the sensorimotor cortex. In line with the vast literature on implicit learning (Reber, 1993. for an overview), we postulate that the human brain can operate effectively in the absence of deliberate engagement. A similar phenomenon was also observed by Nakano et al. (2008) who showed anticipatory modulations in regional blood flow in infants that were asleep.

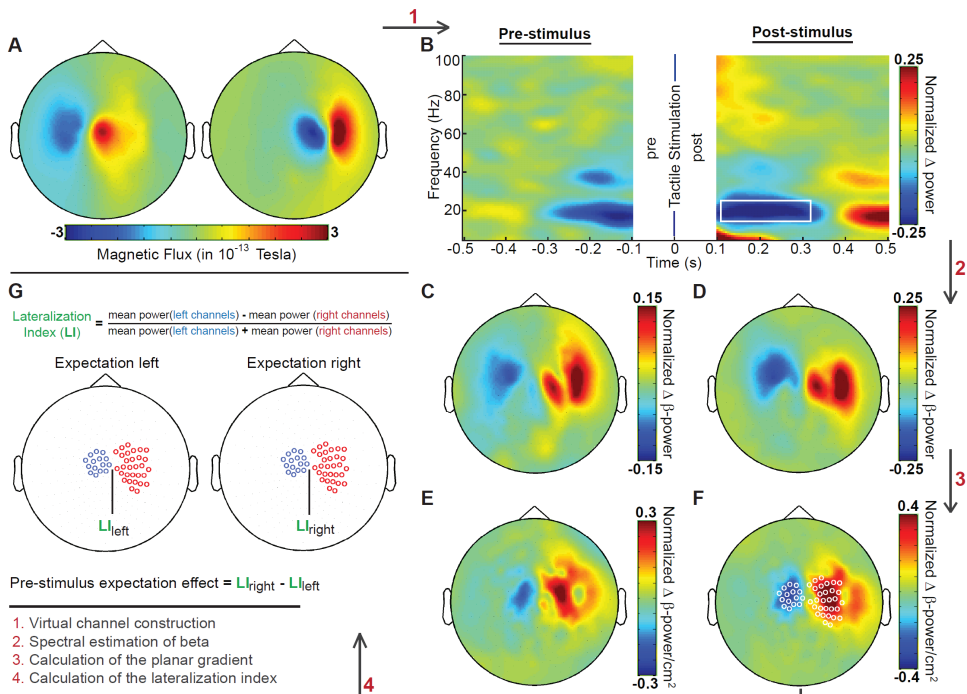
The validity of the above claim depends on whether the tactile stream was truly unattended when participants were detecting auditory deviants. We deliberately presented tactile and auditory events simultaneously and our task explicitly required participants to selectively attend only to a single sensory stream. Furthermore, targets were hard to detect, as is clear from the detection rates. Thus, in order to do the task properly, maximum attention to the cued modality was required. We conclude that expectation modulates beta oscillations both when upcoming tactile events are behaviorally relevant (i.e. attended) and when they are not (i.e. unattended). Additionally, we showed that attention, as operationalized by behavioral relevance, enlarged the size of the expectation-induced modulation.

Conclusion

In the present paper we provided evidence that expectation of a tactile stimulation involves a pre-stimulus modulation of oscillatory neural activity in sensorimotor cortex. This modulation occurred in the beta band and most likely is produced by a contralateral suppression, originating at least partly from S1. We furthermore provided evidence that such an expectation-induced modulation is not restricted to attended events. We argue that the suppression of beta oscillations over the contralateral S1 prepares the system for processing the forthcoming event. Accordingly, the active process of perception starts already prior to sensation.

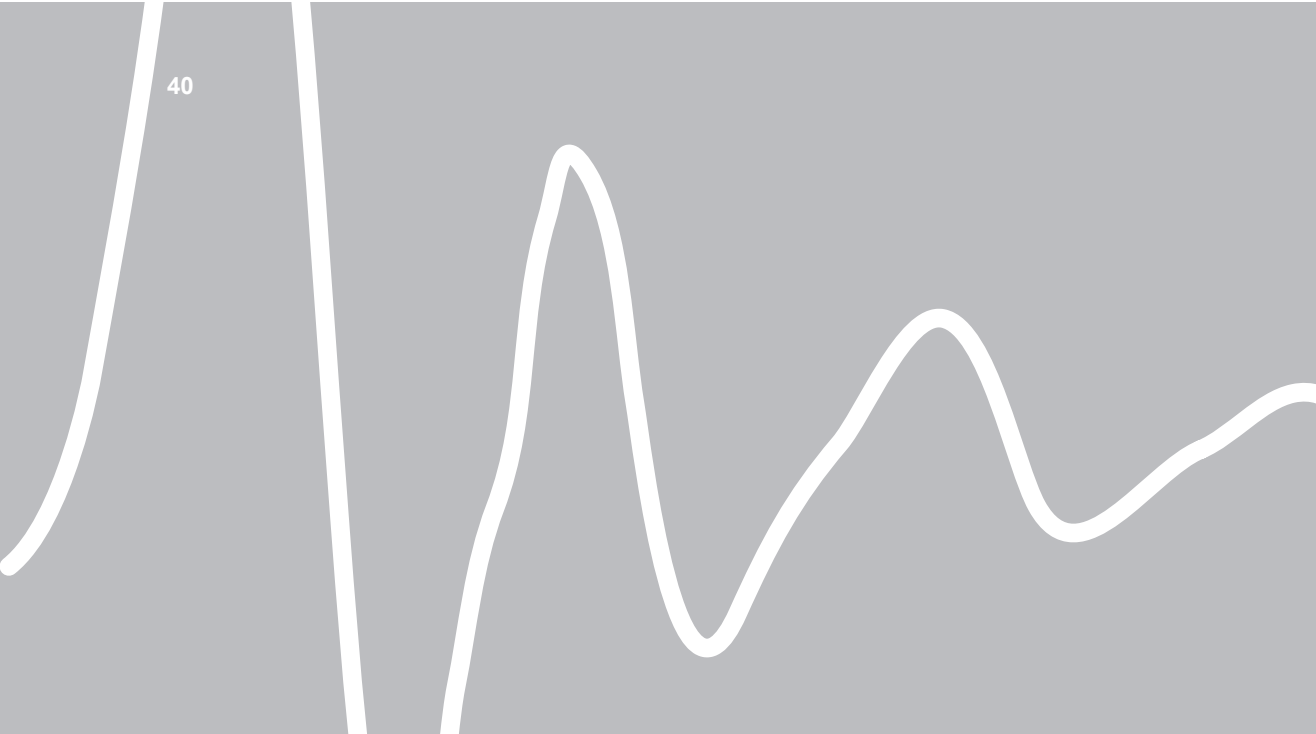


2.5 Supplementary Figure 2.1



Supplementary Figure 2.1. Illustration of analysis procedure and main result for a representative participant. (A) Topographies of the ERF between 40 and 60 ms after right and left hand stimulation, respectively. Two virtual S1 channels were constructed on the basis of these data (step 1 in the Figure). (B) Pre- and post-stimulus representations of the time-resolved power difference between contralateral and ipsilateral virtual S1 channels. The gap in the middle is due to the sliding-window being 200 ms for both pre- and post-stimulus data segments that were cut-out separately. The white box in the post-stimulus TFR represents the selected beta band for this participant. Power in the selected band was then estimated (Step 2 in the Figure). (C) Topography of the beta modulation during attentive-expectation of a lateralized tactile stimulus. Beta power was estimated over a window 350 ms to stimulus onset. Color coded is the normalized difference in beta power between conditions of right and left hand expectation (i.e. [right minus left] / [right plus left]). The modulation topography was calculated on the axial gradiometer data. (D) Topography of the beta modulation following a lateralized tactile stimulus (represented by the white box in B). Same conventions as C. (E, F) Identical to C and D, except topographies were calculated on the synthetic planar gradient data (step 3 in the Figure). White circles superimposed on the post-stimulus modulation topography denote selected channels above left and right S1. Channels were selected on the basis of the same contrast, for which also t-values were calculated (not shown). (G) Illustration of the lateralization index in relation to the expectation effect. After having selected both the individual's spectral (B) and spatial (F) loci of beta, a lateralization index was calculated (step 4 in the Figure). This was done separately for both expectation conditions (left and right). Importantly, the pre-stimulus expectation effect is obtained by contrasting our lateralization index between conditions of right and left hand expectation.





Orienting attention to an upcoming tactile event involves a spatially and temporally specific modulation of sensorimotor alpha- and beta-band oscillations

Adapted from van Ede F, de Lange FP, Jensen O, Maris E (2011) *Orienting attention to an upcoming tactile event involves a spatially and temporally specific modulation of sensorimotor alpha- and beta-band oscillations*. *The Journal of Neuroscience* 31:2016-2024.

3

Abstract

Our perception is facilitated if we know where and when a sensory stimulus will occur. This phenomenon is accounted for by spatial and temporal orienting of attention. Whereas spatial orienting of attention has repeatedly been shown to involve spatially specific modulations of ongoing oscillations within sensory cortex, it is not clear to what extent anticipatory modulations of ongoing oscillations are involved in temporal orienting of attention. To address this, we recorded MEG while human participants performed a tactile identification task. We cued participants to the left or the right hand, after which a tactile stimulus was presented at one of several fixed temporal delays. We thus assessed whether and how ongoing sensorimotor oscillations are modulated during tactile anticipation. We provide evidence for three phenomena. First, orienting to an upcoming tactile event involves a spatially specific contralateral suppression of alpha- and beta-band oscillations within sensorimotor cortex. Second, this modulation is deployed with temporal specificity, and this is more pronounced for beta- as compared to alpha-band oscillations. Third, the contralateral suppression of beta-band oscillations is associated with faster responses to subsequently presented tactile stimuli. Control measures showed that these results cannot be explained by motor planning or execution. We conclude that the modulation of ongoing oscillations within sensory cortex reflects a unifying mechanism underlying both spatial and temporal orienting of attention.

3.1 Introduction

Understanding perception requires an understanding of the top-down influences that affect it. Anticipation is such a top-down influence, and it has been shown to involve a spatially specific modulation of ongoing oscillations within sensory cortex, prior to the presentation of a stimulus. For example, in anticipation of a lateralized visual stimulus, posterior alpha-band (8-12 Hz) oscillations are increased ipsilateral and decreased contralateral to the expected visual input (Worden et al., 2000; Sauseng et al., 2005; Kelly et al., 2006; Thut et al., 2006). We have recently observed a similar phenomenon in the tactile modality, i.e. expectation of a lateralized tactile stimulus involves an accordingly lateralized modulation of pre-stimulus sensorimotor beta-band (15-30 Hz) oscillations (**chapter 2**).

The anticipatory modulations of ongoing alpha- and beta-band oscillations have consequences for neural processing and behavior. Neurophysiologically, these oscillations are inversely related to cortical excitability (Chen et al., 1998; Tamura et al., 2005; Romei et al., 2008; Sauseng et al., 2009). Behaviorally, they are inversely related to perceptual detectability (Ergenoglu et al., 2004; Hanslmayr et al., 2007; Romei et al., 2010), discriminability (van Dijk et al., 2008), and speed of visual and motor processing (Thut et al., 2006; Zhang et al., 2008b; Pogosyan et al., 2009). These findings suggest a functional role of the anticipatory modulations: upcoming sensory processing will be enhanced when the sensory input arrives during a state of high excitability (involving contralaterally suppressed ongoing oscillations), and likewise intrusion of distracting input is blocked when arriving during a state of low excitability (involving ipsilaterally enhanced ongoing oscillations). Accordingly, the observed anticipatory modulations of ongoing oscillations within sensory cortex have been put forward as a physiological mechanism of spatial attention.

Perception is not only facilitated by knowledge of where a stimulus is likely to occur (spatial attention), but also by knowledge of when this stimulus is likely to occur (temporal attention; Nobre, 2001). Like spatial attention, temporal attention is associated with modulations in brain activity (Nobre, 2001; Ghose and Maunsell, 2002; Nobre et al., 2007; Lakatos et al., 2008). However, it is at present unclear to what extent modulations in the amplitude of ongoing oscillatory activity are involved in temporal orienting of attention.

We hypothesized that a temporally specific modulation of ongoing oscillatory activity may constitute a physiological mechanism underlying temporal orienting of attention. Therefore, the modulation of ongoing oscillations, with specificity in both space and time, may be a unifying mechanism underlying both spatial and temporal selective attention. To address this, we recorded MEG while participants performed a tactile identification task. We cued participants to the left or the right hand, after which a tactile stimulus was presented at one of several fixed temporal delays. We thus investigated the spatial and temporal specificity with which ongoing sensorimotor oscillations are modulated during tactile anticipation. Additionally, we addressed whether such a modulation is constituted by a contralateral suppression or an ipsilateral enhancement. Finally, we assessed the behavioral consequences of pre-stimulus oscillatory activity.

3.2 Materials and Methods

Participants

A total of 20 healthy subjects voluntarily participated in the experiment (9 male, mean age: 26y, range: 19-48y). All participants provided written consent and were paid in accordance with guidelines of the local ethics committee (CMO Committee on Research Involving Humans subjects, region Arnhem-Nijmegen, the Netherlands).

Experimental design & paradigm

The experiment was designed to induce both spatial and temporal expectation. Figure 3.1 depicts the experimental paradigm. Every trial started with an auditory cue indicating whether the tactile stimulus would follow on the left or the right hand (with 100 % validity). Left and right hand cues were randomly drawn for each trial. The cues for left and right-hand stimulation were a low (500 Hz) and high pitch (1000 Hz) pure tone. These tones had a duration of 50 ms and were binaurally presented via MEG compatible air-tubes. Their association with the side of tactile stimulation was counterbalanced across participants. Following the cue, the tactile stimulus would be presented after 1, 2, or 3 s with probabilities governed by one of two hazard rate functions. The hazard rate is the conditional probability of observing an event (here, a tactile stimulus) given that it has not yet occurred. At the beginning of each trial, the subject does not know at which temporal position the tactile stimulus will be presented, but as the trial progresses, his/her expectation becomes more specific. Therefore, the behaviorally relevant quantity is the hazard rate, which is updated after every temporal position at which the stimulus does not occur. The first hazard rate function is characterized by the probabilities 0.33, 0.43, and 0.23, which produce the hazard rates 0.33, 0.66, and 1. The second hazard rate function is characterized by the probabilities 0.33, 0.00, and 0.66, which produce the hazard rates 0.33, 0.00, and 1 (see Fig. 3.1). In contrast with the first hazard rate, in the second hazard rate the tactile stimulus is never presented at the second temporal position (i.e. 2 s after the cue). We used the above probabilities such that (1) the conditional probabilities would increase linearly with time and (2) both hazard rates would differ only at the second temporal position. The first and the second hazard rate function are therefore called the three-point and the two-point hazard rate, respectively. It is crucial to note that a tactile stimulus is always presented at one of three possible temporal positions in a trial, and never in between. In other words, we used discrete rather than continuous hazard rate functions. This allowed us to assess the temporal specificity with which anticipatory modulations of oscillations can be deployed. Because temporal specificity requires accurate mental timing, we assisted subjects by presenting a binaural 750 Hz pure tone at temporal positions at which the tactile stimulus did not occur.

Tactile stimuli were produced by piezoelectric Braille cells (Metec, Stuttgart, Germany). A single Braille cell consists of eight pins, aligned in 2 series of 4, that can be raised and lowered. Five such cells, together with a response button, were built into a graspable device (see Supplementary Fig. 3.1), one for each hand. Tactile stimuli were



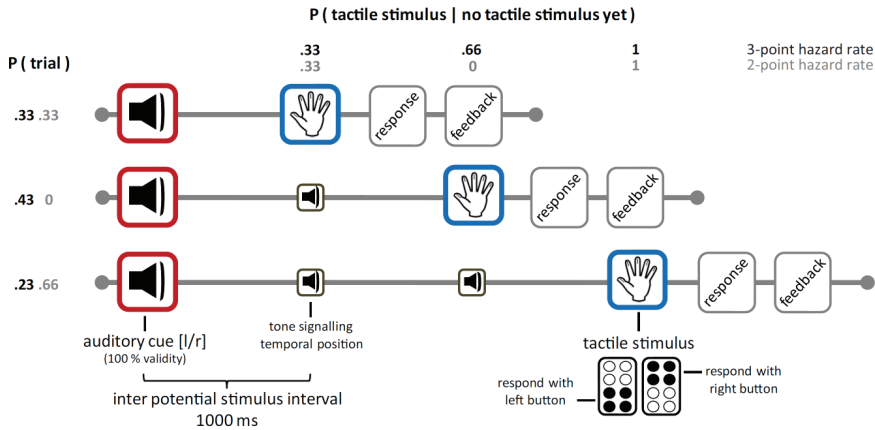


Figure 3.1. Experimental paradigm. Each trial starts with a randomly drawn auditory cue that indicates with 100 % validity whether the tactile stimulus will be presented to the left or the right hand. In the three-point hazard rate condition, the tactile stimulation follows after 1, 2 or 3 s, and in the two-point hazard rate condition, it follows after 1 or 3 s. The probabilities as well as the hazard rates (conditional probabilities given that the stimulus has not been presented yet) can be read from the figure. When the tactile stimulus is not presented, a binaural auditory stimulus is presented that indicates the temporal position, and thus signals that the tactile stimulus can occur 1 s later. When the tactile stimulus is presented, the upper 4 or the lower 4 pins of all Braille cells stimulating the fingertips of the cued hand are transiently raised. The participant is then required to discriminate between these alternatives (upper or lower pins) and respond by pressing the right or left button, respectively. Then, after 1 s feedback is presented. A correct response is followed by a single transient stimulation of both hands, while an incorrect response is followed by a double transient stimulation of both hands. 1 s after the feedback, the next trial is presented.

produced by transiently raising the pins of all Braille cells overlying the five fingertips of a single hand. The pins were lowered into the cells again 20 ms after being raised, rendering the subjective experience of a tactile stimulus as a tap on the fingers.

When a tactile stimulus was presented, the participant was required to discriminate between two stimulus types, involving the stimulation of all digits of the hand with either the upper or lower 4 Braille cell pins. Participants responded by pressing the left button for the lower 4 pins and the right button for the upper 4 pins (see Fig. 3.1). The two stimulus types (upper and lower pins) were equally often presented on the left and the right hand. As a result, our design was balanced with respect to the response side and the side of the tactile stimulus. After the response, feedback was presented. A correct response was followed after 1 s by a single tactile stimulus presented to both hands, whereas an incorrect response was followed by a double tactile stimulus (ISI = 200 ms), also presented to both hands. The next trial was presented 1 s after the feedback.

The experiment consisted of 2 separate sessions that each contained 10 blocks. Each session lasted about 1 hour. Within each block, 50 trials were presented. Within each session, 6 consecutive blocks contained trials in which the stimulus probabilities were governed by the three-point hazard rate function. The other 4 consecutive blocks contained trials in which the stimulus probabilities were governed by the two-point hazard rate function. The order of the two hazard rate supra-blocks was counterbalanced across sessions and

participants. Immediately prior to a change in hazard rate, participants were informed about this change. The complete experiment was programmed and run using the software package Presentation (Neurobehavioral Systems, USA).

MEG recording

The MEG system (CTF MEG TM Systems Inc., Port Coquitlam, Canada) contained 275 axial gradiometers and was housed in a magnetically shielded room. We also recorded bipolar surface EMG from both arms using two pairs of Ag/AgCl electrodes. These electrode pairs were placed across the flexors of the forearm, with one electrode placed near the wrist and the other near the elbow, allowing us to measure digit non-specific contractions. Three localization coils, fixed to anatomical landmarks (nasion, left ear, right ear), were used to determine the position of the head relative to the gradiometers. All data were low-pass filtered by an anti-aliasing filter (300 Hz cutoff), digitized at 1200 Hz, and stored for offline analysis. No EOG data were recorded because subjects were instructed to close their eyes during the experiment (in fact, during the experiment the lights were turned off).

Data analysis

Data were analyzed using FieldTrip (Oostenveld et al., 2011), an open source Matlab toolbox developed at the Donders Institute for Brain, Cognition and Behaviour (Nijmegen, the Netherlands).

All data epochs of interest were visually inspected and those contaminated by artifacts were removed. Excessively noisy channels were also removed. Line noise was removed by means of the Discrete Fourier Transform (DFT). More specifically, we used the DFT to estimate the amplitudes and the phases of the 50, 100 and 150 Hz components and subtracted the sine waves that were constructed from these DFT-estimated amplitudes and phases. Finally, we removed the DC-component of the signals (which includes the offset of the SQUIDS) by subtracting the mean of every epoch.

Channel and frequency band selection. For each participant, we selected a subset of channels as well as a frequency band on the basis of the stimulus-induced modulation in the post-stimulus epoch. These selected channels were subsequently used for the analysis of the pre-stimulus epochs of interest. We now describe this channel and frequency band selection procedure, of which a graphical depiction is shown in Supplementary Figure 3.2. The procedure is based on the tactile stimulus-induced modulation of beta-band oscillations that is known to originate from sensorimotor cortex (Salenius et al., 1997b; Gaetz and Cheyne, 2006; **chapter 2**). Specifically, we estimated beta power (see frequency analysis) for all MEG channels in the range of 15-30 Hz and in the time window from 100 to 300 ms after stimulation, both of which were defined a priori. We then contrasted the beta power following left and right hand stimulation using the index $[(\text{right} - \text{left}) / (\text{right} + \text{left})]$ and selected the 15 channels with the highest (lowest) index value, which were found over the right (left) sensorimotor cortex. This was done using the planar gradient (see planar



gradient calculation). Using these channels, we then calculated a single contra-over-ipsi power ratio (see calculation of a contra-over-ipsi power ratio). In order to optimize the participant-specific selection of channels, we selected (on the basis of visual inspection) the participant-specific time window and frequency band of the post-stimulus beta modulation and repeated the above steps. Importantly, the stimulus-induced beta modulation could be observed in all participants. On average, beta ranged between 13 and 31 Hz, and was modulated between 120 and 400 ms post-stimulus. Post-stimulus modulations of alpha-band oscillations could not be observed in all subjects. For alpha we therefore used a fixed frequency-band of 8-12 Hz.

Planar gradient calculation. Data were collected using an MEG system with axial gradiometers, which measure the first spatial derivative of magnetic field (i.e. magnetic flux) in the axial direction relative the surface of the skull. From these axial gradiometer data we calculated synthetic planar gradient data (Bastiaansen and Knosche, 2000). The planar gradient has the benefit that the activity is concentrated above the source (Hämäläinen et al., 1993). The synthetic planar gradient for a given channel consists of two components, of which one measures the spatial derivative along the anterior-posterior axis of the MEG-helmet, and the other along the left-right axis. By linearly combining (rotating) these components (using coefficients that maximize the power of this linear combination), we obtained a single-component measure (in our case of oscillatory power) per channel. We refer to this as the planar gradient.

Calculation of the contra-over-ipsi power ratio. We based our calculation on a time-resolved power estimate (see frequency analysis) for all selected channels. In the first step, the channels over the left and the right sensorimotor cortex were averaged separately. In the second step, for the left (right) sensorimotor channel we calculated the ratio between the power during anticipation/stimulation of the right (left) hand and the power during anticipation/stimulation of the left (right) hand. In other words, we obtained a single left and a single right sensorimotor power ratio by dividing the oscillatory power during contralateral anticipation/stimulation by the oscillatory power during ipsilateral anticipation/stimulation. In the third step, the left and the right power ratios were averaged, and the resulting measure will be denoted as the contra-over-ipsi power ratio. It is important to note that this measure is not affected by spatially non-specific effects of time, bilateral effects of potential motor preparation, and processing of the binaurally presented tones, because these effects are identical for channels ipsi- and contralateral to the anticipated side.

Frequency analysis. We calculated oscillatory power estimates by means of the Fourier transform in combination with two tapering methods: a single Hanning taper and multiple discrete prolate spheroidal tapers (the multitaper method; Percival and Walden, 1993). We calculated oscillatory power estimates both with and without time resolution. All calculations

with time resolution involved a 300 ms sliding time window that was advanced in steps of 25 ms. Power estimates were calculated for frequencies between 5 and 50 Hz, and each one of them was based on a single Hanning taper. Non-time-resolved power estimates were calculated only for the frequency bands that were selected for the individual participants (see channel and frequency band selection). For the participant-specific beta-bands, power was estimated using the multitaper method, and for the alpha-band it was estimated using a single Hanning taper.

Source analysis. We calculated source-level power estimates by means of adaptive spatial filtering (beamforming). For every point source of interest, a source-level power estimate is calculated from a spatial filter that has unit gain for the point source of interest while maximally attenuating surrounding sources. This is accomplished by taking the cross-spectral density matrix into account. This method is known as Dynamic Imaging of Coherent Sources (DICS; Gross et al., 2001; Liljestrom et al., 2005), although we used it only for the estimation of source-level power. In practice, we set out by discretizing each individual's MRI into a grid with 1 cm resolution. For each grid point, a leadfield matrix was calculated using a forward model based on a single shell volume conductor (Nolte, 2003). A spatial filter was then constructed for each point in the grid that was then applied to estimate the power at that source location. This power was subsequently contrasted between conditions of interest, analogous to the channel-level analyses. We were able to apply this beamforming analysis to 17 out of our 20 subjects. For the remaining 3 subjects, due to technical problems, no head-localization was possible at the time of MEG data acquisition.

EMG analysis. Raw EMG traces were high-pass filtered (40 Hz cut-off) and subsequently rectified. We then calculated an ipsi-over-contra ratio, similar to the contra-over-ipsi ratio as was described for the MEG data. That is, we contrasted the high-pass filtered and rectified EMG traces between two sets of trials: trials in which the (expected) event of interest occurs ipsilateral to the side of the EMG electrodes, and trials in which it occurs contralateral.

Analysis of spatial specificity. We investigated whether orienting to an upcoming tactile event involves a spatially specific modulation of sensorimotor oscillations. We analyzed the first second after the cue for which we calculated the time-resolved contra-over-ipsi power ratio. We also constructed a topography of the difference between left and right hand expectation as described above for the post-stimulus window. For this, we used a pre-stimulus window of 350 ms to stimulus onset. The choice for this window was based on a previous study (**chapter 2**). Additionally, we analyzed the same [right - left] contrast in source-space. Finally, for all channels we linearly regressed time-resolved alpha- and beta-band power on time. This was done separately for anticipation of a left and a right hand stimulus. The t-values of the resulting regression coefficients were taken as a normalized measure of the slope of alpha/beta power on time, and averaged across participants.



Analysis of temporal specificity. We assessed whether the spatially specific modulation of sensorimotor oscillations is deployed with temporal specificity. We analyzed all trials for which the stimulus occurred at the last temporal position ($t = 3$). We calculated the time-resolved contra-over-ipsi ratio with respect to power in the alpha- and the beta-band. This was done separately for both hazard rates. Temporal specificity was evaluated by means of two separate statistical analyses. First, we assessed whether the contra-over-ipsi power ratio time-courses differed between the three-point- and the two-point hazard rate conditions. For this, we used a cluster-based permutation test. This test is well suited for controlling the false-alarm rate when facing multiple comparisons (as in our case, when conditions are contrasted for multiple time-points). Specifically, the false-alarm rate is controlled by using a cluster-statistic that is evaluated under a single permutation distribution (see Maris and Oostenveld, 2007). Secondly, we assessed temporal specificity within each hazard rate. Temporal specificity should manifest itself as a stronger lateralization (indexed by our contra-over-ipsi power ratio) just prior to an expected event versus in between two expected events. To test this hypothesis, we used the trials in which the stimulus was presented at $t = 3$. We pooled the data-points that estimated power in the last 300 ms prior-to an expected event (three-point hazard rate: $t = 0.85$, $t = 1.85$, $t = 2.85$; two-point hazard rate: $t = 0.85$, $t = 2.85$) and contrasted this with another measure that pooled the data-points that estimated power in-between expected events (hazard rate 1: $t = 1.5$, $t = 2.5$; hazard rate 2: $t = 2$). We evaluated this contrast by means of a paired sample t-test, treating the participants as the statistical replications.

Analysis of behavioral consequences. We investigated how the pre-stimulus oscillatory lateralization related to behavioral performance. For this, we separated for each participant both correct and incorrect trials as well as the fastest and the slowest trials (based on a median split) and analyzed these trials separately in the same ways as described above. We did this for the second that preceded the tactile stimulus to which the response was made. For statistical evaluation, we performed a cluster-based permutation test on the contra-over-ipsi power ratio time-courses of the data that was separated according to behavioral performance.

3.3 Results

Behavior

Participants correctly discriminated, on average, 76 (SD = 12) % of the tactile stimuli, and responded with an average latency of 1008 (SD = 349) ms. No differences in identification performance were observed for stimuli presented at the 3 different temporal positions ($F_{(2,38)} = 1.3$; $p = 0.286$). In contrast, response times were significantly shorter for stimuli that were presented on a later as compared to an earlier position ($F_{(2,38)} = 9.1$; $p < 0.005$; see Supplementary Fig. 3.3). Importantly, stimuli that are presented on a later position have a higher hazard rate (see Materials and Methods) than stimuli presented on an earlier position.

Orienting to an upcoming tactile event involves a pre-stimulus suppression of contralateral sensorimotor alpha- and beta-band oscillations

We assessed whether orienting to an upcoming tactile event involves a spatially specific modulation of sensorimotor oscillations. For this, we analyzed the first second after the cue that indicated whether the tactile stimulation would occur on the left or the right hand. Figure 3.2A shows the time-resolved ratio of oscillatory power between contra- and ipsilateral sensorimotor channels relative to the expected tactile stimulus. In anticipation of a lateralized tactile stimulus, there is less alpha- (8-12 Hz) and beta-band (15-30 Hz) activity over the contralateral as compared to the ipsilateral sensorimotor cortex. This effect is most pronounced for the beta-band, and we will focus on this frequency band in the

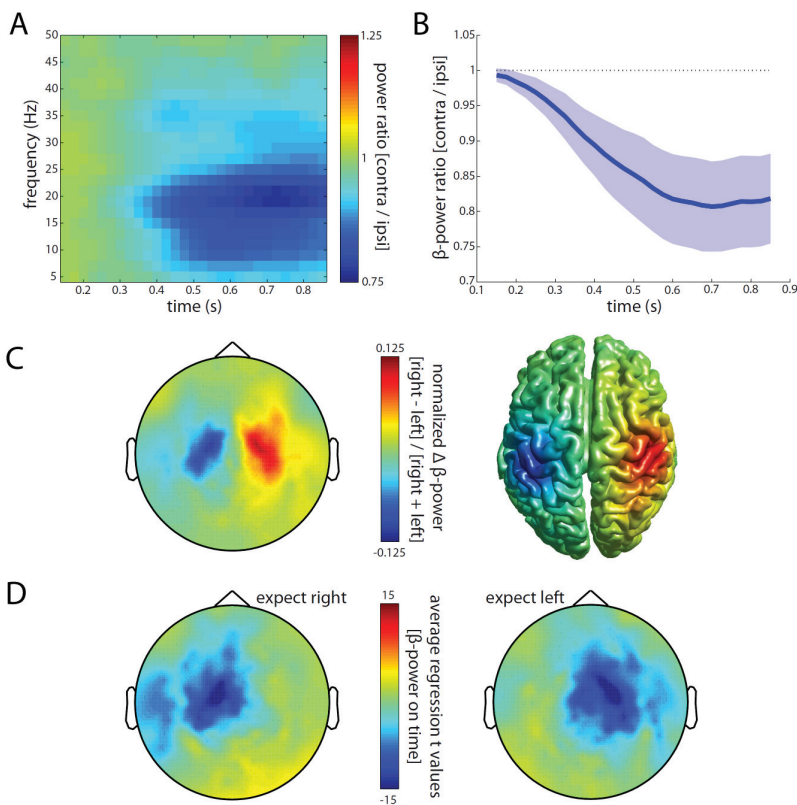


Figure 3.2. Spatial orienting involves a lateralization of beta-band oscillations. (A) Time-resolved power ratio between sensorimotor channels contralateral and ipsilateral to the anticipated tactile stimulus (see Materials and Methods). At time 0, the cue is presented. The first position at which the tactile stimulus may occur is 1 s after the cue. (B) Time-resolved beta power ratio including its 95 % confidence interval, with the standard error calculated using the variance across participants. (C) Topography and source reconstruction of the lateralized pre-stimulus beta power modulation. The color code reflects the normalized difference in beta power between anticipation of a left and right hand stimulation: [(right - left) / (right + left)]. Beta power was estimated over the last 350 ms prior to the first expected event. (D) Topographies of the regression of beta power on time, separately for anticipation of left and right hand stimulation. The color code reflects the t-statistics for the regression coefficients that were obtained for each participant and subsequently averaged.

following. The corresponding results for the alpha-band are highly similar and are shown in Supplementary Figure 3.4. This spatially specific modulation of pre-stimulus beta-band oscillations is highly consistent across subjects, as is evident from Figure 3.2B that shows the beta modulation together with its 95 % confidence interval. Additionally, the modulation becomes stronger towards the expected event, which is consistent with a role in sensory preparation.

Next, we investigated the spatial topography of the observed beta modulation. For every channel, we calculated the beta power in the last 350 ms preceding the time point of the first potential stimulus, separately for left and right hand anticipation, and subtracted the two. The resulting topography is shown in Figure 3.2C, together with the corresponding source reconstruction (see Materials and Methods). Over left sensorimotor cortex, beta power is lower in anticipation of a right as compared to a left hand stimulus, whereas the reverse is true for the right sensorimotor cortex. The minimum and the maximum of the corresponding source-reconstructed power differences are both in the post-central gyrus (i.e. S1).

These observations clearly show a spatially specific modulation of sensorimotor beta-band oscillations in anticipation of a tactile event. However, they do not distinguish between two possible constituents of such a modulation: a contralateral decrease or an ipsilateral increase in beta power. If the decrease over time in the contra-over-ipsi ratio of oscillatory power (depicted in Fig. 3.2B) is produced by a contralateral decrease, then the beta power over contralateral channels must decrease with time. Analogously, if it is produced by an ipsilateral increase, then the beta power over ipsilateral channels must increase with time. To investigate this, for all channels, we linearly regressed time-resolved beta power on time, separately for anticipation of a left and a right hand stimulus. Figure 3.2D depicts the results obtained from this analysis. In anticipation of a right hand stimulus, the beta power over left sensorimotor channels decreases with time. Likewise, in anticipation of a left hand stimulus, the beta power over right sensorimotor channels also decreases with time. This shows that the observed spatially specific modulation of sensorimotor beta-band oscillations is produced by a contralateral suppression.

It is important to note that this pre-stimulus beta modulation is highly similar to the observed post-stimulus modulation (see Supplementary Fig. 3.5), both in terms of frequency content and spatial topography. This is suggestive of a common neural generator of the beta oscillation that is suppressed not only by tactile input but also by its anticipation. Moreover, the strength of the pre-stimulus beta modulation is almost as strong as the strength of the post-stimulus modulation (compare Fig. 3.2B with Supplementary Fig. 3.5B). Note that these observations casts serious limitations to the use of pre-stimulus baseline corrections to predictable events (see Supplementary Fig. 3.5D and E for the severe effect of pre-stimulus baseline correcting induced activity that follows an anticipated tactile event). This correspondence between pre- and the post-stimulus oscillatory activity is specific to alpha and beta. In fact, in the post-stimulus period, there is a lateralized modulation of gamma-

band (60–80 Hz) oscillations (in accordance with Bauer et al., 2006) that was not observed in anticipation of a tactile stimulus (see Supplementary Fig. 3.5D).

It is important to rule out that the anticipatory beta modulation is related to motor planning or execution. With respect to motor planning, it is important to note that the expected side of the tactile stimulus and the expected side of the button-press response were balanced. That is, a left (right) hand stimulus required as often a left hand as a right hand button press. Furthermore, no bias was observed with respect to the side of the button press in relation to the side of the stimulation (side congruent – side incongruent responses: $t_{(19)} = -1.02$; $p = 0.32$). To control for expectation-related motor behavior (such as contracting the hand on which the tactile stimulus was expected to occur) we recorded EMG activity over both arms. We observed no significant difference between ipsi- and contralateral EMG activity during tactile anticipation. This null finding is unlikely to be due to an insensitive EMG measure because lateralized button-presses as well as explicitly requested contractions resulted in significant differences between ipsi- and contralateral EMG activity (see Supplementary Fig. 3.6). On the basis of these considerations, we argue that the observed beta-modulation is related to anticipation of an upcoming tactile event. Accordingly we argue that this modulation occurs at least partially within the primary somatosensory cortex.

Anticipatory modulations of ongoing sensorimotor oscillations are deployed with temporal specificity

Next, we assessed whether the spatially specific modulation of sensorimotor oscillations is deployed with temporal specificity. For this, we restricted our analysis to those trials in which the tactile stimulus was presented after 3 s and thus had been expected at 1, 2 and 3

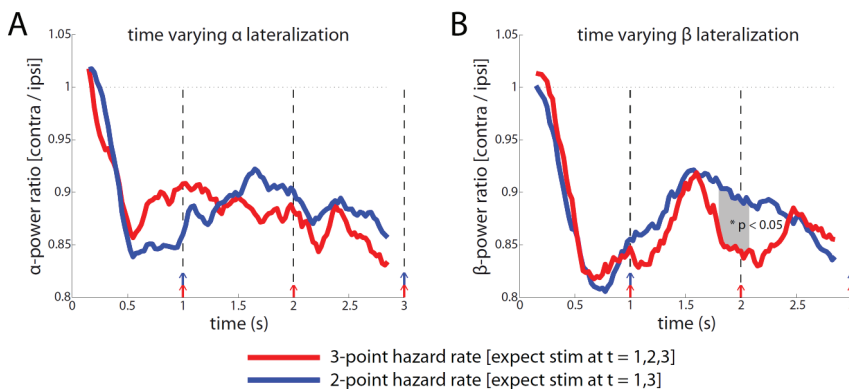


Figure 3.3. Temporal orienting modulates the lateralization of alpha- and beta-band oscillations. (A) Time-resolved ratio of contralateral and ipsilateral alpha power, for both hazard rates. (B) Same as panel A, but now for beta power. Shading indicates the time window for which the two hazard rates significantly differ (permutation test; $p < 0.05$). Dashed lines indicate the three temporal positions at which tactile stimuli were expected. Blue and red arrows indicate whether a stimulus was expected in the corresponding hazard rate. Note that the depicted data are only from those trials in which the tactile stimulus occurred 3 s after the cue.

s (three-point-hazard rate) or at 1 and 3 s (two-point hazard rate). Crucially, the stimulus was never expected in between these three time-points. To assess temporal specificity, we compared the two hazard rate conditions as well as the time-points within each of the two hazard rate conditions.

Figure 3.3 shows the time courses of the alpha- (Fig. 3.3A) and beta-band (Fig 3.3B) contra-over-ipsi ratios of oscillatory power, separately for the two hazard rates. Comparing the two hazard rates by means of a cluster-based permutation test (see Materials and Methods) yielded a significant cluster ($p < 0.05$) exactly in the time window where the two hazard rates differ. However, this significant difference was only observed for beta-band oscillations (Figure 3.3B). This shows that the contralateral suppression of beta-band oscillations is determined not only by a cue that directs spatial attention, but also by whether or not an event is expected at a specific moment in time. Note that this difference cannot be explained by the auditory pacing tones, as these occurred identically in the two- and three-point hazard rates.

Comparing the contra-over-ipsi power ratios within each hazard rate revealed an even more striking temporal specificity. Focusing on the three-point hazard rate (red line), we observe that the beta lateralization (Fig. 3.3B) is strongest just prior to each expected event and relaxes in between. To assess this pattern quantitatively, we statistically compared the power ratios between two sets of time windows: time windows prior to expected events and time windows in-between expected events (see Materials and Methods). This comparison showed a significant effect of temporal specificity ($t_{(19)} = -3.12$; $p < 0.01$). This effect was even stronger in the two-point hazard rate condition (blue line; $t_{(19)} = -5.20$; $p < 0.001$). Interestingly, for the alpha lateralization (Figure 3.3A), a significant temporal modulation was observed only in the two-point hazard rate condition (blue line; $t_{(19)} = -2.79$; $p < 0.05$). Thus, alpha lateralization relaxes when successive time points of interest are spaced 2 s apart, but not when these are spaced only 1 s apart. These results show that spatially specific modulations of ongoing oscillations track the temporal positions at which an event is expected to occur, and that this temporal specificity is more pronounced for sensorimotor beta- as compared to alpha-band oscillations.

Anticipatory modulation of oscillatory power was also quantified by separate contra-over-baseline and ipsi-over-baseline power ratios. Outcomes of these analyses are depicted in Supplementary Figure 3.7.

Beta suppression over contralateral sensorimotor cortex is associated with faster responses to subsequently presented tactile stimuli

We were interested in whether the observed contralateral alpha- and beta-suppression also leads to better task-performance. For this, we separated trials with correct and incorrect responses as well as with a slow and a fast response (based on a median split). No significant differences were found between trials separated on the basis of accuracy. However, significant differences were found between trials separated on the basis of response time. This was

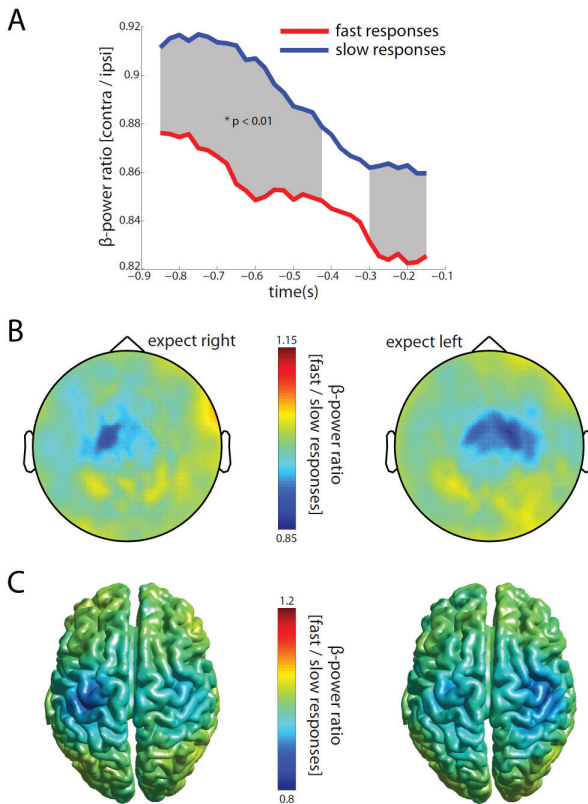


Figure 3.4. The contralateral pre-stimulus beta-suppression is associated with faster responses to tactile stimuli. (A) Ratio between contralateral and ipsilateral beta power, separately for fast and slow responses. Fast and slow responses were separated by a participant-specific median split on the response times. Shading indicates the time windows for which slow and fast responses differ significantly (permutation test; $p < 0.01$). (B) Topographies of the pre-stimulus beta power ratio between fast and slow responses [fast / slow], separately for anticipation of left and right hand tactile stimuli. Beta power was estimated for the last 350 ms preceding the tactile stimulus. (C) Identical to panel B, except that the pre-stimulus beta power ratio between fast and slow responses was calculated in source space.

er over primarily the contralateral sensorimotor cortex.

This relation between response time and the contra-over-ipsi beta power ratio does not reflect motor anticipation. In fact, prior to the stimulus, motor preparation cannot be lateralized. The relation between response time and the beta power ratio is also not simply mediated by temporal position. In fact, although response times decreased with the position of the stimulus in the trial, the pre-stimulus contra-over-ipsi beta power ratio did not change across the possible positions of the stimulus, as can be observed in Figure 3.3B. Thus, we conclude that pre-stimulus contralateral beta power relates to the efficacy by which the upcoming tactile stimulus can be processed and subsequently responded to.

the case only for beta-band oscillations, on which we report below.

Figure 3.4A shows the contra-over-ipsi beta power ratio for the second prior to the tactile event to which the response was made, separately for the fast (on average 723 ms) and the slow (on average 1329 ms) responses. Fast responses are preceded by a significantly lower contra-over-ipsi beta power ratio as compared to the slow responses. The cluster-based permutation test identified two significant clusters ($p < 0.01$) of which one extends up to a second prior to the stimulus. Figure 3.4B shows the topographies of the differential pre-stimulus beta power for the fast and slow responses, separately for subsequent left and right hand stimuli. Figure 3.4C shows the corresponding source reconstructed images. These figures show that fast as compared to slow responses are associated with lower pre-stimulus beta power

3.4 Discussion

We set out to investigate whether anticipation of a tactile event involves a spatially as well as temporally specific modulation of ongoing alpha- and beta-band oscillations within sensorimotor cortex. We observed three phenomena. First, orienting to an upcoming tactile event involves a spatially specific modulation of alpha- and beta-band oscillations within sensorimotor cortex. This modulation is most prominent for beta-band oscillations and is constituted by a contralateral suppression. Second, this modulation is deployed not only with spatial, but also with temporal specificity. This temporal specificity is more pronounced for beta- as compared to alpha-band oscillations. Third, the contralateral suppression of beta-band oscillations is associated with faster responses to subsequently presented tactile stimuli. These observations cannot be explained by motor preparation or execution and are thus associated with preparation for the upcoming sensory event.

Knowing when an event is likely to occur facilitates its perception, a phenomenon that is accounted for by temporal orienting of attention (Nobre, 2001). This temporally selective form of attention is associated with activation of numerous brain areas (Coull and Nobre, 1998), modulation of event-related potentials (Miniussi et al., 1999) and firing rates (Ghose and Maunsell, 2002), and a phase-alignment of delta-band oscillations (Lakatos et al., 2008). We show that temporal orienting of attention also involves a temporally specific modulation of the pre-stimulus amplitudes of ongoing oscillations within sensory cortex. This pre-stimulus modulation may underlie the observed post-stimulus modulations of both event-related potentials (Miniussi et al., 1999) and firing rates (Ghose and Maunsell, 2002), as well as the facilitation of perception that is produced by temporal orienting of attention (Nobre, 2001). While the former pertain to an open question, we provide evidence for the latter. In fact, pre-stimulus suppression of beta-band oscillations within contralateral sensorimotor cortex is associated with faster responses to subsequently presented tactile stimuli. We believe that these faster responses result from more efficient processing of the tactile input when these arrive during a state of suppressed beta-band oscillations. Because this state is most pronounced at times when stimuli are expected to occur, the observed modulation constitutes a mechanism by which temporal orienting of attention can facilitate perception.

As compared to temporally selective attention, spatially selective attention has been studied more extensively. Several studies have shown that spatial orienting of attention involves spatially specific modulations of ongoing oscillatory activity within sensory cortices. This phenomenon is well established for orienting to an upcoming visual event (Worden et al., 2000; Sauseng et al., 2005; Kelly et al., 2006; Thut et al., 2006), and we and others have recently observed a similar modulation for orienting to an upcoming tactile event (Jones et al., 2010; **chapter 2**). The present study adds to these findings by showing that this modulation (1) is flexibly modulated by temporal predictability (2) is constituted by a contralateral suppression (3) occurs in both the alpha- and the beta-band and (4) improves behavioral performance in terms of response times. To complete the picture, a

recent study has shown modulations of alpha-band oscillations associated with feature-specific anticipation (Snyder and Foxe, 2010). In sum, there is good empirical evidence for a general mechanism of attentional orienting that deploys anticipatory modulation of ongoing oscillations both across modalities (visual, somatosensory) and dimensions (space, time, feature).

Alpha- and beta-band modulations are characterized by a different degree of temporal specificity. In contrast, the spatially specific modulations of the alpha- and the beta-band oscillations are highly similar. Evidence for the different degree of temporal specificity is that only for beta-band oscillations, a difference could be observed between the two hazard rates. Moreover, while the lateralized modulation of beta-band oscillations relaxed in between two successive anticipated events that are spaced by only 1 s, the lateralized modulation of alpha-band oscillations relaxed only between two successive anticipated events that are spaced by 2 s. The difference may originate from a different physiological origin of the two sensorimotor oscillations. In fact, in a modeling study, Jones et al. (2009) showed that, whereas alpha-band oscillations may be produced by a thalamo-cortical feedforward drive, beta-band oscillations require an additional feedback drive from higher order cortical areas. However, it cannot be ruled out that the observed difference between alpha- and beta-band oscillations resulted from our data-analysis being more sensitive to the beta-band (see Materials and Methods). Despite this possible data-analytic disadvantage for alpha-band oscillations, we did observe a robust spatially specific modulation of alpha-band oscillations. For this reason, we conclude that the observed difference in temporal specificity between the alpha and beta modulation is of physiological origin. An open question pertains to whether these differences between alpha- and beta-band modulations are restricted to tactile anticipation or are likewise observed in anticipation of sensory events in different modalities. A further open question pertains to whether a similar degree of temporal specificity would have been obtained if we had not used pacing tones to induce temporal expectancy.

Related to the functional differentiation of alpha- and beta-band oscillations with respect to somatosensation, is the issue of their localization. Traditionally, rolandic alpha is considered to be primarily a post-central rhythm whereas rolandic beta is considered to be primarily a pre-central rhythm (Salmelin and Hari, 1994). Accordingly, beta is attributed to the motor and alpha to the somatosensory system. This notion is in conflict with our observation of beta-band oscillations as an index of somatosensory anticipation. However, recent evidence suggests that this traditional view is probably an oversimplification. First, tactile stimulation induces changes in beta power (Salenius et al., 1997b; Cheyne et al., 2003; Bauer et al., 2006; Gaetz and Cheyne, 2006). Second, intracranial electrophysiological measurements directly on the post-central gyrus, have shown beta-band oscillations that originated from S1 (Crone et al., 1998; Brovelli et al., 2004). Witham and Baker (2007a) even recorded stronger beta-band oscillations in S1 than in M1. Third, pre- and post-stimulus beta-band oscillations are related to detectability of tactile stimuli (Linkenkaer-



Hansen et al., 2004; Palva et al., 2005; Jones et al., 2010) as well as the speed with which tactile stimuli are responded to (present study). All three sets of observations show that beta-band oscillations play a role in somatosensation. Further, from a more theoretical perspective, Engel and Fries (2010) propose that beta-band oscillations play a central role in the maintenance of cognitive and sensorimotor states, both within and outside of the motor system. They hypothesize that anticipation of a change is associated with a suppression of beta- and a concomitant increase in gamma-band oscillations. Although our data do not support their prediction with respect to gamma, they are fully in line with their prediction with respect to beta.

A fundamental question pertains to the mechanism by which the pre-stimulus suppression of ongoing alpha- and beta-band oscillations facilitates perception. Although there is ample evidence that these oscillations relate inversely to both excitability (Chen et al., 1998; Sauseng et al., 2005; Tamura et al., 2005; Romei et al., 2008) as well as the efficacy with which information is processed (Ergenoglu et al., 2004; Linkenkaer-Hansen et al., 2004; Thut et al., 2006; Hanslmayr et al., 2007; van Dijk et al., 2008; Zhang et al., 2008b; Romei et al., 2010), it is at present an open question what the underlying mechanisms are. In the following, we speculate about a neurophysiological mechanism by which a pre-stimulus suppression of alpha- and beta-band oscillations can facilitate perception. Reductions in EEG/MEG oscillatory power are commonly interpreted as the result of a desynchronization of underlying neuronal activity (Pfurtscheller and Lopes da Silva, 1999). Accordingly, our observations might reflect the instantiation of a desynchronized neural context that allows for enhanced processing of future sensory input. This may occur via both intra- and interareal processes. With regard to the former, theoretical analysis has shown that the signal-to-noise ratio of pooled neuronal activity increases when the neuronal population desynchronizes (Zohary et al., 1994). Along these lines, attention has been shown to decorrelate neuronal activity in monkey area V4 (Mitchell et al., 2009; Cohen and Maunsell, 2009). Between cortical areas, an efficacious neural context may be provided by selective oscillatory coupling between upstream and downstream populations (Fries, 2005). Selective neuronal gating occurs when multiple competing upstream populations do not oscillate in synchrony (i.e. are desynchronized), allowing only the selected (attended) population to engage in information exchange with the downstream population (Fries, 2005). We thus speculate that the suppression of alpha- and beta-band oscillatory power may reflect a desynchronization of the underlying neuronal populations that (1) increases the signal-to-noise ratio of the pooled neuronal activity (within S1) and (2) allows for a selective gating of neuronal activity (e.g., between S1 and S2). Future work is required to test and understand the physiological mechanisms underlying the anticipatory power reduction reported here.

In conclusion, anticipation of a tactile event involves a spatially as well as temporally specific modulation of ongoing sensorimotor alpha- and beta-band oscillations. The modulation of ongoing oscillations within sensory cortex may therefore constitute a unifying mechanism underlying both spatial and temporal orienting of attention.

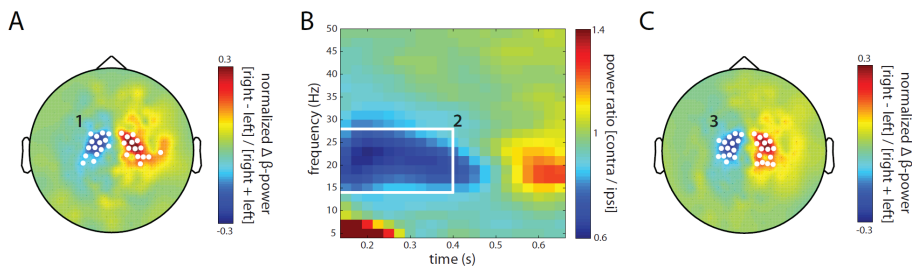


3.5 Supplementary Figures (3.1 - 3.7)

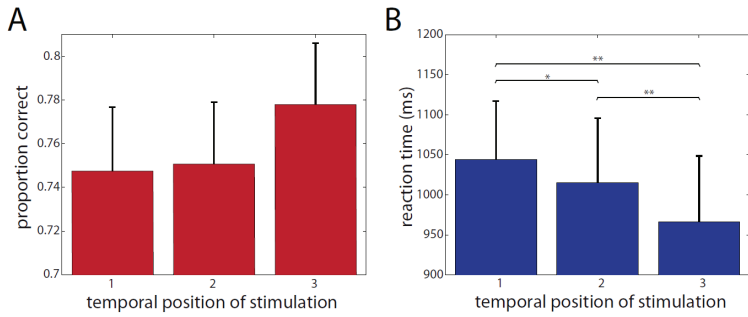


Supplementary Figure 3.1. Braille stimulator. A Braille stimulator has five Braille cells built-in (four on the side, one on the top) and a response button (also on the top). Each Braille cell contains 8 pins, aligned in 2 series of 4, that can be raised and lowered. Individual Braille cell positions are adjustable. When grasped, all five fingertips overlie a Braille cell. Two such devices were used in the experiment, one for each hand.

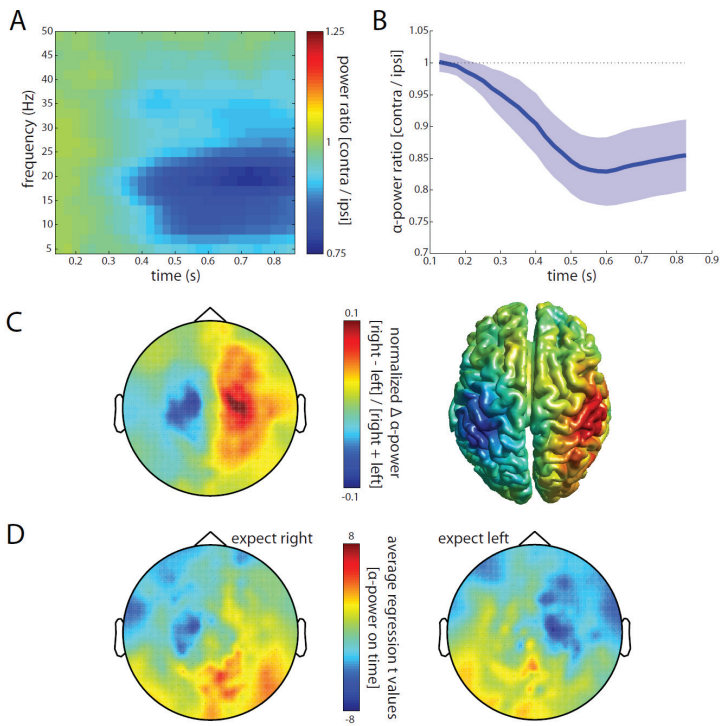
- Step 1: estimate β -power over the a-priori defined time window and spectral band (100-300 ms; 15-30Hz), contrast right and left hand stimulations and select the 15 most negative and the 15 most positive channels to represent S1 left and S1 right, respectively
- Step 2: contrast the 15-channel averaged time-resolved power estimates between contralateral and ipsilateral stimulation [contra/ipsi], pool both S1 contrasts and select the participant-specific time window and spectral band of the post-stimulus β -power modulation
- Step 3: repeat step 1, using the participant-specific time window and spectral band; obtain the participant-specific S1 left and S1 right channels



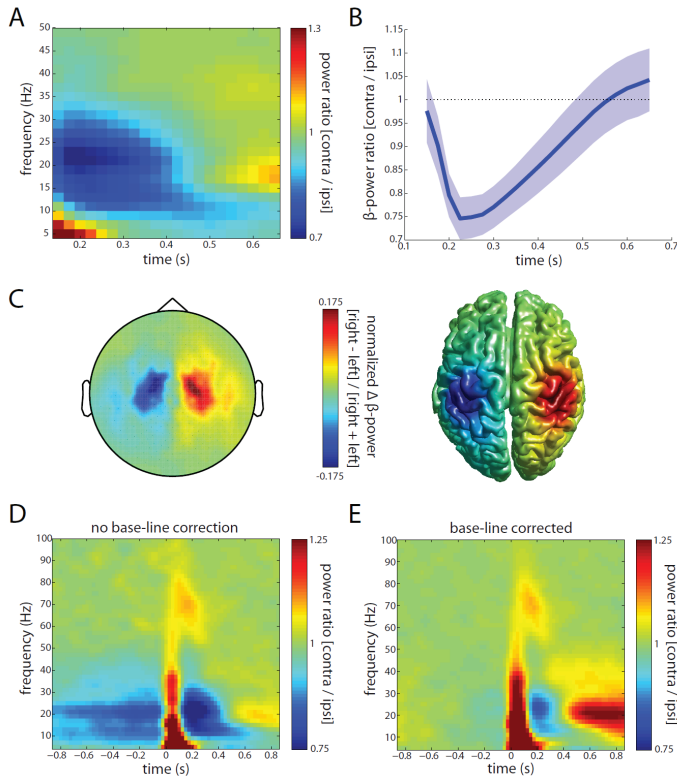
Supplementary Figure 3.2. Channel selection protocol, illustrated for a representative participant. (A) Topography of the post-stimulus normalized beta power difference between right and left hand tactile stimulation $[(\text{right}-\text{left})/(\text{right}+\text{left})]$. Beta-power in the 15-30 Hz band is estimated over the a-priori defined time window of 100-300 ms after the stimulus. White circles indicate channels with the 15 highest and 15 lowest contrast values. (B) Time-resolved power ratio between channels contralateral and ipsilateral to the tactile stimulation, which occurs at 0 s. For the construction of the contra-over-ipsi power-ratio, the channels marked in panel A were used. The white box indicates the participant-specific temporal and spectral locus of the stimulus-induced beta modulation. (C) Topography calculated in the same way as for panel A, but now using the participant-specific beta modulation time window and spectral band that is indicated by the white box in panel B.



Supplementary Figure 3.3. Behavioral data. (A) Proportions correct for tactile stimuli occurring 1, 2 or 3 s after the cue (temporal positions 1, 2 and 3 respectively). (B) Average reaction times for tactile stimuli occurring 1, 2 or 3 s after the cue. Error bars represent 1 standard error above the mean; * $p < 0.05$, ** $p < 0.01$.

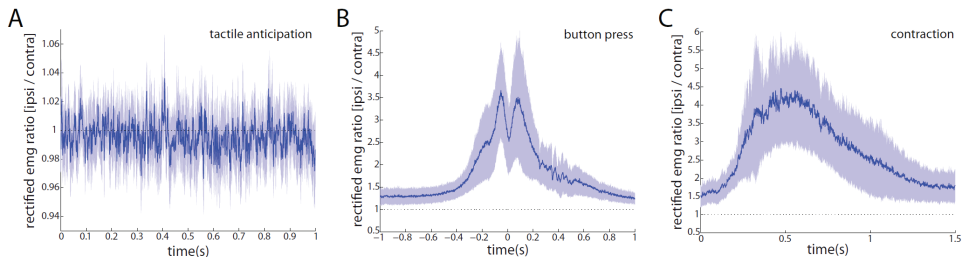


Supplementary Figure 3.4. Spatial orienting involves a lateralization of alpha-band oscillations. Panel A is identical to panel A of Figure 3.2. Panels B-D are calculated in the same way as the corresponding panels of Figure 3.2, but now for the alpha- instead of the beta-band.

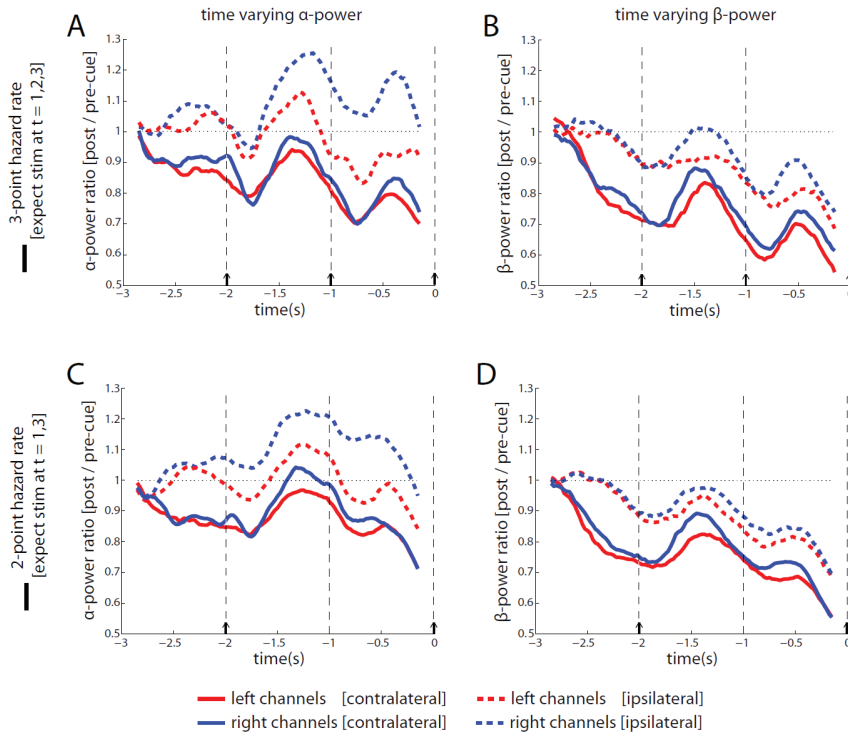


Supplementary Figure 3.5. Tactile stimulus-induced modulations and the effect of pre-stimulus baseline correction for a predictable tactile stimulation. (A) Time-resolved power ratio between sensorimotor channels contralateral and ipsilateral to the tactile stimulus occurring at 0 s. (B) Time-resolved beta power ratio including its 95 % confidence interval, with the standard error calculated using the variance across participants. (C) Topography and source reconstruction of the lateralized stimulus-induced beta power modulation. The color code reflects the normalized difference in beta power following left and right hand stimuli [(right - left) / (right + left)]. Beta power was estimated over the interval [100-350] ms after the stimulus. (D) Same calculation as for panel A, but now for a time axis that involves both the

pre- and the post-stimulus period, and for a frequency axis that ranges from 5 to 100 Hz. (E) Same calculation as for panel D, except that the raw power was baseline corrected prior to the calculation of the contra-over-ipsi power ratio. The baseline correction was performed by dividing the raw power in all time points by the frequency-specific time-averaged power calculated over the pre-stimulus window from -1 to 0 s.



Supplementary Figure 3.6. Rectified EMG activity during motor behavior and tactile anticipation. (A) Time-resolved ratio between ipsilateral and contralateral rectified EMG traces during tactile anticipation. Blue shading indicates the 95 % confidence interval, with the standard error calculated using the variance across participants. The cue is presented at 0 s, and the first position at which the tactile stimulus may occur is at 1 s. Note that the corresponding MEG data is depicted in Figure 3.2B. (B) Same calculation as for panel A, but now applied to EMG traces centered at a left or right hand button press. The button was pressed at 0 s. (C) Same calculation as for panel A, but now applied to EMG traces that follow a cue requesting the participant to contract his left or right hand. This cue was presented at 0 s.



Supplementary Figure 3.7. Time-varying power over contralateral and ipsilateral sensorimotor cortex, relative to the power in a pre-cue baseline. (A) Baseline-corrected time-resolved alpha power in the three-point hazard rate condition, separately for the left (red lines) and right (blue lines) channels, and for anticipation of a contralateral (solid lines) and an ipsilateral (dashed lines) stimulus. Black arrows indicate the temporal positions at which tactile stimuli were expected. Only trials for which the tactile stimulation occurred at 3 s after the cue were analyzed. Baseline correction was performed by dividing the raw time-resolved power by the frequency-specific time-averaged power calculated over the pre-cue window from -3.5 to 3 s. (B) Same calculations as for panel A, but now for power in the beta-band. (C) Same calculations as for panel A, but now for the two-point hazard rate condition. (D) Same calculations as for panel A, but now for power in the beta-band and the two-point hazard rate condition. This quantification thus shows that the temporal specific modulations that are depicted in Fig. 3.3 manifests themselves not only on the contralateral but, to a lesser extent, also on the ipsilateral channels. This quantification furthermore shows that, at least so for the beta-band (panels B and D), power decreases over time, in parallel with the increase in hazard rate (i.e., the more likely for a stimulus to occur in the next interval, the lower the power). Unfortunately, it is not clear to what extent these modulations are driven by nonspecific effects of time, bilateral motor preparation, and/or the bilateral presentation of the tones.

Attentional cues affect accuracy and reaction time via different cognitive and neural processes

Adapted from van Ede F, de Lange FP, Maris E (2012) *Attentional cues affect accuracy and reaction time via different cognitive and neural processes*. *The Journal of Neuroscience* 32:10408-10412.

4

Abstract

We investigated whether symbolic attentional cues affect perceptual accuracy and reaction time (RT) via different cognitive and neural processes. We recorded Magnetoencephalography (MEG) in 19 humans while they performed a cued somatosensory identification task in which the cue-target interval was varied between 0 and 1000 ms. Comparing behavioral and neural measures we show that (1) attentional cueing affects accuracy and RT with different time courses and (2) the time course of our neural measure (anticipatory suppression of neuronal oscillations in stimulus-receiving sensory cortex) only accounts for the accuracy time course. A model is proposed in which the effect on accuracy is explained by a single process (preparatory excitability increase in sensory cortex), whereas the effect on RT is explained by an additional process that is sensitive to cue-target compatibility (post-target comparison between expected and actual stimulus location). These data provide new insights into the mechanisms underlying behavioral consequences of attentional cueing.

4.1 Introduction

Cognitive processes are typically inferred from behavioral data such as accuracy and reaction time (RT). For example, through such data, it is now well-accepted that perception is improved by knowledge of upcoming stimuli, through *voluntary orienting of attention*. This is inferred from both RT decreases (Posner, 1980a; 1980b; Coull and Nobre, 1998) and perceptual accuracy increases (Carrasco, 2011) to validly (as compared to invalidly) cued stimuli.

It is often implicitly assumed that task-induced changes in accuracy and RT are a manifestation of the same underlying cognitive and neural process. An important question pertains to whether this common belief holds true. This is important because it is the cognitive and neural architecture that we are ultimately interested in. Dissociable influences of an experimental manipulation on accuracy and RT will inform us about the existence of distinct underlying cognitive and neural processes.

We investigated the effects on accuracy and RT of a symbolic cue, which allows for voluntary spatial orienting of attention. To address the dissociability of accuracy and RT effects, we looked for two types of evidence. First, we investigated the time course of the effect of a symbolic cue on both accuracy and RT. These time courses were extracted by presenting target stimuli at varying cue-target intervals. In case of dissimilar time courses for accuracy and RT, this implies distinct underlying causes. Second, we investigated the correspondence between these behavioral time courses and the time course of a recently proposed neurophysiological mechanism underlying voluntary attentional orienting: anticipatory suppression of neuronal oscillations in the stimulus-receiving sensory cortex (Worden et al., 2000; Thut et al., 2006; Jones et al., 2010; **chapters 2 and 3**). If this neurophysiological time course corresponds to only one of the two behavioral time courses, this directly shows distinct underlying processes.

Our results show that (1) cueing affects accuracy and RT with different time courses and (2) the neurophysiological time course (indexing anticipatory suppression of neuronal oscillations) only accounts for the accuracy time course. At surprisingly short cue-target intervals, RT effects occur in the absence of both accuracy improvement and anticipatory suppression of neuronal oscillations. To explain these effects, we propose a model in which the accuracy effects are fully explained by a single process (preparatory excitability increase in relevant sensory cortex), whereas the RT effects are at least partly explained by another process (post-target comparison between expected and actual stimulus location).

4.2 Materials and Methods

Participants, design, & task

Nineteen right-handed healthy participants (13 male; age: $M = 27.95$, $SD = 5.38$) took part in the experiment. Two participants were excluded from the analyses because they performed at chance level. The experiment was conducted in accordance with guidelines of the local ethical committee (Committee on Research Involving Human Subjects, Region Arnhem-

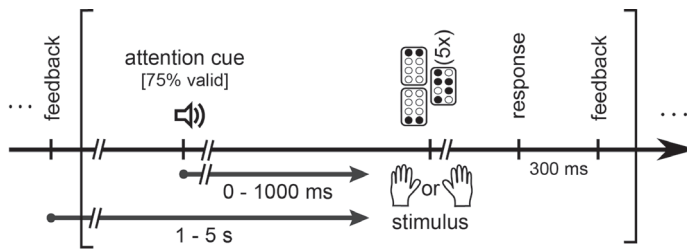


Figure 4.1. Task. A symbolic auditory cue indicates with 75 % validity whether a tactile stimulus will occur on the left or the right hand. Between 0 and 1000 ms after this cue, the target stimulus is presented to the upper or lower part of all fingertips (using the upper or lower pins of the Braille-cells; see black dots) of either hand. This is followed by 5 masks without spatial structure. Participant's task is to discriminate the target (upper or lower) and respond with the right (upper target) or left (lower target) button. After a response, feedback is presented.

of the fingertips of all fingers of a single hand (Fig. 4.1). For tactile stimulation, we used a custom-built Braille-device that has been described previously (**chapters 2 and 3**). On 80 % of the trials, this tactile stimulus was preceded by an auditory cue (25 ms duration) that indicated with 75 % validity on which hand the to-be-discriminated stimulus would occur. Cue type (white noise or a 750 Hz pure tone) was counterbalanced across participants. In order to investigate behavioral time courses, we varied the interval between auditory cue and tactile target. Per trial, this interval was randomly drawn from a uniform distribution with values between 0 and 1000 ms. The remaining trials consisted of two baseline conditions (tactile target presented without a preceding cue or simultaneously with a valid cue) and trials in which no stimulus followed the cue.

The tactile target (see Fig. 4.1) was followed by 5 masks that contained no spatial structure (individual masks lasted 20 ms, inter-mask interval was 50 ms). Masking of the target was used to increase the difficulty of the identification, thus allowing attentional orienting to improve performance. For both hands, tactile stimulation by the upper (lower) pins required a right (left) hand button-press. Because of this, the side of the (expected) target and the side of the subsequently required button-press were uncorrelated. Responses were self-paced. Tactile feedback was presented 300 ms after the response. A correct (incorrect) response was followed by a single (double) 20 ms tap to both hands. The interval between feedback and the next stimulus was drawn from a truncated negative exponential distribution (range: 1-5 s). Because this distribution has a nearly flat hazard rate, the onset of the next cue could not be predicted on the basis of elapsed time since the last cue. In two sessions of approximately 1 hour each, we collected approximately 1500 trials.

Analysis of behavioral data

We calculated time-resolved measures of accuracy and RT, with the time pertaining to the different cue-target intervals. We calculated average behavioral performance for stimuli occurring within a 250 ms cue-target interval window. This window was advanced in 60 steps from 125 ms to 875 ms post-cue. For each participant, we then normalized these

Nijmegen, The Netherlands).

Participants performed a cued somatosensory identification task that required the identification of a tactile stimulus (20 ms duration) that was presented at either the lower or the upper part



data in two ways: (1) we expressed performance on validly and invalidly cued stimuli as a percentage change from the average of our two baseline conditions (Fig. 4.2A,C) and (2) we contrasted validly and invalidly cued trials, and expressed this contrast as a percentage change (Fig. 4.2B,D). With this second normalization we calculate so-called *cue validity effect time courses*.

Recording & analysis of neural data

Recordings and analyses of neural data were highly similar to previous reports from our lab (**chapters 2 and 3**). Data were collected using a 275 axial gradiometers MEG system (CTF MEG TM Systems Inc., Port Coquitlam, Canada), and analyzed in FieldTrip (Oostenveld et al., 2011). From the axial gradiometer signal, we calculated the planar gradient (Bastiaansen and Knosche, 2000), which is maximal above the neuronal sources. Using the post-stimulus data, we selected for each participant (1) the 10 channels above left and right primary somatosensory cortex (S1), and (2) the individual frequency-band that showed the strongest stimulus-induced lateralization (left- versus right-hand stimulus). We estimated oscillatory amplitude using the multitaper method (Percival and Walden, 1993). For both left and right channels we contrasted contralateral and ipsilateral anticipation (Fig. 4.2E,F). Then left and right channels were averaged. This *anticipatory neural lateralization* was then analyzed with the same sliding time-window that was used for the calculation of the behavioral time courses. We only used data from epochs without tactile stimulation.

Comparing time courses

We fitted three-parameter logistic functions to the observed behavioral (cue validity effect) and neural (anticipatory neural lateralization) time courses:

$$f(t) = \frac{p_1}{1 + e^{-(t-p_2)/p_3}}$$

This is a sigmoid function of which right and left asymptote are determined by p_1 and p_2 , and the slope by p_3 . Parameters were estimated using a nonlinear least-square algorithm in Matlab (Mathworks, <http://www.mathworks.com>).

We wanted to compare the cue dependent time courses for accuracy, RT and the anticipatory neural lateralization, which have different scales and different signs. We determined the effect size of each measure by calculating the right asymptote of the fitted logistic function. We then scaled the time course of each measure with respect to its maximal effect size. Accuracy increase, RT decrease and stronger neural lateralization (i.e. lower contra- minus ipsilateral amplitude) were expressed as positive effects with their time courses increasing monotonically from 0 to 1 (Fig. 4.3).

To statistically compare the three time courses, we fitted and normalized logistic functions per participant and calculated the areas under these curves. Under the null hypothesis of identical normalized time courses, this metric does not differ. We evaluated this null hypothesis using paired sample t-tests (alpha = 0.05, two-tailed).

4.3 Results

On average, participants correctly discriminated between the two tactile patterns (Fig. 4.1) on 70 ± 1.5 (mean ± 1 s.e.m.) % of the trials. Average reaction time was 931 ± 77 ms.

Figure 4.2 reveals accuracy and RT as a function of time after the attentional cue. These time courses are derived from responses to target stimuli occurring at various cue-target intervals (see Materials and Methods). For example, after a valid cue, perceptual accuracy increases between 200 and 600 ms after this cue (red line, Fig. 4.2A). This did not

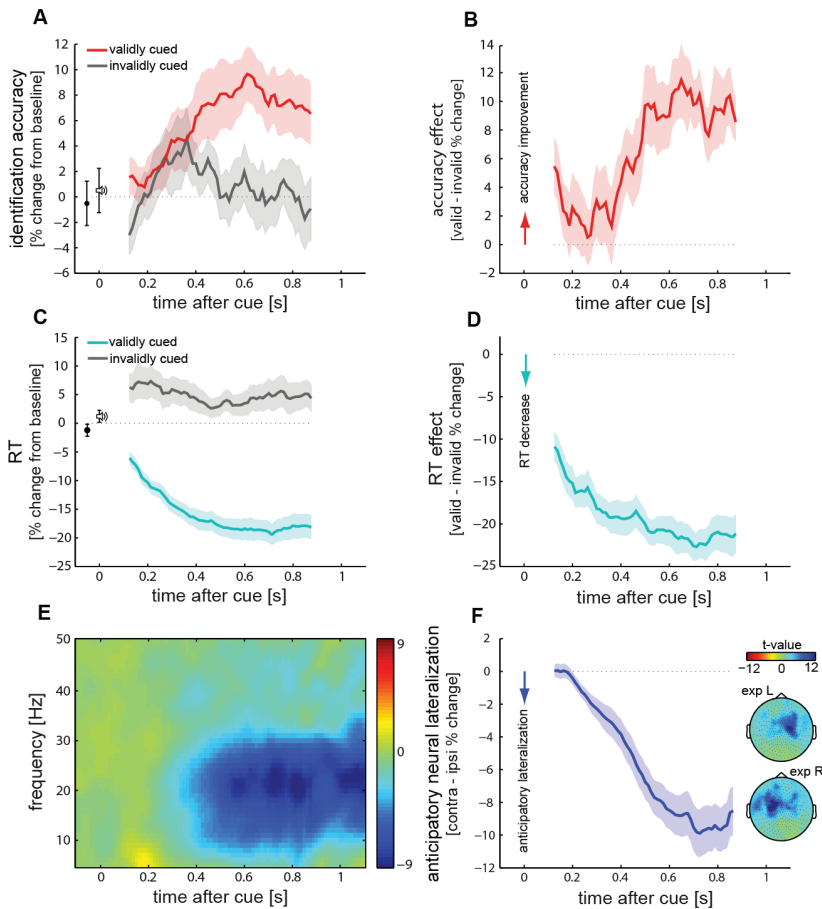


Figure 4.2. Behavioral and neural time courses following a symbolic attentional cue. (A) Tactile identification accuracy, as a function of cue-target interval and cue validity. Data are expressed as the percentage change from the average of two baseline conditions: stimulus occurring without a cue (depicted before $t = 0$) or simultaneous with a cue (depicted at $t = 0$). (B) Cue validity effect (valid minus invalid) on accuracy, expressed as a percentage. (C, D) similar to A and B, for RT. (E) Anticipatory neural lateralization as a function of frequency and time after the cue. Color-code denotes the difference in amplitude between contralateral and ipsilateral primary somatosensory cortex with respect to the cued location. (F) Same as E, except that data are extracted for a single frequency range (between 8-30 Hz, see Method), containing the alpha- and/or beta-band. Insets depict t-valued topographies of the correlation between oscillatory amplitude and time-after-cue. Error bars and colored patches surrounding the time courses represent ± 1 s.e.m.

occur on invalidly cued trials (grey line, Fig. 4.2A), as there was no clear deviation from baseline (no cue or a target presented simultaneously with a cue).

Assuming that validly and invalidly cued trials differ only in the induced direction of spatial attention (contra- versus ipsilateral to the upcoming target), contrasting the two time courses directly reveals the effect of this spatial orienting of attention. Figure 4.2B shows the time course of this cue validity effect for accuracy. This time course is well in line with several previous studies in the visual modality (Muller et al., 1998; Busse et al., 2008; Andersen and Muller, 2010). Following a symbolic cue, perceptual accuracy starts to improve around 200-300 ms, continues to increase till 500-700 ms and then stabilizes.

If multiple behavioral consequences of a symbolic cue are all due to a single underlying process (spatial orienting of attention), then the time courses of these behavioral consequences (i.e. accuracy and RT) must be identical. However, this is not what we observe. The time course of the cue validity effect for RT (Fig. 4.2D) follows a distinct time course, starting much earlier after the cue and changing less rapidly. (This time course did not qualitatively differ between correct and incorrect responses, and therefore these responses were collapsed.) These data indicate that the time courses of the two behavioral consequences of cue validity must be caused, at least in part, by distinct underlying cognitive and neural processes.

Next to the time courses of behavioral cue validity effects, we also investigated the time course of a neural phenomenon that has been proposed to underlie the behavioral consequences of attentional orienting: anticipatory suppression of alpha- and beta-band oscillations in the stimulus-receiving sensory cortex (Worden et al., 2000; Thut et al., 2006; Jones et al., 2010; **chapters 2 and 3**). Concurrently with the behavioral data, we collected MEG signals that were analyzed with the same time resolution (250 ms, see Materials and Methods). We analyzed an anticipatory neural lateralization time course by contrasting anticipation of contralateral and ipsilateral targets. Like the behavioral cue validity effects, this reflects a spatially specific (and thus comparable) measure. Figure 4.2E shows anticipatory neural lateralization with frequency resolution. Clearly, anticipation involves a lateralized modulation of oscillatory activity in the alpha- and the beta-bands (together 8-30 Hz). The time course of this effect is depicted in Figure 4.2F. Because the time courses of alpha- and beta-band lateralizations were highly similar, they were considered together. Anticipatory neural lateralization starts around 200 ms, continues to increase up to 600-700 ms, and then stabilizes. This lateralization is the result of a contralateral suppression. In fact, the amplitude over contralateral MEG channels correlates negatively with the time following the cue (insets Fig. 4.2F; cf. **chapter 3**, Fig. 3.2D).

We investigated whether the time course of this anticipatory neural lateralization could account for the time courses of the behavioral cue validity effects (accuracy and/or RT). To address this question, we fitted logistic functions to these behavioral and neural cue dependent time courses (see Materials and Methods). Results are depicted in Figure 4.3. While the time course of the anticipatory neural lateralization is highly similar to the

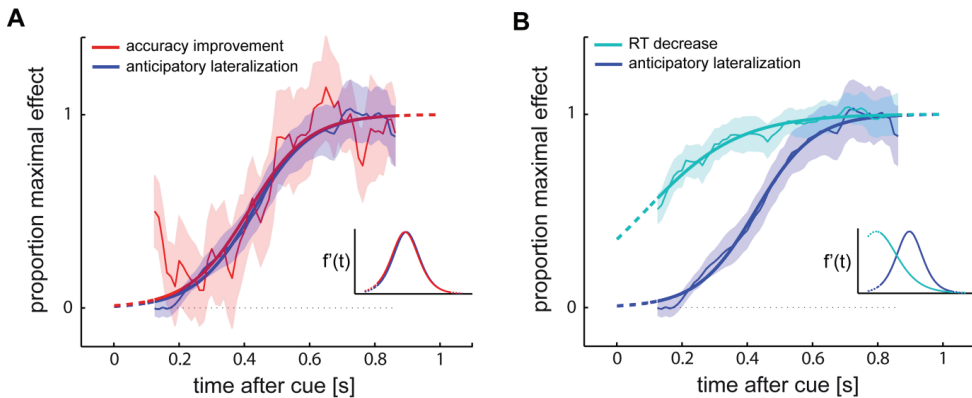


Figure 4.3. Anticipatory neural lateralization accounts for cue validity effect on accuracy but not RT. (A) Overlay of cue validity effect on accuracy and anticipatory neural lateralization. Plots include fitted logistic functions that are normalized to their maximal effect (see Method). An effect of 0 signifies no difference between validly and invalidly cued stimuli (accuracy) or contra- and ipsilateral S1 alpha- and beta-band amplitude (anticipatory neural lateralization). Inset shows rates of change of these functions. (B) Identical to A, except RT is depicted instead of accuracy.

time course for cue validity effect on perceptual accuracy (panel A), the cue validity effect on RT precedes the neural lateralization (panel B). To quantify these phenomena, we fitted these logistic functions to single-subject data, and calculated a single metric that allows for a comparison of the three time courses (see Materials and Methods). This showed that the cue validity effect on RT systematically preceded the cue validity effect on accuracy ($t_{(16)} = -2.337$, $p = 0.033$) as well as the anticipatory neural lateralization ($t_{(16)} = -7.2378$, $p < 10^{-5}$). Time courses of the cue validity effect on accuracy and the anticipatory neural lateralization did not differ significantly ($t_{(16)} = 1.148$, $p = 0.268$).

4.4 Discussion

We observe that the two most-studied behavioral consequences of attentional cueing (perceptual accuracy increase, RT decrease) follow dissimilar time courses: the cue validity effect on RT precedes the effect on accuracy. This implies that distinct cognitive and neural processes underlie the different behavioral consequences of symbolic cueing. We investigated one such neural process, anticipatory suppression of alpha- and beta-band oscillations in contralateral primary sensory cortex, and observed that this accounts only for the cue validity effect on accuracy. To account for the cue validity effect on RT, at least one additional underlying process must be postulated.

Our results add to the existing literature in two important aspects. First, we show a dissociation between accuracy and RT following a manipulation of voluntary (endogenous) spatial attention (by comparing validly and invalidly cued stimuli). Previously, such a dissociation has only been reported between two different forms of attention, voluntary and involuntary (Prinzmetal et al., 2005). Second, our data reveal that the anticipatory



suppression of neuronal oscillations is an important process underlying accuracy improvement with symbolic cueing. Previously this neural phenomenon has been associated with both accuracy (Thut et al., 2006; Yamagishi et al., 2008; Haegens et al., 2011a) and RT improvement (Thut et al., 2006; Haegens et al., 2011a; **chapter 3**). Our results show that RT improvement can also occur in the absence of this neural phenomenon, namely at short cue-target intervals. It is important to point out that this does not invalidate previous observations showing that anticipatory alpha- and beta-band modulation is related to RT. Instead, it shows that, in order to give a *complete* account of cue validity effects on RT, additional neural processes must be identified. An important goal for future research will be to quantify exactly how much of the cue validity effect on RT can be accounted for by the anticipatory suppression of alpha- and beta-band oscillations.

We propose that at least two processes are involved in the behavioral consequences of symbolic cueing. The first process is preparatory (occurs prior to the target) and affects both accuracy and RT. This is the process to which behavioral consequences of symbolic cueing are typically attributed. The second process is non-preparatory (occurs after the target) and affects only RT. This process has not been postulated before.

Our model (Fig. 4.4) applies to tasks in which participants receive a symbolic cue that contains information about the likely spatial location of the upcoming target (e.g. Posner's cueing paradigm). Once the meaning of the cue has been extracted, participants can initiate spatially specific preparatory processes, such as an increase in neuronal excitability in the relevant (stimulus-receiving) sensory cortex. Upon arrival of validly cued stimuli, this leads to enhanced processing of sensory information, which in turn leads to more accurate as well as faster stimulus identification (Fig. 4.4, long cti, accuracy and RT₁ effect). In our model, this process accounts for accuracy improvement with attentional orienting. Our main evidence for this claim is that the time course of the cue validity effect for accuracy is accounted for by the time course of the anticipatory amplitude suppression, which has been associated with increases in neuronal excitability (Romei et al., 2008; Sauseng et al., 2009; Haegens et al., 2011b).

To explain the cue validity effect for RT, an additional, non-preparatory, process is postulated. The non-preparatory nature of this process is suggested by the reliable RT effect at very short cue-target intervals. In fact, the average response to stimuli that occurred within 250 ms after the cue was $10.98 \pm 1.69\%$ faster after a valid as compared to an invalid cue. Moreover, extrapolation to a cue-target interval of 0 ms would indicate a substantial RT effect at this time point (Fig. 4.3B). Because it is unlikely that the meaning of the symbolic auditory cue is extracted at such short intervals, the early RT effect is unlikely accounted for by processes occurring between cue and target. (Note also that this early effect cannot be accounted for by concurrent processing of the cue and the target, because this occurs irrespective of cue validity.) In addition, this early RT effect occurred in the absence of a neurophysiological signal of pre-target increase in neuronal excitability. The early RT effect must thus be explained by a post-target process.

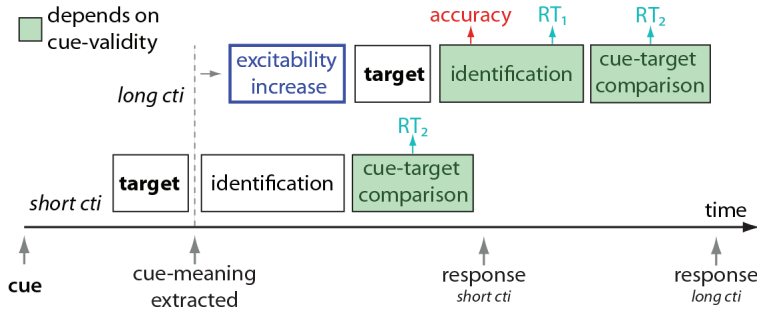


Figure 4.4. Schematic of processes underlying accuracy and RT consequences of symbolic attentional cueing. When stimuli occur at very short cue-target intervals (*short cti*), cue validity effects on RT (as the one we observed) must be explained by processes occurring post-target. This is because cue-meaning is only extracted post-target. One possibility is that, post-target, expected and actual location of the stimulus are compared (cue-target comparison), e.g. to update cue-target contingency. If this process occurs faster in valid compared to invalid trials (a compatibility effect), then this will lead to a cue validity RT effect (RT_2). (While this process is here depicted following identification, it might in reality occur parallel to the identification process.) When stimuli occur at longer intervals after the cue (*long cti*), spatially specific preparatory processes increase neuronal excitability in stimulus-relevant areas, affecting target identification in a cue validity dependent manner. This will affect both accuracy and RT (RT_1). Because cue validity dependent RT_1 and RT_2 effects cannot be disambiguated, it is problematic to infer preparatory processes solely on the basis of RT data.

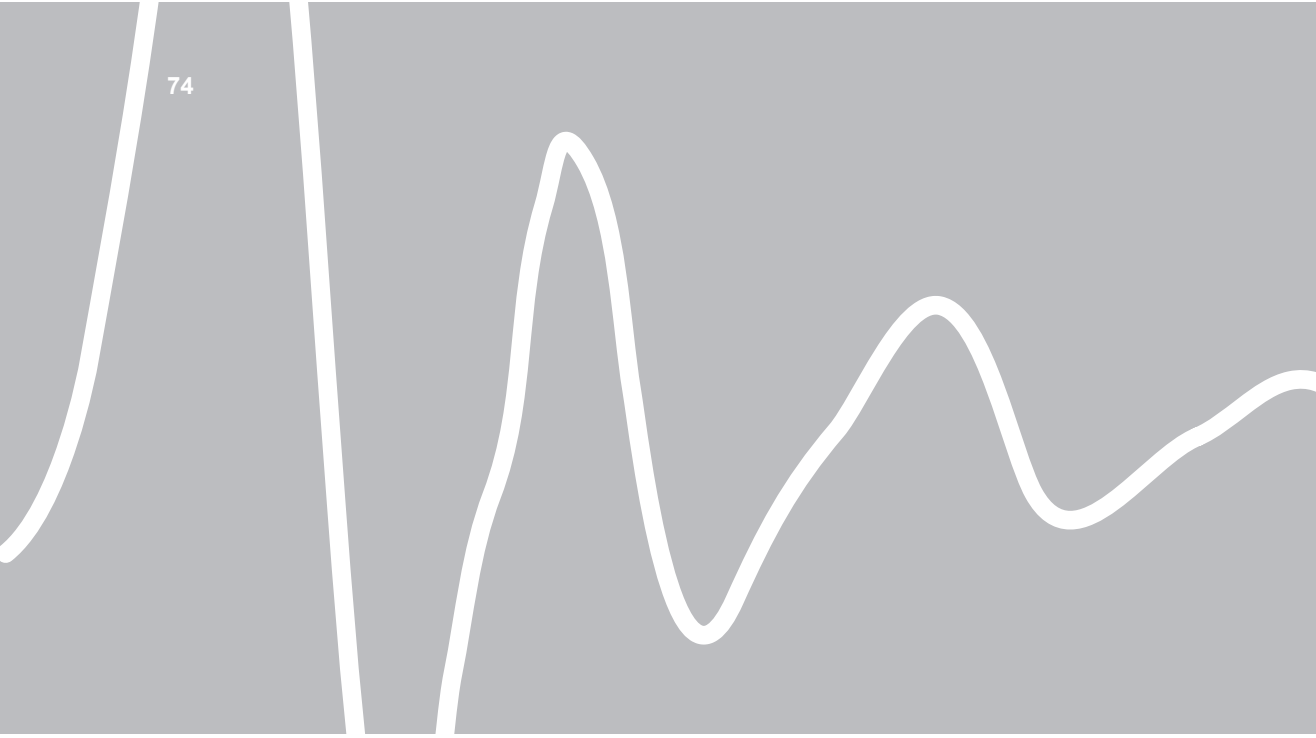
To show the role of this post-target process, we consider trials with a very short cue-target interval (Fig. 4.4, *short cti*). Target stimuli occurring very shortly after the cue cannot benefit from spatially specific preparatory processes, and hence no spatially specific accuracy improvement occurs. However, if the extraction of the meaning of the symbolic cue continues beyond target-presentation, then this information likely becomes available before the response and thus might still affect RT. One possible scenario is that, post-target, the cue information is compared to the actual target location, e.g. to update the cue-target contingency. This process may occur faster for valid as compared to invalid stimuli (i.e. a compatibility effect; Fig. 4.4, RT_2 effect), and this then explains the observed cue validity effect on RT. Although speculative, this gives rise to the notion that such RT effects need not reflect an improvement in perception. As a consequence, at longer cue-target intervals, one cannot infer perception-improving preparatory processes from RT effects only, because these may also be due to a compatibility effect.

Besides the post-target compatibility effect, also other post-target processes could explain our observed dissociation between accuracy and RT. In fact, it has also been put forward (Thut et al., 2006) that accuracy and RT might be differentially affected by reflexive re-orienting of attention, occurring after unexpected (i.e. invalidly cued) stimuli. While re-orienting will improve accuracy, it increases RT. For this alternative explanation to be valid for our data set, one would have to assume that anticipatory spatial orienting of attention does occur at short (< 200ms) cue-target intervals. No validity effect on accuracy is observed because the benefit due to anticipation (on valid trials) can be matched by

the benefit obtained from attentional re-orienting (on invalid trials). A validity effect on accuracy only becomes visible at longer cue-target intervals, when the anticipation has grown so much that attentional re-orienting can no longer match its effect. Validity effects on RT occur, also at short cue-target intervals, because anticipatory processes facilitate target-processing on valid trials (decreasing RT), while attentional re-orienting occurs on invalid trials (increasing RT). While this provides an alternative explanation, a number of aspects in our experimental setup and data make this scenario rather unlikely. First, re-orienting of attention can only affect accuracy if the stimulus is still present or can be easily retrieved from memory following the re-orienting. Our target-stimulus lasted only for 20 ms and was followed by a mask. Second, re-orienting should increase RT (in invalidly cued trials) more at longer cue-target intervals. However, this was not observed (Fig. 4.2C). Third, under the notion that the anticipatory orienting of attention is indexed by the anticipatory neural lateralization, its time course is expected to follow the RT time course. This was clearly not the case (Fig. 4.3). Fourth, re-orienting of attention requires that the meaning of the cue is extracted before target-onset. However, as discussed above, our RT effect occurs at intervals after the cue for which it is unlikely that the meaning of the cue is extracted. Despite these arguments, re-orienting of attention can be another source via which accuracy and RT might dissociate. This mechanism may be particularly important when cue-target intervals are long, and targets are salient or not masked, as in Thut et al. (2006).

In conclusion, symbolic attentional cues affect accuracy and RT in part via different cognitive and neural processes. While the effect of symbolic cueing on accuracy is likely explained by a single process (preparatory excitability increase), an additional, non-preparatory, process likely underlies its effect on RT.





Beyond establishing involvement: Quantifying the contribution of anticipatory alpha- and beta- band suppression to perceptual improvement with attention

Adapted from van Ede F, Köster M, Maris E (2012) *Beyond establishing involvement: Quantifying the contribution of anticipatory α - and β -band suppression to perceptual improvement with attention.* Journal of Neurophysiology 108:2352-2362.

5

Abstract

Systems and cognitive neuroscience aim at understanding the neurophysiological mechanisms that underlie cognition and behavior. Many studies have revealed the involvement of many types of neural signals in diverse cognitive and behavioral phenomena. Here, we go beyond establishing such involvement and address two fundamental, yet largely unaddressed, questions: (1) exactly how much does a given neural signal contribute to a cognitive or behavioral phenomenon of interest? and (2) to what extent are distinct neural signals independently related to this phenomenon? We recorded brain activity using Magnetoencephalography (MEG) while human participants performed a cued somatosensory detection task. Using a novel method, we then quantified the contribution (in a predictive but not causal sense) of two well-established neural phenomena to the improvement in perception with attentional orienting. In our sample, the anticipatory suppression of extracranially recorded oscillatory alpha- and beta-band amplitudes from the contralateral primary somatosensory cortex (S1) could account for maximally 29 % of the attention-induced improvement in tactile perception. In addition, although amplitude suppressions in the alpha- and beta-bands both contributed to this improvement, their contribution was largely shared. These data reveal the upper limit of the cognitive/behavioral relevance of this type of signal and show that at least 71 % of the perceptual improvement with attention must be accounted for by other signals.

5.1 Introduction

Systems and cognitive neuroscience aim at understanding the neurophysiological mechanisms that underlie cognition and behavior. To date this has resulted in a wealth of knowledge concerning the involvement of particular neural signals in cognitive functions and behavior. Despite this progress, studies up to now have left two fundamental questions largely unaddressed. First, how much does a given neural signal contribute to a cognitive or behavioral phenomenon of interest? Second, to what extent are distinct neural signals independently related to this phenomenon?

We report on a study in which both these questions were addressed. In particular, we quantified the contribution of well-established neural phenomena (anticipatory suppression of oscillatory amplitude in sensory cortex, occurring in multiple frequency bands) to a well-established behavioral phenomenon: the improvement in perception that occurs with attentional orienting.

Knowing when and where a stimulus will occur allows for orienting of attention and improves perception (Posner, 1980a; 1980b). Such attentional orienting involves a prestimulus modulation of oscillatory electromagnetic signals with their amplitude being lower over relevant, as compared to irrelevant sensory cortex. This has been established for posterior alpha-band (8-12 Hz) oscillations during visual orienting of attention (Foxe et al., 1998; Worden et al., 2000; Thut et al., 2006; Siegel et al., 2008; Wyart and Tallon-Baudry, 2008; Snyder and Foxe, 2010; Gould et al., 2011), and somatosensory alpha- and beta-band (15-30 Hz) oscillations during tactile orienting of attention (Jones et al., 2010; Anderson and Ding, 2011; Haegens et al., 2011a; **chapters 2-4**). These modulations are specific to the timing (Rohenkohl and Nobre, 2011; **chapter 3**) and features (Snyder and Foxe, 2010) of an expected stimulus, and their deployment depends on stimulus probability (Gould et al., 2011; Haegens et al., 2011a). These properties suggest that oscillatory amplitude modulation reflects an important mechanism underlying the orienting of attention. This is further supported by the observation that low amplitude in the alpha- and beta-band is associated with an enhancement in (1) cortical excitability (Romei et al., 2008; Sauseng et al., 2009; Haegens et al., 2011b), (2) blood-oxygenation-level dependent (BOLD) activity (Ritter et al., 2009; Scheeringa et al., 2011), and (3) psychophysical performance in visual (Thut et al., 2006; van Dijk et al., 2008) and tactile (Jones et al., 2010; Haegens et al., 2011a; **chapters 3 and 4**) tasks.

Despite this coherent picture, two fundamental aspects remain unclear. First, exactly how much of the improvement in perception with attentional orienting can be accounted for by these anticipatory amplitude modulations? While we acknowledge that the relation between prestimulus amplitude and perception has previously been investigated with quantitative measures (e.g. correlation coefficients), inferences have so far remained qualitative. Specifically, it was assessed whether or not a correlation of interest was statistically significant, allowing the qualitative inference of whether or not a relation existed between the two variables (“establishing involvement”). As we will

outline in our Discussion, based on these conventional correlational analyses, only this type of qualitative inference is justified. In the present paper, our goal is not qualitative but quantitative inference. In other words, our goal is determining the effect size. A second fundamental aspect that has remained unclear is to what extent modulations in the alpha- and the beta-band independently contribute to the improvement in perception that occurs with attentional orienting. To address these two questions we developed a novel method that allows for a quantification of the cognitive/behavioral relevance (in a predictive, but not causal sense) of a particular set of neural signals. In contrast to conventional quantitative measures (such as the correlation coefficient), our method produces a quantification that is neither affected by noise in our predictor variables (i.e. our amplitude estimates), nor by variability in our criterion variable (detection responses) that is independent of the cognitive variable under investigation (attentional orienting; see Discussion). We applied our method to extracranial signals that were acquired during a somatosensory detection task using Magnetoencephalography (MEG). In our sample, the anticipatory suppression of the rolandic alpha- and beta-band oscillatory amplitudes together accounted for maximally 29 % of the improvement in tactile perception with attentional orienting. Moreover, while amplitude suppressions in both frequency bands contributed to this improvement, their contributions were largely shared.

5.2 Materials and Methods

Participants & experimental design

Our study was conducted in accordance with the Declaration of Helsinki and approved by the local ethics committee (CMO Region Arnhem-Nijmegen). Informed consent was obtained from all subjects.

Fourteen healthy subjects (5 male; 22–49 years) participated in the study. Two subjects were excluded from analysis. For one subject, no stable behavioral performance could be obtained; another subject fell asleep.

Subjects performed a somatosensory detection task in which the spatial and temporal locations of target stimuli was either cued or not (Fig. 5.1). The central event in a trial was the occurrence of a brief auditory stimulus (50 ms, white noise), that was paired with an electro-tactile stimulus (0.5 ms electric pulse close to threshold intensity) in half the trials. This tactile stimulus was delivered using either of two constant current high voltage stimulators (type DS7A, Digitimer) to the left or the right thumb. Stimulus intensity was set before the experiment. For this, we used a Bayesian staircase algorithm (QUEST; Watson and Pelli, 1983), that adjusts the stimulus intensity such that the hit rate in the cued condition (see below) was approximately 80 % (see also Fig. 5.2A). This algorithm was implemented in the Matlab (Mathworks) Psychophysics Toolbox (Brainard, 1997). Intensities were 1.400 ± 0.066 and 1.747 ± 0.077 mA for the left and the right hand, respectively.

In the experiment, subjects indicated whether a tactile stimulus was presented or not at the time of the central event, which was marked by a brief auditory stimulus. In



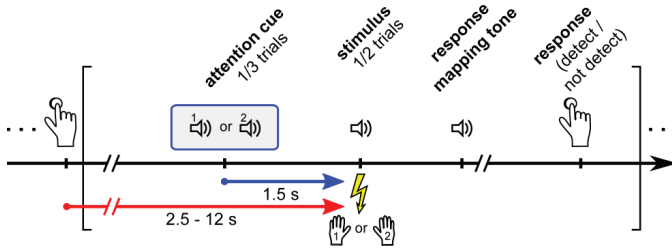


Figure 5.1. Experimental paradigm. Subjects performed a somatosensory detection task in which time (after 1.5 s) and location (left/right thumb) of the upcoming event was either cued or uncued. This event consisted of a brief tone that, in half the trials, was paired with an electric stimulus on one of the subject's thumbs. In each trial, subjects had to indicate whether they had felt a stimulus or not. Responses were delayed and the mapping of the perceptual decisions onto the response buttons was indicated by a response mapping tone (see Materials & Methods). Uncued and cued trials were randomly interleaved.

the uncued condition, it was made as difficult as possible to predict the time of the central event as well as the location at which the tactile stimulus might occur. Concerning time, we drew the interval between a response and the next central event from a truncated negative exponential distribu-

(mean 3.5 s; limited to the range 2.5 to 12 s). A negative exponential distribution has a hazard rate (the probability of an event at time t given that it has not occurred yet) that does not depend on this time t , and therefore is unpredictable. Concerning location, the tactile stimulus could, in case of a stimulus-present trial, occur at either thumb. In the cued condition, the time of the central event and the location at which the tactile stimulus might occur were fully predictable: 1.5 s before the central event, an auditory cue (150 ms, pure tone) was presented, informing with 100 % validity about the time (after 1.5 s) and location (left/right thumb) at which the stimulus might occur. Cue pitch (500/1000 Hz) informed location and was counterbalanced across participants. Cued and uncued trials were randomly interleaved. In total, one third of the trials were cued.

Participants indicated whether a stimulus was presented or not by pressing a button with the left or the right index finger. To indicate the presence of a tactile stimulus, subjects pressed a button on the side where a lateralized auditory response-mapping tone (150 ms, 1000 Hz) was presented, and to indicate its absence, they pressed the button on the other side. This mapping of the perceptual decision onto the response was varied from trial-to-trial to prevent specific motor preparation in the anticipation period of interest. Auditory feedback was presented, indicating hits and misses (50 ms upgoing, respectively, downgoing frequency sweeps between 500 and 1000 Hz).

Participants completed around 1000 trials in two consecutive MEG sessions lasting approximately 70 minutes each. Within each block (72 trials), cue presence, cue side, stimulus presence, and stimulus side were counterbalanced. After each session, an S1 localizer experiment was performed: 200 suprathreshold stimuli were delivered to each thumb. The day before the experiment, subjects practiced the task for approximately one hour.

Data acquisition & preprocessing

The MEG system (CTF MEG TM Systems, Coquitlam, Canada) contained 275 axial gradiometers and was housed in a magnetically shielded room. We also recorded bipolar surface electromyogram (EMG) from the flexors of the forearm (cf. **chapter 3**). Localization coils, fixed to anatomical landmarks (nasion, left, right ear), determined head position. All data were low-pass filtered (300 Hz cutoff), digitized at 1200 Hz, and stored for offline analysis. Line noise was removed offline using a discrete Fourier transform filter. Epochs contaminated by artifacts were removed based on visual inspection. T1-weighted MR-images were acquired and subject-specific single-shell models (Nolte 2003) for source reconstruction were calculated.

Data analysis

Data were analyzed using FieldTrip (Oostenveld et al., 2011), an open-source Matlab toolbox.

Frequency analysis. We calculated oscillatory amplitude by means of the Fourier transform, with and without time resolution. For calculations with time resolution (Fig. 5.2C), we used a 500 ms sliding time window (advanced in steps of 50 ms) and a Hanning taper. Non-time-resolved amplitude estimates (Figs. 5.3-5.5) were calculated for the alpha- and the beta-band using the multitaper method (Percival and Walden, 1993). The alpha-band was defined as 8 to 12 Hz for all subjects whereas the beta-band (which is more variable in frequency) was individually determined per subject based on the post-stimulus response (cf. **chapters 2-4**). On average, beta-bands ranged from 16 to 28 Hz.

Source reconstruction. We reconstructed oscillatory brain activity originating from putative S1. This involved three steps. First, we used the localizer data to find, per participant, the left and right sources that showed the strongest response to right and left tactile stimuli, respectively. This was done in source space using beamforming (dynamic imaging of coherent sources; Gross et al., 2001). Beamforming reconstructs source-power using spatial filters that have unit gain for the point source of interest while maximally attenuating other sources. This is accomplished by taking the cross-spectral density matrix into account. Per voxel (0.5 cm resolution), we calculated the difference between the beta-band amplitudes recorded after left and right thumb stimulation. The maximum and minimum voxels in this contrasted volume were used as loci for left and right sources of interest (hereafter referred to as S1; cf. Haegens et al., 2011a; **chapter 3**). We then estimated optimal spatial filters for reconstructing activity from left and right S1, again using beamforming (now using the cross-spectral density for the 5-50 Hz band, calculated across all epochs of interest). Finally, we applied the obtained filters to our time-domain data (275 channels) to reduce it to one left and one right virtual S1 channel.



Quantifying the contribution of amplitude to behavior. For every trial, we calculated four prestimulus amplitude estimates: alpha- and beta-amplitude in left and right S1. To allow pooling of data over recording sessions and hemispheres, we normalized all amplitude estimates by linearly transforming them to the percentage change from the mean amplitude in the uncued condition of the respective session and hemisphere. Amplitudes from left and right S1 were reassigned as contralateral or ipsilateral to the stimulus.

Our quantification procedure, which was performed per subject, involved the following steps. First, we modeled the relation between perceptual performance and prestimulus amplitude using linear (for reaction times) and logistic (for hit rate) regression in the uncued trials (Fig. 5.3A-C, middle panels). Second, we quantified the anticipatory amplitude modulation in the cued condition. This modulation is the difference between the mean amplitudes in the cued and the uncued trials (red and blue vertical lines in Fig. 5.3A,B, lower panels). Third, we used the amplitude-perception regression coefficients from step 1 to predict the improvement in perceptual performance that would follow from the anticipatory modulation from step 2. Finally, we compared this prediction with the actual improvement that occurred with cueing. By dividing the predicted improvement with the observed improvement (and multiplying it by 100), we quantified how much of the improvement in perception with attentional orienting can be accounted for by anticipatory amplitude modulation: the percentage explained improvement.

Because the regression lines of the cued and uncued condition were roughly linear and parallel over the range in which our amplitudes occurred (Fig. 5.3), our quantification could be based on the regression line of only the uncued condition together with the average attention-induced change in amplitude and perception in the cued condition. If the regression lines would not have been linear and parallel, one would have to use a calculation that is more generally applicable (i.e., to nonlinear and non-parallel regression lines). This more general calculation comes from the statistical literature on the contribution of covariates (in order to correct for them) when estimating treatment effects in observational studies (Maris, 1998; Rubin, 1974; 1977). The formal theory behind this literature also applies to other estimation problems, such as ours, and involves estimating the extent to which the difference between groups (cued and the uncued trials) on some dependent variable (detection performance) can be explained by a another variable (oscillatory amplitude).

Our logistic regression modeled the probability of a hit as a function of prestimulus amplitude according to:

$$P(\text{hit}) = \frac{\exp(\beta_0 + \beta_1 * \text{amplitude})}{1 + \exp(\beta_0 + \beta_1 * \text{amplitude})}$$

We also performed logistic regression using two predictor variables, the single-trial alpha- and beta-band amplitudes. For this, we added a $\beta_2 * \text{amplitude}$ term in the exponent. Coefficients were estimated using the maximum likelihood criterion.

Correcting for noisy amplitude estimates. Noise in our amplitude estimates will attenuate the slopes of the amplitude-perception regression lines that form the basis of our quantification. To obtain a veridical (i.e. noise-free) quantification, the slope-attenuating effect of this noise must be corrected for. We did this in two ways.

First, we corrected single-trial amplitudes for variability in single-trial head position (which was derived from our localization coils) by (1) calculating head position as the Euclidian distance between the center of the head and the center of the MEG-helmet, (2) modeling the relation between head position and amplitude using linear regression, and (3) using these regression coefficients (per subject, session and frequency band) to correct single-trial amplitudes for variability in single-trial head position. We used this metric of height-in-the-helmet because we expected amplitude-estimates from left and right S1 (which are positioned at the top-centre of the helmet) to be most affected by it (this might be different for different cortical regions). Because head-height accounted for only a small percentage of the variance in amplitude across trials ($< 5\%$), we decided not to perform more sophisticated head-position correction algorithms.

Second, we corrected for noise in the single-trial estimates. For this, we used a simulation approach (depicted in Fig. 5.5A-C) with which we derived which true amplitude-perception regression slope formed the basis of our observed slope, given the observed amount of noise. First, we log-transformed our amplitude estimates, such that their distribution closely approximated a normal distribution (Fig. 5.5A,D). As before, we linearly transformed them as percentage change from the mean amplitude in the uncued trials. Second, we estimated the sampling variance of these log- and linearly-transformed amplitude estimates. For this, we made use of the fact that the multitaper method calculates multiple independent Fourier coefficients per trial, one per taper. Per trial, we calculated the log- and linearly-transformed amplitudes of these taper-specific Fourier coefficients, calculated their variance across tapers and divided this variance by the number of tapers to estimate the trial-specific sampling variance. We then averaged this quantity across trials. It is crucial to specify under which conditions this trial-averaged sampling variance estimate is unbiased. That is, under which conditions it neither over- nor underestimates the true sampling variance. We will consider this point in detail below. In the third step, we used the estimated sampling variance to reconstruct the true log amplitude distribution as a normal distribution with mean equal to the observed mean and variance equal to the observed across-trial variance minus the estimated sampling variance (Fig. 5.5A). Using this distribution together with the noise distribution (normal distribution with zero mean and variance equal to the estimated sampling variance), by means of simulation, we derived which “true” amplitude-perception regression slope would, after adding noise, yield the empirically observed one (Fig. 5.5B,C).

In our simulation method, we used a one-dimensional grid (100 steps) of regression coefficients centered on the empirically observed coefficient. For every point in this grid, we randomly drew trial-specific amplitudes from our reconstructed true distribution and



assigned every trial to be a hit or miss, depending on the probability of a hit given the simulated regression coefficient and the drawn amplitude value. We then randomly drew noise from our noise distribution, added it to the amplitudes drawn from the reconstructed true distribution, performed a logistic regression, and calculated the simulated percentage explained improvement. To obtain a reliable estimate, we repeated all the above steps for the full grid numerous times. After every repetition, we calculated, for each grid-point, the running average of the simulated percentage explained improvement. We then identified the best grid point as the point for which this running average was closest to the empirically observed percentage. Absolute deviations were as small as 0.109 ± 0.024 % for the single predictor model and 0.015 ± 0.004 % for the dual-predictor model (discussed below). We continued until the 95 % confidence interval (calculated across simulations) of this simulated percentage for the best grid point fell within ± 1 %. As our estimate of the true regression slope, we took the regression coefficient belonging to the best grid point. With this estimated true regression coefficient, the true percentage explained improvement was derived. These simulations were performed for each participant separately, and outcomes were averaged across participants.

This quantification of the explained improvement is only unbiased if the signal is stationary, because only in this case our estimate of the “true” amplitude-perception regression slope is unbiased. This is because, only under this assumption of a stationary signal, we can rely on the standard theory of multitaper estimation to obtain an unbiased estimate of the single trial noise variance from the Fourier coefficients of the multiple independent tapers (Percival and Walden 1993, p. 360, point [2]; Thomson 1982, section IV). Under violation of this assumption, the signal’s noise is overestimated because part of the within-trial variance across tapers is due to the non-stationarity of the true underlying signal. This leads to an overestimation of the true amplitude-perception regression slope and thereby also the percentage explained improvement. It is important to realize that the percentage explained improvement is potentially overestimated, but cannot be underestimated. For this reason, it is a conservative strategy to consider our quantification as the *maximal* percentage explained improvement. Because perfect stationarity is unlikely to hold, the real percentage explained improvement likely lies between the percentages that are obtained before and after noise correction.

Finally, we extended our simulations to the combined alpha- and beta-amplitude model by drawing from bivariate normal distributions. Besides the sampling variances of the alpha- and the beta log amplitudes, we also calculated their sampling covariance, making use of the within-trial covariance across the tapers. Likewise, we calculated the covariance across trials. This allowed us to reconstruct noise and true bivariate distributions required for our simulation. Simulated percentage explained improvement was calculated using multiple logistic regression and simulations were performed for a two-dimensional grid (25 x 25 steps) containing coefficients for alpha and beta. As our estimate of the true pair of regression coefficients, we took the pair of coefficients belonging to the best grid point.

Statistics

All reported statistical tests were performed across subjects by means of one-sample or paired-samples t-tests (two-tailed, $\alpha = 0.05$). All reported measures of spread are \pm one standard error of the mean (s.e.m.).

5.3 Results

Attentional orienting improves perception and involves suppression of contralateral oscillatory alpha- and beta-band amplitude

As depicted in Figure 5.2A,B, orienting attention improved perception by increasing the hit rate from $52 \pm 3\%$ (mean over subjects \pm s.e.m) in the uncued condition to $81 \pm 2\%$ in the cued condition ($t_{(11)} = 8.491$, $p < 0.001$), and by decreasing reaction times from 685 ± 83 ms to 513 ± 40 ms ($t_{(11)} = -3.291$, $p < 0.01$). False alarm rates did not differ between conditions (uncued $27 \pm 3\%$; cued $24 \pm 3\%$; $t_{(11)} = 1.023$, $p = 0.328$) and were lower than hit rates for all subjects. This indicates performance well above chance.

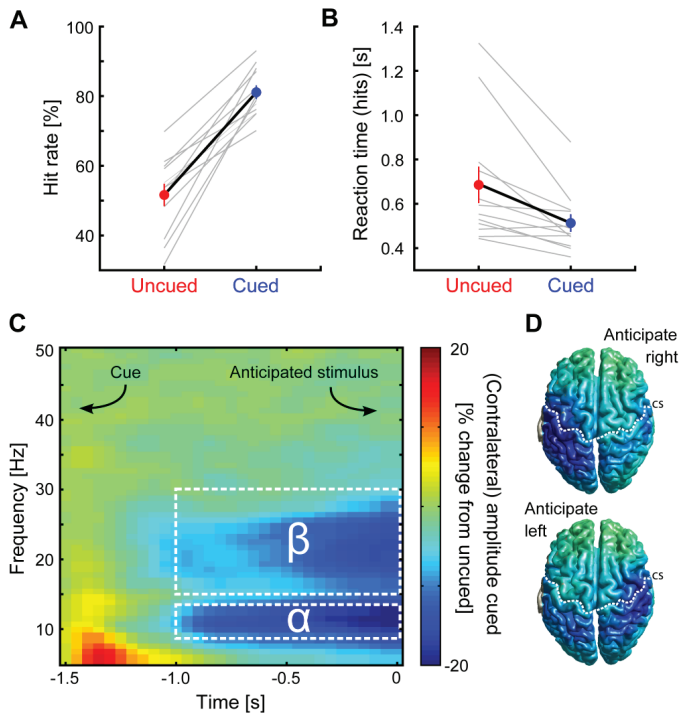


Figure 5.2. Attentional orienting improves perception and involves anticipatory suppression of contralateral alpha- and beta oscillatory amplitudes. (A) Hit rate in the uncued and the cued condition. Colored data points indicate means \pm s.e.m. Gray lines show individual subjects. (B) Same as A, but now showing reaction times in hit trials. (C) Time-frequency representation of oscillatory amplitude in S1 following a cue to the contralateral side, expressed as the percentage change from the uncued condition. White boxes indicate the time-frequency window used in subsequent analyses. (D) Source-reconstructed amplitude modulation in anticipation of a right and left thumb tactile stimulus, averaged over the alpha- and beta-band in a 1 s prestimulus window. Dashed white lines indicate the central sulci (cs).

It is well-established that attentional orienting to upcoming sensory events involves an anticipatory modulation of oscillatory amplitude within sensory cortex (Foxe et al., 1998; Worden et al., 2000; Thut et al., 2006; Siegel et al., 2008; Wyart and Tallon-Baudry, 2008; Snyder and Foxe, 2010; Jones et al., 2010; Anderson and Ding, 2011; Gould et al., 2011; Haegens et al., 2011a; Rohenkohl and Nobre, 2011; **chapters 2-4**). To verify this in our data we computed time- and frequency-resolved oscillatory amplitudes for the reconstructed source signals originating from left and right primary somatosensory cortex (S1; see Materials and Methods). Figure 5.2C shows the time-frequency representation of oscillatory amplitude in S1 following a cue to the contralateral side, expressed as the percentage change from the uncued condition. Orienting attention to an upcoming tactile event involved an attenuation of oscillatory amplitude in both the alpha- and the beta-band (contralateral alpha: $t_{(11)} = -5.523$, $p < 0.001$; contralateral beta: $t_{(11)} = -7.215$, $p < 0.001$). Figure 5.2D shows source reconstructions of this anticipatory modulation, separately for anticipation of a left and a right thumb stimulus. Consistent with previous findings (**chapters 3 and 4**), the anticipatory suppression occurs predominantly contralateral to the cued hand and includes S1.

We now ask how much of the perceptual improvement can be accounted for by these neural signals.

Quantifying the contribution of anticipatory amplitude suppression to perceptual improvement with attention

Spontaneous fluctuations in oscillatory amplitude are correlated with perceptual performance (Jones et al., 2010; Linkenkaer-Hansen et al., 2004; van Dijk et al., 2008). We capitalized on this relation to quantify the contribution of the anticipatory amplitude suppression to the perceptual improvement with attention.

Figure 5.3 illustrates the rationale of our quantification (see also Materials and Methods). First, we used data from the uncued condition to estimate the relation between prestimulus amplitude and perceptual performance in the absence of attentional orienting (red data points). For visualization of this relation, we sorted trials by amplitude and grouped them into 8 non-overlapping bins (cf. Jones et al., 2010; Linkenkaer-Hansen et al., 2004). As can be seen in the upper panels of Figure 5.3, there is a close-to-monotone relation between prestimulus amplitude and perceptual performance, with lower prestimulus amplitude predicting higher perceptual performance. As part of our quantification we modeled this relation at the level of the single-trial data. As adequate models for these empirically observed close-to-monotone relations, we used logistic regression for detection responses (hit / miss; a dichotomous variable) and linear regression for reaction times (a continuous variable; Fig. 5.3 middle panels). These models will be denoted as *amplitude-perception regression lines*. Our rationale is as follows: if perception were fully determined by alpha- and beta-band amplitudes, then attention-induced changes in perception should be fully accounted for by attention-induced changes in these variables. In this case, the amplitude-

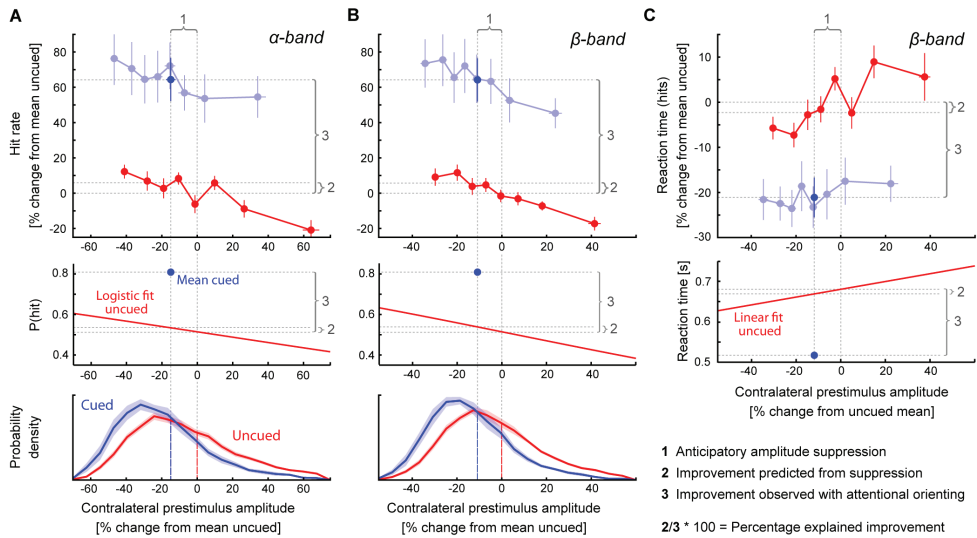


Figure 5.3. Rationale for the quantification of the percentage of attentional improvement explained by amplitude suppression. (A) Upper panel, hit rate as a function of prestimulus amplitude in the alpha-band. Trials from the uncued (red) and cued (blue) condition were separately sorted by amplitude and grouped into 8 bins. Data are normalized as the percentage change from the mean in the uncued condition. The dark blue data point shows mean amplitude and hit rate in the cued condition, which was used for calculation of the percentage explained improvement. Error bars indicate s.e.m. Middle panel, fitted regression slope, analogue to binned data in upper panel. Slope is depicted for the average subject. In practice, quantification was performed per subject. Lower panel, distribution of prestimulus amplitudes, separately for cued and uncued trials. Vertical dashed lines indicate mean amplitude. (B) Same as A, for amplitudes in the beta-band. (C) Same as A showing reaction time (in hit trials) as a function of beta-band amplitude. Quantification of the percentage explained improvement involved (1) estimating the anticipatory amplitude suppression, (2) calculating the predicted improvement in perception that would follow from this anticipatory suppression and (3) comparing the predicted improvement with the observed improvement. This calculation was based on the fitted regression lines (middle panels).

perception regression lines should overlap between the cued and the uncued conditions. Alternatively, the degree to which these regression lines do not overlap (as quantified by the vertical distance between them) indicates the degree to which attention-induced changes in perception cannot be explained by these variables.

Before describing the steps in our quantification, note that the relations between amplitude and perception are highly similar for the uncued (red data points) and the cued (blue data points) conditions. This shows that the relation between amplitude and perception is itself not altered by attentional cueing. Moreover, for the ranges in which our amplitudes occurred, the cued and uncued regression lines were roughly linear and parallel. Because of this, our quantification could be based on the regression line of only the uncued condition together with the average attention-induced change in amplitude and perception in the cued condition (see Materials and Methods).

Our quantification involved three steps (numbered 1-3 in Fig. 5.3). First, we quantified the anticipatory amplitude suppression as the difference between the mean amplitudes in



the cued and uncued condition (blue and red vertical lines in Fig. 5.3A,B lower panels). Second, we used the amplitude-perception regression line from the uncued condition to predict the improvement in perception that would follow from this anticipatory amplitude suppression in the cued condition (i.e. the leftward shift along the regression line equal to the decrease in amplitude after cueing; cf. Fig. 5.2C). Third, we calculated the percentage of the attentional improvement that can be explained by the amplitude suppression (denoted *the percentage explained improvement*) by taking the ratio of predicted over actual attentional improvement and scaling it as a percentage. As illustrated by the vertical distance between the amplitude-perception regression line and the mean cued amplitude (blue data point), only part of the attentional improvement can be explained by the anticipatory amplitude suppression. For example, according to the relation between amplitude and perception in Figure 5.3A upper panel, the anticipatory amplitude suppression in the alpha-band would lead to an improvement of approximately 5 % in hit rate. The actual improvement was approximately 65 %, and therefore the anticipatory amplitude suppression explains $5/65 * 100 = 7.7$ % of the attentional improvement.

The percentage explained improvement was calculated for each subject and averaged subsequently. Explained improvement was highest for contralateral amplitudes: for the alpha-band this was 5.8 ± 1.5 % ($p < 0.005$), and for the beta-band this was 7.0 ± 1.5 % ($p < 0.001$).

For reaction times (Fig. 5.3C), only contralateral beta-band amplitude predicted behavior ($t_{(11)} = 2.938$, $p < 0.05$) and explained 12.5 ± 6.0 % of the attentional improvement. This phenomenon was less robust and therefore we will exclusively focus on hit rate in the following.

We investigated to what extent alpha- and beta-band amplitude in the contralateral hemisphere contributed independently to the explained improvement. We found that combining contralateral alpha and beta explained only an additional 1.7 ± 0.8 % ($t_{(11)} = 2.065$, $p = 0.063$) of the improvement compared to using only contralateral beta (an increase in explained improvement from 7 to 8.7 %). This small and non-significant improvement is a consequence of the fact that amplitude fluctuations in the alpha- and beta-band are highly correlated and therefore their influence on somatosensory perception is not unique. In fact, we observed an average across-trial correlation between alpha and beta amplitude of 0.564 ± 0.038 . (Because of the inherent unreliability of the amplitude estimates, this correlation underestimates the true correlation. We will correct for this later.)

We may have underestimated the explained improvement because our predictor variables may not have been the most predictive ones. To assess this, we investigated to what extent the explained improvement depends on the spatial, spectral, and temporal aspects of our predictor variables. First, it may be that the S1 sources, which were extracted using a localizer, did not reflect the perceptually relevant alpha- and beta-band amplitudes. We therefore extracted sources from the spatial topography of the anticipatory modulation (Fig. 5.2D) and performed the same analysis. With these new sources we obtained highly

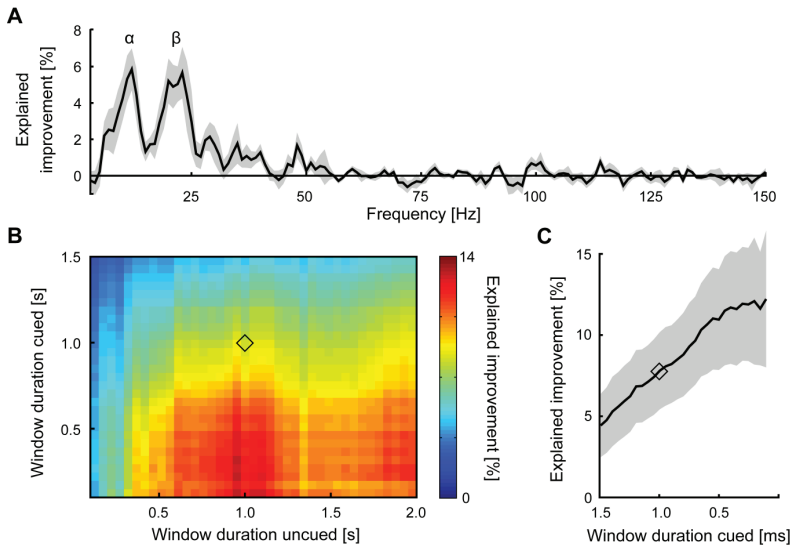


Figure 5.4. Explained improvement is frequency specific and depends on the duration of the time window. (A) Percentage explained improvement in hit rate as a function of the frequency of the prestimulus amplitude. Amplitude was estimated in a 1 s prestimulus window with 4 Hz frequency smoothing. Shading indicates s.e.m. Alpha and beta are the only frequency bands that contribute to the explanation of the attentional improvement. (B) Percentage explained improvement as a function of the time window duration used to estimate the amplitude in the uncued (horizontal axis) and the cued (vertical axis) trials. Contralateral alpha- and beta-band amplitude were used as joint predictors. (C) Percentage explained improvement as a function of the time window duration in the cued trials. Time window duration for the uncued trials was fixed to 1 s. The diamonds in panels B and C indicate the time window durations used in previous analyses. Time windows always ended at stimulus onset.

similar results (alpha: 4.9 ± 1.5 %; beta: 7.1 ± 1.8 %). Second, also pertaining to the spatial aspect, instead of unilateral amplitudes, we tested amplitude lateralization (the difference between contra- and ipsilateral S1 amplitude, cf. Thut et al. 2006) as a predictor. Fluctuations in amplitude lateralization did not predict performance (alpha: 1.8 ± 0.9 %, $p = 0.066$; beta: 0.5 ± 1.2 %, $p = 0.669$). Third, we performed a frequency-resolved analysis of the percentage explained improvement, of which the results are depicted in Figure 5.4A. We found that alpha and beta are the only frequency bands that contribute to the prediction. Finally, we investigated the dependence of our results on the prestimulus time windows used to estimate oscillatory amplitude. In line with studies in other groups (Jones et al. 2010; Linkenkaer-Hansen et al. 2004), we had initially used a 1 s prestimulus window for both cued and uncued trials. We now independently varied the duration of the two windows: the prestimulus window in the uncued trials used to estimate the regression slope, and the prestimulus window in the cued trials used to estimate the anticipatory modulation. Figure 5.4B shows the explained improvement as a function of both window durations, which we obtained using the combined model with contralateral alpha- and beta-band amplitude as predictors. The relation between amplitude and hit rate in the uncued condition is relatively stable for time windows longer than 600 ms. However, the anticipatory suppression in the

cued trials increases with shorter time windows leading to a higher percentage explained improvement. After a cue, it takes some time to suppress oscillatory amplitudes, and hence the closer the window to the actual stimulus, the stronger the modulation (Fig. 5.4C; see also Fig. 5.2C). Using the best selection of time-windows (950 ms uncued, 250 ms cued) the explained improvement was $13.1 \pm 4.0\%$ (compared with the $8.7 \pm 1.8\%$ using the original time windows; diamond in Fig. 5.4B,C).

Correcting for noisy amplitude estimates

Up to this point we have treated our amplitude estimates as an accurate representation of neural activity. However, in reality these estimates reflect a combination of true amplitudes (i.e. produced by alpha and beta oscillations originating from contralateral S1) and noise. This is important to consider because noise in the predictor variable biases the slope of the regression line towards 0. This phenomenon is known as regression attenuation. This implies that noise in the amplitude estimates will lead to an underestimation of the slope of the true amplitude-perception regression lines and therefore of the explained improvement. (Note that variability in the criterion variable around the regression line, does not affect our quantification; see Discussion).

We dealt with this concern in two ways, one dealing with across-trial and another with within-trial noise. First, we corrected for the across-trial amplitude fluctuations caused by trial-by-trial fluctuations in head position (i.e. height of the head in the MEG helmet). Fluctuations in head position accounted for less than 5% ($r^2 = 0.048 \pm 0.015$) of the total variance in amplitude across trials. Correcting single-trial amplitudes based on single-trial head positions did not alter the slope of the amplitude-perception regression lines (alpha: $t_{(11)} = 0.392$, $p = 0.703$; beta: $t_{(11)} = -0.318$, $p = 0.757$). Second, we corrected for within-trials noise. For estimation of the noise variance, we made use of the fact that the multitaper method (Percival and Walden, 1993) of spectral estimation provides multiple independent amplitude estimates from a single data window, namely one per taper (see Materials and Methods). Using a simulation approach (see Materials and Methods) we reconstructed the true (noise-free) amplitude-perception regression slope with which we could estimate the true percentage explained improvement. (Note that this percentage is only “true” under the assumption of signal stationarity. Alternatively it may be considered an upper bound to the percentage explained improvement; see Materials and Methods). Specifically, we drew data from a reconstructed true amplitude distribution (Fig. 5.5A) and investigated the consequences of adding the empirically observed amount of noise (Fig. 5.5B). By simulating multiple amplitude-perception regression slopes and adding noise to these, we derived which true amplitude-perception regression slope would have yielded the one that was actually observed (Fig. 5.5C). This is called the *estimated* true amplitude-perception relation. Figure 5.5D shows the fitted logistic regression lines belonging to the originally observed (noise-dependent and thus attenuated), the head position corrected, and the estimated true slopes, all three obtained using beta-amplitude as predictor.

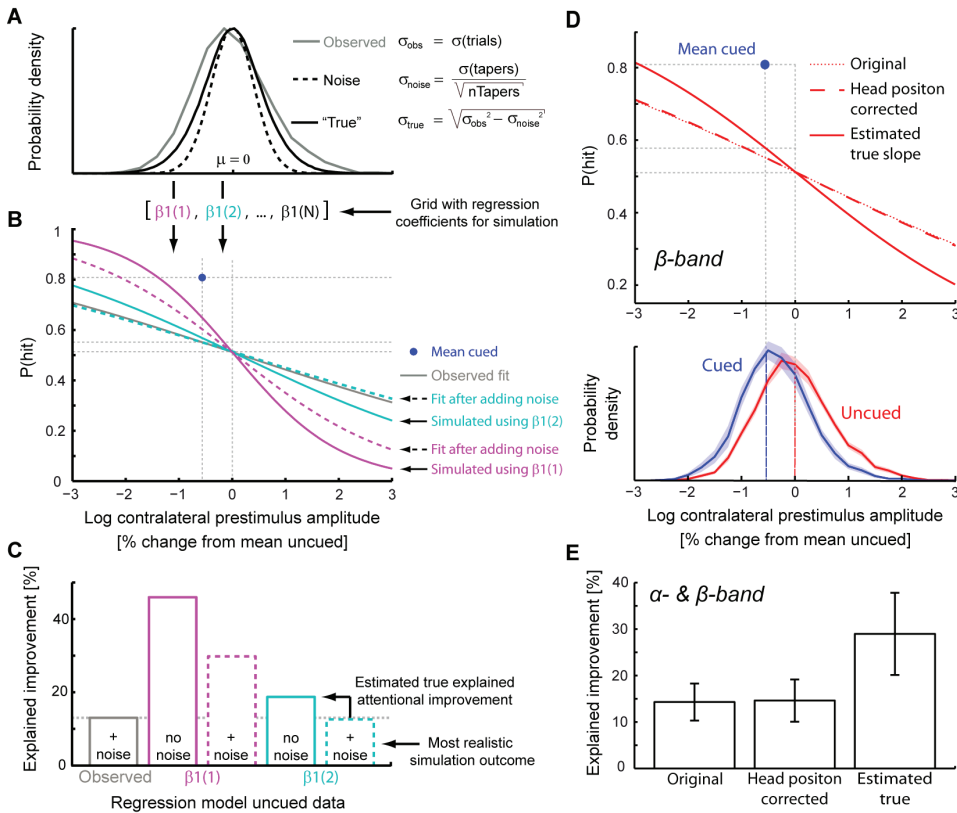


Figure 5.5. Correcting for noise reveals maximal explained improvement. (A) Observed amplitude, derived noise, and reconstructed true amplitude distributions used in the simulation procedure. The observed distribution involves log-transformed amplitude and resembles a normal distribution. The noise distribution is modeled as a normal distribution with standard deviation equal to the standard error calculated across tapers. The true amplitude distribution is modeled as a normal distribution with variance equal to the difference between the observed and the noise variance. (B) True slopes were estimated by simulating the effect of adding the observed amount of noise to numerous (see grid between panel A and B) noise-free slopes. (C) The simulated noise-free slope which, after adding noise, most closely resembled our observed slope was taken as the estimated true slope. With this slope, estimated true percentage explained improvement was calculated. Data in panels A-C represent the average participant (in reality we performed this simulation per participants and averaged the outcomes). For our multiple predictor model (involving both alpha- and beta amplitude) we performed similar simulations using bivariate observed, noise and true distributions. (D) Logistic regression fits for the originally observed, head-position-corrected, and combined head-position- and noise-corrected (estimated true) relation between prestimulus beta-amplitude and hit rate probability. Lower panel shows log-transformed amplitude distributions, which approximate normal distributions (a requirement for our simulations). (E) Percentage explained improvement using the original, head-position-corrected and estimated true slopes. Error bars indicate s.e.m. Alpha- and beta-band amplitudes were used as combined predictors and estimated over 950 and 250 ms windows for uncued and cued data respectively (Fig. 5.4).

We performed similar simulations using the model with both alpha- and beta-amplitudes as predictors. For these simulations we used bivariate true and noise distributions for which the covariance structures were determined by the true amplitude correlation (across trials)

and the noise correlation (across tapers), respectively. Because the within-trial noise of alpha- and beta-band amplitude estimates were largely uncorrelated ($r = 0.048 \pm 0.009$) we had previously underestimated the signal correlation: the estimated true correlation was 0.791 ± 0.037 . Figure 5.5E shows the results for this combined model. When correcting for noise in our amplitude estimates, the anticipatory suppression of oscillatory amplitudes can account for maximally 29 ± 8.8 % of the improvement in perception that occurs with attentional orienting.

5.4 Discussion

Systems and cognitive neuroscience have been very successful in identifying neural signals that are involved in cognitive functions and behavior. This is an important first step in understanding the neurophysiological mechanisms by which cognition and behavior are realized. An essential next step is quantifying how much particular signals, either alone or in combination, contribute to cognition and behavior. Here, we employed a novel method that produces such a quantification by using the relation between spontaneous neural and behavioral fluctuations to determine how much of the task-induced behavioral modulation can be explained by the co-occurring neural modulations. We show that (1) extracranially recorded amplitude modulations from the contralateral primary sensory cortex can, at best, account for 29 % of the perceptual improvement with attentional orienting, and (2) distinct aspects of this signal – alpha and beta band oscillatory amplitudes – have a largely shared contribution.

Discussing the results of our study, one can focus on the explained or the unexplained part of the attentional improvement. The maximal percentage explained (29%) was obtained from local oscillatory amplitudes extracted from a extracranial signals that were recorded using MEG. It is commonly believed that this oscillatory activity reflects synchronized post-synaptic currents (Hari and Salmelin, 1997), with amplitude suppression resulting from desynchronization of these currents (Pfurtscheller and Lopes da Silva, 1999; Naruse et al., 2010). Crucially, post-synaptic currents are not related in a one-to-one fashion to neuronal spiking, the signal for targeted communication between brain areas. From this perspective, it is revealing that a signal that depends on desynchronization of neuronal input, and that is recorded extracranially, might explain up to 29 % of the attentional improvement. An important question therefore pertains to how anticipatory desynchronization in S1 influences the efficacy by which upcoming sensory information (coded as spiking-activity) is represented and transmitted between brain areas. Concerning representation, desynchronization might reduce common (noise) fluctuations between neurons, thereby increasing the coding capacity of the neuronal population (Zohary et al., 1994). Indeed, the desynchronized state is a fundamental aspect of cortical processing (Harris and Thiele, 2011) and a reduction of correlated spike-rate fluctuations by attention has been observed in sensory cortex (Cohen and Maunsell, 2009; Mitchell et al., 2009). Concerning transmission, recordings in multiple layers of sensory cortex have revealed that

attention-induced desynchronization of alpha oscillations occurs primarily in infragranular layers (Buffalo et al., 2011). Because these layers project to upstream areas (Buffalo et al., 2011), the observed anticipatory desynchronization in S1 might reflect preparatory regulation of the efficacy by which thalamic relay nuclei can impact on S1 (Suffczynski et al., 2001).

At the same time, our data show that at least 71% of the attentional improvement must be explained by signals from different areas and/or different types of signals. Importantly, this holds only for signals that are at least partially uncorrelated with the amplitude modulations that we observed. For example, a frontoparietal control region might be involved in orienting of attention (Bressler et al., 2008), but its signals will not explain additional attentional improvement if its only function is to induce amplitude modulations in sensory cortex (Capotosto et al., 2009). Concerning signals from different areas, there may be a central role for the thalamus (Saalmann and Kastner, 2011). Consistent with this, thalamic activity is modulated by attention (O'Connor et al., 2002) and ongoing fluctuations in thalamic BOLD activity predict somatosensory detection (Boly et al., 2007). Next, secondary somatosensory cortex (S2) is also modulated by attention (Chapman and Meftah el, 2005; Steinmetz et al., 2000). Importantly, attentional modulation in S1 and secondary somatosensory cortex may occur independently (Chapman and Meftah el, 2005), allowing for additional explained improvement. Finally, previous studies have suggested that perception is influenced by the balance in activity between relevant (contralateral) and irrelevant (ipsilateral) cortical areas (Drevets et al., 1995; Thut et al., 2006; but see Cohen and Maunsell, 2011). However, this could not be confirmed in our study: (1) the anticipatory modulation only involved a contralateral suppression (Fig. 5.2D; in line with **chapters 3 and 4**), and (2) the balanced amplitude measure [contralateral – ipsilateral] did not predict performance. Concerning different types of signals, additional attentional improvement is likely accounted for by signals on a finer spatial scale (e.g. anticipatory spike-rate increases; Luck et al., 1997; Meftah el et al., 2009). Note here that such different signal types might explain additional attentional improvement, not because of differences in signal quality (because noise is corrected for in our quantification), but because they are sensitive to distinct neural processes. An important goal for future experiments will be to reveal the extent to which these signals and the observed oscillatory amplitude suppression independently contribute to attentional improvement.

We found that both alpha- and beta-band amplitude modulations explain the attentional improvement: amplitude in both frequency bands is suppressed during tactile anticipation (present study; Jones et al., 2010; Anderson and Ding 2011; **chapters 3 and 4**) and is related to perceptual performance (present study; Jones et al., 2010; Haegens et al., 2011a; **chapters 3 and 4**). However, because alpha- and beta-band amplitudes were highly correlated, their contributions to somatosensory perception and its improvement with attentional orienting were largely shared. This contrasts with a number of observations that suggest a dissociation between alpha- and beta-band oscillations: compared to alpha, beta



band oscillations (1) localize more anterior (Salmelin and Hari, 1994), (2) are modulated with a higher temporal flexibility during temporal orienting of somatosensory attention (**chapter 3**), and (3) rebound earlier after tactile input (Cheyne et al., 2003). Open questions remain with respect to the functional overlap between alpha- and beta-band oscillations and their underlying neurophysiological mechanisms (Jones et al., 2009).

A common method to establish the involvement of a neural signal in behavior is demonstrating its correlation with that behavior. However, we believe that demonstrating a correlation is inferior to the quantification proposed in this paper. The main problem with the correlation coefficient is its dependence on sources of variability that are not of interest from the perspective of the phenomenon under investigation (in our case, behavioral improvement with attention). This becomes most clear when this irrelevant variability is reduced by trial-averaging the neural and behavioral measures. For example, we observed that binned prestimulus beta amplitude (Fig. 5.3B) correlated almost perfectly ($r = -0.976$) with hit rate. This contrasts with the trial-by-trial correlation between hit-rate and beta-amplitude, which was as low as -0.078 ± 0.020 . There are two reasons for this low correlation: (1) the measured neural signals are inherently unreliable and (2) single-trial fluctuations in behavioral responses to an identical stimulus are partly determined by stochastic fluctuations that are irrelevant to the neural mechanisms that underlie some cognitive phenomenon of interest (e.g., in our set-up, electrical conductivity fluctuations at the thumb due to sweating, which are most likely unrelated to attention). This second reason is the most important one, because the attenuating effect of the unreliability of the measured neural signals (the first reason) can be corrected for in a similar way as we did for our quantification. The crucial point is that, in contrast to conventional correlational analyses, behavioral variability due to irrelevant stochastic fluctuations does not affect our quantification. In fact, this variability contributes to the variability around the regression lines, whereas our quantification only depends on the vertical distance between these regression lines.

As pointed to above, our quantification is not affected by fluctuations in variables that affect behavior, as long as these fluctuations occur independently of our experimental conditions (i.e. the cued and uncued conditions). This holds true even for cognitively relevant fluctuations, such as those involved in motivation. Throughout the experiment, motivation might fluctuate, and this may affect behavior. (This may occur via fluctuations in amplitude, which might contribute to the slopes of our perception- amplitude regression lines.) Crucially, however, if these fluctuations occur independently of the experimental conditions, they will leave the ratio between the predicted and the actual improvement unaltered. (Analogously, our quantification is unaffected by the motivation of the subject: subjects who pay more attention with cueing will have a larger shift in both amplitude and perception, but not a larger ratio between the two.) Alternatively, those variables whose fluctuations do depend on our experimental conditions (e.g. motivation might be higher in cued trials), are considered attentional by definition, and these will go into our quantification. As desired, the part via which such variables influence perception through

amplitude modulations will go into the explained part, while the part via which they influence perception through neural processes that are not reflected in this signal will go into the unexplained part.

The knowledge provided by a cognitive or systems neuroscience experiment relies on the relations between a cognitive state or behavior and a limited set of neural signals, none of which reflect all relevant aspects of neuronal processing. To evaluate the scope of any such observed relation, it is thus important to explicitly take into account the degree to which the investigated signal is behaviorally relevant. Unfortunately, for many signals a quantification of this relevance has not been established yet. In our study, we used oscillatory amplitudes that were recorded extracranially using MEG, and carefully scanned the spatial, spectral and temporal dimensions of this signal (Fig. 5.4). We demonstrate substantial behavioral relevance. At the same time, our quantification reveals the degree to which relevant neuronal processes are invisible in extracranially (MEG) recorded oscillatory amplitudes, and thus must be explored in different signals or, alternatively, in different aspects of the same signal, such as oscillatory amplitude *and* phase (e.g. Busch et al., 2009).

The paradigm that is introduced here can be more widely applied to investigate the contribution of other neural signals to attentional improvement. First, the contribution of similar signals in different sensory modalities can be investigated (e.g. occipital alpha in a visual task). Second, instead of behavioral performance, the response variable can be a neurophysiological signal that is affected by attention (e.g. an evoked response). Third, the neurophysiological signal that is used to predict behavior can be recorded during stimulus processing, rather than during anticipation. Fourth, other signals, such as BOLD or spiking activity, can be used to represent the brain state. In addition, by combining multiple predictors in a regression model it is possible to investigate to what extent distinct signals independently contribute to the response variable. This can be used to investigate, for example, whether frontoparietal, thalamic and sensory regions independently contribute to the attentional improvement and also whether this holds for BOLD and simultaneously recorded electrophysiological signals, or anticipatory and stimulus-induced signals.

Concluding, we have, to our knowledge, for the first time quantified the cognitive/behavioral relevance of a particular neural signal in the context of attentional orienting: MEG-recorded anticipatory alpha- and beta-band amplitude modulations have a largely shared contribution and account for maximally 29% of the improvement in perception that occurs with attentional orienting. Our study reveals the behavioral relevance of extracranially recorded oscillatory signals and our method provides a new means to quantify how much a particular set of neural signals contribute to cognitive, behavioral and neurophysiological phenomena.



Anticipation increases tactile stimulus processing in the ipsilateral primary somatosensory cortex

Adapted from van Ede F, de Lange FP, Maris E (In press) *Anticipation increases tactile stimulus processing in the ipsilateral primary somatosensory cortex*. *Cerebral Cortex*.
Published ahead of print on May 3 2013, doi:10.1093/cercor/bht111.



6

Abstract

Stimulus anticipation improves perception. To account for this improvement, we investigated how stimulus processing is altered by anticipation. In contrast to a large body of previous work, we employed a demanding perceptual task and investigated sensory responses that occur beyond early evoked activity in contralateral primary sensory areas: stimulus-induced modulations of neural oscillations. For this, we recorded Magnetoencephalography (MEG) in 19 humans while they performed a cued tactile identification task involving the identification of either a proximal or a distal stimulation on the fingertips. We varied the cue-target interval between 0 and 1000 ms such that tactile targets occurred at various degrees of anticipation. This allowed us to investigate the influence of anticipation on stimulus processing in a parametric fashion. We observe that anticipation increases the stimulus-induced response (suppression of beta-band oscillations) originating from the *ipsilateral* primary somatosensory cortex (S1). This occurs in the period in which the tactile memory trace is analyzed and is correlated with the anticipation-induced improvement in tactile perception. We hypothesize that this ipsilateral response indicates distributed processing across bilateral primary sensory cortices, of which the extent increases with anticipation. This constitutes a new and potentially important mechanism contributing to perception and its improvement following anticipation.

6.1 Introduction

Anticipating a stimulus improves its perception (Posner 1980a; 1980b; Carrasco, 2011). What are the neurophysiological mechanisms underlying this improvement? To answer this question, both pre- and post-stimulus neural activity must be considered. Concerning pre-stimulus activity, it is now well-established that anticipation of a behaviorally-relevant stimulus involves a modulation of neural activity in the stimulus-receiving contralateral sensory cortex, as indexed by preparatory increases in spike-rate (e.g. Luck et al., 1997) and regional blood flow (e.g. Kastner et al., 1999) and decreases in neuronal oscillations in the alpha- and beta-bands (e.g. Thut et al., 2006; **chapters 3-5**). These phenomena are associated with improved perception (e.g. Ress et al., 2000; Thut et al., 2006; Jones et al., 2010; **chapter 5**), and are therefore relevant for understanding how anticipation improves perception.

The improvement of perception by anticipatory processes must occur through altered sensory processing of the anticipated sensory information. In order to explain perceptual improvement by anticipation, it is thus important to also consider this post-stimulus sensory processing phase. However, despite a large body of prior investigations (e.g. Mangun and Hillyard, 1991; Miniussi et al., 1999), this literature has been limited by three important aspects. First, this literature has focused almost exclusively on evoked neural activity reflecting early processing stages in brain areas contralateral to sensory input. Second, this has typically been investigated in the context of simple perceptual tasks such as detection. Especially in the context of more demanding perceptual tasks, such as identification, relevant sensory processing is likely not confined to these early and contralateral processing stages. Therefore, to obtain a comprehensive understanding of perception and its improvement with anticipation, it is essential to also investigate sensory processing beyond these early stages. Finally, the relation between neural modulations and perceptual improvement has often remained unaddressed.

Here, we investigated how anticipation alters neural activity beyond early processing stages by employing a demanding perceptual identification task and focusing on stimulus-induced modulations of oscillatory neural activity. This type of sensory response typically persists up to a second after a transient stimulus and occurs in both contra- and ipsilateral sensory cortices (e.g. Chatrian et al., 1959; Cheyne et al., 2003; see also Results). Crucially, because this type of response does not require precise locking in time of the underlying events, it is also sensitive to perceptually-relevant cognitive processes of which the precise timing varies between trials.

One particular process that is important in more demanding perceptual tasks is the online maintenance of relevant sensory information. Such maintenance allows further processing of the sensory information after it has physically disappeared. Interestingly, recent literature suggests that primary sensory cortices are important for such maintenance. For example, visual information kept in working memory can be decoded from patterns of

fMRI activity in primary visual cortex (V1; Harrison and Tong, 2009; Serences et al., 2009; Sneve et al., 2012). Likewise, cueing of visual (Sergent et al., 2011) and somatosensory (Spitzer and Blankenburg, 2011) stimuli *after* their disappearance modulates, respectively, V1 and S1 activity. Moreover, this type of process is also reflected in induced modulations of oscillatory neural activity (Spitzer and Blankenburg, 2011).

Because previous studies on anticipation have focused mainly on early sensory processing stages in simple perceptual tasks, it has remained unclear whether and how the above-sketched memory-dependent processing stage (i.e. the process of maintaining and/or manipulating information in sensory memory after stimulus disappearance) is affected by anticipation. To address this, we employed a demanding tactile identification task in which brief (20 ms) tactile stimuli required substantial further processing (reaction times were in the order of 1 s) – thus relying on memory-dependent perceptual processing. As a manipulation of anticipation we presented these stimuli at variable intervals after a symbolic attentional cue. Because anticipatory processes build up over time, this manipulation of the cue-target interval allowed us to investigate stimulus processing as a function of degree of anticipation.

In our data, anticipation modulates an induced response (the suppression of beta-band oscillations) that occurs in the period in which the sensory memory trace is analyzed: 300–600 ms post-stimulus. Moreover, this modulation is correlated with the anticipation-induced improvement in tactile accuracy. Strikingly, however, this response originates from the *ipsilateral* primary somatosensory cortex (S1). We hypothesize that the primary sensory cortex is involved in identifying the fine detail of a sensory memory trace and that this can occur even when the sensory information is not received via direct afferent pathways. The increased ipsilateral response might reflect an increase in the distribution of sensory processing across bilateral primary sensory cortices, and this may contribute to the perceptual improvement following stimulus anticipation.

6.2 Materials and Methods

Materials and methods of this experiment were reported previously (**chapter 4**). We here reiterate those elements that are essential for understanding the results of the present study, and describe in more detail those methods that are specific to the currently presented analyses.

Participants

Nineteen humans (13 male, age: $M = 28$, $SD = 6$) participated in the experiment. Two participants were excluded from the analyses because of chance-level performance. The experiment was conducted in accordance with guidelines of the local ethical committee (Committee on Research Involving Human Subjects, Region Arnhem-Nijmegen, The Netherlands).



Design, task, & procedure

Participants performed a cued somatosensory identification task. Figure 6.1 depicts the trial-sequence. In each trial, a binaural auditory cue (25 ms duration) indicated with 75 % validity on which side (i.e. which hand) the to-be-identified tactile target would occur. The side was indicated by the type of auditory stimulus (white noise or 750 Hz pure tone) that was counterbalanced across participants. Tactile targets consisted of a stimulation of either the upper (distal) or the lower (proximal) part of all fingertips of a single hand. Targets were delivered using a custom-built Braille device housing five Braille cells (Metec, Stuttgart, Germany; see also **chapters 2 and 3**) that can be individually adjusted. Before starting, each fingertip was positioned over one such Braille cell. For upper (lower) targets we transiently raised the upper (lower) two Braille pins for each fingertip (Fig. 6.1). For both hands, tactile stimulation by the upper (lower) pins required a right (left) hand button-press. Because of this, (anticipated) target side was uncorrelated with the required response side. More specifically, left and right hand button presses were required equally often for targets on either hand. This independence between target and response sides was also reflected in the behavioral responses: side-congruent responses (same target- and response-sides) did not occur more frequently ($t_{(16)} = 0.314$; $p = 0.758$), and were not faster ($t_{(16)} = 0.777$; $p = 0.449$) than side-incongruent responses. This implies that neural activity that lateralized according to (anticipated) target side cannot be due to response preparation and/or execution. To increase difficulty, targets were followed, on the same hand, by five masks that contained no spatial structure. Target and masks together lasted 270 ms (20 ms stimulations, 50 ms inter-stimulus-intervals). Responses were self-paced. Following responses, tactile feedback was presented after 300 ms. A correct (incorrect) response was followed by a single (double) 20 ms tap to both hands. The interval between feedback and the next stimulus was drawn from a truncated negative exponential distribution (range: 1–5 s). Because this distribution has a

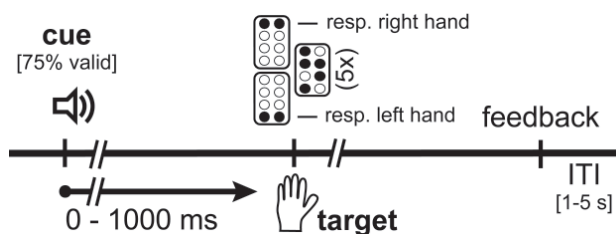


Figure 6.1. Task. A 75% valid symbolic auditory cue indicates whether a tactile stimulus will occur on the left or the right hand. Between 0 and 1000 ms after this cue, the tactile target stimulus is presented to the upper or lower part of all fingertips (using the upper or lower pins of the Braille-cells; see black dots) of either hand. This is followed by 5 masks without spatial structure. Participant’s task is to identify the target (upper or lower) and respond with the right (upper target) or the left (lower target) hand. Following a response participants receive feedback. The inter-trial-interval (ITI) is drawn from a truncated negative exponential distribution with values between 1 and 5 s.

nearly flat hazard rate, the onset of the next cue could not be predicted on the basis of elapsed time since the last cue.

The crucial manipulation in this study is the manipulation of the degree of anticipation. This was realized by varying the interval between the auditory cue and the tactile target. Per trial, this interval was randomly drawn from a uniform dis-

tribution with values between 0 and 1000 ms.

Before recording, subjects received instructions and practiced the task for about ten minutes. In two recording sessions of approximately 1 hour we collected about 1500 trials. Each session contained between 9, 10 or 11 blocks (depending on the subject's motivation) of 75 trials. Left and right cued trials were randomly intermixed. Intervals between blocks were self-paced by the participants.

Recording & extraction of neural data of interest

Recordings and analyses of neural data were highly similar to previous reports from our lab (e.g. **chapters 3 and 4**). Data were collected using a 275 axial gradiometers MEG system (CTF MEG TM Systems Inc., Port Coquitlam, Canada), and analyzed using FieldTrip (Oostenveld et al. 2011). From the axial gradiometer signal, we calculated the planar gradient (Bastiaansen and Knosche, 2000; see also **chapters 2-4**), which is maximal above the neuronal sources.

Per participant, ten channels above both left and right S1 were selected after contrasting all left and right hand stimulations with respect to beta-band (13-30 Hz) amplitude in the 150-400 ms post-target window. Because beta-band amplitude is more suppressed across contralateral as compared to ipsilateral S1 in this time window (e.g. Chatrian et al., 1959; Cheyne et al., 2003; **chapters 2 and 3**), the contrast [left minus right hand stimulation] results in negative values for right S1 and positive values for left S1. We thus selected the ten most negative and ten most positive channels to represent right en left S1 respectively. Note that this channel selection is independent of the main analysis (involving the correlation between neural activity and cue-target interval) because it is based on all target stimuli, independent of cue-target interval.

Oscillatory amplitudes were estimated using Fourier analysis with and without time- and/or frequency resolution. Estimates with frequency-resolution were based on a Hanning-taper, while estimates without frequency-resolution were based on the multitaper method (Percival and Walden, 1993). The multitaper method allows for the estimation of a spectral band (i.e. 13-30 Hz; the beta-band). For analyses with time-resolution, a 250 ms sliding time window was used that was advanced in 12.5 ms steps.

Investigating neural activity as a function of degree of anticipation

The manipulation of the cue-target interval allowed us to investigate target-processing as a function of the degree of anticipation. We did this separately for validly and invalidly cued targets. For our main analysis, we sorted trials into four cue-target interval bins (targets following the cue within [0-250], [250-500], [500-750], or [750-100] ms). After sorting the trials in this way, we used linear regression analyses to reveal which spatial, temporal and spectral aspects of the data varied with degree of anticipation. Because anticipation increases roughly linear over the first second after a cue (i.e., across the four cue-target interval bins; **chapter 4**), this type of analysis is well-suited to reveal which aspects of stimulus processing depend on anticipation.



We initially focused on the target-induced *lateralization* as an index for target processing. We did this for two reasons. First, it reduces the spatial dimension to a single value. Second, it is unaffected by sensory processing of the auditory cue (which was presented binaurally) as well as motor preparation or execution. With respect to the latter, this holds because motor preparation and execution do not lateralize according to target side; left and right hand targets required as often a left as a right hand button press.

We first describe how we quantified the relation between the cue-target interval and the target-induced lateralization indices (steps 1-2; Fig. 6.2A). Thereafter, we describe how we statistically evaluated this relation (steps 3-5; Fig. 6.2B). Together, this analysis involved five steps that are also depicted in Figure 6.2. In step 1, we separated trials by their cue-target interval (placing them into one of the four consecutive cue-target interval bins) and for each bin we calculated the normalized difference in amplitude between contra- and ipsilateral tactile stimulation ($[\text{contra} - \text{ipsi}] / [\text{contra} + \text{ipsi}]$). We did this in a time- and frequency-resolved manner. Importantly, these lateralization indices were calculated on target-centered data (with time 0 defining target onset). This analysis thus resulted in four sets of target-induced modulations, with the only difference between the sets being the interval between the preceding cue and the target (see Fig. 6.2A for these data of a representative participant). To evaluate where in time- and frequency neural activity depended on cue-target interval, we estimated the linear regression coefficient describing the relation between the modulation indices and the cue-target interval (step 2). We did this separately for each time-frequency point.

Because we did not have an hypothesis about where in time and frequency neural activity might vary with degree of anticipation, we used a statistical test that was time- and frequency-uninformed. More precisely, we blindly scanned the full time-frequency space for a statistically significant dependence of amplitude lateralization on cue-target interval. For this we used a cluster-based permutation test (Maris and Oostenveld, 2007). Importantly, this statistical analysis controls the false-alarm rate when facing multiple comparisons, as in our case, where the correlation with cue-target interval is evaluated for multiple time- and frequency samples. The details of this analysis are described and depicted (Fig. 6.2B) in steps 3-5.

In step 3, we obtained our cluster-statistics of interest by (1) evaluating, per time-frequency point, the regression coefficients from step 2 at the group level using a one-sample t-test, (2) clustering the t-values of neighboring time- and frequency-samples in case these exceeded the threshold corresponding to a univariate t-test at the 0.05 level (two-tailed), and (3) summing the t-values per cluster (called *cluster-level statistics*). Using a permutation approach, we then evaluated these cluster-level statistics against the null hypothesis of statistical independence between cue-target interval and oscillatory amplitude lateralization (steps 4 and 5). In step 4, the order of the four cue-target interval bins was permuted (at the single-subject level) and steps 2 and 3 were repeated. This was done 1000 times. The idea here is that, by randomly permuting the order of the cue-target interval

bins, all systematic variations with cue-target interval will be removed. In other words, all clusters observed after random permutation must be due to chance. The distribution that is

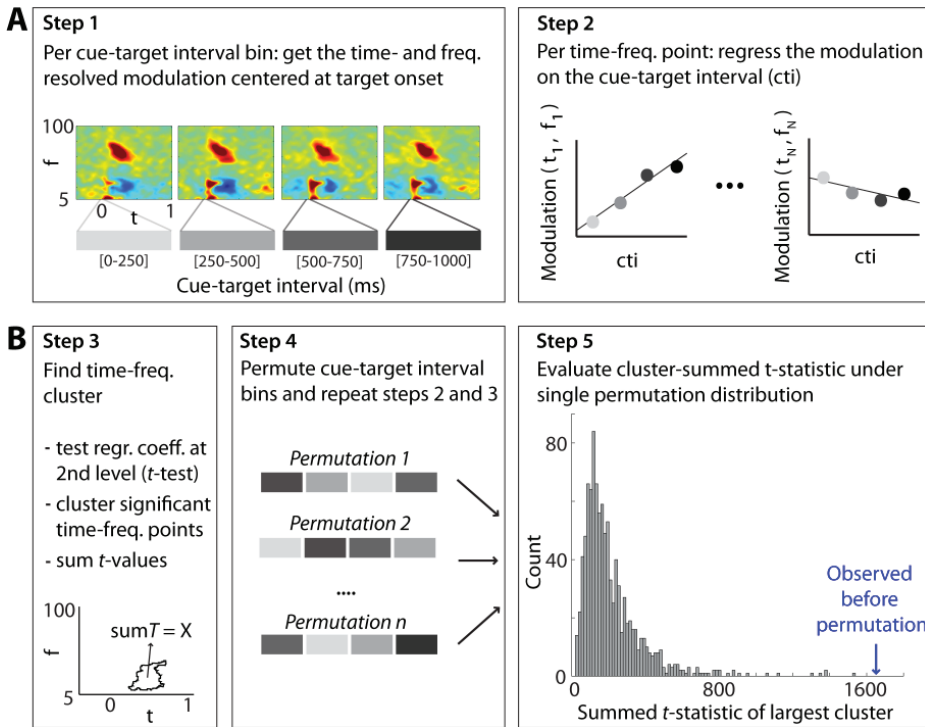


Figure 6.2. Schematic of our analysis: evaluation of where in time and frequency neural activity depends on the degree of anticipation. (A) Quantification of where in time and frequency neural activity depends on the degree of anticipation (operationalized by cue-target interval). We binned trials into four sets based on their cue-target interval and for each set calculated the time- and frequency resolved lateralized modulation indices that were centered on target-onset (step 1). Note that the time-axis for these modulation indices (with time 0 corresponding to target onset) is different from that of the cue-target interval (where 0 corresponds to a target that occurred 0 ms after the cue). The Figure shows these modulation indices for each of the four consecutive cue-target interval bins for a representative participant. In step 2 we evaluated where in time- and frequency neural activity depended on cue-target interval by estimating the linear regression coefficient describing the relation between the modulation indices and the cue-target interval. We did this separately for each time-frequency point. (B) Statistical evaluation. Because there are as many regression coefficients as there are time-frequency points, we face a large multiple comparisons problem. To deal with this problem, we used a cluster-based permutation approach (Maris E and R Oostenveld, 2007), of which the essential steps are depicted in steps 3-5. In step 3 we obtained our cluster-statistic of interest by (1) evaluating, for each time-frequency point, the regression coefficient from step 2 at the second level (i.e. across participants), (2) clustering together neighboring time-frequency points that exceeded the statistical threshold, and (3) summing their t-values. In step 4, we permuted cue-target interval bins (at the single-subject level) and repeated steps 2 and 3. This was repeated 1000 times. Each time we only kept the maximum cluster-statistic. In step 5, the summed t-statistics of the clusters observed before permutation were evaluated under the permutation distribution of these maximum cluster-statistics obtained in step 4. The histogram in the Figure depicts the positive tail of the actual permutation distribution obtained for valid trials and includes the cluster-statistic of the largest positive cluster obtained before permutation (i.e., the post-target beta-band cluster between 300-600 ms; also depicted in step 3; see also Fig. 6.3A). Because none of the cluster-summed t-statistics of the permuted data exceeded that of the original data, the pattern in the original data is unlikely to have resulted by chance ($p < 0.001$ in this one-tailed test).

obtained by randomly permuting the order of the cue-target interval bins (each time keeping the maximum cluster-level statistic) is a distribution under the null hypothesis of statistical independence between cue-target interval and oscillatory amplitude lateralization. In step 5 we assessed the significance of the time-frequency clusters observed in the original data by evaluating them under the permutation distribution of the maximum cluster-statistic ($\alpha = 0.05$, two-tailed). Because this involves a *single* distribution by means of which the full time-frequency space is evaluated, this analysis bypasses the multiple comparison problem.

Significant clusters were used as masks for the time- and frequency resolved plot of the correlation (Pearson's r) between oscillatory amplitude lateralization and cue-target interval (Fig. 6.3A,C). Thus, the masked clusters in Figure 6.3A,C represent clustered time-frequency samples of which the lateralization index scales linearly with cue-target interval, more so then can be explained by chance. For masking we applied an opacity mask ($\alpha = 0.25$ in Matlab) to all non-significant time-frequency points.

Our statistical analysis revealed a highly significant cluster at 300-600 ms post-target, in the 12-28 Hz band (Fig. 6.3A). Having established this statistically significant cluster of interest (in a time- and frequency-uninformed way), we further investigated this effect in three ways. First, we mapped its spatial topography. For every channel, we calculated the correlation between degree of anticipation and the data in this time-frequency window. This was done separately for left and right hand targets (Fig. 6.3A, topographies) that were followed by left and right hand responses (Fig. 6.4). Second, we separately mapped contralateral and ipsilateral time-resolved 12-28 Hz amplitude for stimuli occurring after short (0-250 ms), middle (375-625 ms) or long (750-1000 ms) intervals after the cue. Time was expressed relative to target-onset. Amplitude was expressed as a percentage change from a -1500 to -1125 ms pre-target (and therefore pre-cue) baseline (Fig. 6.3B,D). Note that these two analyses were done solely for descriptive purposes. Third, we investigated the correlation across participants between this neural effect and tactile identification accuracy (Fig. 6.5). We did this as a function of cue-target interval. For this, we analyzed both variables (proportion correct responses and ipsilateral beta-amplitude 300-600 ms post-target) with time-resolution using a 250 ms sliding time window was advanced in 12.5 ms steps across cue-target intervals. For normalization purposes we expressed these variables as a percentage change from the average of two neutral conditions (target without, or simultaneously with a cue).

6.3 Results

We employed a cued somatosensory identification task in which tactile stimuli were delivered to either the left or the right hand. In this task, stimuli required substantial further processing: on average, participants required 931 ± 77 ms (mean \pm 1 s.e.m.) to obtain an accuracy level of 70 ± 1.5 % correct.

Because we had presented stimuli between 0 and 1000 ms after a symbolic attentional cue, and because anticipatory processes build up over the first second after a cue (see **chapter**

4), we could use linear regression analysis to reveal what aspects of stimulus processing varied systematically with degree of anticipation. For this, we separated four sets of trials based on their cue-target intervals (i.e. stimuli occurring at [0-250], [250-500], [500-750], [750-1000] ms after the cue; see also Materials and Methods and Fig. 6.2), and evaluated the strength of the linear relation across these four sets.

Because we did not have an hypothesis about where in time and frequency neural activity might depend on anticipation, we scanned the full time-frequency space using a cluster-based permutation approach (Maris and Oostenveld, 2007; see also Materials and Methods as well as Fig. 6.2). Outcomes of this approach (i.e. the region in time-frequency space in which neural activity varied significantly across the four consecutive cue-target interval bins) are depicted in Figure 6.3.

Anticipatory processes build up over time

Before describing the influence of anticipation on post-target processing, which is the main objective of this manuscript, we briefly highlight the neural processes involved in the anticipatory period itself. For a more elaborate coverage of these results we refer the reader to our previous study that is based on data from the same experiment. In that study, we specifically focused on the relation between these anticipatory signals and the perceptual improvement with attentional cueing (**chapter 4**).

First, we consider data locked to validly cued stimuli (i.e. when the tactile target occurred on the hand that was indicated by the cue). Figure 6.3A shows the time- and frequency-resolved linear correlation between the cue-target interval (as an operationalization of degree of anticipation) and oscillatory amplitude lateralization (S1 contralateral minus ipsilateral to the target), masked by statistical significance (see Materials and Methods, as well as Fig. 6.2 for the rationale behind this analysis).

Before target-onset there is a strong negative correlation between cue-target interval and alpha- and beta-band amplitude lateralization (cluster- $p < 0.001$). This reflects a well-established anticipatory phenomenon that develops within the first second after the cue (e.g. Worden et al., 2000; Thut et al., 2006; Jones et al., 2010; **chapters 3-5**) and is constituted by a stronger contralateral suppression, at least in our data (**chapters 3-5**). This is also visible from the blue lines in Figure 6.3B depicting ipsi- and contralateral baseline-corrected beta-amplitude for trials in which the cue preceded the target between 750 and 1000 ms. Strikingly, in contrast to previous observations (e.g. Haegens et al., 2012), we did not observe an increase in the amplitude ipsilateral to the anticipated target. In fact in ipsilateral channels beta-amplitude also decreased during anticipation. While an elaborate discussion of this observation is beyond the scope of the current manuscript, we would like to point to two possible explanations for this apparent discrepancy. First, in our experiment, no distracters were anticipated on the uncued hand, an issue that is further discussed in **chapter 3**. Second, a potential increase in ipsilateral amplitude might be overshadowed by a potential bilateral effect of motor preparation. Importantly, note that the possibility of such



bilateral motor preparation would not be a confound for our main results, because these are based on lateralized modulations (see Materials and Methods for details).

Interestingly, on validly cued trials (Fig. 6.3A), at target-onset ($t = 0$) this correlation vanishes, implying a discontinuation of this anticipatory brain state. In contrast, on invalidly cued trials (Fig. 6.3C,D), the anticipatory brain state (now represented by a *positive* cluster, because the subject prepares for the opposite hand; cluster- $p < 0.001$) does continue beyond target-onset. This occurs contralateral to the expected target (thus ipsilateral to the actual target; see topographies) and likely reflects the fact that it requires approximately 200 ms to re-orient attention.

These results thus confirm that anticipation builds up over the first second after the cue (as we had previously reported: see **chapter 4**). As such, these results validate the use of the cue-target interval as an operationalization of the degree of anticipation. In the following, we will use this fact to investigate what aspects of target processing vary with this degree of anticipation, which is the main objective of this manuscript.

Anticipation increases the ipsilateral beta-band response to a unilateral tactile target

In addition to the anticipatory cluster discussed above, we also observed a strong correlation between degree of anticipation and neural activity at 300-600 ms post-target in the low frequencies, with a peak in the classical beta-band (13-30 Hz; Fig. 6.3A; cluster- $p < 0.005$). To evaluate whether this correlation originated from the ipsi- or the contralateral hemisphere, we correlated cue-target interval and oscillatory beta-band amplitude in the 300-600 ms interval separately for left and right hand tactile targets (Fig. 6.3A, topographies). Clearly, beta-band amplitude in this time window correlated negatively with cue-target interval over the sensorimotor cortex *ipsilateral* to the stimulated hand. Thus, a higher degree of anticipation is associated with lower amplitude in channels above the sensorimotor cortex ipsilateral to the stimulated hand.

This observation is further explored by zooming in on the time-resolved beta-band amplitude for stimuli occurring at three different degrees of anticipation (Fig. 6.3B): after short (0-250 ms; orange), middle (375-625 ms; green) or long (750-1000 ms; blue) cue-target intervals (note that the amount of bins is arbitrary and that we depict three bins solely for visualization purposes). Ignoring the amplitude increase around target onset (which is a consequence of the evoked response), there are two clear target-induced responses. First, unilateral tactile stimulation strongly suppresses contralateral beta-band oscillations between 150-400 ms post-target. The strength of this suppression is independent of the degree of anticipation (i.e. identical for the three traces) and can therefore be considered a *mandatory* response. Second, unilateral tactile stimulation also suppresses ipsilateral beta-band oscillations (see also Chatrian et al., 1959; Cheyne et al., 2003). This occurs around 300-600 ms post-target, slightly delayed relative to the contralateral response. Crucially, in contrast to the contralateral response, this ipsilateral response *does* depend on degree of

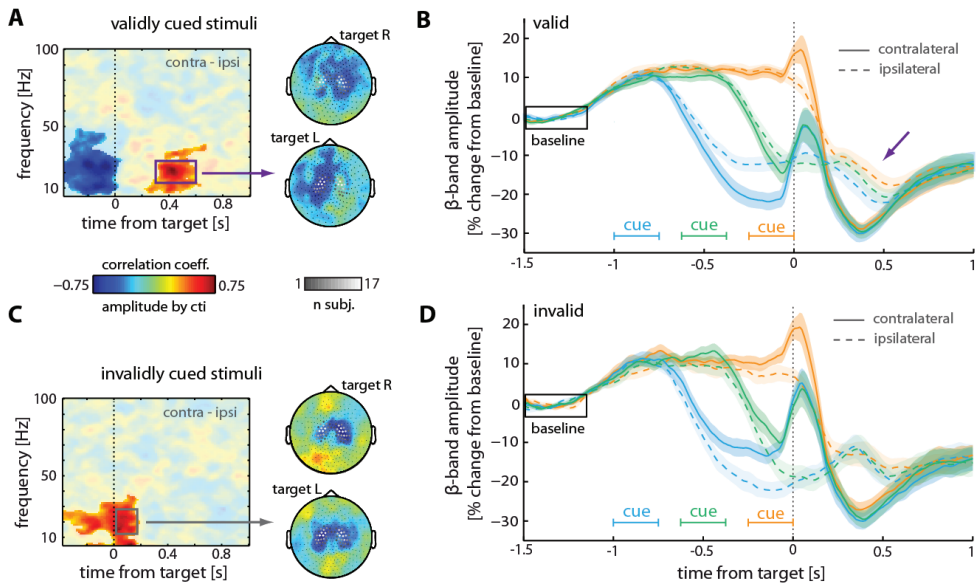


Figure 6.3. Anticipation increases the ipsilateral beta-band response to a unilateral tactile target. (A) Left: time- and frequency-resolved correlation between cue-target interval (cti) and oscillatory amplitude lateralization (contralateral minus ipsilateral S1), masked by significant clusters. Right: topographies of the correlation for the indicated cluster, separately for left and right hand targets. Highlighted channels represent selected channels above left and right S1 (see Materials and Methods for selection procedure). Channel colors show the number of subjects for which a given channel was selected (we adopted this strategy from Siegel M et al., 2007). (B) Time-resolved contralateral and ipsilateral beta-band amplitude, plotted for stimuli that occurred at short (0-250 ms; orange), middle (375-625 ms; green) or long (750-1000 ms; blue) intervals after the symbolic cue. Color patches represent ± 1 s.e.m. Purple arrow indicates the phenomenon of interest. (C,D) Same as A and B, for invalidly cued stimuli.

anticipation: a higher degree is associated with a stronger suppression (Fig. 6.3B, purple arrow). Anticipation thus increases the ipsilateral hemisphere's response to a unilateral tactile target. This is a robust effect, because it is this effect that was revealed as a significant cluster ($p < 0.005$) by our time- and frequency-uninformed statistical analysis.

We did not observe any post-target consequence of anticipation in invalidly cued trials (Fig. 6.3C,D). Importantly, this cannot be explained by the lower number of invalid as compared to valid trials: using this number of valid trials, we observed qualitatively the same results as in Figure 6.3A.

Importantly, the anticipation-dependent ipsilateral response in valid trials cannot be simply explained by a continuation of the anticipatory brain state. In fact, if this were the case, then the strongest effect should be observed in invalid trials directly following target-onset, because in this window the anticipatory suppression is larger in the ipsi- than the contralateral hemisphere (Fig. 6.3D). Instead, the effect only occurs in valid trials and is initiated only at the time when the ipsilateral response is initiated, which is 300 ms post-target (see also Chatrian et al., 1959; Cheyne et al., 2003). Thus, rather than a passive consequence of the prestimulus state, the effect involves the modulation of an existing stimulus-induced response.

The increased ipsilateral response is related to perception

It is important to rule out motor preparation and/or execution as possible explanations for the anticipation-dependent ipsilateral response. In this respect, we must first note that, in our experiment, target and response sides were uncorrelated (see Materials and Methods). Because our main statistical analysis was based on neural lateralization relative to the side of the target, the effect cannot be due to response preparation and/or execution. We could also show this empirically. We calculated, for all channels, the correlation between cue-target interval and beta amplitude at 300-600 ms post-target. We did this separately for trials separated by target and by response side. As can be seen in Figure 6.4A, the negative correlation with cue-target interval remains ipsilateral to the target side, irrespective of the subsequent response side. For example, following a left tactile target, this correlation occurs in channels above the left (ipsilateral) sensorimotor cortex, irrespective of whether the subsequent response followed with the left or right hand. This pattern is also evident from Figure 6.4B depicting these correlations for selected channels above ipsi- and contralateral S1 (see see panel A for the location of these channels and Materials and Methods for details of our selection procedure). Thus, the correlation occurs ipsilateral to the target, irrespective of whether the subsequent response was given with the same or the opposite hand. These observations, combined with the fact that the response is clearly lateralized and observed in channels above primary sensorimotor cortex, suggest that the modulation originates from the ipsilateral S1.

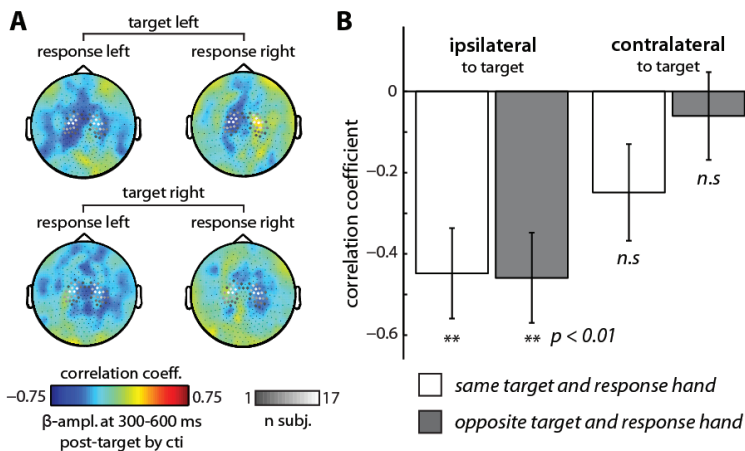


Figure 6.4. The anticipation-dependent beta-band response occurs ipsilateral to the target, irrespective of the side of the motor response. (A) Topographies of the correlation between cue-target interval (cti) and beta-band amplitude at 300-600 ms post-target, separated by target and response hand. Highlighted channels represent selected channels above left and right S1 (see Materials and Methods for selection procedure). Channel colors show the number of subjects for which a given channel was selected (we adopted this strategy from Siegel M et al., 2007). (B) Bar-chart showing the average correlation coefficient between beta-amplitude at 300-600 ms post-target and cue-target interval separately for the selected channels above ipsi- and contralateral S1 relative to target side. Data were separated for trials in which the response (a button press with the thumb) was made on the same or the opposite side as the target. Error bars represent ± 1 s.e.m.

The increased ipsilateral response is associated with perceptual improvement

Our data also provide evidence for the perceptual relevance of this post-target ipsilateral modulation. Figure 6.5A shows the dependence of this response on the cue-target interval. Strikingly, the ipsilateral response depends on the cue-target interval in much the same way as the tactile identification accuracy (Fig. 6.5A). For example, after a cue, both the ipsilateral response and tactile identification accuracy increase between 250 and 600 ms. Note that, as we showed previously (**chapter 4**), the effect of anticipation on reaction time follows a different time course.

More direct evidence for the perceptual relevance of the increased ipsilateral response is shown by its correlation with the improvement in perceptual accuracy. For each cue-target interval bin depicted in Figure 6.5A, we correlated the anticipation-induced change in ipsilateral response with the change in tactile identification accuracy across our 17 participants (change was calculated from the average of two baseline conditions; see Materials and Methods). Strikingly, participants with a stronger increase in the ipsilateral response also benefit more from anticipation in terms of perceptual accuracy (for data averaged across all cue-target intervals: $r = -0.499$, $p = 0.042$). Following the cue, this correlation occurs from 250 ms onwards (Fig. 6.5B), which is consistent with the time it takes before anticipation affects neural responses and behavior (**chapter 4**). Thus, when anticipatory processes come into play, the more they increase the ipsilateral response, the larger the corresponding improvement in perceptual accuracy.

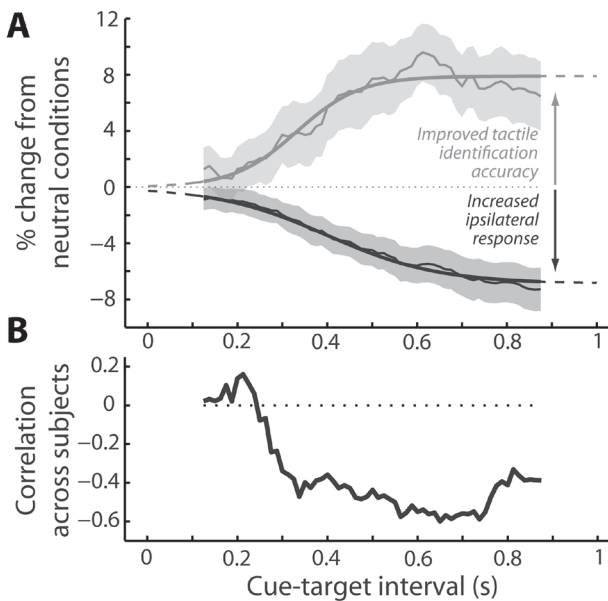


Figure 6.5. The increased ipsilateral response is associated with the anticipation-induced improvement in tactile perception. (A) Upper panel: tactile identification accuracy (grey) and ipsilateral beta-band amplitude at 300-600 ms post-target (black), as a function of cue-target interval. Data are expressed relative to the average of two neutral conditions (target without, or simultaneously with a cue). Patches represent ± 1 s.e.m. (B) Correlation across subjects between the variables in the upper panel. Only data from validly cued trials are shown.

6.4 Discussion

We investigated how anticipation affects stimulus processing and how this improves perception. We observed that anticipation of a unilateral tactile stimulus increases the ipsilateral S1 response (suppression of beta-band oscillations at 300-600 ms post-stimulus) to this stimulus, and that this increased response is associated with the improvement in perception. Three implications stand out. First, anticipation also affects relevant sensory processing beyond early, contralateral stages. Second, ipsilateral primary somatosensory cortex likely plays a more active role in tactile perception than is commonly believed. Third, our data suggest a new mechanism contributing to perception and its improvement with anticipation: distributed sensory processing across bilateral sensory cortices. In the following we will discuss these points in more detail.

Anticipation and late sensory processing stages

In the context of demanding perceptual tasks, behaviorally relevant sensory processing is likely not confined to the early and contralateral processing stages on which most previous investigations have focused. Specifically, previous studies mainly focused on evoked responses, reflecting processes that are precisely locked in time (e.g., neural activity propagating through fixed feedforward and feedback anatomical connections). In sensory cortex, such responses typically occur within the first 200-300 ms post-stimulus. In our tactile identification task, subjects required on average 931 ms to identify the target. This indicates that the memory trace of the transiently presented target was analyzed for at least 600-700 ms before a response was planned. An important question thus becomes whether such late-stage stimulus processing is also influenced by anticipation, and if so, in which brain regions? Scanning spatial, temporal and spectral dimensions of oscillatory neural activity, we observe that anticipation can also affect sensory processing 300-600 ms post-stimulus (see Wyart and Tallon-Baudry, 2008) for another example of such a “late effect” in the visual modality). Moreover, to our surprise, this occurred in the primary sensory cortex *ipsilateral* to the stimulus.

The involvement of primary sensory cortex in later stages of sensory processing fits well with recent literature. In fact, a number of studies provide evidence for the active role of primary sensory cortices in the maintenance of sensory information after stimulus disappearance (Harrison and Tong, 2009; Serences et al., 2009; Sergent et al., 2011; Sneve et al., 2012). In a demanding perceptual task like ours, in which target stimuli are only presented briefly, such maintenance likely plays a central role in perception. Interestingly, in a recent electrophysiological study investigating such sensory maintenance, Spitzer and Blankenburg (2011) also observed a suppression of induced neural oscillations in S1. Here we show that this type of response is modulated by anticipation. Considering the ipsilateral nature of this modulation in our data, it is interesting to note that the utilization of primary sensory cortex for sensory maintenance need not be restricted to the sensory cortex in which sensory information was initially received. Indeed, even perceptual imagery – a condition

without sensory input – can engage primary sensory cortices (Kosslyn et al., 1995). Possibly via the same mechanism, the non-recipient ipsilateral primary sensory cortex might also be utilized for perception. To corroborate this interpretation, experiments are required in which both anticipation and sensory maintenance are explicitly manipulated. For example, if the stimulus must be maintained for several seconds, would the anticipation-dependent ipsilateral response maintain over this period as well?

In the following we first review other available evidence suggesting that ipsilateral S1 can contribute to the perception of unilateral tactile stimuli. We then further elaborate on possible mechanisms via which this increased ipsilateral response might mediate perceptual improvement.

Ipsilateral S1 and tactile perception

Above we suggested that ipsilateral primary sensory cortex might be utilized for perception via purely top-down pathways (i.e. pathways that are also employed by perceptual imagery). In line with this, computational modeling has suggested that S1 beta oscillations might depend critically on inputs to the supragranular (feedback receiving) layers of cortex (Jones et al. 2009). In addition, the utilization of ipsilateral S1 might proceed via bottom-up pathways existing within the somatosensory system. In this system, contralateral S1 is the primary cortical recipient of tactile information. This likely explains the stronger as well as earlier post-stimulus beta-band response over contralateral (as compared to ipsilateral) S1 (Fig. 6.3B,D). At the same time, there is evidence suggesting that ipsilateral S1 also gains access to some of this information. Ipsilateral responses to unilateral tactile stimuli have been observed not only in beta-band oscillations (Chatrian et al., 1959; Cheyne et al., 2003; current study, Fig. 6.3B,D), but also in regional cerebral blood flow (Hlushchuk and Hari, 2006; Lipton et al., 2006; Tommerdahl et al. 2006), dendritic current flow (Lipton et al. 2006), and action potentials (Iwamura et al., 1994; Wiest et al., 2005; Lipton et al., 2006). However, it is currently not clear whether these different types of responses are related to the same underlying principles. For example, while some studies point to inhibition of ipsilateral processing (Hlushchuk and Hari, 2006; Lipton et al., 2006; but see Wiest et al., 2005), our data most likely reflect the opposite. This is because inhibition has been associated with an *increase* in beta-band amplitude (Jensen et al., 2005; Pogosyan et al., 2009). One important difference between our study and the aforementioned ones is that our tactile stimulus required substantial further processing.

Ipsilateral S1 responses likely involve pathways that pass via contralateral S1, in particular Brodmann area 2 (BA2). In BA2, Iwamura et al. (1994) observed numerous cells with bilateral receptive fields for hands and digits. Ablation and inactivation of contralateral S1 abolished bilateral receptive fields, implying that the ipsilateral responses are transmitted via contralateral S1. One likely pathway involves a callosal connection between left and right BA2 (Iwamura et al. 1994). Alternatively, contralateral S1 might project to ipsilateral



S1 indirectly via secondary somatosensory cortex (S2) or the thalamus (Blankenburg et al., 2008). Noteworthy, a pathway between left and right S1 has behavioral advantages because tactile information is often co-registered between both S1 cortices, as a result of bimanual exploration of tactile objects. Because this feature might be central to both somatosensation and action, so might be the ability to distribute processing across the hemispheres. Indeed, analogous to our observations in the tactile domain, ipsilateral primary motor cortex has been implicated in motor-processing (Crone et al., 1998; Donchin et al., 1998; Mehring et al., 2003).

Several lines of evidence suggest that these responses may also contribute to perception. First, processing of sensory information in contralateral S1 is modulated by ipsilateral sensory stimulation (Schnitzler et al., 1995; Wiest et al., 2005). This points to integration of sensory information between bilateral S1, and thus argues for a functional role of ipsilateral S1 in perception. On a behavioral level, Harris et al. (2001) showed that the memory trace of a unilateral tactile stimulus is maintained with specificity for the finger on which the to-be-remembered stimulus occurred. Crucially, this specificity of the tactile memory trace also applied to the corresponding fingers on the other hand. Because this finger specificity implies working memory maintenance within somatotopically organized brain regions (S1 and/or S2), the intermanual transfer implies maintenance in ipsilateral S1 and/or S2. Moreover, similar to the present report (Fig. 6.5B), such working memory performance has been reported to correlate positively with the degree of ipsilateral beta-band suppression in the retention interval (Li Hegner et al., 2007). These observations are thus consistent with a scenario in which the improvement in tactile accuracy following anticipation is mediated by an increased ipsilateral response, as reported in this paper. We next turn to possible mechanisms via which the increased ipsilateral response might mediate the corresponding improvement in perception.

Improved perception through distributed processing

Ample evidence exists that oscillatory neural activity is related to information processing in underlying neural populations. In fact, these oscillations interact with local spiking activity (e.g. Fries et al., 2001; Haegens et al., 2011b). Directly relevant to our observations, the suppression of beta-band oscillations in sensorimotor cortex has been associated with an increase in cortical excitability (Pogosyan et al., 2009; Maki and Ilmoniemi, 2010) as well as an improvement in tactile detection performance (Palva et al., 2005; Jones et al., 2010; **chapter 5**). Because both contra- and ipsilateral S1 show this type of response, we propose that the increase in the ipsilateral response with anticipation reflects an increase in the distribution of sensory processing across contra- and ipsilateral S1.

It is commonly believed that anticipation improves perception through selective focusing of attention, involving amplification of relevant signals and/or suppression of irrelevant signals (Carrasco, 2011). Our task also involved selective attention: subjects anticipated a stimulus on one of their hands, allowing selective spatial attention. Therefore,

our results point to an additional mechanism via which this type of attention might improve perception: the extent to which sensory processing is distributed across contra- and ipsilateral sensory cortices. In line with this hypothesis, we show that the degree to which the ipsilateral response increases (in essence, the degree to which the response becomes more bilateral or distributed) predicts the amount of perceptual improvement with spatial attention.

What type of sensory processing might benefit such distribution across the hemispheres within the context of our tactile identification task? An important notion is that performance in this task relies on the matching of the incoming sensory stimulus to memory templates of the possible targets. In our set-up, these targets differed in a fine spatial aspect (stimulation of the upper versus the lower part of the fingertips), and therefore only S1 might have the appropriate neural circuitry for storing their templates and matching the incoming sensory information. Moreover, throughout our experiment, identical targets occurred on both the left and the right hand, and therefore these templates might have been formed within both left and right S1. In this scenario, optimal matching of the incoming sensory information might involve both contra- and ipsilateral templates. Thus, the increased ipsilateral S1 response might reflect an increase in the extent to which the unilaterally presented sensory information is maintained and matched to the ipsilaterally stored template (in addition to the contralateral one). Alternatively, such template matching might occur downstream of S1. In this case, functional roles of the ipsilateral S1 response might involve: (1) solely holding online the sensory memory trace as long as up- or downstream areas need to read this out, or (2) elaborate processing of the sensory information preceding such read out.

Why is the influence of anticipation only visible in the ipsi-, but not the contralateral beta-band response? We can only speculate about this unexpected result. An important observation is that the stronger contralateral suppression of beta-band oscillations reaches a plateau, independently of degree of anticipation (Fig. 6.3B). This plateau might reflect saturation in the processing capacity of contralateral S1, which might be the reason for utilizing ipsilateral S1 for additional processing. Because a higher degree of anticipation involves more strongly suppressed contralateral beta-band oscillations prior to the target, the additional contralateral suppression following the target is more easily accomplished when the subject is more prepared (compare blue and orange solid lines, Fig. 6.3B) and this may allow additional engagement of ipsilateral S1.

We have put forward the hypothesis that ipsilateral S1 assists in the processing of the tactile memory trace and that anticipation increases this process to improve perception. However, contrary to this hypothesis, previous investigations into the neural correlates of tactile working memory maintenance, did not reveal involvement of S1 (reviewed in Romo and Salinas, 2003). At least three factors might explain this discrepancy. First, the work by Romo and Salinas, (2003) focused on local neural spiking activity, while we focused on a large-scale population aggregate of post-synaptic potentials. Indeed, this latter type of signal has been associated with tactile working memory operations (Spitzer and



Blankenburg, 2011). Second, in addition to online maintenance, our identification task required manipulation of the sensory memory trace (e.g., matching of the sensory memory trace to the stored templates). These additional operations may engage additional neural populations. Third, in contrast to our human subjects, the monkeys in the experiments by Romo and colleagues were highly overtrained. This is relevant because neural dynamics can change with practice (e.g. Wan et al., 2011). Despite these arguments, it is important to keep in mind that our results do not necessarily imply that there are also anticipation-dependent modulations of the spiking activity in ipsilateral S1. For example, work by Das and colleagues (Sirotin and Das, 2009; Cardoso et al., 2012) has revealed anticipation related modulations in hemodynamic signals which are poorly related to local spiking activity. It is currently not clear to what extent such a dissociation may also hold for the beta-band oscillations in the MEG, the neural signal studied here. For example, these oscillations might reflect rhythmic fluctuations of subthreshold dendritic currents (e.g. Jones et al., 2009). Thus, at present we cannot exclude that such modulations of spiking activity occurs elsewhere, such as in the contralateral S1 or bilateral S2, and produce synchronized subthreshold activity in connected cortical areas (i.e. the ipsilateral S1). The ipsilateral response might thus reflect the consequence of stimulus processing that takes place elsewhere. However, this account would predict that the influence of anticipation should also be observed in channels above the contralateral S1 / bilateral S2. This was not the case (Fig. 6.3A,B).

Conclusion

We conclude that anticipation can also affect memory-dependent perceptual processing in primary sensory cortex, and that the ipsilateral S1 likely plays a more active role in tactile perception than is commonly thought. Increasing the extent to which sensory processing is distributed across bilateral primary sensory cortices might constitute an important mechanism contributing to the improvement in perception following stimulus anticipation.





Dissociable spectral signatures of somatosensory attention during anticipation and stimulus processing

Adapted from van Ede F, Szabényi S, Maris E (Submitted) *Dissociable spectral signatures of somatosensory attention during anticipation and stimulus processing.*

7

Abstract

What are the neural correlates of attention? Here we show that the answer to this question depends critically on the sensory context in which attention is deployed. We recorded magnetoencephalography (MEG) in humans and investigated tactile spatial attention in two different sensory contexts: in anticipation and during the processing of sustained tactile stimuli. We observe a double dissociation between these contexts and two key electrophysiological correlates of attention: in anticipation we primarily observe an attentional suppression of contralateral alpha- and beta oscillations (8-12 and 15-30 Hz, respectively), whereas during stimulus processing we primarily observe an attentional amplification of contralateral gamma oscillations (55-75 Hz). This dissociation is well explained by the different neural states that occur prior and during the stimulus, and on which attention can exert its influence. We propose that attention must be understood as a mechanism that modulates existing patterns of neural activity, and not as a fixed set of specific neural correlates. Consequently, different correlates of attention may contribute to perception in different contexts and, as our data reveals for the attentional modulation of alpha oscillations, these are not always required for attention to improve perception.

7.1 Introduction

A major challenge in cognitive and systems neuroscience is to understand the neural mechanisms via which attention allows the selective processing of one aspect of the environment while ignoring others (Desimone and Duncan, 1995). To date, studies into the neural mechanisms of attention have revealed multiple neural correlates. For example, in regions of sensory cortex that process the task-relevant stimulus, attention has been shown to increase firing rate (e.g. Luck et al., 1997), blood flow (e.g. Kastner et al., 1999) and gamma oscillations (e.g. Fries et al., 2008), and decrease spike-rate (noise) correlations (e.g. Cohen and Maunsell, 2009) and alpha and beta oscillations (e.g. Worden et al., 2000; **chapters 3-5**). A key question that emerges is whether these different correlates are merely different reflections of the same underlying processes (and thus collectively *constitute* attention) or, rather, whether they relate to distinct components of attention and therefore might dissociate between experimental conditions. Here we addressed this question with regard to two of the aforementioned electrophysiological correlates of spatial attention: (1) the suppression of oscillations in the alpha- and beta bands, and (2) the amplification of oscillations in the gamma band.

Although both these correlates have been well-established over the past 15 years, careful inspection of the literature reveals an important distinction. The attentional suppression of alpha oscillations in the visual modality (Worden et al., 2000; Thut et al., 2006) and alpha and beta oscillations in the somatosensory modality (Jones et al., 2010; Haegens et al., 2011; **chapters 3-5**) is typically reported in studies that investigate attention in the interval between a symbolic spatial cue and an anticipated target (i.e. in anticipation). In contrast, the attentional amplification of gamma oscillations is almost exclusively reported in studies in which attention is directed to a sustained stimulus (i.e. during stimulus processing; Fries et al., 2008; Siegel et al., 2008; Gregoriou et al., 2009). Thus, while both correlates are well-established, an important issue has remained obscure: whether these different correlates co-occur or, alternatively, are unique to the specific sensory context in which attention is investigated (i.e. before or during the stimulus).

If the neural correlates of attention are context-dependent, then this has several implications. First, it would suggest that the neural implementation of attention cannot be understood in relation to a fixed set of its correlates. Instead, it might be better understood as a mechanism that modulates existing patterns of neural activity. We provide direct evidence for this: corresponding to the stimulus-induced change in the oscillatory patterns of neural activity, we observe that attention primarily suppresses contralateral alpha and beta oscillations in anticipation, while it primarily amplifies gamma oscillations during stimulus processing. Second, the context-dependence of neural correlates of attention would restrict the behavioral relevance of the different correlates of attention to specific sensory contexts. In fact, we report a large attentional improvement in perception without any concurrent attentional alpha modulation during sustained stimulus processing. This reveals that this specific correlate is not always required for attention to improve perception.

7.2 Materials and Methods

Participants

18 subjects (12 male; age-range: 22-50 years) participated in the experiment. One participant was excluded due to chance level performance, another due to an incomplete understanding of our instructions as a result of a language barrier. The experiment was conducted in accordance with guidelines of the local ethical committee (Committee on Research Involving Human Subjects, Region Arnhem-Nijmegen, The Netherlands).

Tactile stimulation

We used two custom-built Braille stimulators containing 8 pins per fingertip and a response button at the thumb (see also **chapters 2 and 3**). Tactile stimulation always occurred on both hands (all fingers, excluding the thumbs), at a rate of 50 Hz. Stimuli contained two features (a proximity and a motion feature; Fig. 7.1), each having two levels (proximal/distal and leftward/rightward, respectively). For each trial we randomly drew these levels independently per feature and per hand. The proximity feature involved a higher percentage of pins presented to either the proximal or distal part of the fingertips. For example, at every 50 Hz cycle of a *distal* stimulus, each of the four distal pins would have a probability of 0.12 to be presented versus a probability of 0.01 for each of the four proximal pins. For the motion feature, one finger per hand received a stronger stimulus ($p = 0.85$ for all pins) and this stimulus jumped left- or rightward across the fingers every 300 ms (3.3 Hz/finger), inducing a sensation of sweeping motion. Following a practice session we adjusted the above probabilities slightly in several participants.

Task & procedure

We employed a cued tactile identification task (Fig. 7.1). Each trial started with a 300 ms visual cue. A word instructed subjects to identify the proximity or the motion feature of the stimulus (attend trials), or to ignore this stimulus (ignore trials). In the attend trials, this instruction was paired with an arrow pointing to the left or right, indicating the hand for which the identity of the tactile stimulus should be evaluated (the attended hand). Following cue-onset, there was a 2.5 s anticipation interval followed by a 2.5 s stimulation interval. A response screen followed 500 ms after stimulation. In 10 % of the attend trials, prior to the response screen, subjects were asked about the identity of the stimulus on the unattended hand (invalid trials).

In proximity trials, subjects pressed the left (right) button to indicate a proximal (distal) stimulus; in motion trials, they pressed the left (right) button to indicate a leftward (rightward) moving stimulus. Confidence was indicated by a bar that filled up as long as the button remained pressed. In ignore trials, subjects required to bring the confidence bar to a predetermined location, indicated by a line on the screen. As feedback, the fixation-cross turned red (incorrect) or green (correct) for 200 ms. Inter-trial-intervals were between 1 and 2.5 s. Trial types occurred with equal probability and were randomly intermixed. In 2 sessions of an hour, subjects completed around 700 trials.



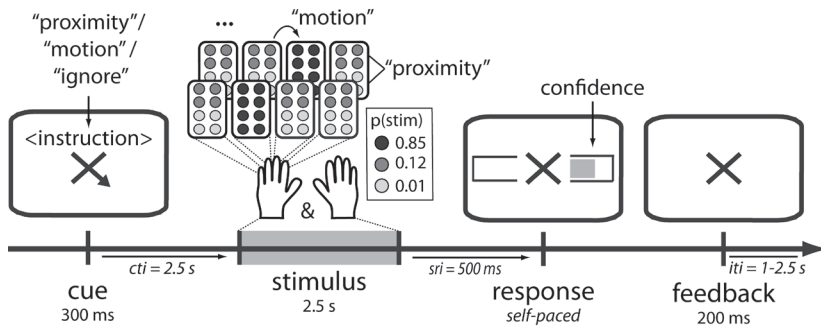


Figure 7.1. Cued tactile identification task. Each trial started with a 300 ms visual cue. A word instructed subjects to identify the “proximity” or the “motion” feature of the stimulus (attend trials), or to “ignore” this stimulus (ignore trials). In attend trials, this instruction was paired with an arrow pointing to the left or right, indicating the hand for which the identity of the tactile stimulus should be evaluated. Following cue-onset, there was a 2.5 s anticipation interval followed by a 2.5 s stimulation interval. Stimuli were always presented to both hands and contained both a proximity and a motion feature (that was independent between the hands). In proximity trials, subjects were required to identify whether at the cued hand the stimulus was on average more proximal or distal. In motion trials, subjects were required to identify whether at the cued hand the stimulus contained a leftward or a rightward motion (see Materials and Methods for details). 500 ms after stimulation, a response screen was presented. In proximity trials subjects pressed the left (right) button to indicate a proximal (distal) stimulus; in motion trials subjects pressed the left (right) button to indicate a leftward (rightward) moving stimulus. Confidence was indicated by a bar that filled up as long as the button remained pressed. A change in color of the fixation cross served as feedback.

Recording & analysis

Neural activity was recorded using a 275-channel CTF MEG system (1200 Hz sampling) and analyzed in Matlab, using FieldTrip (Oostenveld et al., 2011). All channel-level analyses were based on the synthetic planar gradient, which is maximal above the source (Bastiaansen and Knosche, 2000; see also **chapters 2 and 3**). Channels were selected above the left and right S1 by contrasting 8-30 Hz power during the stimulus with that prior to the cue, and selecting the 10 left and the 10 right channels that showed the maximal response to the tactile stimulus. Attentional modulation was quantified as the difference between trials in which the attended hand was contra- or ipsilateral to these channels, expressed as a percentage change (i.e. $((\text{contra} - \text{ipsi}) / \text{ipsi}) * 100$). This was done separately for the left and right channels, which were then pooled. Epochs between 0.5-2.5 and 3-5 s were used to quantify the attentional modulation in the anticipation and stimulation intervals. Because all observations in this paper were highly similar between the proximity and the motion trials, these were collapsed.

Oscillatory power was estimated using conventional Fourier analysis in combination with multi-tapering which allows for control over spectral smoothing (Percival and Walden, 1993). Smoothing parameters are stated in our figure captions. Alpha, beta and gamma were defined as, respectively, 8-12, 15-30 and 55-75 Hz. Analyses with time-resolution were based on a 500 ms sliding time window that was advanced in 100 ms steps. Sources were reconstructed using beamforming (Gross et al., 2001). We placed grids of 0.75 cm^3 voxels in the individual MRIs. Per voxel, power was reconstructed separately for left and right

attention trials and subsequently contrasted between them. Data were normalized to MNI coordinates before averaging across participants.

We made sure that all reported modulations could not be attributed to motor preparation and/or execution. First, we separated all trials for which the response was made with the same hand as the attended one, from the trials in which these hands were different. If the attentional modulation reflects motor preparation, then the attentional modulation indices should reverse between these two sets of trials. Following the same logic, we also separated trials based on their muscular activity. We had recorded this activity using two bipolar electrode pairs that were placed across the flexors of the left and right forearms. We measured muscular contraction by a signal that was obtained by first high-pass filtering (40 Hz cut-off) and subsequently rectifying the raw EMG traces. We separated trials in which the muscular contraction was higher on the attended than the unattended hand, from those in which this was the other way around. Again, if the attentional modulations reflect overt motor behavior, then these modulations should reverse between these two sets of trials.

7.3 Results

Attention improves perception

Attention significantly improved perception as indexed by higher accuracy (improvement of 27 %; $t_{(15)} = 5.20$; $p < 0.005$) faster reaction times (22.29 %; $t_{(15)} = -5.80$; $p < 0.001$) and higher confidence ratings (42.37 %; $t_{(15)} = 4.47$; $p < 0.005$) to stimuli that were preceded by valid, compared to invalid, spatial cues (Fig. 7.2).

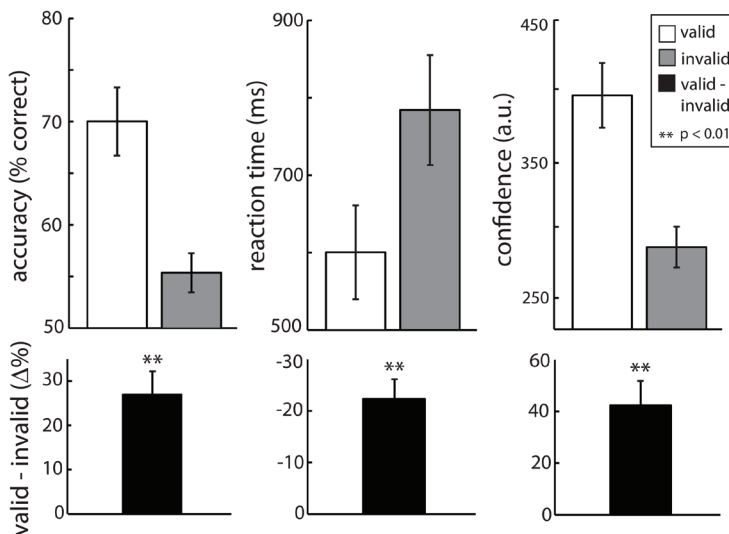


Figure 7.2. Attention improves perceptual accuracy, speeds up perceptual judgments and increases confidence. On invalid trials, after stimulus presentation, subjects were asked to report the identity of the unattended stimulus. Confidence is indexed by button-press duration in ms. Error bars represent ± 1 SEM.

Neural correlates of spatial attention are different during anticipation and stimulus processing

To investigate the neural correlates of tactile spatial attention, we contrasted neural activity in MEG channels above the left and right primary somatosensory cortex (S1) between trials in which the attended hand was contra- (“attend in”) or ipsilateral (“attend out”) to these channels. Note that, because the stimulus was always presented to both hands (only one of which was attended in any given trial), this contrast is exclusively sensitive to the side of attentional deployment. This measure can therefore be compared between the anticipatory and the stimulus processing intervals, without being confounded by changes in neural activity that are a direct consequence of the bottom-up sensory input. Of course, neural correlates of attention might still be *mediated* by stimulus presence, as we will argue below.

Figure 7.3A depicts this contrast as a function of time and frequency and shows our primary observation: a dissociation in the neural correlates of attention between anticipation and stimulus processing. Specifically, in anticipation of the upcoming stimulus (0-2.5 s; also denoted “pre”), the attentional

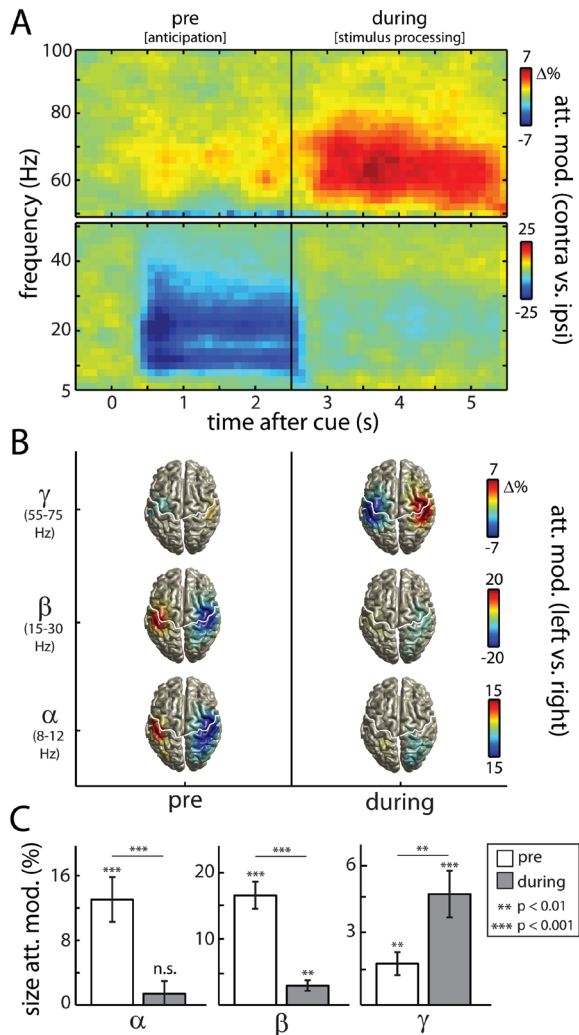


Figure 7.3. Neural correlates of attention dissociate between anticipation and stimulus processing. (A) Time and frequency resolved representation of the attentional modulation of neural activity. Attentional modulation is calculated using selected channels above left and right S1 by contrasting trials in which the attended hand was contra- (“attend in”) or ipsilateral (“attend out”) to these channels. At time 0 the cue is presented. Stimulation occurs from 2.5 to 5 s. For frequencies > 50 Hz we applied a ± 4 Hz frequency smoothing. (B) Source reconstructions of the attentional alpha, beta and gamma modulations (here quantified as left vs. right attention). Colored voxels exceeded the significance-threshold of the univariate t-statistics. (C) Size of the attentional modulations (contra vs. ipsi). Error bars represent ± 1 SEM.

modulation was predominant in the alpha and beta frequency bands, whereas during stimulus processing (2.5-5 s; also denoted “during”) this modulation was predominant in the gamma band (Fig. 7.3A). This dissociation is demonstrated most strikingly with respect to the alpha band: for this frequency band, we observed a strong and highly significant modulation in anticipation (size modulation: 13.04 %; $t_{(15)} = 4.79$, $p < 0.001$) that was completely abolished during the stimulus (1.39 %; $t_{(15)} = 0.92$, $p > 0.3$). Although for the beta and gamma bands this dissociation was not absolute (i.e. a small but significant beta modulation was also observed during stimulus processing, and a small but significant gamma modulation was also observed in anticipation), for these bands the pattern of results was also dominated by the difference in the attentional modulation between anticipation and stimulus processing. This pattern of results was highly robust and is summarized in Figure 7.3C.

The observed dissociation could also be demonstrated with a source analysis in which we contrasted attention to the left and right hand (Fig. 7.3B). In addition, this analysis revealed that the attentional modulation in all three frequency bands originated from the same cortical areas: the primary sensorimotor cortices (i.e. all modulations were centered on the central sulci which are indicated by the white lines in Fig. 7.3B).

These modulations could not be attributed to motor preparation or execution (Fig. 7.4). If these modulations would reflect response preparation, then they should reverse between trials in which the response was made with the same or the opposite hand as the hand

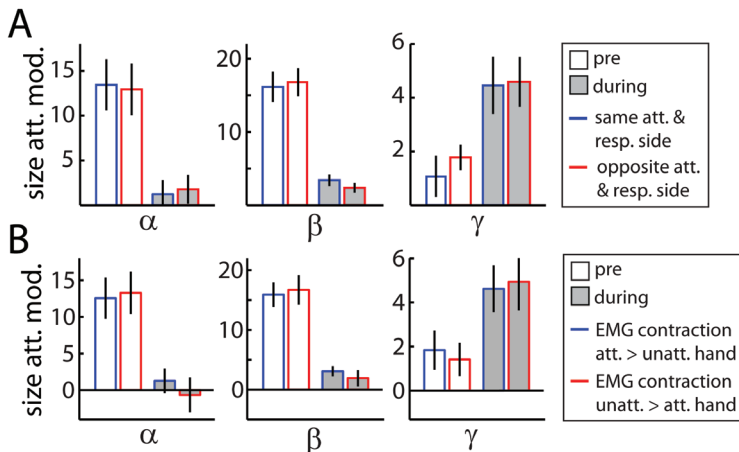


Figure 7.4. The observed attentional alpha, beta and gamma modulations are not due to response preparation or overt motor behavior. (A) Comparable to Figure 7.3C, except data are split by response side. Crucially, all attentional modulations are highly similar between trials in which the response was made with the same or with the opposite hand as the hand that was attended. If these modulations represented response preparation, then the attentional modulations should have reversed between these two sets of trials, and this is clearly not the case. (B). This follows the same logic as panel A, except we here split the trials by EMG contraction, i.e., whether the attended or the unattended hand showed a stronger muscular contraction. Again, if the observed attentional modulations were due to overt motor behavior, then these modulations should reverse between these two sets of trials and this is clearly not the case. Thus, both response preparation and overt motor behavior cannot account for the attentional modulations of alpha, beta and gamma oscillations.

that was attended. This was clearly not the case (Fig. 7.4A). Likewise, if these modulations would reflect overt motor behavior, then these modulations should reverse between trials in which the muscular contraction was stronger on either the attended hand or the unattended hand. Measuring muscular contraction by the rectified high-pass (>40 Hz) filtered EMG, we observed that this was clearly not the case (Fig. 7.4B). Therefore, these modulations must be attributed to covert tactile attention and therefore most likely originate (at least partly) from S1. Finally, as we show in Figure 7.5B, these modulations all originate from the contralateral hemisphere, with alpha and beta decreasing with attention (primarily in anticipation) and gamma increasing (primarily during stimulus processing).

Attention interacts with the stimulus-induced change in neural activity

The difference between anticipation and stimulus processing in essence entails a difference in sensory context, i.e., the difference between the absence and presence of the stimulus. We therefore evaluated the hypothesis that the observed dissociation (Fig. 7.3) is mediated by a stimulus-induced change in neural activity within sensory cortex. If attention mainly operates on existing neural activity, then a change in neural activity induced by the stimulus must be paired with a change in the type of activity that attention can modulate. To evaluate this, we first investigated the change in the pattern of neural activity due to the stimulus itself. For this, we had included trials in which the stimulus could be ignored, which allowed us to investigate the pure (i.e. attention-free) effect of the stimulus. We compared neural activity prior to the stimulus with neural activity during the stimulus, the result of which is depicted in Figure 7.5A (top panels). Most importantly, the stimulus strongly suppressed alpha and beta oscillations, while at the same time it induced gamma oscillations. This observation provides a parsimonious explanation for the observed dissociation (Fig. 7.3). Because alpha and beta oscillations are largely abolished by the stimulus, attention can no longer modulate these oscillations when the stimulus is present, hence the lack of a modulation during stimulus processing (also depicted in the lower panels in Fig. 7.5A). Analogously, because gamma oscillations are most pronounced during the stimulus, this is when attention can amplify these oscillations, hence the stronger modulation of gamma during stimulus processing.

These observations are also confirmed by the time courses of power for, on the one hand, the alpha- and beta bands and, on the other hand, the gamma band (Fig. 7.5B; note that we collapsed across the alpha- and beta bands because they showed a highly similar pattern). Again, the black lines indicate our ignore condition and show the pure stimulus-driven change in neural activity. Evidently, the attentional modulation of gamma power is most pronounced when the stimulus is present and generates gamma: there is a stimulus-induced gamma increase in the ignore condition, and this increase is amplified with a factor > 2 when attention is directed to the contralateral hand (upper panel Fig. 7.5B). At the same time, because the stimulus itself leads to a strong attenuation of alpha and beta oscillations (see the ignore condition in the lower panel of Fig. 7.5B), these oscillations cannot be further

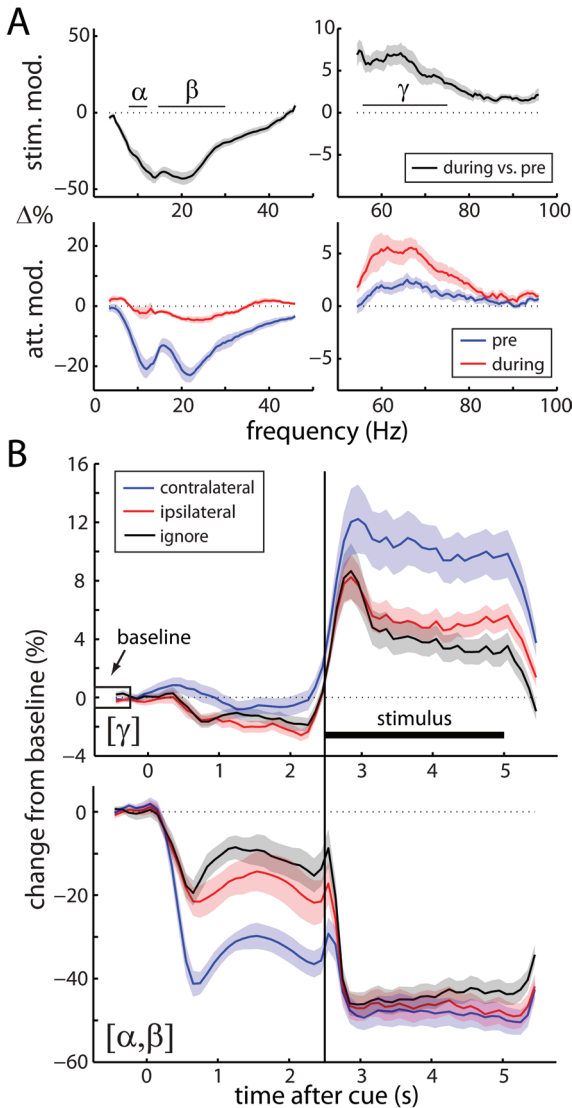


Figure 7.5. Attention interacts with stimulus-induced changes in neural activity. (A) Frequency-spectra of the stimulus-induced (top) and attentional (bottom) modulations of oscillatory power. Stimulus-induced modulations are based on the ignore condition. Spectra were estimated with ± 2 Hz smoothing. (B) Time courses of gamma (upper panel) and alpha/beta (lower panel) power when the attended hand was contra- or ipsilateral to the selected channels, or when the stimulation was ignored. Data are expressed as a percentage change from a pre-cue (-0.75 to -0.25 s) baseline. Shadings represent ± 1 SEM.

suppressed by attention in this interval (a floor effect). This contrasts with the anticipatory interval, where they are selectively suppressed contralateral to the attended hand.

Additional factors that shape the neural correlates of attention

The neural correlates of attention are further shaped by individual characteristics and the details of the experimental task. First, we observed large inter-individual differences in the degree to which the sustained tactile stimulus induced gamma oscillations (as evaluated using the trials in the ignore condition). While in some subjects the stimulus clearly induced gamma oscillations, in other subjects the same stimulus did not. Crucially, this measure of gamma responsiveness was tightly correlated with the size of the *attentional* gamma modulation (Fig. 7.6), both during anticipation ($r = 0.62$, $p < 0.05$) and during stimulus processing ($r = 0.77$, $p < 0.001$). Second, we noted an important difference between our current dataset and two closely related datasets that we had recorded previously

(**chapters 3 and 5**). In those datasets, we had initially not observed any anticipatory gamma modulation. We therefore reanalyzed these datasets with the same settings that we used

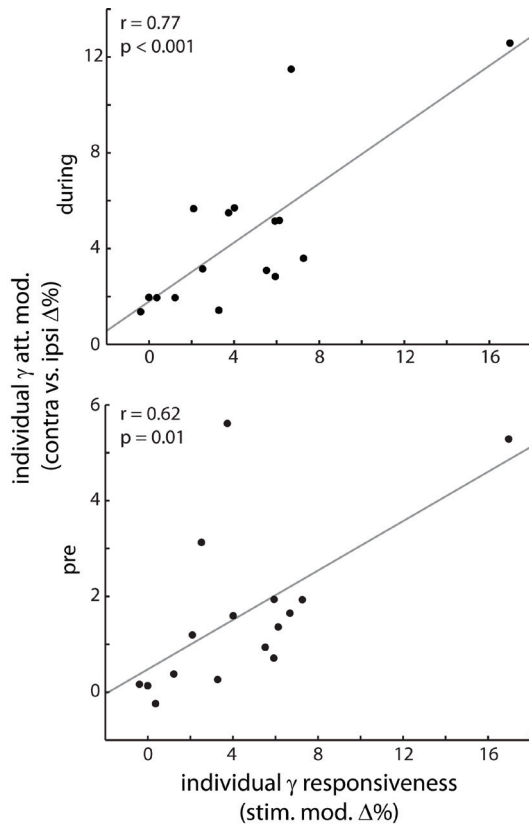


Figure 7.6. Participant-specific gamma responsiveness predicts the size of the attentional gamma modulations. For each participant we quantified the gamma responsiveness as the percentage increase in gamma power during the stimulus, compared with the prestimulus period. We only used ignore trials. This responsiveness strongly predicts the size of the participant-specific attentional gamma modulation, both in anticipation (bottom panel) and during stimulus processing (top panel).

of the anticipated tactile stimulus, which was different in the different studies (we return to this in our Discussion).

7.4 Discussion

We report that the neural correlates of attention critically depend on the sensory context in which attention is deployed. By focusing on the neural correlates of tactile spatial attention, we have shown that attention primarily suppresses contralateral alpha and beta oscillations in anticipation, while it primarily amplifies contralateral gamma oscillations during stimulus processing. Moreover, the attentional modulation of gamma oscillations is further shaped by the specific experimental task and the individual participant in which gamma is investigated.

here; this time making use of the knowledge about the relevant gamma frequency band. We also pooled the data across both previous experiments. This revealed a small but significant anticipatory gamma modulation, also in these data (size of the modulation: 0.61 %; $t_{(31)} = 3.65$, $p < 0.001$). However, in the current dataset, this modulation was almost three times as large as in the previous datasets (1.77 % vs. 0.61 %), and this difference was statistically significant ($t_{(46)} = 2.65$, $p < 0.05$). In contrast, no differences were observed with respect to the anticipatory alpha and beta band modulations (alpha: $t_{(46)} = 0.43$, $p > .65$; beta: $t_{(46)} = 0.99$, $p > 0.3$), suggesting that this observation is not due to global differences between the experiments (e.g. differences in difficulty or motivation). Rather, it might be attributed to the distinct nature

Our data suggest that attention must be understood as a cognitive operation that has a modulatory rather than a driving influence on patterns of neural activity. Generalizing beyond the experimental manipulations of the present study, any factor that shapes the patterning of neural activity, in principle, may also shape the neural activity patterns on which attention can exert its influence and hence shape the observable correlates of attention. This implies that the neural implementation of attention cannot be understood in relation to a fixed set of specific neural correlates. In fact, particular correlates of attention need not be inherent to attention because they can be exclusive to specific contexts. In our data, this was the case for the attentional modulation of alpha oscillations.

Alpha oscillations and attention

Alpha oscillations have been suggested to reflect an inhibitory state, such that the attentional suppression of alpha oscillations in task-relevant (relative to task-irrelevant) neural populations enhances the processing of attended information (e.g. Jensen and Mazaheri, 2010). Based on a number of observations, this particular type of modulation has been put forward as a generic mechanism of attention: (1) it has been well-documented in the visual (Worden et al., 2000; Thut et al., 2006), somatosensory (Jones et al., 2010; Haegens et al., 2011; **chapters 2-5**) and auditory (Muller and Weisz, 2012) modalities, (2) with regard to spatial (Worden et al., 2000; **chapters 2-5**), temporal (Rohenkohl and Nobre, 2011; **chapter 3**) and feature-based (Snyder and Foxe, 2010) attention, and (3) follows the time course of the attentional deployment of attention, as indexed by behavior (**chapter 4**). To our knowledge, the present data for the first time reveal a breakdown in the generality of this type of modulation. Specifically, we observed that the attentional modulation of alpha oscillations was completely abolished during the stimulus.

Crucially, the breakdown of the attentional alpha modulation during the stimulus was not paired by a breakdown in the attentional improvement in perception (Fig. 7.2). This contrasts with numerous previous studies that have related this type of modulation directly to the attentional improvement in perception (Thut et al., 2006; Jones et al., 2010; Haegens et al., 2011; **chapter 5**). In fact, we have previously quantified that up to 30 % of this improvement can be explained by this type of modulation (**chapter 5**). The present data suggest that this perceptual relevance is likely restricted to situations in which attention influences perception through anticipatory processes. This is primarily the case when sensory stimuli can be anticipated and are only brief, such as in a Posner cueing paradigm (Posner; 1980a; 1980b). In the present experiment, we used sustained stimuli that required accumulation of sensory information over time. Therefore, in our current task, the most relevant interval is the interval during the stimulus, and in this interval we did not observe any attentional modulation of alpha oscillations. Assuming that the observed lack of the attentional alpha modulation reflects a true lack in the underlying populations, we must conclude that the attentional modulation of alpha oscillations, although frequently observed, is not a *necessary* component of attention.



The extent to which alpha oscillations, and thereby the attentional modulation of alpha oscillations, will be abolished during the stimulus likely depends on the specific properties of the stimulus, such as its strength and size. In fact, previous studies did observe an attentional alpha modulation during stimulation (e.g. Handel et al., 2011). Nevertheless, our data provide an important proof of principle: that attention *can* improve perception without a concurrent modulation of alpha oscillations during the deployment of attention to the stimulus.

Gamma oscillations and attention

The attentional amplification of gamma oscillations has also been proposed as a generic mechanism of attention. Specifically, it has been proposed that increased gamma oscillations result in more synchronized neuronal output, rendering communication to downstream areas more effective (Fries, 2005; Fries et al., 2008). Indeed, several studies have revealed that attention increases the amplitude of gamma oscillations within neural populations that represent the attended stimulus (Fries et al., 2008; Siegel et al., 2008; Gregoriou et al., 2009; Lima et al., 2011). However, this has been shown exclusively during stimulus processing and exclusively in the visual modality. Here we confirm in the somatosensory modality that the attentional modulation of gamma oscillations is largely restricted to contexts in which gamma prevails (during the stimulus and in those subjects who show gamma). At the same time, our data show that the sustained stimulus-induced and attentional amplification of gamma oscillations during stimulus processing are generalizable phenomena across the different sensory cortices. In fact, to our knowledge, our data for the first time reveal a sustained, band-limited, attentional gamma modulation in the somatosensory modality. Previously, such a modulation has only been observed with transient gamma oscillations, following brief tactile stimuli (Bauer et al., 2006). Noteworthy, the frequency band in which we observe our gamma modulations is comparable to the gamma band that has previously been observed in human MEG data in the visual modality (Hoogenboom et al., 2006).

We did also observe a small but reliable attentional modulation of gamma oscillations in anticipation. This modulation was of the same sign, originated from the same location, and occurred in the same frequency band as the modulation during the stimulus. To our knowledge, our data for the first time demonstrate such a band-limited and sustained anticipatory increase in gamma oscillations. Interestingly, while we also observed this anticipatory increase in our previous experiments, it was much weaker there. Most likely, this is due to the specific stimuli and task that we used. While in previous experiments our stimuli consisted of either a brief single tap to the fingers or a brief single electrical pulse to the thumb, our current stimuli consisted of patterns that unfolded across time and across the fingers. Although speculative, it is likely that anticipation of this type of stimulus involves more vivid imagery of the possible identity of the upcoming stimulus, and that this is reflected in the anticipatory attentional gamma modulation (see also Hamame et al., 2012). If correct, this shows that even the experimental context such as the type of target

stimulus can shape the neural correlates of attention, and that this can be so even in the interval prior to this stimulus.

With regard to the anticipatory gamma modulation two open questions stand out. First, in the light of our proposal that attention has a modulatory (rather than driving) influence on patterns of neural activity, a relevant question pertains to whether the anticipatory gamma modulation reflects the modulation of already present (albeit weak) gamma oscillations, or rather the emergence of gamma oscillations due to attention. Second, in a similar experiment in the visual modality, Siegel et al. (2008) reported an anticipatory modulation of gamma oscillations from early visual areas that was of opposite sign as the one we observed (i.e. they observed a contralateral decrease). It remains unclear what might account for this discrepancy.

Feedforward versus feedback accounts of gamma and alpha

It has recently been suggested that gamma oscillations are primarily associated with feedforward processing while alpha oscillations are associated with feedback processing (Buffalo et al., 2011). This suggestion is based on the laminar profiles of oscillations in these distinct bands: whereas alpha predominantly occurs in the deep (feedback receiving) layers, gamma predominantly occurs in the superficial (output) layers. In line with this suggestion, we observed the strongest modulation of gamma when there was a driving stimulus. In this interval, gamma oscillations might render cortical communication to downstream areas more effective (Fries, 2005; Fries et al., 2008). At the same time, we observed no attentional alpha modulation during the stimulus, although top-down feedback projections most likely play a vital role during this interval. To further dissect this discrepancy, it will be essential to investigate the laminar profile of the here reported double dissociation between sensory context and the different neural correlates of attention.

Conclusion

The neural correlates of attention are profoundly shaped by the context in which attention is deployed. This implies that the neural implementation of attention cannot be described by a fixed set of specific neural correlates, but rather must be understood as a mechanism that modulates existing patterns of neural activity. As a consequence, the different correlates of attention contribute to perception in different contexts and, as our data revealed, are not always required for attention to improve perception.





128

Somatosensory demands modulate muscular beta oscillations, independent of motor demands

Adapted from van Ede F, Maris E (2013) *Somatosensory demands modulate muscular beta oscillations, independent of motor demands*. The Journal of Neuroscience 33:10849-10857.



8

Abstract

Neural oscillations in the beta band (15-30 Hz) occur coherently throughout the primate somatomotor network, comprising somatomotor cortices, basal ganglia, thalamus, cerebellum and spinal cord, with the latter resulting in beta oscillations in muscular activity. In accordance with the anatomy of this network, these oscillations have traditionally been associated strictly with motor function. Here we show in humans that somatosensory demands, both in anticipation and during the processing of tactile stimuli, also modulate beta oscillations throughout this network. Specifically, somatosensory demands suppress the degree to which not only cortical, but also muscular activity oscillates in the beta band. This suppression of muscular beta oscillations by perceptual demands is specific to demands in the somatosensory modality and occurs independent of movement preparation and execution: it occurs even when no movement is required at all. This places touch perception as an important computation within this widely distributed somatomotor beta network and suggests that, at least in healthy subjects, somatosensation and action should not be considered as separable processes, not even at the level of the muscles.

8.1 Introduction

Neural oscillations in the beta band (15-30 Hz) are a defining feature of one of the most prominent networks in the primate nervous system: the somatomotor network. These oscillations occur coherently throughout this network comprising the primary somatosensory (S1) and motor (M1) cortices (Brovelli et al., 2004; Witham and Baker, 2007), premotor cortex (Ohara et al., 2001), basal ganglia (reviewed in Jenkinson and Brown, 2011), thalamus (Marsden et al., 2000; Paradiso et al., 2004), cerebellum (Aumann and Fetz, 2004; Soteropoulos and Baker, 2006) and even the spinal cord (as evidenced from oscillations in muscular activity; Kilner et al., 2004; Baker, 2007).

In agreement with the anatomy of this network, this type of neural activity has traditionally been considered in relation to motor functions such as the preparation and execution of movement (when beta oscillations are suppressed; Pfurtscheller and Lopes da Silva, 1999; Paradiso et al., 2004), holding of posture (when beta oscillations are pronounced; Gilbertson et al., 2005) and the integration of proprioception with action plans during movement (Baker, 2007). At the same time, evidence has accumulated that beta oscillations recorded over the contralateral primary somatomotor cortex are also related to touch perception. Most prominently, several groups have shown that the amplitude of these oscillations is related to tactile perception, with lower pre- (Jones et al., 2010; **chapter 5**) and post- (Palva et al., 2005) stimulus amplitude being associated with higher detection performance. Moreover, and in accordance with this relation, these oscillations are suppressed over the contralateral primary somatomotor cortex by somatosensory demands, which occurs both in anticipation (Jones et al., 2010; Bauer et al., 2012; **chapters 2-7**) and during the processing of tactile stimuli (Chatrian et al., 1959; Cheyne et al., 2003; **chapters 2, 3, 6 and 7**).

An important question pertains to whether these beta oscillations that are relevant for tactile perception are actually part of the large-scale coherent somatomotor network that has traditionally been studied only in the context of motor tasks. Based on the inter-areal coupling of these oscillations (e.g. Baker et al., 1997; Brovelli et al., 2004), we hypothesize that if this is the case, then beta modulations associated with somatosensory demands should also be observed in motor parts of the network.

To address this, we investigated beta oscillations in muscular activity while human participants performed cued somatosensory identification and detection tasks. In these tasks, cortical beta oscillations are suppressed both in anticipation and during the processing of tactile stimuli (**chapters 2-7**). We here report highly similar modulations of beta oscillations in muscular activity, even when no movement is required at all. This confirms that the beta oscillations that are modulated by somatosensory demands are part of the larger somatomotor network, placing touch perception as an important computation within this network. In addition, these data suggest that modulations of neural activity in populations involved in somatosensation do not occur independently from those involved in action, not even at the level of the muscles.

8.2 Materials and Methods

We analyzed electromyographic activity (EMG) from three experiments in which participants anticipated left or right hand tactile stimuli while magnetoencephalography (MEG) and EMG were recorded. The MEG results of these experiments have previously been reported, together with detailed descriptions of the employed materials and methods (Experiment 1: **chapter 3**; Experiment 2: **chapter 4**; Experiment 3: **chapter 5**). We here re-iterate those elements that are essential for understanding the results presented in this manuscript. Next to these three experiments, we ran a fourth control experiment in which we only recorded EMG (see *Follow-up control experiment*).

Participants

20, 19 and 14 healthy subjects (27 males; age-range 19-49) participated in the three experiments respectively. Four participants were excluded due to chance-level performance. Experiments were conducted in accordance with guidelines of the local ethics committee (Committee on Research Involving Human Subjects, Region Arnhem-Nijmegen, The Netherlands).

Paradigm

Our main analysis involved the data of Experiment 1 because this experiment contained the largest set of data (both in terms of amount of subjects and usable trials) and employed the cleanest stimulation protocol (a single suprathreshold tap to all fingertips of a single hand). In Experiment 1, subjects performed a cued somatosensory identification task. An auditory cue instructed subjects to orient their attention to their left or right hand. At the cued hand, a tactile target would occur one, two or three seconds later. The cue was presented binaurally with the pitch of the cue (500/1000 Hz) indicating the side of the upcoming tactile stimulus. Moreover, the association between pitch and stimulus side was counterbalanced across participants. Because our main analyses focused on lateralized modulations relative to (anticipated) target side, our results can neither be explained by sensory processing of the cue, nor by its potentially arousing effect. The tactile target consisted of a stimulation of all fingertips of the cued hand at either proximal or distal sites. We used Braille-cells for tactile stimulation (see **chapter 3** for details). Subjects indicated whether the stimulus was perceived as proximal or distal by pressing a button with the left or right thumb respectively. On average subjects responded 1008 ± 349 ms after the stimulus.

Crucially, somatosensory demands were independent of response demands because left and right hand button presses were equally often required for targets on either hand. This is because response side depended on the perceived pattern of the stimulus, not its side. Because both patterns (proximal and distal) occurred equally often on either hand, stimulus side was independent of the required response side. Note that this also holds for the cued side, because the cue predicted the side of the stimulus, not its pattern. Importantly, we also observed this independence in our behavioral data: on average, side-congruent



responses (same stimulus- and response-sides) occurred neither more frequent (proportion of congruent responses: 0.49 ± 0.01 , denoting mean ± 1 s.e.m.; $t_{(19)} = -1.02$; $p = 0.322$), nor faster (congruent: 1079 ± 71 , incongruent: 983 ± 64 ms; $t_{(19)} = 1.65$; $p = 0.116$) than side-incongruent responses. We did note significant biases for some subjects towards either congruent or incongruent responses (as assessed by subject-specific chi-square tests). However, these biases occurred in both directions: some subjects were biased towards congruent responses, while others were biased towards incongruent responses, and hence we did not observe any bias on average. Moreover, these subject-specific biases did not predict the effect of interest, the muscular beta-band modulation. More precisely, neither the subject-specific proportion of congruent responses nor the subject-specific chi-square statistic correlated with the size of this effect (in both cases, $|r| < 0.25$, $p > 0.3$).

This spatial independence between stimulus and response sides implies that EMG activity that lateralized according to (anticipated) stimulus-side (Fig. 8.2) cannot be due to response preparation or execution. We thus deliberately focused our analysis on lateralized EMG activity. In addition to this important aspect of our data, we also (1) directly investigated the effect of any potential response bias (by separating trials by their relation between stimulus and response side) and (2) ran a control experiment in which we removed the motor response from the trial (see *Follow-up control experiment*).

EMG recording & analysis

Bipolar surface EMG was recorded from the flexors of the forearms by means of two pairs of Ag/AgCl electrodes. Both pairs were placed on the insides of the forearms. Per pair, one electrode was placed approximately 5 cm proximal to the wrist and another was placed approximately 5 cm distal to the inner tendon of the elbow. This resulted in an electrode placement with an inter-electrode distance of approximately 20 cm. This inter-electrode distance is much larger than the distances that are typically used to measure digit specific EMG. In fact, this electrode placement was chosen because we were interested in the digit non-specific EMG. In our experiments, investigating covert somatosensory attention, we were interested in such a global measure because the movement of any of the fingers would be considered a motor confound.

Data were analyzed using FieldTrip (Oostenveld et al., 2011). All analyses were done on mean-corrected EMG.

First, we analyzed the frequency content of the EMG traces, as well as their coherence with the cortical activity recorded with MEG (Fig. 8.1). For this we divided our dataset into consecutive epochs of 2 s (irrespective of experimental conditions) and applied conventional Fourier analysis in combination with multi-tapering. Multi-tapering allows control over spectral smoothing (Percival and Walden, 1993), and for these analyses we applied 4 Hz smoothing. For the analysis of cortico-muscular coherence (i.e. coherence between MEG and EMG; Fig. 8.1C) we used previously selected MEG channels above left and right primary somatomotor cortices (**chapter 3**). MEG channels above left and right sensorimotor cortices were selected based on stimulus-induced responses to left and right

tactile stimuli. Specifically, we contrasted left and right stimuli [right – left] with respect to beta band amplitude between 100-300 ms post-stimulus, and selected the 15 channels with the lowest (highest) value which were found on the left (right) somatomotor cortex; see also **chapter 3**).

Second, we investigated lateralized modulations in EMG activity as a function of (anticipated) stimulus- and response-sides (Figs. 8.2-8.4). We contrasted trials in which (anticipated) stimulus- or response-side was ipsilateral to the arm from which the EMG was recorded with those trials in which this event occurred contralateral to the recorded EMG. We expressed this contrast as a percentage change: $[(\text{ipsi-contra}) / \text{contra}] * 100$. We did this separately for left and right EMG and pooled the percentages. (Note that these contrasts are analogous to the previously reported cortical modulations, which were calculated by contrasting activity in MEG channels above left and right primary somatomotor cortices between contra- and ipsilateral anticipation and stimulation; **chapter 3**). We calculated this contrast for two measures: (1) time- and frequency-resolved power, and (2) high-pass filtered (40 Hz cut-off) and subsequently rectified EMG activity (as an index of muscle tone/contraction). Time-resolved oscillatory power (measure 1) was estimated using a sliding time-window of 300 ms that was advanced in steps of 25 ms (analogous to the analysis of the cortical MEG data). Statistical significance was evaluated for beta (15-30 Hz) power lateralization by means of a cluster-based permutation test (Maris and Oostenveld, 2007) in which temporally adjacent thresholded data-points were clustered and evaluated under a single permutation distribution (thereby controlling false-positive rate).

Third, we calculated trial-by-trial correlations between cortical and muscular beta lateralization (Fig. 8.5). We focused on the anticipatory modulations over the [400-1000] ms window after the cue, because the anticipatory modulation is most pronounced in this time window (see Fig. 8.2A). Per trial, we calculated the normalized difference between the left and right recording sites: for cortical lateralization we calculated $[(R-L) / (R+L)]$ and for muscular lateralization we calculated $[(L-R) / (L+R)]$. Separately for left and right cued trials, we sorted the trials according to cortical lateralization and placed them into 5 consecutive bins. For each bin we then calculated both the average cortical and the average muscular lateralization. Binned data were then averaged across subjects.

Fourth we calculated the Pearson correlation across subjects between, on the one hand, the muscular lateralization measure, and on the other hand, the cortical lateralization measure and the cortico-muscular coherence (Fig. 8.6). Similarly, we calculated the correlation between, on the one hand, the level of background muscle tone, and on the other hand, the cortical and muscular lateralization measures. As a measure of background muscle tone we averaged amplitudes across all frequencies of the calculated power spectra (see step 1 above). For the two correlations with muscle tone, we also evaluated their difference by means of the Hotellings-Williams test for the difference between two dependent correlations (Williams, 1959). For these correlation analyses, we included data from all three experiments. We again focused on the lateralization measures calculated over the last



600 ms before the anticipated stimulus (i.e. [400-1000] ms post-cue in Experiments 1 and 2; [900-1500] ms post-cue in Experiment 3). (Note that in experiment 2 we had presented stimuli at variable cue-target intervals between 0-1000 ms. Despite this, we were able to obtain a stimulus-uncontaminated measure of the anticipatory modulation. To achieve this, we calculated time-resolved beta power between 0-1000 ms post-cue, using a sliding time window of 300 ms. For every trial, we only used estimates from time bins that occurred before the stimulus. For example, if the stimulus occurred at 800 ms post-cue, the last time bin from which we used the data was between 500-800 ms, and data from later time bins were omitted. For every time bin we first averaged data across trials, and then also across the time bins that showed anticipatory activity, being the bins from 400 ms post-cue onwards. Because the time bins never included the stimulus, this resulted in a stimulus-uncontaminated measure of the anticipatory activity. We could estimate anticipatory activity up to 1000 ms, because we had also included catch trials in which no stimuli followed the cue.). Because these lateralization measures (muscular: [ipsi minus contra]; cortical: [contra minus ipsi]) have negative values (due to a stronger ipsilateral-muscular and contralateral-cortical *suppression*), we inverted the contrasted values to express the modulation *strengths* as a positive number.

Differences between experiments

There are two important differences between the three experiments that are considered here. The first difference concerns stimulation protocols. In Experiments 1 and 2, mechanical tactile stimuli were applied to all fingers of one hand, while in Experiment 3 threshold electrical stimuli were applied to the thumb. For this reason, we did not compare stimulus-induced beta modulations across experiments. The second important difference concerns bodily postures. In Experiment 1, participants lay in the MEG (which was put into supine position) with their arms stretched out to grasp our Braille-stimulators (see Supplementary Fig. 3.1 in **chapter 3** for a depiction of one such stimulator). In Experiment 2, the same Braille-stimulators were used, but a subset of participants was recorded while seated. Finally, in Experiment 3, subjects sat while resting their arms on the MEG-chair's arm rests, and stimulation electrodes were taped to the thumbs. These different body postures are important when considering the reported differences in background muscle tone (Fig. 8.7).

Follow-up control experiment

In a follow-up experiment we addressed two remaining questions. First, we investigated whether the observed EMG modulation by sensory demands is specific to demands in the somatosensory modality. Second, we investigated whether this modulation also occurs when no motor response is required at the end of a trial. To this end, we asked 7 subjects (5 males, age-range 27-51), who previously showed this modulation, to return to the lab for a follow-up experiment. In this experiment, we only recorded EMG and used the same electrode placing as described above.

The experiment consisted of two cued detection tasks, one in the somatosensory

modality and one in the visual modality. In both tasks, we presented auditory cues (the same cues that were used in Exp. 1) that instructed subjects to orient their attention to either the left or the right side (in case of the tactile task, the left or right hand; in case of the visual task, the left or right side of the screen). One second after this cue, a stimulus occurred with probability 0.5 at the cued location and the subjects' task was to judge whether or not they felt (tactile blocks) or saw (visual blocks) a stimulus. Tactile stimuli were applied for 1 ms to the left or right median nerve using either of two constant-current stimulators (Digitimer; type DS7A) that were taped to the body. Visual stimuli were presented for a single frame (16.7 ms) on the left or right side of the screen, and consisted of filled white circles with a diameter of approximately 1 cm. Before the experiment, intensities of the stimuli (respectively, the electrical current and the visual contrast) were adjusted to a level where the stimuli were just above perceptual threshold (based on verbal report). Tactile and visual blocks (each containing 10 trials), were randomly interleaved. The relevant modality was indicated to the subject by means of the text "tactile task" or "visual task" that remained on the screen throughout the block.

In this control experiment, the trials did not include a motor response. Instead, subjects had to count the number of stimuli presented within a block (which ranged from 0 to 10) and to report this number verbally only at the end of each block. Tasks were equated on difficulty: on average, subjects reported the number of presented stimuli correctly in 56.28 ± 2.56 (visual) and 51.75 ± 3.92 (tactile) percent of the blocks. The average absolute deviation from the correct number was, respectively, 0.83 ± 0.15 and 0.82 ± 0.13 .

Before running this follow-up experiment, we had observed that the EMG modulation of interest requires the presence of background muscle activity (see Fig. 8.7). To achieve this in our control experiment, we asked subjects to hold up a tube (1000 cm wide, 7 cm diameter, 956 gram) throughout the experiment. Subjects were in seated position, rested their elbows on the chair and lifted the tube with both hands (hand palms facing upwards). Importantly, this motor engagement does not induce a confound in our results because the tube was held up in the same way irrespective of the anticipated side and irrespective of the block's modality (see also Fig. 8.8D). Our analyses focused on the difference in activity between ipsi- and contralateral anticipation and the difference between tactile and visual blocks.

8.3 Results

Cortex and muscle couple at beta-frequency

Throughout the cued tactile identification task (Materials and Methods), muscle activity recorded at the flexors of the forearms showed rhythmic activity in the beta range (15-30 Hz; denoted *muscular beta oscillations*). Figure 8.1A depicts an example EMG trace showing these oscillations. These oscillations were observed in the majority of our subjects as revealed by the grand average EMG power spectrum (Fig. 8.1B). Moreover, these oscillations were coherent with those recorded above contralateral primary somatomotor



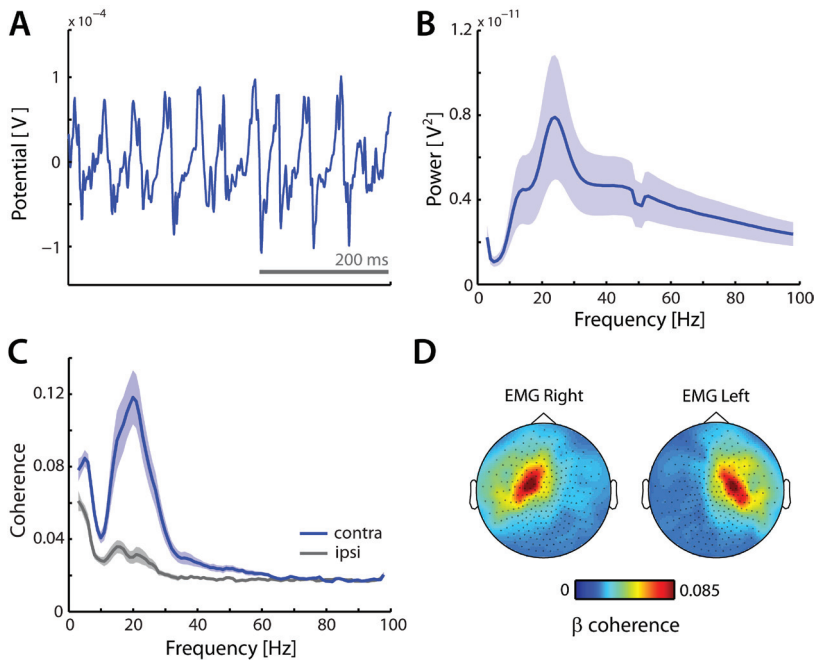


Figure 8.1. Muscular activity oscillates at beta-frequency, coherent with contralateral cortex. (A) Example mean-corrected EMG trace. (B) Grand-average muscular power-spectrum. (C) Grand-average coherence-spectra between EMG and MEG-channels above contra- and ipsilateral primary somatomotor cortices. (D) Topographies of the beta-coherence with the left and right forearm EMG. Blue and grey shadings indicate ± 1 s.e.m. Data are from Experiment 1.

cortex (Fig. 8.1C,D). These observations are consistent with a large body of literature in which this type of activity has been investigated during steady contraction in the context of motor tasks (e.g. Baker et al., 1997; Salenius et al., 1997; Schoffelen et al., 2005).

Muscular beta oscillations are suppressed by strictly somatosensory demands

We investigated EMG activity that lateralized in anticipation (Fig. 8.2A) and during the sensory processing (Fig. 8.2B) of a tactile stimulus to the left or right hand. In several previous reports, we and others have documented that such lateralized tactile anticipation and stimulus processing involves an accordingly lateralized modulation of cortical alpha and beta oscillations (see introduction). Because of the coupling between cortical and muscular beta oscillations (Fig. 8.1C,D), it is conceivable that the muscular beta oscillations are similarly modulated. Precisely this can be observed in the time-frequency representations of the difference in power between ipsi- and contralateral EMG (Fig. 8.2, upper panels; for the corresponding cortical modulations see Fig. 3.2A and Supplementary Fig. 3.5A in **chapter 3**). Time-resolved power differences for the beta band (15-30 Hz; middle panels) reveal the robustness of these modulations (shading represents ± 1 s.e.m; p-values indicate the

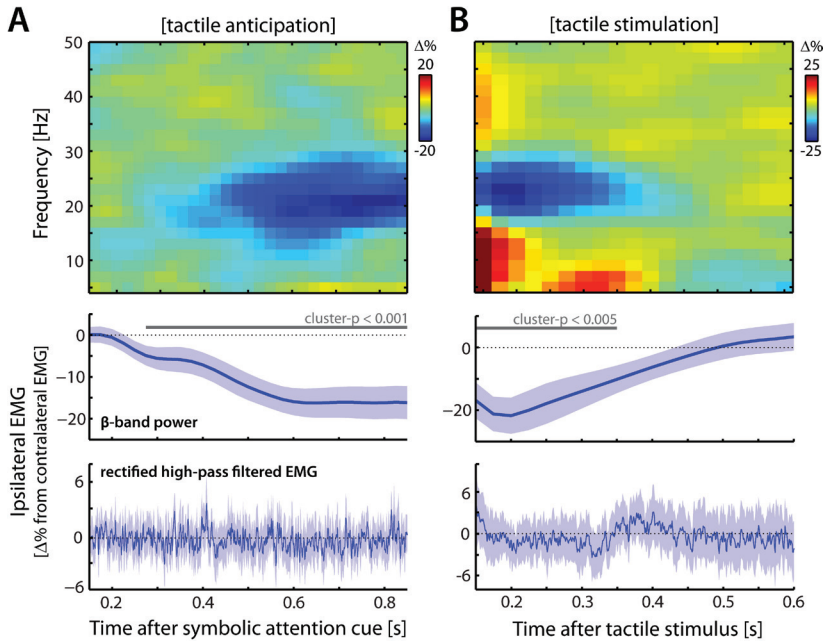


Figure 8.2. Somatosensory demands modulate muscular beta oscillations. Modulations of muscular beta oscillations by lateralized (A) tactile anticipation and (B) tactile stimulation. Modulations are expressed as the difference between EMG recorded on the hand ipsi- and contralateral to the (expected) event ([ipsi minus contra], expressed as a percentage change). Compare with the [contra minus ipsi] contrasts in the MEG data from the primary somatomotor cortices (see Fig. 3.2A and Supplementary Fig. 3.5A in **chapter 3**). Middle panels show time courses of these contrasts for extracted beta band power. Solid grey lines indicate significant clusters (Materials and Methods). Dotted grey lines indicate the null-hypothesis of no difference between contra- and ipsilateral EMG. Lower panels show changes in muscles tone (high-pass filtered and rectified EMG). Blue shadings represent ± 1 s.e.m. Data are from Experiment 1.

significance of the temporal clusters; Materials and Methods). We further assessed whether this lateralization was constituted by an ipsilateral decrease or a contralateral increase by investigating the temporal development of the anticipatory modulation (Fig. 8.2A, middle panel) separately for ipsi- and contralateral EMG. As we observed in cortex (**chapter 3**), the lateralization results from a suppression of beta oscillations in populations representing the task-relevant hand: muscular beta-power *ipsilateral* to the anticipated stimulus *decreases* with time after cue ($r = -0.69 \pm 0.08$; $t_{(19)} = -8.52$, $p < 0.001$). See also Figure 8.8D for the ipsilateral nature of this modulation.

The muscular beta modulation is independent of movement preparation and execution

Several aspects rule out movement preparation and execution as possible explanations for the observed muscular beta modulations. First, in our task, (anticipated) stimulus- and response sides were spatially uncorrelated, both in design and in response behavior (see Materials and Methods). The lateralized modulations with respect to stimulus side (Fig.

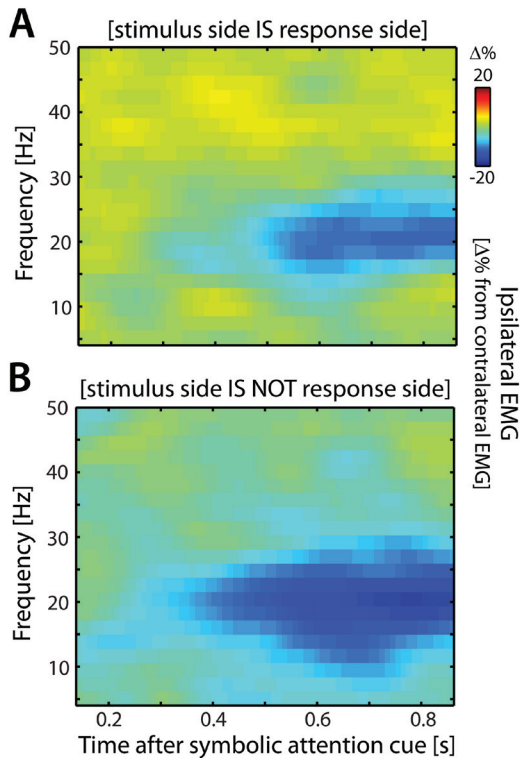


Figure 8.3. The EMG lateralization occurs irrespective of response side. Identical to Figure 8.2A, except that data are split into trials in which the response was made on the same side as the stimulus (panel A), and trials in which the response was made on the opposite side (panel B). Lateralization is depicted relative to anticipated stimulus side. Data are from Experiment 1.

response side (Fig. 8.4). This pattern of EMG activity looks fundamentally different from the pattern associated with tactile anticipation and stimulus processing: it is of opposite sign, occurs in all frequencies, and is more than an order of magnitude larger.

Finally, our observations can also not be attributed to non-response-related movement during anticipation and processing of the tactile stimuli. This is evidenced by the lack of modulation in muscle tone (Fig. 8.2, lower panels; again compare with massive increase during actual motor behavior in Fig. 8.4). Thus, while somatosensory demands reduce the degree to which muscular activity oscillates in the beta range, they leave overall muscle output (as indexed by rectified, high-pass filtered, EMG activity) unaltered. The here-presented modulation can therefore not be explained by (preparation of) movement of the fingers during tactile anticipation and stimulus processing. Rather, as we will show below, it likely occurs as a consequence of the cortical, somatosensory-related, modulation that propagates through the somatomotor network.

8.2) can therefore not be attributed to response preparation and execution. We could further show this in our data. For this, we focused on the anticipatory modulation, and used the following logic: if this modulation is due to response preparation, then the lateralized pattern observed in Figure 8.2A should reverse between trials in which the stimulus is followed by a response on the same versus the opposite side. In contrast, we observed a highly similar anticipatory modulation between these two sets of trials (Fig. 8.3). This directly shows that the lateralization relative to the anticipated stimulus side cannot be attributed to response preparation. Moreover, as we will show later (Fig. 8.8), this anticipatory modulation also occurs when no response is required at all. In addition to this analysis, we also directly investigated EMG activity that lateralized according to

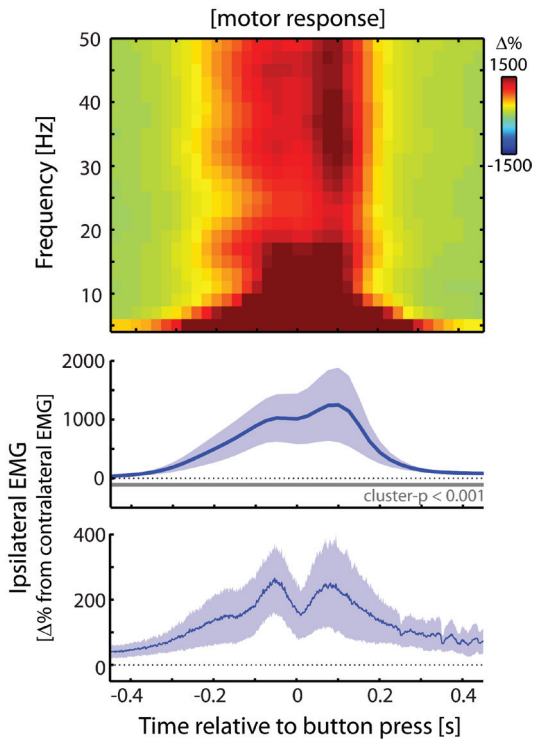


Figure 8.4. EMG activity related to overt motor behavior looks fundamentally different. Identical to Figure 8.2, except muscular activity is now contrasted between ipsi- and contralateral motor responses (i.e. button presses with the left or right thumb). Data are from Experiment 1.

when cortex is in a state of “left anticipation” (when beta power is lower in right compared to left MEG), so are the muscles (when beta power is lower in left compared to right EMG). This correlation is highly robust across subjects: for the binned data this correlation was $r = 0.74 \pm 0.07$ ($t_{(19)} = 10.81$, $p < 0.001$). Moreover, as predicted, this subject-specific across-trial correlation was stronger for subjects with a higher cortico-muscular coherence ($r = 0.64$; $p < 0.01$). Furthermore, analogous to the pattern of cortico-muscular coherence (Fig. 8.1C,D), this across-trial correlation between cortical and muscular power was specific to the beta band (Fig. 8.5B) and to channels above the contralateral primary sensorimotor cortices (Fig. 8.5C).

We also assessed the relation between the cortical and muscular modulations across subjects. For this, we combined data from three experiments, all in which lateralized tactile stimuli were anticipated while MEG and EMG were recorded (Materials and Methods). As depicted in Figure 8.6, the strength of the muscular modulation correlated with the strengths of both the cortical modulation (Fig. 8.6A) and the cortico-muscular coherence (Fig. 8.6B).

The muscular beta modulation reflects a spillover of the cortical beta modulation onto the muscles

If the muscular beta modulation reflects a spillover of the cortical modulation onto the muscles then it is expected (1) to correlate with the cortical modulation on a trial-by-trial basis, (2) to correlate with the strength of the cortical modulation across subjects, and (3) to scale with cortico-muscular coherence. We assessed these predictions with regard to the anticipatory modulation (cf. Fig. 8.2A).

Figure 8.5A shows the trial-by-trial relation between cortical and muscular states (as indexed by beta power lateralization) in anticipation of left and right tactile stimuli (note that we binned data to allow averaging across participants). Clearly, a strong correlation exists between cortical and muscular states. For example,

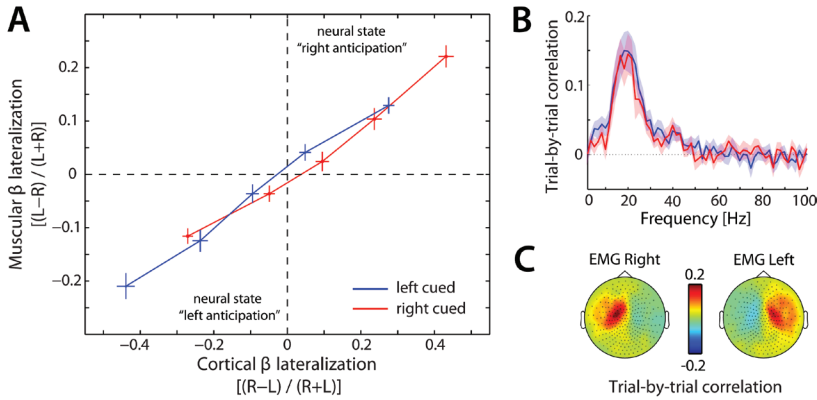


Figure 8.5. Cortical state predicts muscular state on a trial-by-trial basis. (A) Data points represent normalized lateralization indices that were binned according to cortical lateralization in the last 600 ms before the anticipated tactile stimulus (400-1000 ms post-cue, the time window in which this modulation is most pronounced: see Fig. 8.2A). This was done for both left and right hand tactile anticipation; see cueing conditions). Error bars represent ± 1 s.e.m. Neural state “left anticipation” is defined by lower power for right compared to left primary somatomotor cortices together with lower power for left compared to right EMG (vice versa for neural state “right anticipation”). (B) Frequency-spectrum of the trial-by-trial correlation between cortical and muscular lateralization. Blue and red lines represent left and right cued trials respectively. Shadings represent ± 1 s.e.m. (C) Topographies of the trial-by-trial correlation between cortical and muscular beta power, separately for the left and right EMG. Data are from Experiment 1.

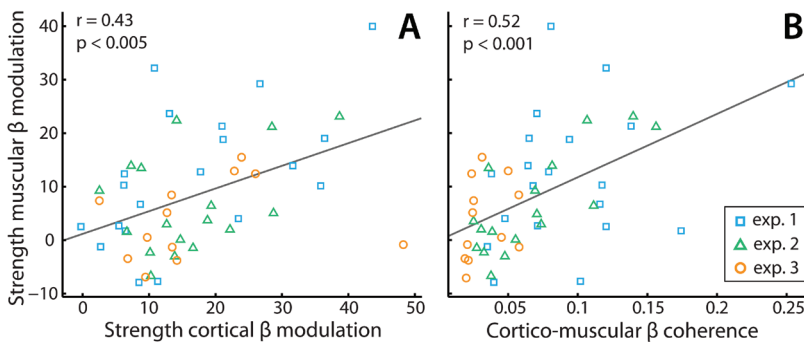


Figure 8.6. Strength of muscular beta modulation depends on strength of cortical modulation and cortico-muscular coupling. (A) Correlation between strengths (Materials and Methods) of the cortical and muscular beta modulations in anticipation of a lateralized tactile stimulus (cf. Fig. 8.2A). Data points represent individual participants. Data are shown from three experiments ($n = 20, 17$ and 12 , respectively). For all experiments, beta power was estimated over the last 600 ms before the anticipated stimulus ([400-1000] ms post-cue for Exp. 1 and 2, [900-1500] ms post-cue for Exp. 3). (B) Identical to A, except cortico-muscular coherence is plotted as predictor.

These correlations remained significant, even when controlling for the factor Experiment (i.e., when we subtracted the mean values per experiment from all the observations in that experiment before calculating these correlations; $r = 0.46$, $p < 0.001$ and $r = 0.44$, $p < 0.005$, respectively). At the same time, we also noted an interesting difference between the three experiments that we further explore below.

The muscular beta modulation is gated by background muscle tone

The three experiments differed drastically in absolute levels of EMG activity (Fig. 8.7A; $F_{(2,46)} = 4.3$, $p < 0.05$), likely due to different postural positions across the experiments (Materials and Methods). This allowed us to investigate to what extent both the cortical and the muscular modulations depend on background muscle tone. In contrast to the cortical modulation, the muscular beta modulation strongly depends on background muscle tone (Fig. 8.7B). In fact, in the experiment in which very little EMG power was observed, we did not observe an anticipatory modulation of muscular beta oscillations ($p > 0.1$), despite a robust cortical modulation. The relation of background muscle tone with the strength of the muscular beta modulation (and likewise, the absence of this relation with the cortical beta modulation) was also revealed by a correlation analysis across subjects (Fig. 8.7C,D). A significant correlation with background muscle tone was observed only for the muscular modulation ($r_{\text{muscle}} = 0.448$, $p < 0.05$; $r_{\text{cortex}} = 0.107$, $p > 0.45$). Completely in line with this observation, the correlation with the muscular modulation was significantly larger than the one with the cortical modulation ($t_{(46)} = 2.4$, $p < 0.05$). Together, these data show that the hypothesized propagation from cortex to muscle is gated by factors determining background muscle tone.

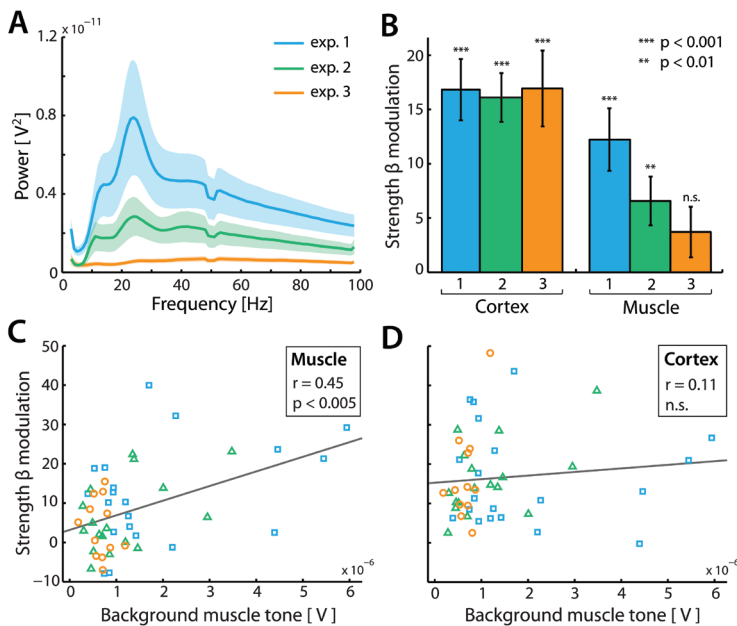


Figure 8.7. Muscular but not cortical beta modulation depends on background muscle tone. (A) Grand-average muscular power-spectra for the three experiments. Colored shadings represent ± 1 s.e.m. (B) Strengths of the cortical and muscular beta modulations in anticipation of a tactile stimulus for the three experiments in panel A. Error bars represent ± 1 s.e.m. P-values represent statistical significance with respect to the null-hypothesis of no lateralization (strength = 0). (C) Correlation between background muscle tone and strength of the anticipatory muscular beta modulation. Background muscle tone is indexed by the average amplitude across all frequencies of the calculated background EMG power spectra (cf. panel A; Materials and Methods for details). (D) Similar to C, except the *cortical* modulation is plotted as the criterion variable.

The muscular beta modulation by sensory demands is specific to the somatosensory modality and does not require a motor response in the trial

In a follow-up control experiment (see Materials and Methods) we addressed whether the muscular beta modulation by sensory demands is specific to the somatosensory modality. To this end, we recorded EMG activity while subjects anticipated either an upcoming tactile or an upcoming visual stimulus. As before, we calculated the lateralized difference in EMG activity as a function of anticipated stimulus side (left or right hand or visual field, respectively). As is evident from Figure 8.8, the modulation is specific to the somatosensory modality (tactile: $t_{(6)} = -2.89$, $p < 0.05$; visual: $t_{(6)} = -0.11$, $p > 0.9$; tactile minus visual: $t_{(6)} = -3.45$, $p < 0.05$). Importantly, this difference cannot be explained by differences in overall muscle tone between the visual and tactile tasks: the overall power in the EMG was highly similar ($t_{(6)} = -1.30$, $p > 0.2$) between our tactile and visual detection tasks (Fig. 8.8D). In fact, the only aspect with respect to which the power spectra differ, concerns our effect of interest: a selective attenuation in the beta band, only in EMG recordings ipsilateral to the anticipated stimulus, and only during tactile anticipation (Fig. 8.8D).

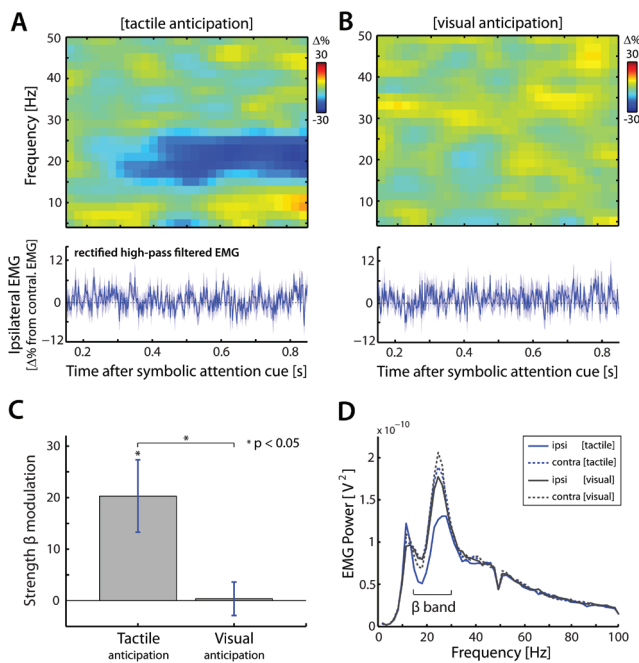


Figure 8.8. The modulation of muscular beta oscillations by sensory demands is specific to the somatosensory modality and does not require a motor response in the trial. Modulations of muscular oscillations by lateralized (A) tactile and (B) visual anticipation. Conventions as in Fig. 8.2A. Data are from our follow-experiment (Materials and Methods), in which subjects did not give a motor response at the end of the trial. (C) Bar graph of the lateralized beta modulation for tactile and visual anticipation. Lateralization was calculated for power in the [400-1000] ms post-cue window. Error-bars represent ± 1 s.e.m. ($n = 7$). (D). Average EMG powerspectra as a function of side (ipsi / contra) and modality (tactile / visual) of the anticipated stimuli. Because these powerspectra were calculated over the [400-1000] ms post-cue window, they also reveal the anticipatory modulation of interest (see the attenuation in 15-30 Hz power in the ipsilateral EMG during tactile anticipation).

In this control experiment, the subjects did not have to give a motor response at the end of the trial (see Materials and Methods). Crucially, this did not alleviate the modulation of muscular beta oscillations. These data thus further strengthen the notion that the reported modulation of muscular beta oscillations can occur independent of motor demands.

8.4 Discussion

We observed that the previously documented cortical modulation of beta oscillations by somatosensory demands – in anticipation and during the processing of tactile stimuli – also manifests itself in oscillatory patterns of muscular activity, independent of movement preparation and execution. This implies that these somatosensory-relevant beta oscillations are part of the large-scale somatomotor network, placing touch perception as an important computation in this network. In addition, these data suggest that, despite specific behavioral demands, it might not be possible to engage populations involved in somatosensation and action independently, not even at the level of the muscles.

The observed muscular beta modulation is likely explained by propagation of this modulation along anatomical pathways from primary somatomotor cortex to muscle. For example, this might occur from S1 (where it is required in our task) to M1 (Brovelli et al., 2004) and then via pyramidal tract neurons to alpha-motor neurons in the spinal cord regulating muscular output. Alternatively, this might also occur through direct efferent pathways that exist between S1 and the spinal cord (Coulter and Jones, 1977; Matyas et al., 2010). Indeed, three observations suggest that the cortical (e.g. **chapter 3**) and muscular (present manuscript) modulations represent the same modulation occurring in the distinct populations within the network: the cortical and muscular modulations (1) have highly similar modulation profiles, (2) are both constituted by a suppression within the populations related to the task-relevant hand, and (3) are highly correlated, both across trials and participants. In addition to the cortical requirements of our task, the cortical origin of the beta modulation is also confirmed by the fact that only the muscular modulation depends on muscle tone. In fact, if the muscular modulation would drive the cortical modulation, a similar dependency should be observed in cortex. We thus propose that the muscular beta modulation reflects a *spillover* from cortex to muscles along descending anatomical pathways. Considering this hypothesis, two points must be clarified. First, the somatosensory nature of our task does not necessarily imply that the modulation is also *initiated* in S1. In fact, it might also be initiated elsewhere in the network and propagate to S1 to assist tactile processing. Second, in contrast to this propagation-profile for the *modulation* of beta oscillations, their *generation* might involve a more complex interplay between de- and ascending cortico-spinal pathways (Baker, 2007).

A critical feature of the here-reported muscular beta modulation is the absence of a concurrent change in muscle tone (i.e. muscle contraction). However, this observation by itself does not preclude a motor account of our data. For example, there is ample evidence (e.g. Pfurtscheller and Neuper, 1997; Miller et al., 2010) that processes such as motor preparation, motor imagery and motor intent (all processes without motor output) also modulate cortical beta oscillations. (To our knowledge, this has not yet been established at the muscular level.) Crucially, we argue that also these processes cannot account for our observations. Considering movement preparation, the muscular modulation occurred irrespective of movement side (Fig. 8.3) and occurred even when no response was required



at all (Fig. 8.8). Considering imagery or intent, it is unlikely that participants imagined or intended *moving* their hand, as this would not help them in the perceptual tasks. This is most obvious in our control experiment, in which the tactile stimulator was taped to the body (Fig. 8.8). We thus conclude that the here-reported muscular modulations must be due strictly to somatosensory demands.

The main implication of our observations is that the somatosensory-related modulation of beta oscillations (and therefore touch perception) must be understood in relation to the large-scale somatomotor beta network. Previous studies already pointed at the interplay between beta oscillations in this network and somatosensation. On the one hand, studies showed that somatosensation might be critical to the occurrence of beta oscillations in this network: (1) S1 drives M1 beta oscillations (in a Granger causality sense; Brovelli et al., 2004) and (2) coherence of muscular (Fisher et al., 2002; Kilner et al., 2004) and cortico-muscular (Riddle and Baker, 2005) beta oscillations is altered by alterations in afferent (periphery to cortex) sensory processing. On the other hand, studies suggested that beta oscillations in this network might itself also contribute to somatosensory perception. For example, timing of action potentials of cells in S1 (including cutaneous areas 3b and 1) can be influenced by beta oscillations recorded elsewhere in the network (i.e., M1 as shown by Witham et al., 2007b). Along the same line, recent MEG studies showed that the amplitude of beta oscillations above contralateral primary somatomotor cortex is inversely related to touch perception (Palva et al., 2005; Jones et al., 2010; **chapters 4 and 5**), and is accordingly suppressed in anticipation and during the processing of tactile stimuli (Jones et al., 2010; Bauer et al., 2012; **chapters 2-7**). An important insight from the current work is that these somatosensory-relevant beta oscillations are in fact part of the large-scale somatomotor beta network. This underscores the notion that touch perception is an important computation within this network, even when no movement is required. At this point it is important to clarify that we do not want to claim that the muscular beta modulation is itself functionally relevant for tactile perception (i.e., that the muscle is doing somatosensory processing). Rather, our data provides evidence for the notion that this *type of signal* (beta-oscillations in a large-scale coherent network), must be understood not only in relation to motor computations, but also somatosensory computations (see also Lalo et al., 2007). While previous studies had already implicated beta oscillations in tactile perception (Jones et al., 2010; **chapter 2-7**), we here show that these oscillations are in fact the same as those often studied in the context of motor tasks (i.e. the beta oscillations that are visible in the EMG).

Strikingly, our data suggest that task-related modulations of neural activity do not occur independently in neural populations involved in somatosensation and action, not even when behavioral demands require their independence, as in our task. This is likely due to the fact that distinct populations in the somatomotor network are strongly interconnected. This strong interconnectedness most likely results from the high frequency with which they interact. In fact, during movement, populations involved in somatosensation and action are in a continuous dialogue: action causes somatosensation, leading to adjusted

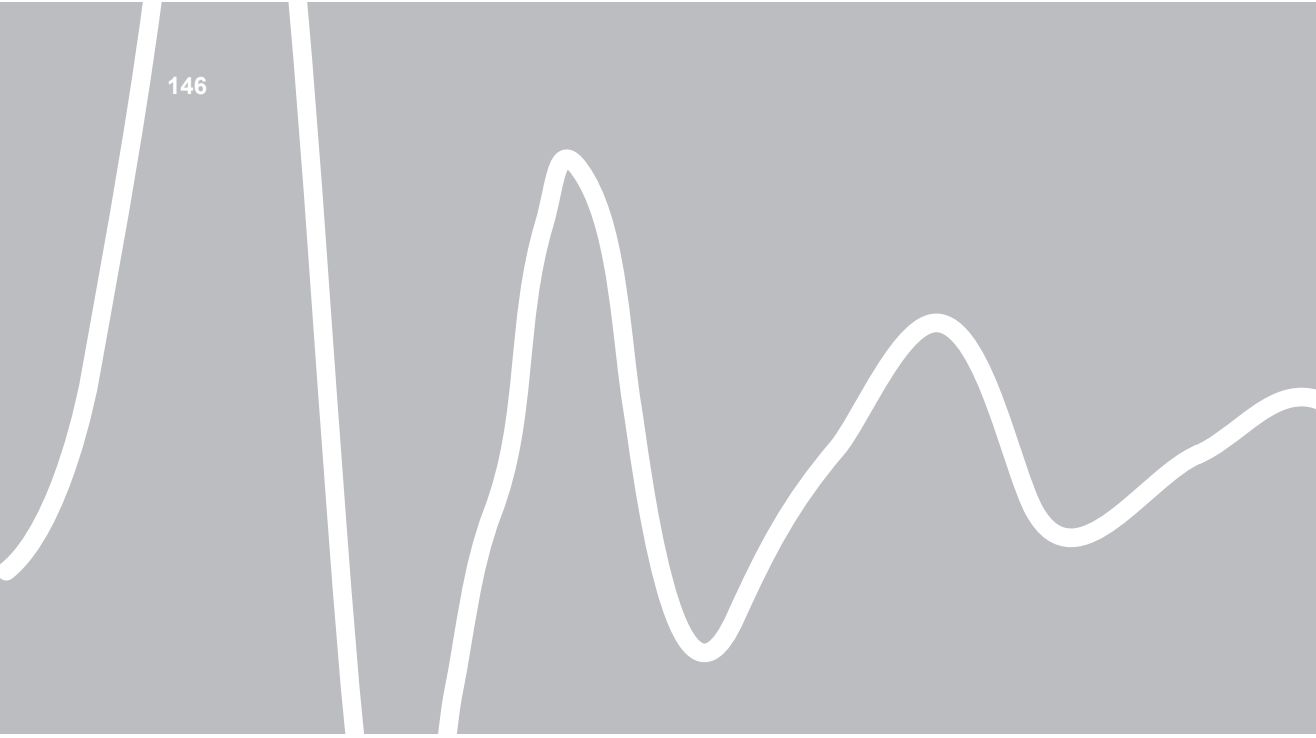
action, etc. However, in several situations (such as in our experiments) touch perception is independent from action. The here-reported observation that in such situations muscular activity is nevertheless modulated therefore reveals a constraint on the flexibility with which neural populations involved in somatosensation and action can independently modulate their activity. Put differently, our data show that, from a physiological perspective, somatosensation and action should not be considered as two fully separable processes. This conclusion is further supported by recent rodent studies implicating primary motor cortex in tactile perception (Ferezou et al., 2007) and primary somatosensory cortex in motor control (Matyas et al., 2010). The current work demonstrates this inherent dependence between somatosensation and action in human. In future investigations it would be interesting to address whether this dependence persists in patients who have lost muscle control after brain or spinal cord injury.

In cortex, somatosensory demands modulate not only beta but also alpha oscillations (**chapters 3-7**). Moreover, in cortex these oscillations are strongly coupled: they show highly similar modulation profiles (at least during tactile anticipation) and their spontaneous fluctuations are highly correlated (**chapter 5**). In contrast, the associated muscular modulations are restricted to the beta band. This suggests that, in primary somatomotor cortex, factors that modulate alpha oscillations also modulate beta oscillations (and vice versa). At the same time, oscillations in these two bands propagate differently throughout the somatomotor network, with only beta oscillations affecting spinal populations (note that these data do not imply that alpha oscillations do not play a role in muscular function; rather, they show that, concerning the somatosensory *modulation* of these oscillations, only the modulation in the beta band propagates to the muscles). As a result, spinal beta oscillations (visible in the EMG) might be modulated by beta modulations elsewhere in the network, a phenomenon of which the present work showcases one example.

Finally, our results have a practical implication by showing that, given an appropriate posture, beta oscillations in muscular activity can index the state of neural activity as it occurs elsewhere in the somatomotor network. Compared with MEG and EEG, this allows for an easier, cheaper, more mobile, and spatially more specific way of assessing the state of the somatomotor network during various tasks, both in fundamental as well as clinical research settings.

We conclude that touch perception is an important computation within the widely distributed somatomotor beta network and that somatosensation and action should not be considered as separable processes, not even at the level of the muscles.





Phase relation diversity in neural oscillations and the interpretation of observed amplitude modulations

9



Abstract

Observed modulations of oscillatory amplitude have emerged as key indices of neural computations and cognition. Here, we first outline three alternative scenarios that may produce such observed modulations. These involve changes in (1) the average phase relations *between* the neural structures that underlie the recording site, (2) the precision of these phase relations, and (3) the source level amplitudes *within* these structures. Next, we provide a first step towards disentangling these alternatives by comparing average phase relations in human magnetoencephalographic (MEG) recordings between conditions that differ markedly in amplitude. We show that, at the spatial scale of neural structures that can be distinguished by MEG, observed amplitude increases are not paired by a reduction in the diversity of the phase relations *between* these structures. Rather, amplitude modulations co-exist in multiple underlying structures, while these maintain their average phase relations. We show this for both ongoing alpha- (8-12 Hz) and visually induced gamma oscillations (50-70 Hz). This narrows down the possible interpretations and functional consequences of observed amplitude modulations. In addition, these data demonstrate that phase relation diversity is a pervasive feature of neural oscillations, even in extracranial MEG recordings.

9.1 Introduction

Over the last 20 years, amplitude modulations of oscillatory neural activity (Fig. 9.1) have emerged as one of the core indices of neural computations. These modulations have been implicated in a multitude of cognitive operations (reviewed in Hari and Salmelin, 1997; Kahana et al., 2001; Jensen et al., 2007; see also **chapters 2-8**). In order for these observations to contribute to a mechanistic explanation of cognition, it is essential to understand how these modulations come about.

There are at least three different scenarios that may produce changes in amplitude, as observed in a recording site at some distance from the sources (Fig. 9.1). First, observed amplitude modulations may reflect changes in the *phase relations* between membrane potential oscillations in the underlying neural structures (with the spatial scale of these structures ranging anywhere from neurons to populations). This interpretation is known as event-related (de)synchronization (ERD/ERS; Pfurtscheller and Lopes da Silva, 1999). When the diversity in phase relations

between these structures becomes smaller (i.e. when oscillations in these structures become more synchronous), their electric/magnetic fields sum up to a signal with higher amplitude at a distant recording site (i.e. a longer average vector in the complex plane; Fig. 9.1). In this scenario, one may observe changes in amplitude at the *sensor level* even when amplitudes remain the same in the underlying structures (called *source level amplitudes*). Alternatively, source level amplitudes in each of these structures may change without a change in their phase relations (Fig. 9.1). As a third mechanism, the precision of the phase relations between these structures might change (i.e. a change in coherence).

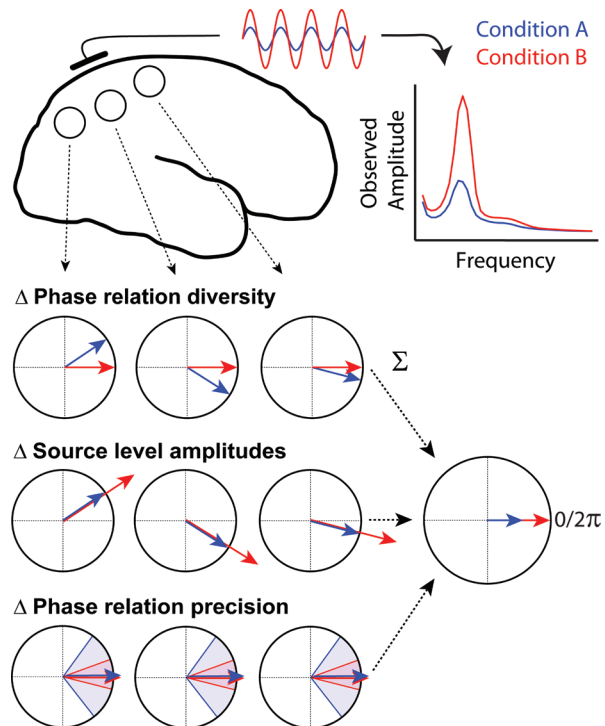


Figure 9.1. Schemes that may underlie changes in observed oscillatory amplitude. The directions of the arrows indicate the average phase relations relative to an arbitrary reference. The lengths of an arrows indicate amplitudes. The relevant aspects pertain to the diversity in the between-population average phase relations, the source level amplitudes, and the phase relation precision (precision is indicated by the shaded areas).

When the average phase relations are 0 (as depicted in Fig. 9.1), this latter mechanism will change the sensor level amplitudes, because an increase in precision implies an increase in synchrony. (However, the situation is more complicated when the average phase relations differ from 0; in that case, an increase in precision does not have to imply that the distribution of phase relations is more concentrated around 0.)

With regard to these alternatives, three clarifications must be considered. First, these scenarios are not mutually exclusive. Second, while the measurement of oscillations in any distant recording site implies a certain level of synchrony between the underlying membrane potential oscillations (because individual membrane potential oscillations do not exceed the noise level of most extracellular recordings), this is orthogonal to our distinction between the scenarios above. Our distinction concerns the interpretation of a *change* in amplitude of an already measurable oscillatory signal. Third, source level amplitude modulations (at every spatial scale larger than individual neurons) may still reflect changes in synchrony at a finer spatial scale. Nevertheless, it is still important to establish whether there exists a spatial scale at which neural structures show amplitude modulations while maintaining their phase relations (i.e. the source level amplitude scenario in Fig. 9.1). For example, this might constrain the ways in which amplitude modulations may impact on neural computations.

To provide a first step towards disentangling these scenarios, we evaluated average phase relations in neural oscillations in conditions that differed markedly in amplitude. Recent work from our lab revealed profound diversity in average phase relations in both monkey V4 (Maris et al., 2013) and human electrocorticography (ECoG; van der Meij et al., 2012). Here, we focused on human MEG and asked two questions. (1) Is diversity in the average phase relations also present in such extracranial recordings? (2) When amplitude increases, does this diversity decrease or remain the same? Thus, we investigate the scenario depicted in the top row of Figure 9.1. If phase relation diversity would decrease, this would provide direct evidence for this scenario.

9.2 Results

We first investigated our two questions for posterior alpha (8-12 Hz) oscillations, which are the strongest oscillations in the MEG signal. We compared two conditions that differed vastly in alpha amplitude: eyes open and eyes closed (Figs. 9.2A, 9.3A). For a representative participant, Figure 9.2A depicts the topographies of alpha amplitudes in the two conditions. To evaluate phase relations, we first selected the channel with the highest amplitude and plotted the epoch-averaged phase relation between this and all other channels (Fig. 9.2B).

If alpha oscillations originate from a single oscillating dipole, then all between-channel phase relations should be either 0 or π (depending on whether the channels are located in the same or the opposite poles). Instead, we observed a rich palette of phase relations. This implies multiple underlying structures that oscillate at diverse phases, with the number of populations ranging from two to a continuum, as in traveling waves (Ermentrout and Kleinfeld, 2001). Crucially, this diversity was highly similar between the

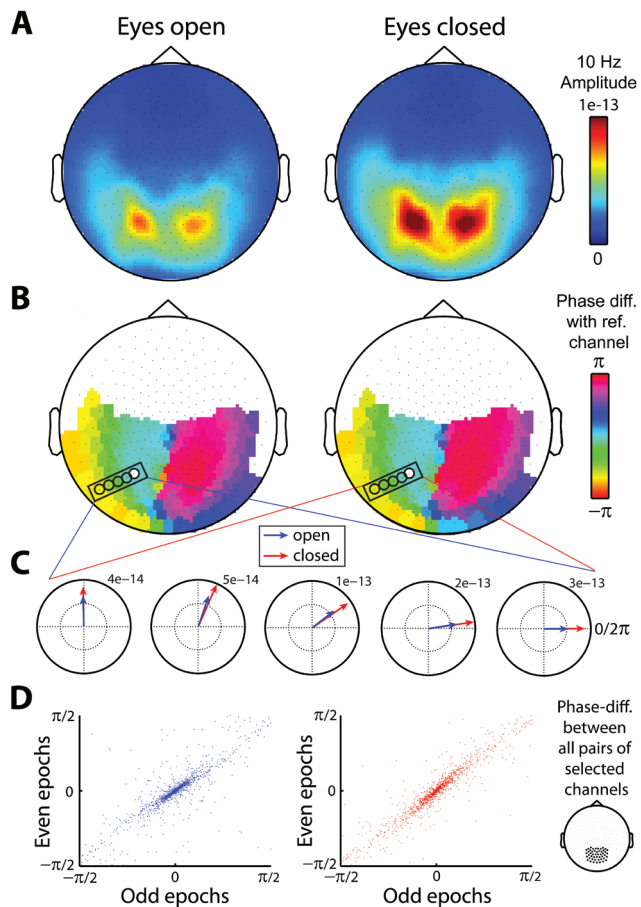
two conditions (Fig. 9.2B), and this was the case for all participants (Supplementary Fig. 9.1). Thus, the increase in amplitude is not paired by a reduction in the diversity of the phase relations between these underlying structures. This is further demonstrated by zooming in on a subset of these channels (Fig. 9.2C): whereas the amplitude increased in each channel, the average phase relations with the reference channel remained the same.

A split-half procedure revealed reliable diversity in the phase relations of a large set of channel pairs (Fig. 9.2D; Supplementary Fig. 9.2 for channel selection). Based on this, we derived a metric of systematic phase relation diversity (Materials and Methods; Supplementary Figs. 9.3 and 9.4). We evaluated this metric for many frequencies, in both conditions, and averaged across all participants (Fig. 9.3B). This confirmed at the group level (1) that posterior alpha oscillations exhibit reliable phase relation diversity, and (2) that this diversity is maintained despite vast changes in amplitude.

These observations generalize to visually induced gamma oscillations (50-70 Hz). We presented inward-moving concentric gra-tings (Hoogenboom et al., 2006) at two contrast levels that induced different amplitudes (Fig. 9.3C). Again, we observed reliable phase relation diversity in these oscillations and again this did not decrease when amplitude increased (Fig. 9.3D).

These observations did not change when we corrected for between-condition differences in the reliability of the phase relation estimates (Supplementary Fig.9.5).

Figure 9.2. Alpha oscillations exhibit a rich palette of phase relations that are maintained when amplitude increases (representative participant). (A) Posterior alpha amplitude is stronger during eyes closed. (B,C) Alpha oscillations exhibit a rich palette of phase relations (rel. to marked channel) that is highly similar between both conditions that differ vastly in amplitude. (D) Phase relations are reliably diverse across a large set of channel pairs (individual data points).



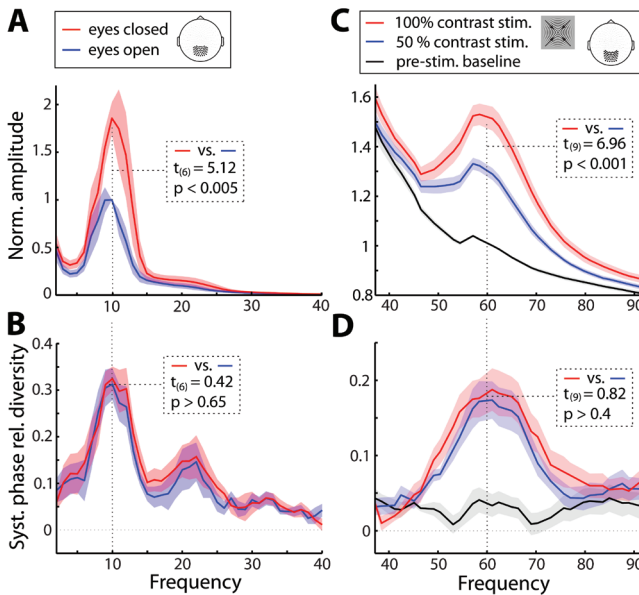


Figure 9.3. Both ongoing alpha and visually induced gamma oscillations exhibit systematic phase relation diversity that is maintained when amplitude increases (group-level data). (A,C) Alpha and gamma amplitudes are significantly higher during eyes closed and 100 % contrast stimulation, respectively. (B,D) Both alpha and gamma oscillations exhibit systematic phase relation diversity (SPHARED; Methods) that does not decrease when amplitude increases. Spectra are based on the indicated channel clusters (cf. Supplementary Fig. 9.2). Shadings indicate ± 1 s.e.m. Insets report relevant t - and p -statistics (two-tailed) at 10 and 60 Hz.

9.3 Discussion

This work provides two new insights. First, we studied the mechanisms underlying observed amplitude modulations. This revealed that, at least for neural structures that can be distinguished by MEG, amplitude increases should not be interpreted as a reduced diversity in the phase relations *between* these structures. Rather, these modulations co-exist in multiple underlying structures, while these maintain their average phase relations. We have demonstrated this for both ongoing alpha- and visually induced gamma oscillations. Nevertheless, changes in observed amplitude may still have (a combination of) three causes: (1) changes in the amplitudes of the underlying membrane potential oscillations (e.g. due to a stronger oscillatory drive received by, for example, the pulvinar; Lopes da Silva et al., 1980), (2) changes in the precision of the phase relations (i.e. coherence) between these structures, and/or (3) changes in phase relation diversity (i.e. synchronization) *within* each of the underlying structures (i.e. at a finer spatial scale). To investigate the contribution of changes in coherence, it will be essential to employ a method that allows for a comparison of the precision of the phase relations, while strictly controlling for differences in signal-to-noise ratio (which also scales with amplitude). To investigate the contribution of synchronization within the MEG-resolvable structures, it will be essential for future studies to extend the here presented approach to recordings at a finer spatial scale, such as between neighboring columns and, ultimately, neurons.

Second, these data also demonstrate that phase relation diversity is a pervasive aspect of neural oscillations, even when recorded extracranially. Again, this was the case for both alpha- and visually induced gamma oscillations. The existence of such phase

relation diversity is interesting by itself and warrants further investigation. For example, relevant questions pertain to the underlying source configuration, and the degree to which this diversity is under cognitive control. Another important question pertains to the functional role of this diversity. In fact, phase relation diversity, combined with amplitude and/or coherence modulations, may have important consequences for neural information processing as reflected in neural spiking activity. Many studies have demonstrated that spike timing depends on field oscillations (reviewed in Fries, 2005), and amplitude increases are typically paired by increases in such spike-field synchrony (e.g. Womelsdorf et al., 2006; Fries et al., 2008). This suggests that phase relation diversity may serve to control the spike timing relations between the different structures, while amplitude and coherence modulations (within and between these structures, respectively) may impact on the precision of these spike timing relations. Although speculative, these aspects may provide key ingredients for the routing of information through cortical circuits with high spatial specificity (see also Fries, 2005; Maris et al., 2013).

9.4 Materials and Methods

Participants

We analyzed data from two experiments. Experiment 1 focused on ongoing alpha oscillations. Eight healthy participants (six male, age range: 24-50) participated in this experiment. We only recorded participants in whom we had observed strong alpha oscillations in previous experiments. One participant was excluded from the analysis because he showed no clear alpha oscillations in the eyes open condition. Experiment 2 focused on visually induced gamma oscillations. This experiment was originally conducted to study genetic contributions to these oscillations. In the original experiment, 160 healthy participants participated. For our purpose, we only analyzed data from the 10 participants (2 male, age range: 18-28) who showed the strongest gamma response to visual stimulation. It is critical to point out that, for both experiments, we selected participants based on oscillatory amplitude alone. This selection is therefore independent of the critical aspect of our study which concerns phase relation diversity. All participants provided written consent. Experiments were conducted in accordance with guidelines of the local ethics committee (Committee on Research Involving Human Subjects, Region Arnhem-Nijmegen, The Netherlands).

Experiment 1

Experiment 1 consisted of two parts. In part 1, every 8, 10 or 12 s, participants heard a man's voice instructing them in alternation to either open or close their eyes. This continued for approximately 30 minutes. Part 1 was immediately followed by part 2 consisting of two continuous blocks of 5 minutes: one with eyes open and the other with eyes closed. Data were cut into epochs of 2 s. Epochs of part 1 and 2 were analyzed together. We analyzed approximately 500 epochs per condition.

Experiment 2

Participants performed a visual change detection task with inward-moving concentric gratings (similar to Hoogenboom et al., 2006; van Pelt et al., 2012). Gratings had a diameter of 8.1 degree visual angle and were presented foveally. Participants were instructed to respond as fast as possible to a speed change of the inward motion. Responses were made with the right index finger. The speed change occurred at an unpredictable time point between 750 and 3000 ms after stimulus onset. We cut the data into epochs of 750 ms and only used epochs prior to the speed change. In different trials, stimuli were presented at either of three different speeds of the inward motion and at two different contrast levels (50 and 100 % contrast). Trial types were randomly intermixed. We only analyzed trials in which the speed of the inward motion was 0.66 degree/sec. The task lasted 1 hour. We analyzed approximately 250 epochs per condition.

MEG recordings & preprocessing

In both experiments, data were collected with a CTF MEG system (Port Coquitlam, Canada) containing 275 axial gradiometers. Data were high-pass filtered at 300 Hz, sampled at 1200 Hz, and stored for offline analyses. Data were analyzed in Matlab (Mathworks, <http://www.mathworks.com>), using FieldTrip (Oostenveld et al., 2011) in combination with custom code. 50 Hz line-noise was removed using a filter based on the discrete Fourier transform. Epochs contaminated by artifacts were removed following visual inspection. From the data of Experiment 1, we additionally subtracted two heartbeat components using Independent Component Analysis (ICA; Bell and Sejnowski 1995). We subtracted those components whose time courses were highly coherent with the electrocardiogram (ECG). In experiment 2 we had not recorded the ECG and so we did not remove the ECG components from the signal.

Analysis of amplitude and phase relations

We performed spectral analysis using a multi-taper approach that allows control over spectral smoothing to achieve optimal spectral concentration (Percival and Walden, 1993; Mitra and Pesaran, 1999). We applied tapers from a family of orthogonal prolate spheroidal functions. For all analyses on alpha oscillations (Experiment 1) we applied ± 2 Hz smoothing; for gamma oscillations (Experiment 2) we applied ± 5 Hz smoothing.

In multitaper estimation, for each taper, the data segment is multiplied with that taper and then Fourier transformed, giving the windowed Fourier transform $\tilde{x}_k(f)$:

$$\tilde{x}_k(f) = \sum_{t=1}^N w_k(t) x_t e^{-2\pi i f t}$$

where x_t ($t = 1, 2, \dots, N$) is the time series of the signal under consideration and $w_k(t)$ ($k = 1, 2, \dots, K$) are K orthogonal taper functions.



The multitaper estimates for the spectrum $S_{xx}(f)$ and cross-spectrum $S_{xy}(f)$ are given by:

$$S_{xx}(f) = \frac{1}{K} \sum_{k=1}^K |\tilde{x}_k(f)|^2 \quad S_{xy}(f) = \frac{1}{K} \sum_{k=1}^K \tilde{x}_k(f) \tilde{y}_k^*(f)$$

For the analysis of amplitude, we took the square root of the taper-averaged power spectrum S_{xx} . We normalized all amplitude spectra before averaging across participants. In Experiment 1, we normalized amplitude to a proportion of 10 Hz amplitude in the eyes open condition. In Experiment 2, we normalized amplitude to a proportion of 60 Hz amplitude in the pre-stimulus baseline condition.

For the analysis of phase relations, we used the spectra $S_{xx}(f)$ and cross-spectra $S_{xy}(f)$ to calculate the coherency $C_{xy}(f)$:

$$C_{xy}(f) = \frac{S_{xy}(f)}{\sqrt{S_{xx}(f) S_{yy}(f)}}$$

Coherency is a complex quantity. The phase of coherency gives the preferred (i.e. average) phase relation between the two time series, x_t and y_t , and ranges between $[-\pi, +\pi]$.

We calculated these phase relations for all channel pairs within a cluster of selected channels above posterior regions of the brain. We used slightly different channel clusters for the analyses of alpha and gamma oscillations because the channels that showed the strongest amplitude for visually induced gamma oscillations were located slightly more posterior than those that showed the strongest amplitude of ongoing alpha oscillations (Supplementary Fig. 9.2).

For illustration purposes, we also selected the channel with the highest amplitude and plotted the average phase relations between this and all other channels (Fig. 9.2B). Because this is only meaningful for channels in which alpha oscillations were observed, we masked all channels in which alpha amplitude was $< 25\%$ of the amplitude in the selected channel. To further zoom in on the effect of interest we also realigned data relative to the peak of alpha in the channel with the highest amplitude and calculated Fourier coefficients for this and neighboring channels. We depict the average, complex valued, coefficients for several channels in Figure 9.2C. In these plots the vector angles represent the phase relations with the selected reference channel and the vector lengths represent the associated amplitudes.

Analysis of phase relation diversity

We quantified the degree to which phase relations were reliably diverse across all selected channel pairs. Our approach is depicted schematically in Supplementary Figure 9.3 and in Supplementary Figure 9.4 we show some applications to the observed data.

We first separated systematic from unsystematic phase relations based on a split-half procedure. Per condition, we divided all epochs into two sets: odd-numbered epochs and even-numbered epochs. For both sets, we estimated epoch-averaged phase relations

between all selected channel pairs. Crucially, if a channel pair has a reliable phase relation, then this relation should be observed in both sets of epochs. In contrast, if the phase relation is not reliable, then both sets will produce a different phase relation.

Figure 9.2D and Supplementary Figure 9.4 shows several examples of this split-half procedure applied to observed data. Note that, specifically for alpha (Experiment 1) and gamma (Experiment 2) oscillations, these phase relations are both diverse across all channel pairs (i.e. spread out over the range $[-\pi, +\pi]$) and reliable (i.e. highly similar for the odd and even data splits). We set out to quantify this pattern in the data using a single metric, which we calculated per frequency bin and per condition (outcomes are depicted in Fig. 9.3B,D). For this, we build on a previously developed metric termed over-Site-pair PHase Relation Diversity (SPHARED; Maris et al., 2012). Although we used slightly modified calculations, we will also refer to our metric as SPHARED. The main reasons for using this metric are twofold: (1) SPHARED is zero whenever the true phase diversity is zero (i.e. when all diversity is due to noise) (2) SPHARED can be calculated in a way that it does not depend on phase relation diversity produced by dipolar patterns (we return to this below).

The pairs of phase relations (with one element from the odd- and the other from the even-numbered epochs; Supplementary Fig. 9.3A) are points in a space that is defined by two circular axes, one for the odd and the other for the even epochs. We first projected every point (channel pair) onto two new axes, with one axis corresponding to the systematic component in the phase relations, and the other to the unsystematic component (Supplementary Fig. 9.3B). Per channel pair, its location on the systematic axis is defined by the *average* phase-relation between the odd and even epochs (represented as points on the unit circle in the complex plane) and the projection on the unsystematic axis is defined as the *difference* in the phase relations between the odd and even epochs (again in the complex plane). Because noise is twice as small on the systematic projection (because noise is reduced by averaging but not by subtracting), we divided all values on our unsystematic axis by 2. The geometrical representation of our projection is the surface of a sphere (Supplementary Fig. 9.3D). For simplicity, we first explain SPHARED for a two-dimensional plane, restricted to all systematic phase relations in the range $[-\pi/2, +\pi/2]$. Thereafter, we return to the spherical representation to explain how we deal with dipolar patterns in our data.

SPHARED is based on the following rationale. If there is diversity in the phase relations between all channel pairs *and* if this is reliable, then the diversity across the systematic axis (which contains both systematic diversity and noise) should be larger than the diversity across the unsystematic axis (which contains only noise). SPHARED is therefore calculated as the difference in diversity between the systematic and the unsystematic axes (systematic minus unsystematic). Diversity is quantified as the absolute deviation from phase relations of 0, averaged across all channel pairs. SPHARED is zero when (1) there is no diversity in the phase relations across channel pairs (i.e. when all signals oscillate in synchrony; the dipole scenario in Supplementary Fig. 9.3B) or (2) when this diversity is not reliable (i.e. when the diversity is equally large across the systematic and the unsystematic axes of the

projection; the noise scenario in Supplementary Fig. 9.3B). In fact, SPHARED will only be positive when there are non-zero phase relations *and* when these are reliable (the true phase relation diversity scenario in Supplementary Fig. 9.3B). We verified this using simulated data.

We now consider systematic phase relations across the full circle (i.e. ranging between $[-\pi, +\pi]$). Here, a single current dipole also produces phase relation diversity because its two poles differ by π . Specifically, in the MEG signal, a single current dipole will simultaneously produce a positive (outward) flux in channels on one side of the dipole and a negative (inward) flux in channels on the opposite side of the dipole. Therefore, an oscillating dipole will produce phase relations of both 0 and π (depending on whether the two channels of a pair are located in the same or the opposite poles). We are not interested in this type of diversity because it is produced by a single underlying source. To deal with this, we split our channel pair data in two halves: one half with systematic phase relations in the range $[-\pi/2, +\pi/2]$ (thus centered at 0), and one half with phase relations outside this range (thus centered at $\pm\pi$). In other words, we split our data according to the two halves of the sphere (Supplementary Fig. 9.3D). We calculated SPHARED separately for each half of the sphere and subsequently pooled these values. Computationally, this was achieved by separating all channel pairs with systematic components outside the range $[-\pi/2, +\pi/2]$, and applying a phase-shift of π to these phase relations before calculating SPHARED. As evident from Supplementary Figure 9.3D, single dipoles only produce diversity *between* both halves of the sphere; not *within* either of them. Therefore, our two-step SPHARED metric is insensitive to all diversity that may result from single dipoles. This is also evident from Supplementary Figure 9.4, lower left panel. In this particular example, we observe at 30 Hz a clear dipolar pattern with strong concentration of phase relations at both 0 and at $\pm\pi$. This is represented by a 5-point cloud in this two-dimensional plane (a 2-point cloud on a sphere; Supplementary Fig. 9.3C,D). Critically, because there is no reliable diversity surrounding each of these clouds, the associated SPHARED value is close to 0, as it should be.

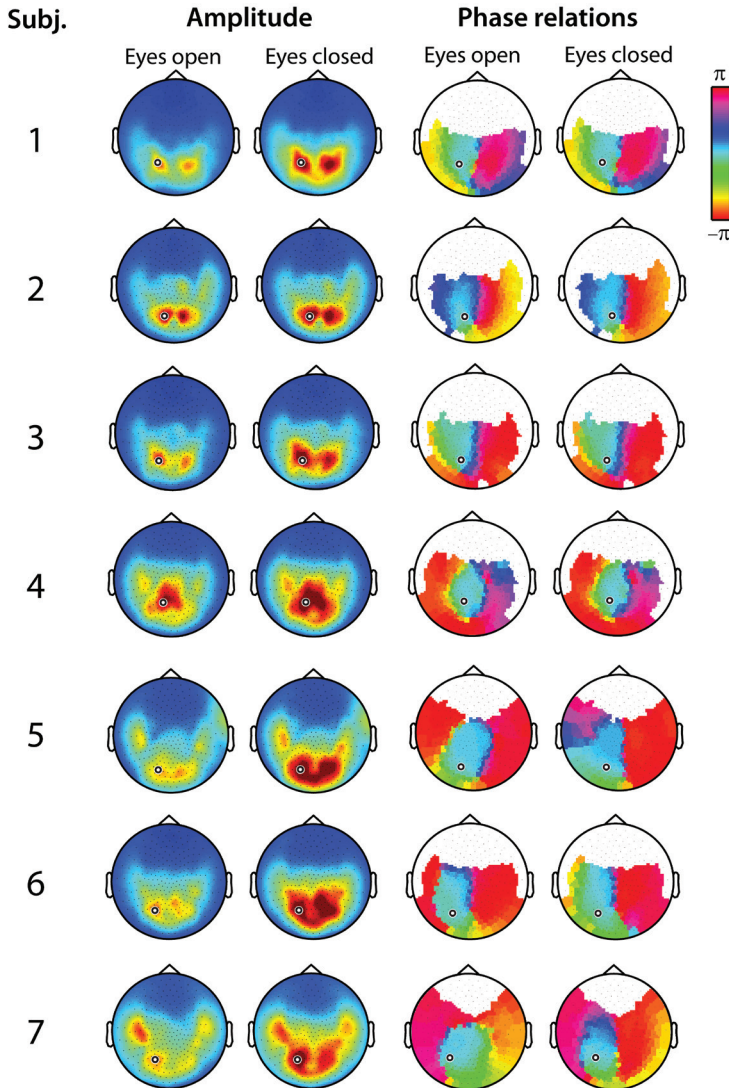
Correction of between-condition differences in phase relation reliability

We corrected for between-condition differences in the reliability of the phase relation estimates by artificially equating the unreliability of these estimates between the conditions. Results of this correction are depicted in Supplementary Figure 9.5. Per channel pair, we added noise to the condition with the more reliable phase relation estimate (typically, the condition with the higher amplitude) before calculating SPHARED. The amount of noise was determined by the between-condition difference in the reliability of the phase relation estimates. Concretely, we performed the following four steps. (1) For each condition and channel pair we estimated the sampling variance of every phase relation estimate using the Jackknife (Efron and Stein, 1981). (2) We doubled this variance to make it appropriate for phase relation estimates based on half the number of epochs, because this is the relevant quantity (our correction involves adding noise to each of the two phase relation estimates

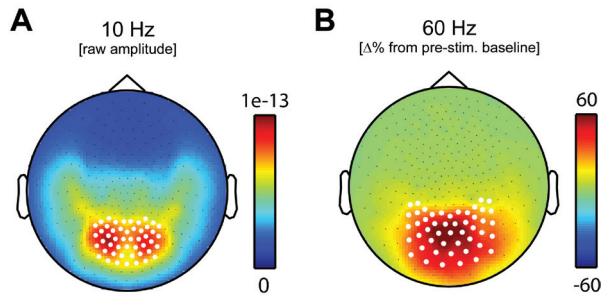
obtained from our split-half procedure; see step 4 below). (3) Per channel pair, we subtracted the sampling variances of the two conditions (largest minus smallest). (4) Per channel pair, we drew two independent values from a normal random distribution with variance equal to the sampling variance difference obtained in step 3. We added these two values to the phase relations obtained for the odd- and the even-numbered epochs. For channel pairs for which the phase relations were less reliable in condition A, we added this simulated noise to the phase relations in condition B, and vice versa. After adding this noise, we recalculated SPHARED (Supplementary Fig. 9.5).



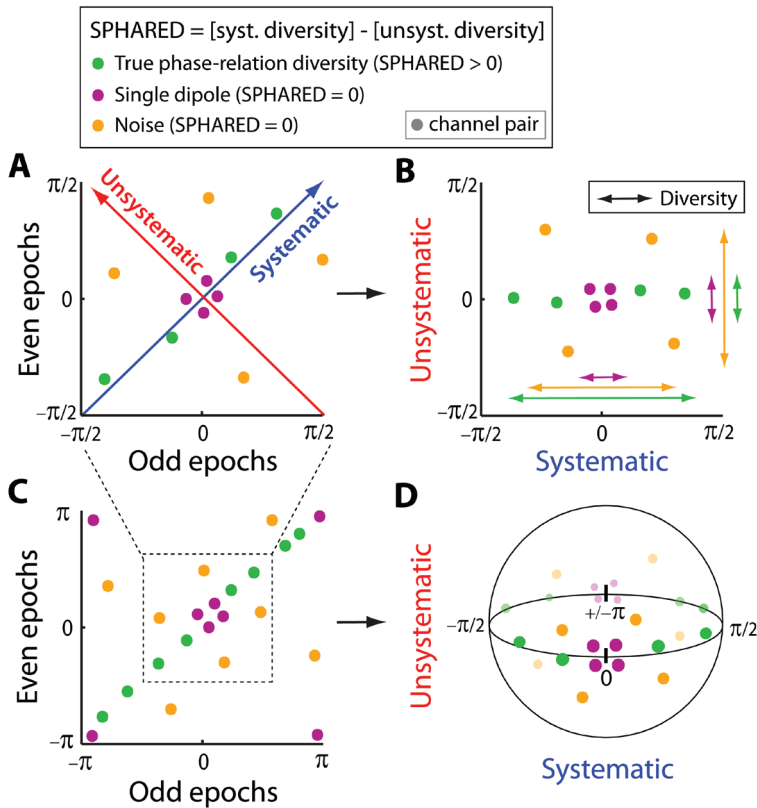
9.5 Supplementary Figures (9.1 - 9.5)



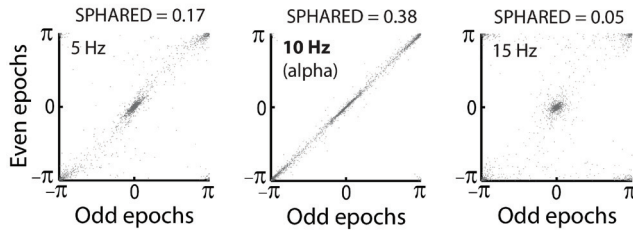
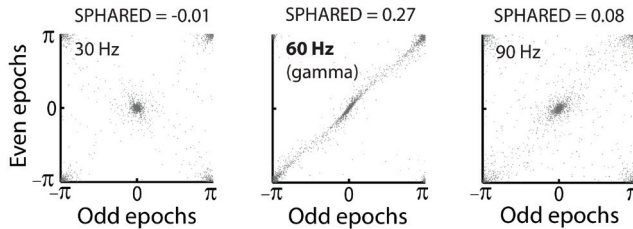
Supplementary Figure 9.1. Experiment 1: In all subjects, alpha oscillations exhibit a rich palette of phase relations that are maintained despite vast changes in amplitude. Amplitude topographies: for each subject the 10 Hz (i.e. alpha) amplitudes are plotted on the same scale for the eyes open and closed conditions. Note that every subject shows an increase in alpha amplitude with the eyes closed. Phase relation topographies: we selected the channel in the left posterior channels that showed the highest alpha amplitude (this channel is marked in all topographies). As in Figure 9.2B, we plotted the average phase relation between this and all other channels. Again, we masked all channels for which the amplitude was $< 25\%$ of the amplitude in the selected channel. Crucially: (1) alpha oscillations exhibit a rich palette of phase relations in each subject, and (2) these relations are highly replicable between the two conditions, within each subject. Different subjects did show different phase relation plots. However, this is likely due between-subject differences in (1) the configuration of the underlying sources (see also the amplitude plots) and (2) the location of the selected channel that we plotted the phase relations with.



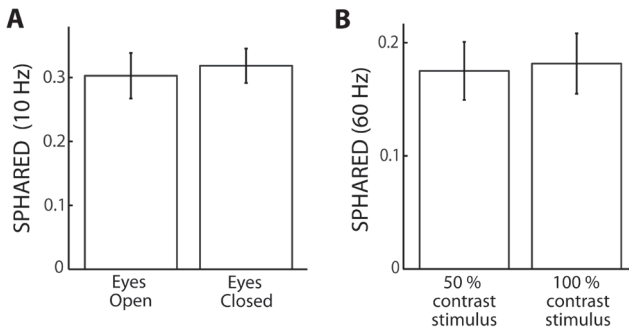
Supplementary Figure 9.2. Channel clusters overlaid on average topographies of ongoing alpha and visually induced gamma oscillations. (a) Grand-average topography of alpha amplitude, collapsed across the eyes open and eyes closed conditions. White disks mark the selected channel cluster used in Figure 9.3a,b. (b) Grand-average topography of gamma amplitude, expressed as a percentage change from a pre-stimulus baseline. Again, 50 % and 100 % contrast stimulus conditions were collapsed. White disks mark the selected channel cluster used in Figure 9.3C,D.



Supplementary Figure 9.3. Schematic of our metric to quantify systematic phase relation diversity across all selected channel pairs (SPHARED). See also Methods. We first describe our metric for all phase relations in the range $[-\pi/2, +\pi/2]$ (panels A and B). We begin by separating all epochs into two sets: odd-numbered and even-numbered epochs (panel A). For each set, we obtained one epoch-averaged phase relation per channel pair. Individual channel pairs are depicted as individual points in the schematic graphs. We depict three different scenarios: true phase relation diversity (green), a single current dipole (purple) and noise (orange). To separate reliable for unreliable phase relations, we projected these data onto a systematic axis (blue) and an unsystematic axis (red). We calculated the diversity of these phase relations across both axes (panel B). SPHARED is defined as the difference between the two diversity measures: the diversity across the systematic axis minus the diversity across the unsystematic axis. SPHARED will only be > 0 when there is substantial diversity (this excludes the dipole scenario) and this is reliable (this excludes the noise scenario). I.e., only for the green data points, the diversity is larger across the systematic compared to the unsystematic axis (as indicated by the length of the horizontal and vertical arrows). Now consider phase relations across the full circle (i.e. between $[-\pi, +\pi]$; panels C,D). Looking at this range, a single dipole does lead to diversity in the phase relations, because it produces phase relations of both 0 and π (Methods for details). To deal with this, we split our phase relation data in two halves: one centered at systematic phase relations of 0 and the other centered at $+\pi/-\pi$. To see the motivation for this split, consider the projection of our phase relations as points on a sphere (panel D). The horizontal plane in panel D contains a circle that is the axis for the systematic component; deviations from this circle in the vertical direction are the values on the axis for the unsystematic component. Note how the four purple points in the corners of panel C are accurately clustered around phase relations of $+\pi/-\pi$. To remove the contributions of dipoles to SPHARED, we calculated SPHARED separately for both halves of this sphere. For several examples of SPHARED applied to observed data, see Supplementary Figure 9.4.

Exp. 1. Eyes closed (Participant 2)**Exp 2. 100% contrast stim. (Participant 1)**

Supplementary Figure 9.4. SPHARED: examples of observed data. Epoch-averaged phase relations for odd- and even-numbered epochs in two representative participants. Each point represents a single channel pair, with its position being determined by the phase relations for the odd- and even-numbered epochs. Channel pairs were taken from a cluster of channels across posterior regions of the brain (Fig. 9.3A,B; Supplementary Fig. 9.2). Associated SPHARED values are stated above each scatterplot. Note that, specifically for alpha and gamma oscillations, these phase relations are both diverse (spread out over the range $[-\pi, +\pi]$) and reliable (highly similar for the odd and even data splits). Note also that our SPHARED metric is insensitive to diversity that results from dipolar patterns in the data. For example, the lower left panel shows a strong concentration of phase relations at both 0 and $\pm\pi$. This dipolar pattern (represented by a 5-point cloud in this two-dimensional plane) is associated with a SPHARED value close to 0.



Supplementary Figure 9.5. SPHARED values for alpha and gamma after correction for between-condition differences in the reliability of the phase relation estimates. We corrected for between-condition differences in the reliability of the phase relation estimates by equating the unreliability of these estimates between the conditions. Specifically, per channel pair, we added noise to the condition with the more reliable phase relation estimate (typically, the condition with the higher amplitude). The amount of noise was determined by the between-condition difference in the reliability of the phase relation estimates. Crucially, for both alpha (A) and gamma (B) oscillations, SPHARED values remained highly similar (compare panels A,B with Fig. 9.3B,D; 10 and 60 Hz, respectively). Therefore, phase relation diversity does not differ between the conditions that differed vastly in amplitude, also not when potential differences in the reliability of the phase relation estimates are corrected for.

General discussion

10



10.1 Summary

I set out to understand the neurophysiological mechanisms via which preparatory attention improves perception. In this section, I list all the key observations detailed in the previous eight chapters of this thesis. Thereafter, in 10.2, I evaluate the progress that we have made based on these observations. Many of these chapters have also revealed additional insights, of which I next highlight three in 10.3. Finally, in 10.4, I provide an outlook with further outstanding questions and in 10.5 I conclude.

We have seen that orienting attention to an expected touch sensation involves a preparatory suppression of alpha and beta oscillations (**chapters 2-8**). We have seen that this occurs, amongst others, in the contralateral primary somatosensory cortex (S1), which is the first cortical stage at which the anticipated tactile information will be processed. This phenomenon:

1. Is strongest during attentive expectations (**chapter 2**)
2. Is specific in both space and time (**chapter 3**)
3. Follows the time course of accuracy, but not reaction time, improvement (**chapter 4**)
4. Accounts for up to 30 % of the attentional improvement in perception (**chapter 5**)
5. Increases the ipsilateral S1 response to tactile input (**chapter 6**)
6. Is mainly restricted to the preparatory interval, and replaced by the attentional modulation of gamma oscillations during stimulus processing (**chapter 7**)
7. Occurs, for beta oscillations, throughout the widely distributed somatomotor network (**chapter 8**)
8. May co-exist in neighboring neural structures that exhibit and maintain diversity in their phase relations (**chapter 9**)

10.2 Evaluation

To evaluate how well these observations answer my central research question, I will divide this question into three sub questions that logically follow each other. Q1: What are the neural signatures (or phenomena) of preparatory selective attention? Q2: How relevant are these signatures for perception? Q3: What are the mechanisms via which these signatures affect perception? With regard to the preparatory modulation of alpha and beta oscillations, the studies presented in this thesis provide good answers to these first two questions and hint at possible answers to this third question. I elaborate on this below.

Q1: What are the neural signatures of preparatory selective attention?

Chapters 2-8 have demonstrated that the preparatory suppression of alpha and beta oscillations constitutes a key neural signature of preparatory selective attention. This phenomenon is highly robust: it was observed in every study and in almost every participant. Together with other literature, this demonstrates that the anticipatory modulation of ongoing

oscillations constitutes a general signature of preparatory selective attention. For example, this has been demonstrated not only in the somatosensory modality (**chapters 2-8**), but also the visual (Worden et al., 2000; Thut et al., 2006) and auditory (Muller and Weisz, 2012) modalities. Moreover, this phenomenon is not only specific to the anticipated location of a stimulus (Worden et al., 2000; Thut et al., 2006; **chapters 2-8**), but also to its anticipated timing (Rohenkohl and Nobre, 2011; **chapter 3**) and its relevant feature (Snyder and Foxe, 2010). These observations place the preparatory modulation of ongoing oscillations on the map as a highly robust signature of preparatory attention that must be considered alongside other signatures of preparatory attention (such as the preparatory increase in blood flow that also occurs in the stimulus-receiving sensory cortices; e.g. Kastner et al., 1999; Carlsson et al., 2000; Voisin et al., 2006).

Q2: How relevant is this signature for perception?

As stated in **chapter 1**, the relevance of any given neural signature of attention is directly related to the extent to which it can account for the associated improvement in perception. **Chapters 4, 5 and 7** have provided key insights into this relevance for the signature that has been central in this thesis. Most prominently, **chapter 5** has revealed that this signature may account for up to 30 % of the attentional improvement in perception. At the same time, **chapters 4 and 7** have revealed that there can also be behavioral effects of attentional cues without any attentional modulation of alpha and beta oscillations. Each of these studies has thus revealed that additional neural phenomena must also be considered to provide a full account of (preparatory) attention. The attentional modulation of gamma oscillations may provide one such phenomenon, although it is largely restricted to the interval during stimulus processing (**chapter 7**).

It will be critical for future studies to investigate the extent to which also other signatures of preparatory attention (such as the preparatory increases in spike-rate and blood flow; e.g. Luck et al., 1997; Kastner et al., 1999) may explain additional parts of the attentional improvement in perception.

Noteworthy, the perceptual relevance of the neural signatures of attention may depend on the specific requirements of the perceptual task. In fact, the studies in this thesis have pointed to the existence of at least two such task-dependencies for the attentional modulations of alpha- and beta oscillations. First, their perceptual relevance may be largely restricted to situations in which stimuli can be anticipated and are only briefly presented (**chapter 7**). Second, these modulations may have more impact on stimulus detection than on stimulus identification. In fact, only in **chapter 5** (the only chapter in which a detection task was employed) could single-trial amplitudes be related to perceptual accuracy. This may be due to the notion that perceptual identification, in contrast to detection, also relies on further processing of the sensory information after its presentation (i.e. from short-term memory). Because this processing may affect identification also of stimuli that occurred during states of low attention (albeit to a lesser extent; e.g. **chapter 6**), identification is



only partly determined by prior brain states. In future studies, it will thus be important to dissect precisely which aspects of perception are influenced by this and other signatures of attention.

Q3: What are the mechanisms via which this signature affects perception?

As stated in **chapter 1**, several studies have demonstrated that the amplitudes of alpha and beta oscillations are inversely related to cortical excitability and information processing. Therefore, the preparatory suppression of these oscillations in the stimulus receiving sensory cortices may instantiate a neural state that is characterized by high excitability and high information processing capacity. Upon sensory input, such a state will ensure that the anticipated sensory information will be processed with immediate high fidelity.

This immediately brings forward the question how the amplitudes of alpha and beta oscillations (as observed in the MEG signal) are related to cortical excitability and information processing capacity. This is by far the most difficult question to answer and our data only provide limited insights into this important issue. In fact, an adequate answer to this question necessitates complementing animal research, in which this can be studied with much higher precision than in human MEG recordings.

There are at least two possibilities via which modulations in the observed amplitudes of alpha and beta oscillations may contribute to perception. First, under a pulsed inhibition account of alpha (and possibly also beta) oscillations (Jensen and Mazaheri, 2010; Mathewson et al., 2011), their observed suppression may reflect weaker ‘pulses of inhibition’ which may lead to longer windows of opportunity and overall less inhibition (see also **chapter 1**, 1.2.2). Thus, when the anticipated sensory information comes in, the receiving cortex (in which these oscillations are suppressed) is more excitable and this may boost the response to this attended stimulus. Alternatively, a reduction in observed amplitude may also reflect a desynchronization of the underlying neural populations (Pfurtscheller and Lopes da Silva, 1999), and this may also improve perception. In particular, this may increase the coding capacity of the population because of the following reason. Imagine a population in which all neurons fire action potentials in perfect synchrony. At any given moment, this population can only code for two states. Now, because desynchronization of the membrane potential fluctuations may decrease the (stimulus unrelated) dependencies between these neurons, this may increase the coding capacity of the population (Zohary et al., 1994; Mitchell et al., 2009; Cohen and Maunsell, 2009; Harris and Thiele, 2011). **Chapter 9** aimed at disentangling these alternative scenarios and showed that, at least for neural structures that can be distinguished by MEG, amplitude modulations are not paired by changes in the average phase relations between these structures. However, besides genuine amplitude decreases of the underlying membrane potential oscillations (the pulsed account), these modulations may still reflect desynchronization at a finer spatial scale (i.e. within the underlying structures). To further distinguish between these alternatives, it will be essential for future studies to extend the approach presented in **chapter 9** to recordings at

the scales of neighboring columns and, ultimately, neurons. In addition, it will be important to investigate the precise functional role of the (amplitude-independent) diversity in the phase relations that was revealed in **chapter 9**.

In addition to understanding the neurophysiological mechanisms that govern oscillatory brain states, a complementary approach to this question is to address how such brain states alter sensory processing. In other words, what are the neural phenomena during stimulus processing that are affected by these prior brain states? **Chapter 6** revealed that such preparatory brain states may increase the size of the induced response from the ipsilateral primary sensory cortex. Moreover, the size of this effect was correlated with the size of the attentional improvement in perception. If this ipsilateral beta response reflects stimulus processing, then this implies that such preparatory brain states may increase the degree to which sensory processing is distributed across the hemispheres. This provides a novel and potentially important mechanism via which preparatory attention may improve perception. Having established this novel phenomenon, the next logical step would be to turn to questions 2 and 3, but now try to answer these for this particular phenomenon. In particular: (Q2) How much of the improvement can be (additionally) explained by this increased ipsilateral response? (Q3) Via what physiological mechanisms does this increased ipsilateral response improve perception, and via what mechanisms does the contralateral preparatory brain state lead to the increased ipsilateral response?

Thus, while these studies have revealed several new insights into how preparatory attention improves perception, they provide a picture that is far from complete and point to several important avenues for future research (see also 10.4 for additional outstanding questions).

10.3 Additional insights

I now turn to three additional insights that these studies have provided. These insights branch out to related issues in cognitive neuroscience and I therefore highlight them briefly.

10.3.1 Are reaction time differences sufficient to infer attentional processes?

A great part of the attention literature is based solely on differences in reaction time to validly- and invalidly cued stimuli. A relevant question thus becomes whether such reaction time differences are sufficient to infer attentional processes. In **chapter 4**, I have shown that attentional cues may already affect reaction times to stimuli that are presented within 200 ms after the symbolic attentional cue. At these latencies, there is no clear effect on perceptual accuracy, and also no corresponding preparatory modulation of alpha and beta oscillations. To account for this early reaction time effect, I have postulated that there might be two sources that lead to faster reaction times to validly cued stimuli: (1) a true attentional effect, and (2) a cue-target compatibility effect. If this is true, then differences in reaction time alone are not sufficient to infer attentional processes, because they could be due solely to a compatibility effect (see **chapter 4** for further discussion).



10.3.2 Do cognitive variables have a fixed set of neural correlates?

It is often assumed that cognitive variables, such as attention, have a fixed set of neural correlates. In **chapter 7**, I have shown that this is not the case: the neural correlates of attention are profoundly shaped by the sensory context in which attention is deployed. Thus, the neural correlates of cognition can be highly context-dependent, even when the cognitive operations, at a functional level, are not (i.e. the focus of attention did not differ between both contexts).

10.3.3 Are somatosensation and action physiologically separable?

Perception and action are often studied in isolation. However, in particular somatosensation and action are heavily interdependent: action leads to somatosensation, leading to adjusted action, etc. Therefore, it is relevant to know whether modulations in neural activity in the somatosensory and motor parts of the brain can actually occur in isolation (in line with the way these are often studied). **Chapter 8** suggests that this is not the case, at least not with respect to beta oscillations in a widely distributed network. Recent studies in the rodent have also implicating primary motor cortex in tactile perception (Ferezou et al., 2007) and primary somatosensory cortex in motor control (Matyas et al., 2010). These observations require us to reevaluate the functional differences between the somatosensory and motor cortices and to work towards paradigms in which somatosensation and action are studied in interaction.

10.4 Further outstanding questions

In my evaluation (10.2), I have pointed to several important avenues for future investigations with respect to the central phenomenon in this thesis. In addition, several other questions stand out, of which I highlight four below.

This thesis has focused on how preparatory selective attention affects neural activity in the primary somatosensory cortex (S1). Clearly, preparatory attention will not be associated with modulations of neural activity in S1 alone. For example, functional Magnetic Resonance Imaging (fMRI) studies into preparatory attention consistently report activations of parietal and frontal cortices that are hypothesized to play a key role in driving the modulations in the sensory cortices (Corbetta and Shulman, 2002; Bressler et al., 2008). Likewise, S1 is not the only brain region in which somatosensory information is processed. For example, this information is also processed in the secondary somatosensory cortices. Despite several efforts, in the studies presented in this thesis, I have not been able to identify robust neural signatures of attention in these areas. How neural activity in these regions is modulated during preparatory attention, and how these modulations are related to the ones presented in this thesis, thus remain relevant questions for future research. In fact, modulations in these other areas of the brain may account for those parts of the attentional improvement that could not be explained by the preparatory modulations of oscillatory neural activity in

the contralateral S1.

Another avenue for future research will be to investigate whether and how the somatomotor beta oscillations that I have studied differ from the beta oscillations that are coherent across the frontal and parietal cortices. While these two types of beta oscillations seem to share a common feature (they are both coherent over relatively large distances), their functional roles may well differ. In fact the latter beta oscillations show an *increase* with attention and are hypothesized to reflect active processing (Liang et al., 2002; Bushman and Miller, 2007; Salazar et al., 2012).

This thesis has also revealed that neural activity in populations involved in somatosensation and action cannot be modulated independently (**chapter 8**). This brings forward the question whether this inseparability also has functional consequences. For example, does action (or action preparation) automatically alter the state of somatosensory cortex to improve somatosensory perception? Likewise, does somatosensation (or somatosensory preparation) automatically induce a state of readiness in the motor system, thereby facilitating (re)action?

Finally, as already alluded to in **chapter 1**, in everyday life, preparatory tactile attention is most prevalent during active behavior, such as when reaching out for objects. It will be essential to establish whether the key observations described in this thesis also generalize to such situations.

10.5 Conclusion

In this thesis, I set out to investigate the neurophysiological mechanisms via which preparatory selective attention improves perception. The central observation in this thesis is that orienting attention to an expected touch sensation involves a preparatory suppression of alpha and beta oscillations in the contralateral (stimulus receiving) primary somatosensory cortex. This thesis has put this type of preparatory modulation of ongoing oscillations on the map as a highly robust phenomenon that is (1) generalizable across the different sensory modalities, (2) specific in both space and time, and (3) relevant for perception. At the same time, several studies in this thesis have revealed that attention can also affect perception independent of this phenomenon, implying that additional neural processes must also be considered to explain how preparatory attention improves perception. These studies have also provided several other new insights into this phenomenon (e.g. its influence on ipsilateral stimulus processing; its propagation to the muscles) as well as into related branches in cognitive neuroscience. In future endeavors it will be critical to (1) advance the understanding of the precise physiological mechanisms via which the preparatory suppression of alpha and beta oscillations improves perception, and (2) uncover which other neural signatures of preparatory attention account for additional parts of this improvement.



References



Anderson KL, Ding M (2011) Attentional modulation of the somatosensory mu rhythm. *Neuroscience* 180:165-180.

Andersen SK, Muller MM (2010) Behavioral performance follows the time course of neural facilitation and suppression during cued shifts of feature-selective attention. *Proc Natl Acad Sci U S A* 107:13878-13882.

Aumann TD, Fetz EE (2004) Oscillatory activity in forelimb muscles of behaving monkeys evoked by microstimulation in the cerebellar nuclei. *Neurosci Lett* 361:106-110.



Babiloni C, Brancucci A, Babiloni F, Capotosto P, Carducci F, Cincotti F, Arendt-Nielsen L, Chen AC, Rossini PM (2003) Anticipatory cortical responses during the expectancy of a predictable painful stimulation. A high-resolution electroencephalography study. *Eur J Neurosci* 18:1692-1700.

Baker SN, Olivier E, Lemon RN (1997) Coherent oscillations in monkey motor cortex and hand muscle EMG show task-dependent modulation. *J Physiol* 501:225-241.

Baker SN (2007) Oscillatory interactions between sensorimotor cortex and the periphery. *Curr Opin Neurobiol* 17:649-655.

Bastiaansen MC, Knosche TR (2000) Tangential derivative mapping of axial MEG applied to event-related desynchronization research. *Clin Neurophysiol* 111:1300-1305.

Bauer M, Oostenveld R, Peeters M, Fries P (2006) Tactile spatial attention enhances gamma-band activity in somatosensory cortex and reduces low-frequency activity in parieto-occipital areas. *J Neurosci* 26:490-501.

Bauer M, Kennett S, Driver J (2012) Attentional selection of location and modality in vision and touch modulates low-frequency activity in associated sensory cortices. *J Neurophysiol* 107:2342-2351.

Bell AJ, Sejnowski TJ (1995) An information-

maximization approach to blind separation and blind deconvolution. *Neural Comput* 7:1129-1159.

Berger H (1929) Über das Elektroenkephalogramm des Menschen. *Archiv für Psychiatrie und Nervenkrankheiten* 87:527-570.

Blankenburg F, Ruff CC, Bestmann S, Bjoertom O, Eshel N, Josephs O, Weiskopf N, Driver J (2008) Interhemispheric effect of parietal TMS on somatosensory response confirmed directly with concurrent TMS-fMRI. *J Neurosci* 28:13202-13208.

Boly M, Baeteau E, Schnakers C, Degueldre C, Moonen G, Luxen A, Phillips C, Peigneux P, Maquet P, Laureys S (2007) Baseline brain activity fluctuations predict somatosensory perception in humans. *Proc Natl Acad Sci U S A* 104:12187-12192.

Brainard DH (1997) The Psychophysics Toolbox. *Spat Vis* 10:433-436.

Bressler SL, Tang W, Sylvester CM, Shulman GL, Corbetta M (2008) Top-down control of human visual cortex by frontal and parietal cortex in anticipatory visual spatial attention. *J Neurosci* 28:10056-10061.

Brovelli A, Ding M, Ledberg A, Chen Y, Nakamura R, Bressler SL (2004) Beta oscillations in a large-scale sensorimotor cortical network: directional influences revealed by Granger causality. *Proc Natl Acad Sci U S A* 101:9849-9854.

Buffalo EA, Fries P, Landman R, Buschman TJ, Desimone R (2011) Laminar differences in gamma and alpha coherence in the ventral stream. *Proc Natl Acad Sci U S A* 108:11262-11267.

Burton H (1976) Second somatosensory cortex and related areas. In: Jones EG, Peters A (Eds.), *Cerebral cortex, Vol 5 Sensory-motor areas and aspects of cortical connectivity*. Plenum Press, New York, pp. 31-98.

Busch NA, Dubois J, VanRullen R (2009) The phase of ongoing EEG oscillations predicts visual perception. *J Neurosci* 29:7869-76.

Buschman TJ, Miller EK (2007) Top-down versus bottom-up control of attention in the prefrontal and posterior parietal cortices. *Science* 315:1860-1862.

Busse L, Katzner S, Treue S (2008) Temporal dynamics of neuronal modulation during exogenous and endogenous shifts of visual attention in macaque area MT. *Proc Natl Acad Sci U S A* 105:16380-16385.



Capotosto P, Babiloni C, Romani GL, and Corbetta M (2009) Frontoparietal cortex controls spatial attention through modulation of anticipatory alpha rhythms. *J Neurosci* 29:5863-5872.

Cardoso MM, Sirotin YB, Lima B, Glushenkova E, Das A (2012) The neuroimaging signal is a linear sum of neurally distinct stimulus- and task-related components. *Nat Neurosci* 15:1298-1306.

Carlsson K, Petrovic, Skare S, Petersson KM, Ingvar M (2000) Tickling expectations: neural processing in anticipation of a sensory stimulus. *J Cogn Neurosci* 12:691-703.

Carrasco M (2011) Visual attention: the past 25 years. *Vision Res* 51:1484-1525.

Chapman CE, Meftah el M (2005) Independent controls of attentional influences in primary and secondary somatosensory cortex. *J Neurophysiol* 94:4094-4107.

Chatrian GE, Petersen MC, Lazarte JA (1959) The blocking of the rolandic wicket rhythm and some central changes related to movement. *Electroencephalogr Clin Neurophysiol* 11:497-510.

Chen R, Yaseen Z, Cohen LG, Hallett M (1998) Time course of corticospinal excitability in reaction time and self-paced movements. *Ann Neurol* 44:317-325.

Cheyne D, Gaetz W, Garnero L, Lachaux JP, Ducorps A, Schwartz D, Varela FJ (2003) Neuromagnetic imaging of cortical oscillations accompanying tactile stimulation. *Brain Res Cogn Brain Res* 17:599-611.

Cohen MR, Maunsell JH (2009) Attention improves performance primarily by reducing interneuronal correlations. *Nat Neurosci* 12:1594-

1600

Cohen MR, Maunsell JH (2011) Using neuronal populations to study the mechanisms underlying spatial and feature attention. *Neuron* 70:1192-1204.

Corbetta M, Shulman GL (2002) Control of goal-directed and stimulus-driven attention in the brain. *Nat Rev Neurosci* 3:201-215.

Coull JT, Nobre AC (1998) Where and when to pay attention: the neural systems for directing attention to spatial locations and to time intervals as revealed by both PET and fMRI. *J Neurosci* 18:7426-7435.

Coulter JD, Jones EG (1977) Differential distribution of corticospinal projections from individual cytoarchitectonic fields in the monkey. *Brain Res* 129:335-340.

Crone NE, Miglioretti DL, Gordon B, Sieracki JM, Wilson MT, Uematsu S, Lesser RP (1998) Functional mapping of human sensorimotor cortex with electrocorticographic spectral analysis. I. Alpha and beta event-related desynchronization. *Brain* 121:2271-2299.



Desimone R, Duncan J (1995) Neural mechanisms of selective visual attention. *Annu Rev Neurosci* 18:193-222.

Donchin O, Gribova A, Steinberg O, Bergman H, Vaadia E (1998) Primary motor cortex is involved in bimanual coordination. *Nature* 395:274-278.

Drevets WC, Burton H, Videen TO, Snyder AZ, Simpson JR, Raichle ME (1985) Blood flow changes in human somatosensory cortex during anticipated stimulation. *Nature* 373:249-252.



Efron D, Stein C (1981) The jackknife estimate of variance. *Ann Stat* 9:586-596.

Engel AK, Fries P, Singer W (2001) Dynamic predictions: oscillations and synchrony in top-down processing. *Nat Rev Neurosci* 2:704-716.

Engel AK, Fries P (2010) Beta-band oscillations – signalling the status quo? *Curr Opin Neurobiol* 20:156-165.

Ergenoglu T, Demiralp T, Bayraktaroglu Z, Ergen M, Beydagi H, Uresin Y (2004) Alpha rhythm of the EEG modulates visual detection performance in humans. *Brain Res Cogn Brain Res* 20:376-383.

Ermentrout GB, Kleinfeld D (2001) Traveling electrical waves in cortex: insights from phase dynamics and speculation on a computational role. *Neuron* 29:33-44.



Ferezou I, Haiss F, Gentet LJ, Aronoff R, Weber B, Petersen CC (2007) Spatiotemporal dynamics of cortical sensorimotor integration in behaving mice. *Neuron* 56:907-923.

Fisher RJ, Galea MP, Brown P, Lemon RN (2002) Digital nerve anaesthesia decreases EMG-EMG coherence in a human precision grip task. *Exp Brain Res* 145:207-214.

Foxe JJ, Simpson GV, and Ahlfors SP (1998) Parieto-occipital approximately 10 Hz activity reflects anticipatory state of visual attention mechanisms. *Neuroreport* 9:3929-3933.

Fries P, Reynolds JH, Rorie AE, Desimone R (2001) Modulation of oscillatory neuronal synchronization by selective visual attention. *Science*. 291:1560-1563.

Fries P (2005) A mechanism for cognitive dynamics: neuronal communication through neuronal coherence. *Trends Cogn Sci* 9:474-480.

Fries P, Womelsdorf T, Oostenveld R, Desimone R (2008) The effects of visual stimulation and selective visual attention on rhythmic neuronal synchronization in macaque area V4. *J Neurosci* 28:4823-4835.

Fries P (2009) Neuronal gamma-band synchronization as a fundamental process in cortical computation. *Annu Rev Neurosci* 32:209-224.



Gaetz W, Cheyne D (2006) Localization of sensorimotor cortical rhythms induced by tactile stimulation using spatially filtered MEG. *Neuroimage* 30:899-908.

Ghose GM, Maunsell JH (2002) Attentional modulation in visual cortex depends on task

timing. *Nature* 419:616-620.

Gilbertson T, Lalo E, Doyle L, Di Lazzaro V, Cioni B, Brown P (2005) Existing motor state is favored at the expense of new movement during 13-35 Hz oscillatory synchrony in the human corticospinal system. *J Neurosci* 25:7771-7779.

Gonzalez-Castillo J, Saad ZS, Handwerker DA, Inati SJ, Brenowitz N, Bandettini PA (2012) Whole-brain, time-locked activation with simple tasks revealed using massive averaging and model-free analysis. *Proc Natl Acad Sci U S A* 109:5487-5492.

Gould IC, Rushworth MF, Nobre AC (2011) Indexing the graded allocation of visuospatial attention using anticipatory alpha oscillations. *J Neurophysiol* 105:1318-1326

Gregoriou GG, Gotts SJ, Zhou H, Desimone R (2009) High-frequency, long-range coupling between prefrontal and visual cortex during attention. *Science* 324:1207-1210.

Gross J, Kujala J, Hamalainen M, Timmermann L, Schnitzler A, Salmelin R (2001) Dynamic imaging of coherent sources: Studying neural interactions in the human brain. *Proc Natl Acad Sci U S A* 98:694-699.



Haegens S, Handel BF, Jensen O (2011a) Top-down controlled alpha band activity in somatosensory areas determines behavioral performance in a discrimination task. *J Neurosci* 31:5197-5204.

Haegens S, Nacher V, Luna R, Romo R, Jensen O (2011b) alpha-Oscillations in the monkey sensorimotor network influence discrimination performance by rhythmical inhibition of neuronal spiking. *Proc Natl Acad Sci U S A* 108:19377-19382.

Haegens S, Luther L, Jensen O (2012) Somatosensory anticipatory alpha activity increases to suppress distracting input. *J Cogn Neurosci* 24:677-685.

Harris JA, Harris IM, Diamond ME (2001) The topography of tactile working memory. *J Neurosci* 21:8262-8269.

Harris KD, Thiele A (2011) Cortical state and attention. *Nat Rev Neurosci* 12:509-523

- Harrison SA, Tong F (2009) Decoding reveals the contents of visual working memory in early visual areas. *Nature* 458:632-635.
- Hämäläinen M, Hari R, Ilmoniemi RJ, Knuutila J, Lounasmaa OV (1993) Magnetoencephalography—theory, instrumentation, and applications to noninvasive studies of the working human brain. *Rev Mod Phys* 65:413-497.
- Hamame CM, Vidal JR, Ossandon T, Jerbi K, Dalal SS, Minotti L, Bertrand O, Kahane P, Lachaux JP (2012) Reading the mind's eye: online detection of visuo-spatial working memory and visual imagery in the inferior temporal lobe. *Neuroimage* 59:872-879.
- Händel BF, Haarmeier T, Jensen O (2011) Alpha oscillations correlate with the successful inhibition of unattended stimuli. *J Cogn Neurosci* 23:2494-2502.
- Hanslmayr S, Aslan A, Staudigl T, Klimesch W, Herrmann CS, Bauml KH (2007) Prestimulus oscillations predict visual perception performance between and within subjects. *Neuroimage* 37:1465-1473.
- Hari R, Karhu J, Hämäläinen M, Knuutila J, Salonen O, Sams M, Vilkmann V (1993) Functional organization of the human first and second somatosensory cortices: a neuromagnetic study. *Eur J Neurosci* 5:724-734.
- Hari R, Salmelin R (1997) Human cortical oscillations: a neuromagnetic view through the skull. *Trends Neurosci* 20:44-49.
- Hlushchuk Y, Hari R (2006) Transient suppression of ipsilateral primary somatosensory cortex during tactile finger stimulation. *J Neurosci* 26:5819-5824.
- Hoogenboom N, Schoffelen JM, Oostenveld R, Parkes LM, Fries P (2006) Localizing human visual gamma-band activity in frequency, time and space. *Neuroimage* 29:764-773.
- 
- Iwamura Y, Iriki A, Tanaka M (1994) Bilateral hand representation in the postcentral somatosensory cortex. *Nature* 369:554-556.
- 
- Jasper H, Penfield W (1949) Electroencephalograms in man: Effect of voluntary movement upon the electrical activity of the precentral gyrus. *Archiv Für Psychiatrie und Zeitschrift Neurologie* 183:163-174.
- Jenkinson N, Brown P (2011) New insights into the relationship between dopamine, beta oscillations and motor function. *Trends Neurosci* 34:611-618.
- Jensen O, Goel P, Kopell N, Pohja M, Hari R, Ermentrout B (2005) On the human sensorimotor-cortex beta rhythm: sources and modeling. *Neuroimage* 26:347-355.
- Jensen O, Kaiser J, Lachaux JP (2007) Human gamma-frequency oscillations associated with attention and memory. *Trends Neurosci* 30:317-324.
- Jensen O, Mazaheri A (2010) Shaping functional architecture by oscillatory alpha activity: gating by inhibition. *Front Hum Neurosci* 4:186.
- Jones SR, Pritchett DL, Sikora MA, Stufflebeam SM, Hamalainen M, Moore CI (2009) Quantitative analysis and biophysically realistic neural modeling of the MEG mu rhythm: rhythmogenesis and modulation of sensory-evoked responses. *J Neurophysiol* 102:3554-3572.
- Jones SR, Kerr CE, Wan Q, Pritchett DL, Hamalainen M, Moore CI (2010) Cued spatial attention drives functionally relevant modulation of the mu rhythm in primary somatosensory cortex. *J Neurosci* 30:13760-13765.
- 
- Kahana MJ, Seelig D, Madsen JR (2001) Theta returns. *Curr Opin Neurobiol* 11:739-744.
- Kastner S, Pinsk MA, De Weerd P, Desimone R, Ungerleider LG (1999) Increased activity in human visual cortex during directed attention in the absence of visual stimulation. *Neuron* 22:751-761.
- Kelly SP, Lalor EC, Reilly RB, Foxe JJ (2006) Increases in alpha oscillatory power reflect an active retinotopic mechanism for distracter suppression during sustained visuospatial attention. *J Neurophysiol* 95:3844-3851.
- Kilner JM, Fisher RJ, Lemon RN (2004)

Coupling of oscillatory activity between muscles is strikingly reduced in a deafferented subject compared with normal controls. *J Neurophysiol* 92:790-796.

Kosslyn SM, Thompson WL, Kim IJ, Alpert NM (1995) Topographical representations of mental images in primary visual cortex. *Nature* 378:496-498.



Lakatos P, Karmos G, Mehta AD, Ulbert I, Schroeder CE (2008) Entrainment of neuronal oscillations as a mechanism of attentional selection. *Science* 320:110-113.

Lalo E, Gilbertson T, Doyle L, Di Lazzaro V, Cioni B, Brown P (2007) Phasic increases in cortical beta activity are associated with alterations in sensory processing in the human. *Exp Brain Res* 177:137-145.

Lamp I, Yarom Y (1993) Subthreshold oscillations of the membrane potential: a functional synchronizing and timing device. *J Neurophysiol* 70:2181-2186.

Liang H, Bressler SL, Ding M, Truccolo WA, Nakamura R (2002) Synchronized activity in prefrontal cortex during anticipation of visuomotor processing. *Neuroreport* 13:2011-2015.

Li Hegner Y, Lutzenberger W, Leiberg S, Braun C (2007) The involvement of ipsilateral temporoparietal cortex in tactile pattern working memory as reflected in beta event-related desynchronization. *Neuroimage* 37:1362-1370.

Liljeström M, Kujala J, Jensen O, Salmelin R (2005) Neuromagnetic localization of rhythmic activity in the human brain: a comparison of three methods. *Neuroimage* 25:734-745.

Lima B, Singer W, Neuenschwander S (2011) Gamma responses correlate with temporal expectation in monkey primary visual cortex. *J Neurosci* 31:15919-15931.

Linkenkaer-Hansen K, Nikulin VV, Palva S, Ilmoniemi RJ, Palva JM (2004) Prestimulus oscillations enhance psychophysical performance in humans. *J Neurosci* 24:10186-10190.

Lipton ML, Fu KM, Branch CA, Schroeder CE (2006) Ipsilateral hand input to area 3b

revealed by converging hemodynamic and electrophysiological analyses in macaque monkeys. *J Neurosci* 26:180-185.

Lopes da Silva FH, Vos JE, Mooibroek J, Van Rotterdam A (1980) Relative contributions of intracortical and thalamo-cortical processes in the generation of alpha rhythms, revealed by partial coherence analysis. *Electroencephalogr Clin Neurophysiol* 50:449-456.

Luck SJ, Chelazzi L, Hillyard SA, Desimone R (1997) Neural mechanisms of spatial selective attention in areas V1, V2, and V4 of macaque visual cortex. *J Neurophysiol* 77:24-42.



Maki H, Ilmoniemi RJ (2010) EEG oscillations and magnetically evoked motor potentials reflect motor system excitability in overlapping neuronal populations. *Clin Neurophysiol* 121:492-501.

Mangun GR, Hillyard SA (1991) Modulations of sensory-evoked brain potentials indicate changes in perceptual processing during visual-spatial priming. *J Exp Psychol Hum Percept Perform* 17:1057-1074.

Maris E (1998) Covariance adjustment versus gain scores revisited. *Psychological Methods* 3:309-327.




Maris E, Oostenveld R (2007) Nonparametric statistical testing of EEG- and MEG-data. *J Neurosci Methods* 164:177-190.



Maris E, Womelsdorf T, Desimone R, Fries P (2013) Rhythmic neuronal synchronization in visual cortex entails spatial phase relation diversity that is modulated by stimulation and attention. *Neuroimage* 74:99-116.


Marsden JF, Ashby P, Limousin-Dowsey P, Rothwell JC, Brown P (2000) Coherence between cerebellar thalamus, cortex and muscle in man: cerebellar thalamus interactions. *Brain* 123 (Pt 7):1459-1470.

Mathewson KE, Lleras A, Beck DM, Fabiani M, Ro T, Gratton G (2011) Pulsed out of awareness: EEG alpha oscillations represent a pulsed-inhibition of ongoing cortical processing. *Front Psychol* 2:99.

Matyas F, Sreenivasan V, Marbach F, Wacongne C, Barsy B, Mateo C, Aronoff R, Petersen CC

- (2010) Motor control by sensory cortex. *Science* 330:1240-1243.
- McMains SA, Fehd HM, Emmanouil TA, Kastner S (2007) Mechanisms of feature- and space-based attention: response modulation and baseline increases. *J Neurophysiol* 98:2110-2121.
- Meftah el M, Bourgeon S, Chapman CE (2009) Instructed delay discharge in primary and secondary somatosensory cortex within the context of a selective attention task. *J Neurophysiol* 101:2649-2667.
- Mehring C, Rickert J, Vaadia E, Cardoso de Oliveira S, Aertsen A, Rotter S (2003) Inference of hand movements from local field potentials in monkey motor cortex. *Nat Neurosci* 6:1253-1254.
- Miller KJ, Schalk G, Fetz EE, den Nijs M, Ojemann JG, Rao RP (2010) Cortical activity during motor execution, motor imagery, and imagery-based online feedback. *Proc Natl Acad Sci U S A* 107:4430-4435.
- Miniussi C, Wilding EL, Coull JT, Nobre AC (1999) Orienting attention in time. Modulation of brain potentials. *Brain* 122 (Pt 8):1507-1518.
- Mitchell JF, Sundberg KA, Reynolds JH (2009) Spatial attention decorrelates intrinsic activity fluctuations in macaque area V4. *Neuron* 63:879-888.
- Mitra PP, Pesaran B (1999) Analysis of dynamic brain imaging data. *Biophys J* 76:691-708.
- Muller MM, Teder-Salejarvi W, Hillyard SA (1998) The time course of cortical facilitation during cued shifts of spatial attention. *Nat Neurosci* 1:631-634.
- Muller N, Weisz N (2012) Lateralized auditory cortical alpha band activity and interregional connectivity pattern reflect anticipation of target sounds. *Cereb Cortex* 22:1604-1613.
- 
- Nagamine T, Kajola M, Salmelin R, Shibasaki H, Hari R (1996) Movement-related slow cortical magnetic fields and changes of spontaneous MEG- and EEG-brain rhythms. *Electroencephalogr Clin Neurophysiol* 99:274-286.
- Nakano T, Homae F, Watanabe H, Taga G (2008) Anticipatory cortical activation precedes auditory events in sleeping infants. *PLoS One* 3:e3912.
- Naruse Y, Matani A, Miyawaki Y, Okada M (2010) Influence of coherence between multiple cortical columns on alpha rhythm: a computational modeling study. *Hum Brain Mapp* 31:703-715.
- Nobre AC (2001) Orienting attention to instants in time. *Neuropsychologia* 39:1317-1328.
- Nobre AC, Correa A, Coull J (2007) The hazards of time. *Curr Opin Neurobiol* 17:465-470.
- Nolte G (2003) The magnetic lead field theorem in the quasi-static approximation and its use for magnetoencephalography forward calculation in realistic volume conductors. *Phys Med Biol* 48:3637-3652.
- 
- O'Connor DH, Fukui MM, Pinsk MA, Kastner S (2002) Attention modulates responses in the human lateral geniculate nucleus. *Nat Neurosci* 5:1203-1209.
- Ohara S, Mima T, Baba K, Ikeda A, Kunieda T, Matsumoto R, Yamamoto J, Matsushashi M, Nagamine T, Hirasawa K, Hori T, Mihara T, Hashimoto N, Salenius S, Shibasaki H (2001) Increased synchronization of cortical oscillatory activities between human supplementary motor and primary sensorimotor areas during voluntary movements. *J Neurosci* 21:9377-9386.
- Oostenveld R, Fries P, Maris E, Schoffelen JM (2011) FieldTrip: Open source software for advanced analysis of MEG, EEG, and invasive electrophysiological data. *Comput Intell Neurosci* 2011:156869.
- 
- Palva S, Linkenkaer-Hansen K, Naatanen R, Palva JM (2005) Early neural correlates of conscious somatosensory perception. *J Neurosci* 25:5248-5258.
- Paradiso G, Cunic D, Saint-Cyr JA, Hoque T, Lozano AM, Lang AE, Chen R (2004) Involvement of human thalamus in the preparation of self-paced movement. *Brain* 127:2717-2731.

- Percival DB, Walden AT (1993) *Spectral Analysis for Physical Applications: Multitaper and Conventional Univariate Techniques*. Cambridge: Cambridge University Press.
- Pfurtscheller G, Neuper C (1997) Motor imagery activates primary sensorimotor area in humans. *Neurosci Lett* 239:65-68.
- Pfurtscheller G, Lopes da Silva FH (1999) Event-related EEG/MEG synchronization and desynchronization: basic principles. *Clin Neurophysiol* 110:1842-1857.
- Pogosyan A, Gaynor LD, Eusebio A, Brown P (2009) Boosting cortical activity at beta-band frequencies slows movement in humans. *Curr Biol* 19:1637-1641.
- Posner MI (1980a) Orienting of attention. *Q J Exp Psychol* 32:3-25.
- Posner MI, Snyder CR, Davidson BJ (1980b) Attention and the detection of signals. *J Exp Psychol* 109:160-174
- Prinzmetal W, McCool C, Park S (2005) Attention: reaction time and accuracy reveal different mechanisms. *J Exp Psychol Gen* 134:73-92.
- 
- Reber S (1993) *Implicit Learning and Tacit Knowledge: An Essay on the Cognitive Unconscious*. Oxford University Press, Oxford.
- Ress D, Backus BT, Heeger DJ, (2000) Activity in primary visual cortex predicts performance in a visual detection task. *Nat Neurosci* 3:940-945.
- Riddle CN, Baker SN (2005) Manipulation of peripheral neural feedback loops alters human corticomuscular coherence. *J Physiol* 566:625-639.
- Rihs TA, Michel CM, Thut G (2007) Mechanisms of selective inhibition in visual spatial attention are indexed by alpha-band EEG synchronization. *Eur J Neurosci* 25:603-610.
- Ritter P, Moosmann M, Villringer A (2009) Rolandic alpha and beta EEG rhythms' strengths are inversely related to fMRI-BOLD signal in primary somatosensory and motor cortex. *Hum Brain Mapp* 30:1168-1187.
- Rohenkohl G, Nobre AC (2011) Alpha oscillations related to anticipatory attention follow temporal expectations. *J Neurosci* 31:14076-14084.
- Romei V, Brodbeck V, Michel C, Amedi A, Pascual-Leone A, Thut G (2008) Spontaneous fluctuations in posterior alpha-band EEG activity reflect variability in excitability of human visual areas. *Cereb Cortex* 18:2010-2018.
- Romei V, Gross J, Thut G (2010) On the role of prestimulus alpha rhythms over occipito-parietal areas in visual input regulation: correlation or causation? *J Neurosci* 30:8692-8697.
- Romo R, Salinas E (2003) Flutter discrimination: neural codes, perception, memory and decision making. *Nat Rev Neurosci* 4:203-218.
- Rubin DB (1974) Estimating causal effects of treatments in randomized and nonrandomized studies *J Educ Psychol* 66:688-701.
- Rubin DB (1977) Assignment to treatment group on the basis of a covariate. *J Educ Stat* 2:1-26.
- 
- Saalmann YB, Kastner S (2011) Cognitive and perceptual functions of the visual thalamus. *Neuron* 71:209-223.
- Salazar RF, Dotson NM, Bressler SL, Gray CM (2012) Content-specific fronto-parietal synchronization during visual working memory. *Science* 338:1097-1100.
- Salenius S, Portin K, Kajola M, Salmelin R, Hari R (1997a) Cortical control of human motoneuron firing during isometric contraction. *J Neurophysiol* 77:3401-3405.
- Salenius S, Schnitzler A, Salmelin R, Jousmaki V, Hari R (1997b) Modulation of human cortical rolandic rhythms during natural sensorimotor tasks. *Neuroimage* 5:221-228.
- Salinas E, Sejnowski TJ (2001) Correlated neuronal activity and the flow of neural information. *Nat Rev Neurosci* 2:539-550.
- Salmelin R, Hari R (1994) Spatiotemporal characteristics of sensorimotor neuromagnetic rhythms related to thumb movement. *Neuroscience* 60:537-550.

- Sauseng P, Klimesch W, Stadler W, Schabus M, Doppelmayr M, Hanslmayr S, Gruber WR, Birbaumer N (2005) A shift of visual spatial attention is selectively associated with human EEG alpha activity. *Eur J Neurosci* 22:2917-2926.
- Sauseng P, Klimesch W, Gerloff C, Hummel FC (2009) Spontaneous locally restricted EEG alpha activity determines cortical excitability in the motor cortex. *Neuropsychologia* 47:284-288.
- Scheeringa R, Fries P, Petersson KM, Oostenveld R, Grothe I, Norris DG, Hagoort P, Bastiaansen MC (2011) Neuronal dynamics underlying high- and low-frequency EEG oscillations contribute independently to the human BOLD signal. *Neuron* 69:572-583.
- Schnitzler A, Salmelin R, Salenius S, Jousmaki V, Hari R (1995) Tactile information from the human hand reaches the ipsilateral primary somatosensory cortex. *Neurosci Lett* 200:25-28.
- Schoffelen JM, Oostenveld R, Fries P (2005) Neuronal coherence as a mechanism of effective corticospinal interaction. *Science* 308:111-113.
- Serences JT, Ester EF, Vogel EK, Awh E (2009) Stimulus-specific delay activity in human primary visual cortex. *Psychol Science* 20:207-214.
- Sergent C, Ruff CC, Barbot A, Driver J, Rees G (2011) Top-down modulation of human early visual cortex after stimulus offset supports successful postcued report. *J Cogn Neurosci* 23:1921-1934.
- Siegel M, Donner TH, Oostenveld R, Fries P, Engel AK (2007) High-frequency activity in human visual cortex is modulated by visual motion strength. *Cereb Cortex* 17:732-741.
- Siegel M, Donner TH, Oostenveld R, Fries P, Engel AK (2008) Neuronal synchronization along the dorsal visual pathway reflects the focus of spatial attention. *Neuron* 60:709-719.
- Sirotin YB, Das A (2009) Anticipatory haemodynamic signals in sensory cortex not predicted by local neuronal activity. *Nature* 457:475-479.
- Sneve MH, Alnaes D, Endestad T, Greenlee MW, Magnussen S (2012) Visual short-term memory: activity supporting encoding and maintenance in retinotopic visual cortex. *Neuroimage* 63:166-178.
- Snyder AC, Foxe JJ (2010) Anticipatory attentional suppression of visual features indexed by oscillatory alpha-band power increases: a high-density electrical mapping study. *J Neurosci* 30:4024-4032.
- Soteropoulos DS, Baker SN (2006) Cortico-cerebellar coherence during a precision grip task in the monkey. *J Neurophysiol* 95:1194-1206.
- Spitzer B, Blankenburg F (2011) Stimulus-dependent EEG activity reflects internal updating of tactile working memory in humans. *Proc Natl Acad Sci U S A* 108:8444-8449.
- Steinmetz PN, Roy A, Fitzgerald PJ, Hsiao SS, Johnson KO, Niebur E (2000) Attention modulates synchronized neuronal firing in primate somatosensory cortex. *Nature* 404:187-190.
- Suffczynski P, Kalitzin S, Pfurtscheller G, Lopes da Silva FH (2001) Computational model of thalamo-cortical networks: dynamical control of alpha rhythms in relation to focal attention. *Int J Psychophysiol* 43:25-40.
- Summerfield C, Egnor T (2009) Expectation (and attention) in visual cognition. *Trends Cogn Sci* 13:403-409.
- 
- Tallon-Baudry C, Bertrand O (1999) Oscillatory gamma activity in humans and its role in object representation. *Trends Cogn Sci* 3:151-162.
- Tamura Y, Hoshiyama M, Nakata H, Hiroe N, Inui K, Kaneoke Y, Inoue K, Kakigi R (2005) Functional relationship between human rolandic oscillations and motor cortical excitability: an MEG study. *Eur J Neurosci* 21:2555-2562.
- Taniguchi M, Kato A, Fujita N, Hirata M, Tanaka H, Kihara T, Ninomiya H, Hirabuki N, Nakamura H, Robinson SE, Cheyne D, Yoshimine T (2000) Movement-related desynchronization of the cerebral cortex studied with spatially filtered magnetoencephalography. *Neuroimage* 12:298-306.
- Thomson DJ. Spectrum estimation and harmonic analysis (1982) *Proc IEEE* 70:1055-1096

Thut G, Nietzel A, Brandt SA, Pascual-Leone A (2006) Alpha-band electroencephalographic activity over occipital cortex indexes visuospatial attention bias and predicts visual target detection. *J Neurosci* 26:9494-9502.

Thut G, Miniussi C, Gross J (2012) The functional importance of rhythmic activity in the brain. *Curr Biol* 22:R658-663.

Tommerdahl M, Simons SB, Chiu JS, Favorov O, Whitsel BL (2006) Ipsilateral input modifies the primary somatosensory cortex response to contralateral skin flutter. *J Neurosci* 26:5970-5977.



van der Meij R, Kahana M, Maris E (2012) Phase-amplitude coupling in human electrocorticography is spatially distributed and phase diverse. *J Neurosci* 32:111-123.

van Dijk H, Schoffelen JM, Oostenveld R, Jensen O (2008) Prestimulus oscillatory activity in the alpha band predicts visual discrimination ability. *J Neurosci* 28:1816-1823.

van Pelt S, Boomsma DI, Fries P (2012) Magnetoencephalography in twins reveals a strong genetic determination of the peak frequency of visually induced gamma-band synchronization. *J Neurosci* 32:3388-3392.

Voisin J, Bidet-Caulet A, Bertrand O, Fonlupt P (2006) Listening in silence activates auditory areas: a functional magnetic resonance imaging study. *J Neurosci* 26:273-278.

Volgushev M, Chistiakova M, Singer W (1998) Modification of discharge patterns of neocortical neurons by induced oscillations of the membrane potential. *Neuroscience* 83:15-25.



Wan Q, Kerr C, Pritchett D, Hamalainen M, Moore C, Jones S (2011) Dynamics of dynamics within a single data acquisition session: variation in neocortical alpha oscillations in human MEG. *PLoS One* 6:e24941.

Watson AB, Pelli DG (1983) QUEST: a Bayesian adaptive psychometric method. *Percept Psychophys* 33:113-120.

Wiest MC, Bentley N, Nicolelis MA (2005)

Heterogeneous integration of bilateral whisker signals by neurons in primary somatosensory cortex of awake rats. *J Neurophysiol* 93:2966-2973.

Williams EJ (1959) The comparison of regression variables. *J Royal Stat Soc* 21:396-399

Witham CL, Baker SN (2007a) Network oscillations and intrinsic spiking rhythmicity do not covary in monkey sensorimotor areas. *J Physiol* 580:801-814.

Witham CL, Wang M, Baker SN (2007b) Cells in somatosensory areas show synchrony with beta oscillations in monkey motor cortex. *Eur J Neurosci* 26:2677-2686.

Womelsdorf T, Fries P, Mitra PP, Desimone R (2006) Gamma-band synchronization in visual cortex predicts speed of change detection. *Nature* 439:733-736.

Worden MS, Foxe JJ, Wang N, Simpson GV (2000) Anticipatory biasing of visuospatial attention indexed by retinotopically specific α -band electroencephalography increases over occipital cortex. *J Neurosci* 20:RC63:1-6.

Wyart V, Tallon-Baudry C (2008) Neural dissociation between visual awareness and spatial attention. *J Neurosci* 28:2667-2679.



Yamagishi N, Callan DE, Anderson SJ, Kawato M (2008) Attentional changes in pre-stimulus oscillatory activity within early visual cortex are predictive of human visual performance. *Brain Res* 1197:115-122.



Zhang Y, Chen Y, Bressler SL, Ding M (2008a) Response preparation and inhibition: the role of the cortical sensorimotor beta rhythm. *Neuroscience* 156:238-246.

Zhang Y, Wang X, Bressler SL, Chen Y, Ding M (2008b) Prestimulus cortical activity is correlated with speed of visuomotor processing. *J Cogn Neurosci* 20:1915-1925.

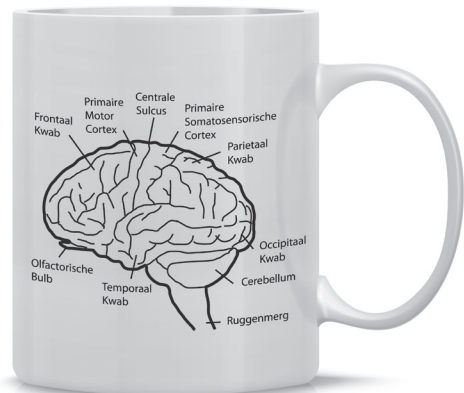
Zohary E, Shadlen MN, Newsome WT (1994) Correlated neuronal discharge rate and its implications for psychophysical performance. *Nature* 370:140-143.

Nederlandse samenvatting (Dutch summary)

Onze zintuigen worden voortdurend geconfronteerd met meer informatie dan kan worden waargenomen. Dit stelt het zenuwstelsel voor de uitdaging om slechts die aspecten van de omgeving te verwerken die relevant zijn voor huidige doelen en andere aspecten te negeren. Bijvoorbeeld, wanneer je doel is om de mok in Figuur 1 op te pakken om hier koffie uit te drinken, dien je de locatie van de mok, de grootte van het oor van de mok, hoe vol de mok is, etc. te verwerken. Andere aspecten, zoals de opdruk op de mok, kun je daarbij negeren. In vergelijking, als je doel is om te leren over de anatomie van het brein, dan dien je selectief de opdruk van de mok te verwerken en kun je andere zaken zoals de grootte van het oor van de mok negeren. Dit proces van het selectief verwerken van informatie die relevant is voor je huidige doelen wordt in de wetenschap beschreven als *selectieve aandacht*.

In veel situaties is het voor de waarneming niet alleen van belang om de relevante zintuiglijke informatie te selecteren uit informatie die op dat moment aanwezig is, maar ook om voorbereid te zijn op deze informatie, alvorens deze zich manifesteert. Dit is met name van belang wanneer deze informatie slechts kort wordt aangeboden of wanneer deze onmiddellijk relevant is. Bijvoorbeeld, bij het oppakken van de mok is van belang dat de zintuiglijke informatie van je vingertoppen vanaf het eerste contact met deze mok direct met grote nauwkeurigheid uitgelezen wordt. Op basis van deze informatie kan namelijk de grijpbeweging worden aangepast en hiermee kan vermeden worden dat de koffie over de tafel wordt gespild. De voorbereiding kan er in zo'n geval voor zorgen dat de verwerking van zintuiglijke informatie in het relevante deel van je omgeving (je rechter hand) een onmiddellijk voordeel heeft t.o.v. het irrelevant deel (je linker hand). Het is dit type *voorbereidende selectieve aandacht* dat centraal staat in mijn proefschrift.

In het laboratorium wordt selectieve aandacht doorgaans bestudeerd door gebruik te maken van symbolische cues die aangeven waar een toekomstige zintuiglijke stimulatie (ook wel *stimulus* genoemd) waarschijnlijk gepresenteerd zal worden. Invloedrijk werk van Michael Posner heeft aangetoond dat zulke cues leiden tot snellere reacties op stimuli die gepresenteerd worden op verwachte locaties t.o.v. onverwachte locatie. Ook hebben studies laten zien dat stimuli het beste worden waargenomen als deze worden gepresenteerd op verwachte momenten. Zulke studies tonen aan dat ons zenuwstelsel verwachtingen gebruikt om zintuiglijke informatie optimaal te verwerken. Dit leidt tot de fundamentele vraag hoe het zenuwstelsel dit voor elkaar



Figuur 1. Mok waarnaar gerefereerd wordt in de tekst.

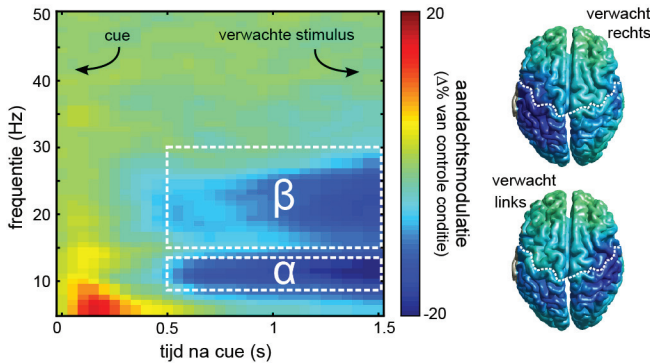
krijgt. Met andere woorden: wat zijn de neurofysiologische mechanismen waar middels voorbereidende selectieve aandacht de waarneming verbetert?

In dit proefschrift heb ik acht studies beschreven naar verschillende aspecten van deze centrale vraagstelling. Deze studies hebben zich geconcentreerd op de rol van hersengolven (ook wel *neurale oscillaties* genoemd) zoals bestudeerd in de zintuiglijke modaliteit van de tastzin (ook wel *somatosensoriek* genoemd).

Conceptueel is dit proefschrift opgedeeld in drie delen. In **deel 1 (hoofdstukken 2 en 3)** heb ik het primaire fenomeen van dit proefschrift beschreven. Dit fenomeen houdt in dat de voorbereiding op een stimulus op één van beide handen gepaard gaat met een suppressie van alfa- en bèta-oscillaties zoals gemeten boven de contralaterale primaire somatosensorische cortex (zie Figuur 2). De contralaterale somatosensorische cortex betreft dat deel van het brein waar deze zintuiglijke informatie verwerkt zal worden. **Hoofdstuk 2** laat voor het eerst zien dat een dergelijk fenomeen ook optreedt in de somatosensorische modaliteit en **hoofdstuk 3** laat voor het eerst zien dat dit fenomeen niet alleen specifiek is met betrekking tot de locatie van de verwachte stimulus, maar ook voor het verwachte moment waarop deze stimulus zal worden aangeboden.

Deel 2 (hoofdstukken 4, 5 en 6) bouwt voort op deze centrale observatie door dit fenomeen te relateren aan de aandachtgerelateerde verbetering van de waarneming (**hoofdstukken 4 en 5**) alsmede de neurale processen tijdens de stimulus verwerking (**hoofdstuk 6**). In **hoofdstuk 4** constateer ik dat het centrale fenomeen van dit proefschrift het tijdsverloop volgt van de verbetering in de accuraatheid (maar niet reactietijd) van de waarneming en in **hoofdstuk 5** blijkt dat dit fenomeen ongeveer 30% van deze verbetering kan verklaren. **Hoofdstuk 6** beschrijft dat dit fenomeen ook gepaard gaat met een grotere ipsilaterale response op de verwachte stimulus, hetgeen mogelijk wijst op een grotere verdeling van de stimulusverwerking tussen de linker en rechter hersenhelften.

In **deel 3 (hoofdstukken 7, 8 en 9)** plaats ik het centrale fenomeen in een breder perspectief door dit te vergelijken met de aandachtsmodulatie van neurale oscillaties tijdens de stimulus verwerking (**hoofdstuk 7**), dit te bestuderen in de context van een wijdverspreid somatomotorisch netwerk (**hoofdstuk 8**) en door de mogelijke mechanismen te beschouwen die ten grondslag kunnen liggen aan het centrale fenomeen (betreffende een amplitude modulatie zoals geobserveerd in een meting van buiten de schedel; **hoofdstuk 9**). Hierbij constateer ik eerst dat de aandachtsgerelateerde suppressie van alfa- en bèta-oscillaties in voorbereiding op een stimulus vervangen wordt door een amplificatie van gamma-oscillaties (60-80 Hz) tijdens de stimulusverwerking (**hoofdstuk 7**). Daarnaast constateer ik dat de modulatie van bèta-oscillaties niet alleen plaatsvindt in de somatosensorische cortex, maar in een uitgebreid netwerk dat zelfs het ruggenmerg omvat (**hoofdstuk 8**). Tenslotte constateer ik dat amplitude modulaties plaatsvinden in meerdere bronnen, terwijl deze hun onderlinge faserelaties behouden (**hoofdstuk 9**).



Figuur 2. Voorbereiding op een verwachte somatosensorische stimulus gaat gepaard met een suppressie van alfa- en bèta-oscillaties in dat deel van het brein waar de verwachte stimulus zal worden verwerkt: de contralaterale somatosensorische cortex.

Samenvattend, in dit proefschrift heb ik de neurofysiologische mechanismen onderzocht waar middels voorbereidende aandacht de waarneming verbetert. Ik heb dit onderzocht voor de tastzin. De centrale observatie is dat voorbereiding op een verwachte stimulatie op de hand gepaard gaat met een suppressie van alfa- en bèta-oscillaties in dat deel van het brein waar de verwachte zintuiglijke informatie verwerkt zal worden. Dit proefschrift zet dit fenomeen op de kaart als een robuust fenomeen dat (1) generaliseerbaar is voor de verschillende zintuiglijke modaliteiten, (2) specifiek is voor zowel de verwachte locatie als het verwachte moment en (3) relevant is voor de waarneming. Dit proefschrift leidt derhalve tot een beter begrip van hoe voorbereidende selectieve aandacht de waarneming verbetert. Tegelijkertijd tonen meerdere studies in dit proefschrift aan dat aandacht ook onafhankelijk van dit fenomeen de waarneming kan verbeteren. Dit impliceert dat er ook andere neurale processen in acht genomen dienen te worden om een volledig beeld te vormen van hoe voorbereiding de waarneming verbetert. In vervolg onderzoek zal het van belang zijn om deze andere neurale processen ook in kaart te brengen. Ook is het van belang om meer inzicht te verwerven in de precieze mechanismen waar middels de anticipatoire suppressie van alfa- en bèta-oscillaties de waarneming verbetert.

Publications

Somatosensory demands modulate muscular beta oscillations independent of motor demands

van Ede F & Maris E

The Journal of Neuroscience, 33(26), 2013, 10849-10857

Anticipation increases tactile stimulus processing in the ipsilateral primary somatosensory cortex

van Ede F, de Lange FP & Maris E

Cerebral Cortex, published ahead of print May 3 2013

Attentional cues affect accuracy and reaction time via different cognitive and neural processes

van Ede F, de Lange FP & Maris E

The Journal of Neuroscience, 32(30), 2012, 10408-10412

Beyond establishing involvement: quantifying the contribution of anticipatory alpha- and beta-band suppression to perceptual improvement with attention

van Ede F, Köster M & Maris E

Journal of Neurophysiology, 108(9), 2012, 2352-2362

Orienting attention to an upcoming tactile event involves a spatially and temporally specific modulation of sensorimotor alpha- and beta-band oscillations

van Ede F, de Lange, FP, Jensen O & Maris E

The Journal of Neuroscience, 31(6), 2011, 2016-2024

Joint action modulates motor system involvement during action observation in 3-year-olds

Meyer M, Hunnius S, van Elk M, **van Ede F** & Bekkering H

Experimental Brain Research, 211(3-4), 2011, 581-592

Prior expectation mediates neural adaptation to repeated sounds in the auditory cortex: an MEG study

Todorovic A, **van Ede F**, Maris E & de Lange FP

The Journal of Neuroscience, 31(25), 2011, 9118-9123

Tactile expectation modulates pre-stimulus β -band oscillations in human sensorimotor cortex

van Ede F, Jensen O & Maris E

NeuroImage, 51(2), 2010, 867-876

Curriculum Vitae

Freek van Ede was born in Den Helder on 18 January 1985. After living in Curaçao and in the United States of America for several years, he returned to the Netherlands where he obtained his high school diploma from the Christelijk Lyceum Veenendaal (Athenaeum, specialisation Nature and Health) in 2003. Freek went on to study Psychology at the University of Utrecht (specialisations Neuropsychology and Cognitive Neuroscience), from which he obtained his Bachelor's degree in 2007. He then moved to Nijmegen to enroll in the Cognitive Neuroscience Research Master at the Radboud University (specialisation Perception, Action and Consciousness), from which he graduated in 2009 with the *judicium cum laude*. During this period, Freek also obtained a TOPtalent PhD scholarship that allowed him to stay at the Radboud University to pursue a doctorate at the Donders Institute for Brain, Cognition and Behaviour (under supervision of Eric Maris and in collaboration with Floris de Lange and Ole Jensen). In August 2013, Freek completed his doctoral studies. In addition to his research, Freek has been involved in teaching and supervising students (Bachelor and Master levels) as well as in the organisation and chairing of scientific meetings at the Donders Institute, such as the Donders Discussions (2010) and the Systems Neuroscience Journal Club (2010 to 2014).

Acknowledgements

Research

Foremost, I am grateful to Eric Maris. I could not have wished for a better doctoral supervisor. Thank you for always being open minded and attentive to my personal research plans, for sharpening my thoughts at the right moments, for always having your door open, for exchanging thoughts with me on a wide range of issues, for involving me in student supervision, for always being clear and fair about each other's roles, for expressing your belief in me, and more. Thank you.

I also thank Floris de Lange and Ole Jensen. Thank you for providing additional support, for including me into your research groups as a full member and for inviting me to retreats and social events. Thank you for allowing me to widen my horizon.

I also thank my promotor Markus Ullsperger for always making time for me, and Malte Köster, Szabolcs Szabényi and Stan van Pelt for their contributions to the research described in, respectively, chapters 5, 8 and 9.

I also thank all people that have participated in the research presented in this doctoral thesis. In particular, I thank Marlene Meyer, Matthias Ekman, Alina Lartseva, Ashley Lewis and Rocio Silva Zunino for participating in several of the reported experiments (as well as pilots and follow-up studies).

Technical

I thank Norbert Hermesdorf and Pascal de Water for constructing the Braille stimulator that I have used extensively, Sander Berends and Paul Gaalman for their support in the MEG and MRI laboratories, the technical group (headed by Erik van den Boogert) for maintaining good computing facilities, and the FieldTrip developers (headed by Robert Oostenveld) for providing an excellent open source toolbox for EEG and MEG data analysis.

Procedural

I thank all involved secretaries for their support during my doctorate. I also thank Pascal Fries, Pieter Roelfsema, Peter Brown and all members of the corona for their role in the manuscript evaluation, Marlene Meyer and Matthias Ekman for being my paranimfs, and Niels van der Wegen for his help with the design of this book.

Social

I thank my parents Ton and Geke, my brothers Joost and Egbert, my partner Rocio and my friends for their interest in my work and their positive encouragements. I also thank all colleagues at the Donders Institute with whom I have engaged in interesting discussions on both research- and non-research related topics.

Thank you all.
Without you this work would not have been possible.

Donders Graduate School for Cognitive Neuroscience Series

1. van Aalderen-Smeets, S.I. (2007). *Neural dynamics of visual selection*. Maastricht University, Maastricht, the Netherlands.
2. Schoffelen, J.M. (2007). *Neuronal communication through coherence in the human motor system*. Radboud University Nijmegen, Nijmegen, the Netherlands.
3. de Lange, F.P. (2008). *Neural mechanisms of motor imagery*. Radboud University Nijmegen, Nijmegen, the Netherlands.
4. Grol, M.J. (2008). *Parieto-frontal circuitry in visuomotor control*. Utrecht University, Utrecht, the Netherlands.
5. Bauer, M. (2008). *Functional roles of rhythmic neuronal activity in the human visual and somatosensory system*. Radboud University Nijmegen, Nijmegen, the Netherlands.
6. Mazaheri, A. (2008). *The influence of ongoing oscillatory brain activity on evoked responses and behaviour*. Radboud University Nijmegen, Nijmegen, the Netherlands.
7. Hooijmans, C.R. (2008). *Impact of nutritional lipids and vascular factors in Alzheimer's disease*. Radboud University Nijmegen, Nijmegen, the Netherlands.
8. Gaszner, B. (2008). *Plastic responses to stress by the rodent urocortinergic Edinger-Westphal nucleus*. Radboud University Nijmegen, Nijmegen, the Netherlands.
9. Willems, R.M. (2009). *Neural reflections of meaning in gesture, language and action*. Radboud University Nijmegen, Nijmegen, the Netherlands.
10. van Pelt, S. (2009). *Dynamic neural representations of human visuomotor space*. Radboud University Nijmegen, Nijmegen, the Netherlands.
11. Lommertzen, J. (2009). *Visuomotor coupling at different levels of complexity*. Radboud University Nijmegen, Nijmegen, the Netherlands.
12. Poljac, E. (2009). *Dynamics of cognitive control in task switching: Looking beyond the switch cost*. Radboud University Nijmegen, Nijmegen, the Netherlands.
13. Poser, B.A. (2009). *Techniques for BOLD and blood volume weighted fMRI*. Radboud University Nijmegen, Nijmegen, the Netherlands.
14. Baggio, G. (2009). *Semantics and the electrophysiology of meaning. Tense, aspect, event structure*. Radboud University Nijmegen, Nijmegen, the Netherlands.
15. van Wingen, G.A. (2009). *Biological determinants of amygdala functioning*. Radboud University Nijmegen Medical Centre, Nijmegen, the Netherlands.
16. Bakker, M. (2009). *Supraspinal control of walking: Lessons from motor imagery*. Radboud University Nijmegen Medical Centre, Nijmegen, the Netherlands.
17. Aarts, E. (2009). *Resisting temptation: The role of the anterior cingulate cortex in adjusting cognitive control*. Radboud University Nijmegen, Nijmegen, the Netherlands.
18. Prinz, S. (2009). *Waterbath stunning of chickens – Effects of electrical parameters on the electroencephalogram and physical reflexes of broilers*. Radboud University Nijmegen, Nijmegen, the Netherlands.
19. Knippenberg, J.M.J. (2009). *The N150 of the Auditory Evoked Potential from the rat amygdala: In search for its functional significance*. Radboud University Nijmegen, Nijmegen, the Netherlands.
20. Dumont, G.J.H. (2009). *Cognitive and physiological effects of 3,4-methylenedioxymethamphetamine (MDMA or 'ecstasy') in combination with alcohol or cannabis in humans*. Radboud University Nijmegen, Nijmegen, the Netherlands.
21. Pijnacker, J. (2010). *Defeasible inference in autism: A behavioral and electrophysiological approach*. Radboud University Nijmegen, Nijmegen, the Netherlands.

22. de Vrijer, M. (2010). *Multisensory integration in spatial orientation*. Radboud University Nijmegen, Nijmegen, the Netherlands.
23. Vergeer, M. (2010). *Perceptual visibility and appearance: Effects of color and form*. Radboud University Nijmegen, Nijmegen, the Netherlands.
24. Levy, J. (2010). *In cerebro unveiling unconscious mechanisms during reading*. Radboud University Nijmegen, Nijmegen, the Netherlands.
25. Treder, M. S. (2010). *Symmetry in (inter) action*. Radboud University Nijmegen, Nijmegen, the Netherlands.
26. Horlings C.G.C. (2010). *A weak balance: Balance and falls in patients with neuromuscular disorders*. Radboud University Nijmegen, Nijmegen, the Netherlands.
27. Snaphaan, L.J.A.E. (2010). *Epidemiology of post-stroke behavioural consequences*. Radboud University Nijmegen Medical Centre, Nijmegen, the Netherlands.
28. Dado – van Beek, H.E.A. (2010). *The regulation of cerebral perfusion in patients with Alzheimer's disease*. Radboud University Nijmegen Medical Centre, Nijmegen, the Netherlands.
29. Derks, N.M. (2010). *The role of the non-preganglionic Edinger-Westphal nucleus in sex-dependent stress adaptation in rodents*. Radboud University Nijmegen, Nijmegen, the Netherlands.
30. Wyczesany, M. (2010). *Covariation of mood and brain activity. Integration of subjective self-report data with quantitative EEG measures*. Radboud University Nijmegen, Nijmegen, the Netherlands.
31. Beurze S.M. (2010). *Cortical mechanisms for reach planning*. Radboud University Nijmegen, Nijmegen, the Netherlands.
32. van Dijk, J.P. (2010). *On the Number of Motor Units*. Radboud University Nijmegen, Nijmegen, the Netherlands.
33. Lapatki, B.G. (2010). *The Facial Musculature - Characterization at a Motor Unit Level*. Radboud University Nijmegen, Nijmegen, the Netherlands.
34. Kok, P. (2010). *Word order and verb inflection in agrammatic sentence production*. Radboud University Nijmegen, Nijmegen, the Netherlands.
35. van Elk, M. (2010). *Action semantics: Functional and neural dynamics*. Radboud University Nijmegen, Nijmegen, the Netherlands.
36. Majdandzic, J. (2010). *Cerebral mechanisms of processing action goals in self and others*. Radboud University Nijmegen, Nijmegen, the Netherlands.
37. Snijders, T.M. (2010). *More than words - Neural and genetic dynamics of syntactic unification*. Radboud University Nijmegen, Nijmegen, the Netherlands.
38. Grootens, K.P. (2010). *Cognitive dysfunction and effects of antipsychotics in schizophrenia and borderline personality disorder*. Radboud University Nijmegen Medical Centre, Nijmegen, the Netherlands.
39. Nieuwenhuis, I.L.C. (2010). *Memory consolidation: A process of integration – Converging evidence from MEG, fMRI and behavior*. Radboud University Nijmegen Medical Centre, Nijmegen, the Netherlands.
40. Menenti, L.M.E. (2010). *The right language: Differential hemispheric contributions to language production and comprehension in context*. Radboud University Nijmegen, Nijmegen, the Netherlands.
41. van Dijk, H.P. (2010). *The state of the brain, how alpha oscillations shape behaviour and event related responses*. Radboud University Nijmegen, Nijmegen, the Netherlands.
42. Meulenbroek, O.V. (2010). *Neural correlates of episodic memory in healthy aging and Alzheimer's disease*. Radboud University Nijmegen, Nijmegen, the Netherlands.
43. Oude Nijhuis, L.B. (2010). *Modulation of human balance reactions*. Radboud University Nijmegen, Nijmegen, the Netherlands.

- Netherlands.
44. Qin, S. (2010). *Adaptive memory: Imaging medial temporal and prefrontal memory systems*. Radboud University Nijmegen, Nijmegen, the Netherlands.
 45. Timmer, N.M. (2011). *The interaction of heparan sulfate proteoglycans with the amyloid protein*. Radboud University Nijmegen, Nijmegen, the Netherlands.
 46. Crajé, C. (2011). *(A)typical motor planning and motor imagery*. Radboud University Nijmegen, Nijmegen, the Netherlands.
 47. van Grootel, T.J. (2011). *On the role of eye and head position in spatial localisation behaviour*. Radboud University Nijmegen, Nijmegen, the Netherlands.
 48. Lamers, M.J.M. (2011). *Levels of selective attention in action planning*. Radboud University Nijmegen, Nijmegen, the Netherlands.
 49. van der Werf, J. (2011). *Cortical oscillatory activity in human visuomotor integration*. Radboud University Nijmegen, Nijmegen, the Netherlands.
 50. Scheeringa, R. (2011). *On the relation between oscillatory EEG activity and the BOLD signal*. Radboud University Nijmegen, Nijmegen, the Netherlands.
 51. Bögels, S. (2011). *The role of prosody in language comprehension: When prosodic breaks and pitch accents come into play*. Radboud University Nijmegen, Nijmegen, the Netherlands.
 52. Ossewaarde, L. (2011). *The mood cycle: Hormonal influences on the female brain*. Radboud University Nijmegen, Nijmegen, the Netherlands.
 53. Kuribara, M. (2011). *Environment-induced activation and growth of pituitary melanotrope cells of *Xenopus laevis**. Radboud University Nijmegen, Nijmegen, the Netherlands.
 54. Helmich, R.C.G. (2011). *Cerebral reorganization in Parkinson's disease*. Radboud University Nijmegen, Nijmegen, the Netherlands.
 55. Boelen, D. (2011). *Order out of chaos? Assessment and treatment of executive disorders in brain-injured patients*. Radboud University Nijmegen, Nijmegen, the Netherlands.
 56. Koopmans, P.J. (2011). *fMRI of cortical layers*. Radboud University Nijmegen, Nijmegen, the Netherlands.
 57. van der Linden, M.H. (2011). *Experience-based cortical plasticity in object category representation*. Radboud University Nijmegen, Nijmegen, the Netherlands.
 58. Kleine, B.U. (2011). *Motor unit discharges - Physiological and diagnostic studies in ALS*. Radboud University Nijmegen Medical Centre, Nijmegen, the Netherlands.
 59. Paulus, M. (2011). *Development of action perception: Neurocognitive mechanisms underlying children's processing of others' actions*. Radboud University Nijmegen, Nijmegen, the Netherlands.
 60. Tieleman, A.A. (2011). *Myotonic dystrophy type 2. A newly diagnosed disease in the Netherlands*. Radboud University Nijmegen Medical Centre, Nijmegen, the Netherlands.
 61. van Leeuwen, T.M. (2011). *'How one can see what is not there': Neural mechanisms of grapheme-colour synaesthesia*. Radboud University Nijmegen, Nijmegen, the Netherlands.
 62. van Tilborg, I.A.D.A. (2011). *Procedural learning in cognitively impaired patients and its application in clinical practice*. Radboud University Nijmegen, Nijmegen, the Netherlands.
 63. Bruinsma, I.B. (2011). *Amyloidogenic proteins in Alzheimer's disease and Parkinson's disease: Interaction with chaperones and inflammation*. Radboud University Nijmegen, Nijmegen, the Netherlands.
 64. Voermans, N. (2011). *Neuromuscular features of Ehlers-Danlos syndrome and Marfan syndrome; expanding the phenotype of inherited connective tissue disorders and investigating the role of the extracellular matrix in muscle*. Radboud University Nijmegen Medical Centre, Nijmegen, the Netherlands.

- Netherlands.
65. Reelick, M. (2011). *One step at a time. Disentangling the complexity of preventing falls in frail older persons*. Radboud University Nijmegen Medical Centre, Nijmegen, the Netherlands.
 66. Buur, P.F. (2011). *Imaging in motion. Applications of multi-echo fMRI*. Radboud University Nijmegen, Nijmegen, the Netherlands.
 67. Schaefer, R.S. (2011). *Measuring the mind's ear: EEG of music imagery*. Radboud University Nijmegen, Nijmegen, the Netherlands.
 68. Xu, L. (2011). *The non-preganglionic Edinger-Westphal nucleus: An integration center for energy balance and stress adaptation*. Radboud University Nijmegen, Nijmegen, the Netherlands.
 69. Schellekens, A.F.A. (2011). *Gene-environment interaction and intermediate phenotypes in alcohol dependence*. Radboud University Nijmegen, Nijmegen, the Netherlands.
 70. van Marle, H.J.F. (2011). *The amygdala on alert: A neuroimaging investigation into amygdala function during acute stress and its aftermath*. Radboud University Nijmegen, Nijmegen, the Netherlands.
 71. de Laat, K.F. (2011). *Motor performance in individuals with cerebral small vessel disease: An MRI study*. Radboud University Nijmegen Medical Centre, Nijmegen, the Netherlands.
 72. Mädebach, A. (2011). *Lexical access in speaking: Studies on lexical selection and cascading activation*. Radboud University Nijmegen, Nijmegen, the Netherlands.
 73. Poelmans, G.J.V. (2011). *Genes and protein networks for neurodevelopmental disorders*. Radboud University Nijmegen, Nijmegen, the Netherlands.
 74. van Norden, A.G.W. (2011). *Cognitive function in elderly individuals with cerebral small vessel disease. An MRI study*. Radboud University Nijmegen Medical Centre, Nijmegen, the Netherlands.
 75. Jansen, E.J.R. (2011). *New insights into V-ATPase functioning: the role of its accessory subunit Ac45 and a novel brain-specific Ac45 paralog*. Radboud University Nijmegen, Nijmegen, the Netherlands.
 76. Haaxma, C.A. (2011). *New perspectives on preclinical and early stage Parkinson's disease*. Radboud University Nijmegen Medical Centre, Nijmegen, the Netherlands.
 77. Haegens, S. (2012). *On the functional role of oscillatory neuronal activity in the somatosensory system*. Radboud University Nijmegen, Nijmegen, the Netherlands.
 78. van Barneveld, D.C.P.B.M. (2012). *Integration of exteroceptive and interoceptive cues in spatial localization*. Radboud University Nijmegen, Nijmegen, the Netherlands.
 79. Spies, P.E. (2012). *The reflection of Alzheimer disease in CSF*. Radboud University Nijmegen Medical Centre, Nijmegen, the Netherlands.
 80. Helle, M. (2012). *Artery-specific perfusion measurements in the cerebral vasculature by magnetic resonance imaging*. Radboud University Nijmegen, Nijmegen, the Netherlands.
 81. Egetemeir, J. (2012). *Neural correlates of real-life joint action*. Radboud University Nijmegen, Nijmegen, the Netherlands.
 82. Janssen, L. (2012). *Planning and execution of (bi)manual grasping*. Radboud University Nijmegen, Nijmegen, the Netherlands.
 83. Vermeer, S. (2012). *Clinical and genetic characterisation of autosomal recessive cerebellar ataxias*. Radboud University Nijmegen Medical Centre, Nijmegen, the Netherlands.
 84. Vrins, S. (2012). *Shaping object boundaries: Contextual effects in infants and adults*. Radboud University Nijmegen, Nijmegen, the Netherlands.
 85. Weber, K.M. (2012). *The language learning brain: Evidence from second language and bilingual studies of syntactic processing*. Radboud University Nijmegen, Nijmegen, the Netherlands.

86. Verhagen, L. (2012). *How to grasp a ripe tomato*. Utrecht University, Utrecht, the Netherlands.
87. Nonkes, L.J.P. (2012). *Serotonin transporter gene variance causes individual differences in rat behaviour: For better and for worse*. Radboud University Nijmegen Medical Centre, Nijmegen, the Netherlands.
88. Joosten-Weyn Banningh, L.W.A. (2012). *Learning to live with Mild Cognitive Impairment: development and evaluation of a psychological intervention for patients with Mild Cognitive Impairment and their significant others*. Radboud University Nijmegen Medical Centre, Nijmegen, the Netherlands.
89. Xiang, HD. (2012). *The language networks of the brain*. Radboud University Nijmegen, Nijmegen, the Netherlands.
90. Snijders, A.H. (2012). *Tackling freezing of gait in Parkinson's disease*. Radboud University Nijmegen Medical Centre, Nijmegen, the Netherlands.
91. Rouwette, T.P.H. (2012). *Neuropathic pain and the brain - Differential involvement of corticotropin-releasing factor and urocortin 1 in acute and chronic pain processing*. Radboud University Nijmegen Medical Centre, Nijmegen, the Netherlands.
92. van de Meerendonk, N. (2012). *States of indecision in the brain: Electrophysiological and hemodynamic reflections of monitoring in visual language perception*. Radboud University Nijmegen, Nijmegen, the Netherlands.
93. Sterrenburg, A. (2012). *The stress response of forebrain and midbrain regions: Neuropeptides, sex-specificity and epigenetics*. Radboud University Nijmegen, Nijmegen, The Netherlands.
94. Uithol, S. (2012). *Representing action and intention*. Radboud University Nijmegen, Nijmegen, The Netherlands.
95. van Dam, W.O. (2012). *On the specificity and flexibility of embodied lexical-semantic representations*. Radboud University Nijmegen, Nijmegen, The Netherlands.
96. Slats, D. (2012). *CSF biomarkers of Alzheimer's disease: Serial sampling analysis and the study of circadian rhythmicity*. Radboud University Nijmegen Medical Centre, Nijmegen, the Netherlands.
97. van Nuenen, B.F.L. (2012). *Cerebral reorganization in premotor parkinsonism*. Radboud University Nijmegen Medical Centre, Nijmegen, the Netherlands.
98. van Schouwenburg, M.R. (2012). *Fronto-striatal mechanisms of attentional control*. Radboud University Nijmegen, Nijmegen, The Netherlands.
99. Azar, M.G. (2012). *On the theory of reinforcement learning: Methods, convergence analysis and sample complexity*. Radboud University Nijmegen, Nijmegen, The Netherlands.
100. Meeuwissen, E.B. (2012). *Cortical oscillatory activity during memory formation*. Radboud University Nijmegen, Nijmegen, The Netherlands.
101. Arnold, J.F. (2012). *When mood meets memory: Neural and behavioral perspectives on emotional memory in health and depression*. Radboud University Nijmegen, Nijmegen, The Netherlands.
102. Gons, R.A.R. (2012). *Vascular risk factors in cerebral small vessel disease: A diffusion tensor imaging study*. Radboud University Nijmegen Medical Centre, Nijmegen, the Netherlands.
103. Wingbermühle, E. (2012). *Cognition and emotion in adults with Noonan syndrome: A neuropsychological perspective*. Radboud University Nijmegen, Nijmegen, The Netherlands.
104. Walentowska, W. (2012). *Facing emotional faces. The nature of automaticity of facial emotion processing studied with ERPs*. Radboud University Nijmegen, Nijmegen, The Netherlands.
105. Hoogman, M. (2012). *Imaging the effects of ADHD risk genes*. Radboud University Nijmegen, Nijmegen, The Netherlands.
106. Trammer, J. J. (2012). *Feedforward and feedback mechanisms in sensory motor*

- control. Radboud University Nijmegen, Nijmegen, The Netherlands.
107. van Eijndhoven, P. (2012). *State and trait characteristics of early course major depressive disorder*. Radboud University Nijmegen Medical Centre, Nijmegen, the Netherlands.
 108. Visser, E. (2012). *Leaves and forests: Low level sound processing and methods for the large-scale analysis of white matter structure in autism*. Radboud University Nijmegen, Nijmegen, The Netherlands.
 109. van Tooren-Hoogenboom, N. (2012). *Neuronal communication in the synchronized brain. Investigating the functional role of visually-induced gamma band activity: Lessons from MEG*. Radboud University Nijmegen, Nijmegen, The Netherlands.
 110. Henckens, M.J.A.G. (2012). *Imaging the stressed brain. Elucidating the time- and region-specific effects of stress hormones on brain function: A translational approach*. Radboud University Nijmegen, Nijmegen, The Netherlands.
 111. van Kesteren, M.T.R. (2012). *Schemas in the brain: Influences of prior knowledge on learning, memory, and education*. Radboud University Nijmegen, Nijmegen, The Netherlands.
 112. Brenders, P. (2012). *Cross-language interactions in beginning second language learners*. Radboud University Nijmegen, Nijmegen, The Netherlands.
 113. Ter Horst, A.C. (2012). *Modulating motor imagery. Contextual, spatial and kinaesthetic influences*. Radboud University Nijmegen, Nijmegen, The Netherlands.
 114. Tesink, C.M.J.Y. (2013). *Neurobiological insights into language comprehension in autism: Context matters*. Radboud University Nijmegen, Nijmegen, The Netherlands.
 115. Böckler, A. (2013). *Looking at the world together. How others' attentional relations to jointly attended scenes shape cognitive processing*. Radboud University Nijmegen, Nijmegen, The Netherlands.
 116. van Dongen, E.V. (2013). *Sleeping to Remember. On the neural and behavioral mechanisms of sleep-dependent memory consolidation*. Radboud University Nijmegen, Nijmegen, The Netherlands.
 117. Volman, I. (2013). *The neural and endocrine regulation of emotional actions*. Radboud University Nijmegen, Nijmegen, The Netherlands.
 118. Buchholz, V. (2013). *Oscillatory activity in tactile remapping*. Radboud University Nijmegen, Nijmegen, The Netherlands.
 119. van Deurzen, P.A.M. (2013). *Information processing and depressive symptoms in healthy adolescents*. Radboud University Nijmegen, Nijmegen, The Netherlands.
 120. Whitmarsh, S. (2013). *Nonreactivity and metacognition in mindfulness*. Radboud University Nijmegen, Nijmegen, The Netherlands.
 121. Vesper, C. (2013). *Acting together: Mechanisms of intentional coordination*. Radboud University Nijmegen, Nijmegen, The Netherlands.
 122. Lagro, J. (2013). *Cardiovascular and cerebrovascular physiological measurements in clinical practice and prognostics in geriatric patients*. Radboud University Nijmegen Medical Centre, Nijmegen, the Netherlands.
 123. Eskenazi, T.T. (2013). *You, us & them: From motor simulation to ascribed shared intentionality in social perception*. Radboud University Nijmegen, Nijmegen, The Netherlands.
 124. Ondobaka, S. (2013). *On the conceptual and perceptual processing of own and others' behavior*. Radboud University Nijmegen, Nijmegen, The Netherlands.
 125. Overvelde, J.A.A.M. (2013). *Which practice makes perfect? Experimental studies on the acquisition of movement sequences to identify the best learning condition in good and poor writers*. Radboud University Nijmegen, Nijmegen, The Netherlands.
 126. Kalisvaart, J.P. (2013). *Visual ambiguity in perception and action*. Radboud University

- Nijmegen Medical Centre, Nijmegen, The Netherlands.
127. Kroes, M. (2013). *Altering memories for emotional experiences*. Radboud University Nijmegen, Nijmegen, The Netherlands.
 128. Duijnhouwer, J. (2013). *Studies on the rotation problem in self-motion perception*. Radboud University Nijmegen, Nijmegen, The Netherlands.
 129. Nijhuis, E.H.J (2013). *Macroscopic networks in the human brain: Mapping connectivity in healthy and damaged brains*. University of Twente, Enschede, The Netherlands
 130. Braakman, M. H. (2013). *Posttraumatic stress disorder with secondary psychotic features. A diagnostic validity study among refugees in the Netherlands*. Radboud University Nijmegen, Nijmegen, The Netherlands.
 131. Zedlitz, A.M.E.E. (2013). *Brittle brain power. Post-stroke fatigue, explorations into assessment and treatment*. Radboud University Nijmegen, Nijmegen, The Netherlands.
 132. Schoon, Y. (2013). *From a gait and falls clinic visit towards self-management of falls in frail elderly*. Radboud University Nijmegen Medical Centre, Nijmegen, The Netherlands.
 133. Jansen, D. (2013). *The role of nutrition in Alzheimer's disease - A study in transgenic mouse models for Alzheimer's disease and vascular disorders*. Radboud University Nijmegen, Nijmegen, The Netherlands.
 134. Kos, M. (2013). *On the waves of language - Electrophysiological reflections on semantic and syntactic processing*. Radboud University Nijmegen, Nijmegen, The Netherlands.
 135. Severens, M. (2013). *Towards clinical BCI applications: Assistive technology and gait rehabilitation*. Radboud University Nijmegen, Nijmegen, Sint Maartenskliniek, Nijmegen, The Netherlands.
 136. Bergmann, H. (2014). *Two is not always better than one: On the functional and neural (in)dependence of working memory and long-term memory*. Radboud University Nijmegen, Nijmegen, The Netherlands.
 137. Wronka, E. (2013). *Searching for the biological basis of human mental abilities. The relationship between attention and intelligence studied with P3*. Radboud University Nijmegen, Nijmegen, The Netherlands.
 138. Lüttjohann, A.K. (2013). *The role of the cortico-thalamo-cortical system in absence epilepsy*. Radboud University Nijmegen, Nijmegen, The Netherlands.
 139. Brazil, I.A. (2013). *Change doesn't come easy: Dynamics of adaptive behavior in psychopathy*. Radboud University Nijmegen, Nijmegen, The Netherlands.
 140. Zerbi, V. (2013). *Impact of nutrition on brain structure and function. A magnetic resonance imaging approach in Alzheimer mouse models*. Radboud University Nijmegen, Nijmegen, The Netherlands.
 141. Delnooz, C.C.S. (2014). *Unravelling primary focal dystonia. A treatment update and new pathophysiological insights*. Radboud University Nijmegen Medical Centre, Nijmegen, The Netherlands.
 142. Bultena, S.S. (2013). *Bilingual processing of cognates and language switches in sentence context*. Radboud University Nijmegen, Nijmegen, The Netherlands.
 143. Janssen, G. (2014). *Diagnostic assessment of psychiatric patients: A contextual perspective on executive functioning*. Radboud University Nijmegen, Nijmegen, The Netherlands.
 144. Piai, V. Magalhães (2014). *Choosing our words: Lexical competition and the involvement of attention in spoken word production*. Radboud University Nijmegen, Nijmegen, The Netherlands.
 145. van Ede, F. (2014). *Preparing for perception. On the attentional modulation, perceptual relevance and physiology of oscillatory neural activity*. Radboud University Nijmegen, Nijmegen, The Netherlands.